



**Faculty of Pharmacy  
with the Division of Laboratory Medicine**  
Medical University of Białystok

**Kamila Buzun**

*Molecular mechanism of anticancer activity of novel  
4-thiazolidinone derivatives*

Doctoral dissertation based on a series of scientific publications  
in medical and health sciences  
in the discipline of pharmaceutical sciences

**Supervisors**

**Prof. Anna Bielawska**, Medical University of Białystok, Department of Biotechnology

**Prof. Roman Lesyk**, Danylo Halytsky Lviv National Medical University, Department  
of Pharmaceutical, Organic and Bioorganic Chemistry

Białystok 2022

*This doctoral dissertation would not have been possible without the support and help of many people, whom I would like to thank at this point.*

*My Supervisors, **Prof. Anna Bielawska** and **Prof. Roman Lesyk**, for giving me the opportunity for scientific development, the substantive direction of this dissertation, trust, patience, knowledge, and experience that you have shared with me.*

***Prof. Krzysztof Bielawski** for his scientific support, valuable remarks, and kindness.*

***Doctor Agnieszka Gornowicz, Doctor Bożena Popławska, and Doctor Robert Czarnomysy** for their scientific support and invaluable help in conducting my research.*

***Prof. Jadwiga Handzlik** and **Prof. Gniewomir Latacz** for their support, and kindness and for the opportunity to complete the scientific internship in the Department of Technology and Biotechnology of Drugs at the Jagiellonian University Medical College.*

***Employees and PhD students** of the Department of Biotechnology, and Department of Synthesis and Technology of Drugs for the friendly working atmosphere, help, and valuable scientific discussions.*

***My parents** for their unwavering faith, unconditional love, and the values they instilled in me.*

***My brothers, Karol and Kuba**, for their support, understanding, and patience.*

***My friends** for their presence, optimism, and understanding.*

## **I. List of publications constituting the doctoral dissertation**

Total Impact Factor for the publication series: **21.311**

Total points according to the list of scientific journals by the MES (Ministry of Education and Science): **520 points**

### **List of publications constituting the doctoral dissertation:**

1. Kamila Buzun, Anna Bielawska, Krzysztof Bielawski, Agnieszka Gornowicz, *DNA topoisomerases as molecular targets for anticancer drugs*, Journal of Enzyme Inhibition and Medicinal Chemistry, 2020, Vol. 35, No. 1, 1781-1799, DOI: 10.1080/14756366.2020.1821676, IF = 5.051, MES scores: 140.00 points
2. Kamila Buzun, Agnieszka Gornowicz, Roman Lesyk, Krzysztof Bielawski, Anna Bielawska, *Autophagy Modulators in Cancer Therapy*, International Journal of Molecular Sciences, 2021, Vol. 22, No. 11, 35 pp., Article ID: 5804, DOI: 10.3390/ijms22115804, IF = 5.924, MES scores: 140.00 points
3. Kamila Buzun, Anna Kryshchyshyn-Dylevych, Julia Senkiv, Olexandra Roman, Andrzej Gzella, Krzysztof Bielawski, Anna Bielawska, Roman Lesyk, *Synthesis and Anticancer Activity Evaluation of 5-[2-Chloro-3-(4-nitrophenyl)-2-propenylidene]-4-thiazolidinones*, Molecules, 2021, Vol. 26, No. 10, 15 pp., Article ID: 3057, DOI: 10.3390/molecules26103057, IF = 4.412, MES scores: 100.00 points
4. Kamila Buzun, Agnieszka Gornowicz, Roman Lesyk, Anna Kryshchyshyn-Dylevych, Andrzej Gzella, Robert Czarnomysy, Gniewomir Latacz, Agnieszka Olejarz-Maciej, Jadwiga Handzlik, Krzysztof Bielawski, Anna Bielawska, *2-{5-[(Z,Z)-2-Chloro-3-(4-nitrophenyl)-2-propenylidene]-4-oxo-2-thioxothiazolidin-3-yl}-3-methylbutanoic Acid as a Potential Anti-Breast Cancer Molecule*, International Journal of Molecular Sciences, 2022, Vol. 23, No. 8, 34 pp., Article ID: 4091, DOI: 10.3390/ijms23084091, IF = 5.924, MES scores: 140.00 points

## Table of contents

<b>I.</b>	List of publications constituting the doctoral dissertation.....	3
<b>II.</b>	Introduction.....	6
<b>III.</b>	Aim of the work.....	14
<b>IV.</b>	Fulfilment of scientific objectives – materials, methods, and results.....	15
<b>V.</b>	Conclusions.....	23
<b>VI.</b>	References.....	24
<b>VII.</b>	Abstract.....	34
<b>VIII.</b>	Streszczenie w języku polskim.....	35
<b>IX.</b>	DNA topoisomerases as molecular targets for anticancer drugs, <i>Journal of Enzyme Inhibition and Medicinal Chemistry</i> , 2020, Vol. 35, No. 1, 1781-1799.....	37
<b>X.</b>	Autophagy Modulators in Cancer Therapy, <i>International Journal of Molecular Sciences</i> , 2021, Vol. 22, No. 11, 35 pp., Article ID: 5804.....	56
<b>XI.</b>	Synthesis and Anticancer Activity Evaluation of 5-[2-Chloro-3-(4-nitrophenyl)-2-propenylidene]-4-thiazolidinones, <i>Molecules</i> , 2021, Vol. 26, No. 10, 15 pp., Article ID: 3057.....	91
<b>XII.</b>	2-{5-[(Z,Z)-2-Chloro-3-(4-nitrophenyl)-2-propenylidene]-4-oxo-2-thioxothiazolidin-3-yl}-3-methylbutanoic Acid as a Potential Anti-Breast Cancer Molecule, <i>International Journal of Molecular Sciences</i> , 2022, Vol. 23, No. 8, 34 pp., Article ID: 4091.....	117
<b>XIII.</b>	Statement of the author of the dissertation.....	151
<b>XIV.</b>	Statements of co-authors of the dissertation.....	152
<b>XV.</b>	Scientific achievements.....	164
	1. List of publications constituting the doctoral dissertation	
	2. List of other publications	
	3. List of conference papers	
	4. List of other scientific activities	

## **Abbreviations**

ADCD – autophagy-dependent cell death

ADME-Tox – absorption, distribution, metabolism, excretion, toxicity

APAF-1 – apoptosis protease-activating factor 1

CMA – chaperone-mediated autophagy

COVID-19 – coronavirus disease 2019

DDIs – drug-drug interactions

DISC – death-inducing signaling complex

DRs – death receptors

eMI – endosomal microautophagy

ESCRT – endosomal sorting complex required for transport

LAMP2A – lysosome-associated membrane protein type 2A

LC3A – microtubule-associated protein 1A/1B light chain 3A

LC3B – microtubule-associated protein 1A/1B light chain 3B

MA – Michael acceptors

MCB – medium control baseline

MES – Ministry of Education and Science

MPF – microplate fluctuation

PAINS – pan-assay interference compounds

PCD – programmed cell death

SAR – structure-activity relationship

Top I – topoisomerase I

Top II – topoisomerase II

Top IIA – topoisomerase IIA

Top IIB – topoisomerase IIB

## II. Introduction

One of the world's leading public health problems and also the second cause of death is cancer. Due to the coronavirus disease 2019 (COVID-19) pandemic, the most recent data on cancer cases and deaths are from 2018 and 2019. Delays in cancer diagnosis and treatment in 2020 and 2021 caused by COVID-19 and the associated limited access to healthcare and hospitals may contribute to an increase in the number of advanced-stage cancer diagnoses and subsequent increases in mortality rates. It is projected, that in 2022 only in the United States, there will be 1,918,030 new cases of cancer (more than 5,000 new cases per day) and 609,360 cancer deaths [1,2].

The discovery of cytostatic anticancer drugs that followed World War II was a real turning point in cancer treatment. Since then, exponential growth in new anticancer drug research has been observed. The beginning of the 1980s brought the second real breakthrough in the pharmacology and oncology area – thanks to cellular and molecular biology studies, it has become possible to develop drugs specific to selected molecular targets involved in tumorigenesis. This, in turn, gave rise to targeted therapy. Chemotherapy and targeted therapy have significantly improved cancer patients' survival and life quality. The turn of the third millennium with the introduction of monoclonal antibodies and immune checkpoint inhibitors brought another breakthrough in clinical pharmacology and oncology. With the development of genetic engineering, treatment of advanced metastatic cancers resistant to current therapies has become possible. Nowadays, cancer studies are focused on the design and development of new therapeutic approaches. There is no doubt that optimal therapy for each patient requires an individualized approach considering diagnosed cancer type, stage of disease, and individual patient's preferences. However, available chemotherapeutic agents are characterized by low therapeutic index and poor selectivity, resulting in numerous side effects.

One of the greatest challenges of modern medicinal chemistry studies is anticancer therapy. The imperfections of modern chemotherapy justify the development of the search for new chemotherapeutic drugs with high therapeutic efficacy and low toxicity. 4-Thiazolidinones and their derivatives became a subject of interest in modern medicinal chemistry in the 1960s. In almost 60 years, numerous reviews, scientific papers, and patents covering 4-thiazolidinone derivatives have appeared [3-7]. Since the 1960s, a substantial increase in pharmacology and medicinal chemistry of this group of compounds has been seen [8-11]. A diverse range of activities of 4-thiazolidinones has been observed – from anticancer, antibacterial, anti-inflammatory, and antidiabetic to antiparasitic [12-15]. Among 4-thiazolidinones, a well-

known class of drugs and patented lead compounds, “small molecules” with anticancer properties are of particular interest to scientists throughout the world. The undeniable evidence for the affinity of 4-thiazolidinone-based compounds to known anticancer biotargets *i.e.* JSP-1, Bcl-X<sub>L</sub>-BH3 (antiapoptotic complex), or TNF- $\alpha$ -TNFRc-1 are found in the literature [16-18].

## 2.1. 4-Thiazolidinones

4-Thiazolidinones are a well-studied group of biologically active compounds [6]. Extensively explored since the 1960s, 4-thiazolidinone derivatives have become the foundation of numerous innovative medicinal compounds *i.e.* Darbufelone (COX-2/5-LOX dual inhibitor) [19], Etozoline (modern diuretic) [7], Epalrestat (inhibitor of aldose reductase) [20], or Pioglitazone and its analogs (hypoglycemic agents) (**Figure 1**) [21]. Rational, privileged substructure-based diversity-oriented synthesis of 4-thiazolidinones, well-known lead compounds in medicinal chemistry, is an important tool in the design of new molecules with drug-like properties [4-6,22-24].

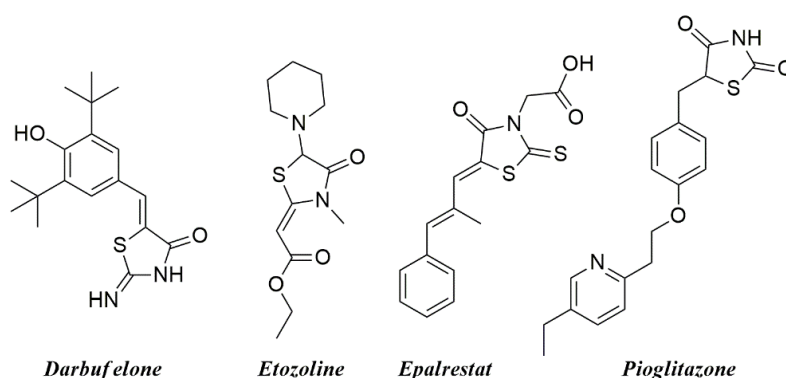


**Figure 1.** Known drugs belonging to the group of 4-thiazolidinones

Among 4-thiazolidinones, 5-ene-4-thiazolidinones have become a subject of special interest in the context of chemical features and pharmacological profiles (many 4-thiazolidinone lead compounds, drug candidates, and 4-thiazolidinone-based drugs belong to the aforementioned subtype) [17]. Conjugation of the 5-ene fragment to the carbonyl group at the C4 position of the thiazolidine core makes the compound potentially reactive and electrophilic due to a possible Michael addition of the nucleophilic protein residues to the exocyclic double bond. Therefore, 5-ene-4-thiazolidinones can be considered Michael acceptors (MA) [3]. In the modern approach to medicinal chemistry, MA possess dualistic nature that characterizes 5-ene-4-thiazolidinone derivatives as frequent hitters (promiscuous inhibitors) or pan-assay interference compounds (PAINS). Usually, PAINS are unusable during drug design due to their possible insufficient selectivity caused by interaction between PAINS

and biotargets (*i.e.* enzymes, receptors) [25-27]. However, in the polypharmacological approach, the low selectivity of MA towards different biotargets can be considered an asset and a foundation for further compound optimization. A lot of MA with anticancer properties are classified as covalent inhibitors (*i.e.* PI3K-, EGFR- or MEK-inhibitors) and the MA-moiety's presence in known ligands, increases their selectivity [17].

Over the last 20 years, 4-thiazolidinones have become a source of anticancer lead compounds and drug candidates [16]. Among 4-thiazolidinone derivatives inhibitors of tumor necrosis factor  $\alpha$  [28], Bcl-X<sub>L</sub> and BH3 (proteins involved in programmed cell death – apoptosis) [29], necroptosis [30], Pim-1 and Pim-2 protein kinases [31], integrin antagonists [32], peroxisome proliferator-activated receptor- $\gamma$  agonists [33,34] and COX-2 inhibitors [35] were found.

## 2.2. Autophagy

A comprehensive description of the autophagy process, known autophagy inhibitors and activators, as well as clinically and preclinically tested compounds is provided in the review article “*Autophagy modulators in cancer therapy*” that is a part of this doctoral dissertation [36].

Autophagy is a process of “*self-eating*” that plays an important role in the intracellular degradation of damaged proteins, organelles, or cellular fragments. It provides an organism's homeostasis and prevents the accumulation of redundant components inside the cell. On the other hand, under stressful conditions *i.e.* chemotherapy, hypoxia, or nutrient deficiency, autophagy can also become the strategy for cell survival [36-39].

“*Autophagy-dependent cell death (ADCD)*”, occurring in all eukaryotic cells, is a type of regulated cell death [40]. ADCD performs important functions in the cell, *i.e.* it is an adaptation mechanism to stressful conditions. This process, through its diverse mechanisms of degradation of redundant organelles, proteins, and other cellular fragments, represents the major catabolic system of eukaryotic cells [41,42]. Furthermore, as an integral part of maintaining cellular homeostasis, autophagy-dependent cell death has an important role in preserving genome integrity and tumor suppression [43].

Differences in the mechanism of delivery of redundant cytoplasmic components to the lysosomes resulted in the distinction of four basic types of autophagy:

- Macroautophagy – the most common type of autophagy [44]. During the initial phase of the macroautophagy process, a fragment of cytoplasm is surrounded by a forming double C-shaped membrane (phagophore). The membrane extends, enclosing



a fragment of cytoplasm with redundant/damaged organelles or proteins inside. Consequently, a 300-900 nm bubble (autophagosome) is formed, which subsequently undergoes a maturation process in which autophagosomes and lysosomes merge. This resulted in the formation of autolysosomes, where accumulated macromolecular substrates are degraded to fatty acids using hydrolytic lysosomal enzymes [45,46]. Macroautophagy may play a dual role in tumorigenesis. Through degradation of redundant or damaged cells, proteins or organelles, this process can lead to tumor suppression. In contrast, metabolite recycling or the cytoprotective effect of autophagy in response to applied chemotherapy may stimulate cancer cell development [47].

- Selective autophagy – its mechanism is based on the degradation of specific organelles: endoplasmic reticulum (ER-phagy), mitochondria (mitophagy), proteasomes (proteaphagy), ribosomes (ribophagy), peroxisomes (pexophagy), lipid droplets (lipophagy), lysosomes (lysophagy) and nuclei (nucleophagy). The mechanism of action of selective autophagy is related to the binding of specific organelles. Autophagy receptors bind a selected cargo and thereafter its degradation occurs in lysosomes/vacuoles [48-51]. Its ability to degrade selected organelles makes selective autophagy important for maintaining cellular homeostasis [52]. Dysfunctions of the selective autophagy may result in various diseases, *i.e.* cancer [53,54], neurodegenerative diseases [55,56] or heart failure [57].
- Microautophagy – a non-invasive process of cytoplasmic material absorption through lysosomal membrane invaginations [58]. In mammals, microautophagy occurs on late endosomes and is defined as endosomal microautophagy (eMI) [59]. selectively or randomly collected substrates are transported to endosomes in vesicles. On the endosome surface, membrane invagination occurs involving the endosomal sorting complex required for transport (ESCRT) machinery [59,60]. The substrates of the eMI process are integrated into intraluminal vesicles and therefore may be degraded or excreted outside the cell [61].
- Chaperone-mediated autophagy (CMA) – one of the pathways of intracellular protein degradation which occur in lysosomes. The identification of substrates for the CMA process is based on the presence of specific sequences (KFERQ-like motifs) in proteins. The substrates of the CMA process are selected by a cytosolic chaperone – heat shock cognate protein 70 (Hsc70), and transported to the surface of lysosomes by Hsc70 and co-chaperones [62,63]. Thereafter, delivered proteins bind to lysosome-associated membrane protein type 2A (LAMP2A), and the formed protein-LAMP2A complex

allows for onward transport of substrates into the lysosome lumen. Finally, the delivered substrate proteins are degraded using hydrolytic enzymes [62].

In light of cancer therapy, we observe a dual role of autophagy – it can induce or inhibit cancer cell development [64]. As a growth-promoting mechanism for cancer cells, autophagy preserves cells from the negative influence of different forms of cellular stress. In anticancer therapy, that process is referred to as “*adaptive autophagy*”. Sustaining cancer cell development enhances the tumor’s chances for survival despite the use of chemotherapy or radiation therapy. Nevertheless, targeted inhibition of adaptive autophagy results in reversal of the process and resensitization of the cells to the applied therapy [65,66]. Among well-known autophagy inhibitors, we can list, *i.e.* Chloroquine, Verteporfin, Clarithromycin, 3-Methyladenine. In turn, Temsirolimus, Everolimus, and Metformin are classified as autophagy activators [36].

### **2.3. Apoptosis**

Apoptosis or programmed cell death (PCD), is a process that leads to the efficient and organized elimination of cells, where DNA damages or other defects have occurred during development. The mechanism of PCD is very complex and precisely regulated at the gene level. We can distinguish two main apoptotic pathways: intrinsic and extrinsic (**Figure 2**). In the intrinsic pathway, when damages are detected, the cell itself initiates the degradation mechanism. The extrinsic apoptotic pathway requires the involvement of so-called death receptors. In both cases, initiating signals lead to the activation of initiator caspases (caspase-8 or caspase-9). Active caspases initiate the signaling cascade which results in the activation of executioner caspases (caspase-3, caspase-6, and caspase-7). This results in several events, *i.e.*: DNA fragmentation, nuclear protein destruction, or formation of apoptotic bodies, resulting in cell death [67].

As mentioned above, the intrinsic apoptotic pathway is initiated inside the cell. The apoptotic triggers, such as irreversible DNA damage, oxidative stress, hypoxia, or extremely high concentration of  $\text{Ca}^{2+}$  cause a collapse in mitochondrial membrane potential and subsequent release of cytochrome c from mitochondrial intermembrane space [68]. Released to the cytosol, cytochrome c combines with apoptosis protease-activating factor 1 (APAF1) and inactive procaspase-9 to form a multiprotein complex – the apoptosome. This leads to the activation of procaspase-9 to its active form – caspase-9, followed by the activation of executioner procaspases. Finally, activated executioner caspases induce cell death [69].

The extrinsic apoptotic pathway is initiated through so-called death receptors (DRs). Macrophages or natural killer cells produce death ligands which then bind with DRs localized at the cell surface. After ligand binding, DRs accumulate into clusters in the cell membrane and promote the recruitment of adaptor proteins, which then interact with procaspase-8 [70]. Death receptor combines with death ligand, an adaptor protein, and procaspase-8 to form death inducing signaling complex (DISC). DISC leads to the transformation of procaspase-8 to its active form – caspase-8. Subsequently, caspase-8 triggers an executioner caspase cascade, resulting in cell death [71].

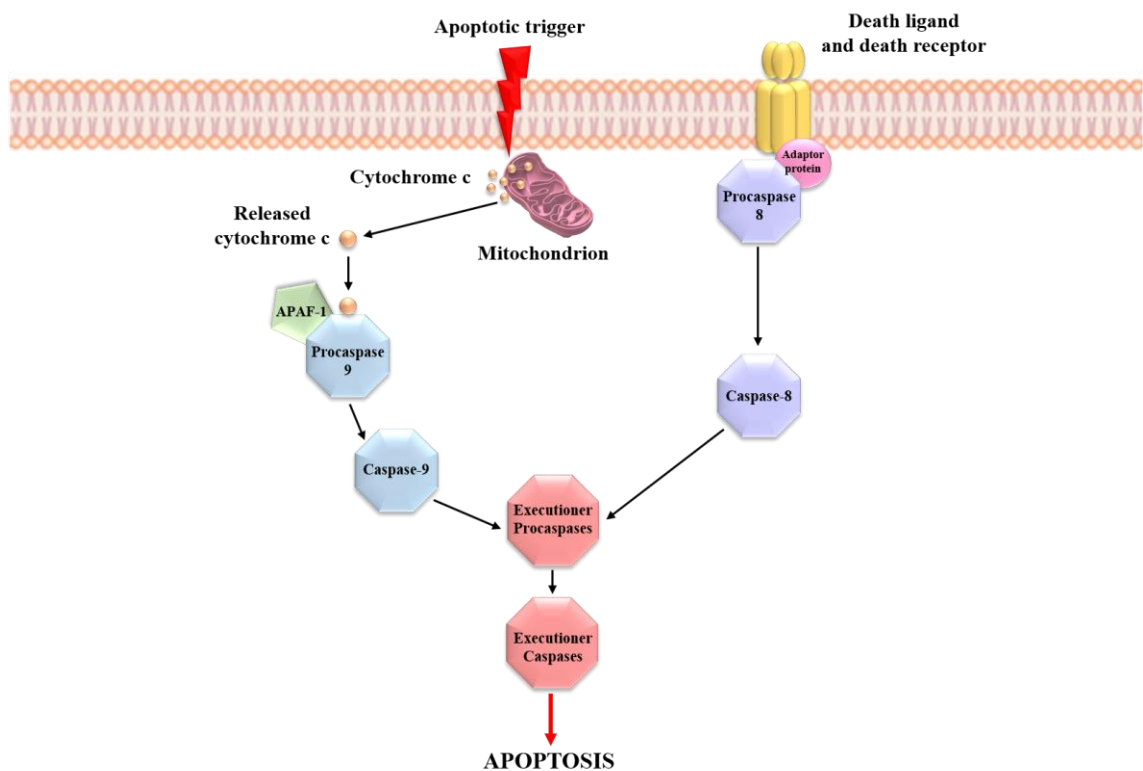


**Figure 2.** Apoptotic pathways

Carcinogenesis is the result of a series of genetic changes that transform a normal cell into a cancerous cell [72]. One of the key mechanisms related to the survival and progression of cancer cells is their evasion of PCD. Deregulation of apoptosis is associated with uncontrolled cell proliferation, cancer development and progression, and the treatment resistance of cancer cells [73]. Unlike necrosis, PCD does not induce inflammation and it represents the preferred cell death pathway for anticancer therapies. Selective induction of PCD and the regulation of apoptotic pathways regulation by therapeutic compounds is currently focusing the attention of many scientists as a promising approach to cancer therapy [74-81].

Recognition and understanding of the molecular factors involved in the apoptosis signaling pathway are crucial for the development of new anticancer strategies. Considering the

fact that impairments of PCD are one of the hallmarks of cancer cells, stimulation of apoptosis represents one of the most promising strategies in the design and development of new, more effective anticancer compounds.

The correlation between apoptosis and autophagy processes and its influence on cell viability has been noted and accurately described in Chapter 3 of the review paper “*Autophagy modulators in cancer therapy*” [36].

## **2.4. Topoisomerases**

Topoisomerases (Top), discovered by Jim Wang in 1971, are enzymes that control the topology of DNA [82,83]. They participate in many essential processes taking place in cells e.g. replication, transcription, and recombination of DNA and chromosomes condensation. Topoisomerases covalently bind to the phosphorus group in DNA, split the single or double DNA strand, and eventually religate them. According to the mechanism of action, we can distinguish two main types of enzymes: topoisomerases I (Top I) and topoisomerases II (Top II). Furthermore, these types of Top can be divided into five subfamilies. A detailed description of Top I and Top II subfamilies can be found in the review paper “*DNA topoisomerases as molecular targets for anticancer drugs*” included in this dissertation [84]. Due to their extremely important biological functions, structure, or mechanism of action, these enzymes have been one of the major molecular targets for anticancer drug design for nearly 30 years. Topoisomerase II is an attractive molecular target as its enhanced activity is observed in many cancers [85].

Topoisomerases II, which are divided into two subtypes (topoisomerase IIA and IIB) are found in many living organisms. Topoisomerases IIA (Top IIA) are found in bacteria, eukaryotes, humans, and several archaeon species. The sequences of all the enzymes belonging to the Top IIA show considerable similarity with the only differences occurring in the quaternary structures of these proteins. In contrast, topoisomerases IIB (Top IIB) are found mainly among archaea, plants, and some algae species. The DNA double-strand topology change caused by Top IIA is based on the “*two-gate*” mechanism. Initially, Top IIA attaches to the DNA strands. As a result of the ATP to ADP hydrolysis in presence of  $Mg^{2+}$  ions, tyrosine molecules from both monomers of Top IIA attack the DNA phosphodiester bond, causing cleavage of both DNA strands. The tyrosine covalently binds to the 5' end of the cut DNA fragment (G-segment). By cleaving the DNA helix, a “*gate*” is created that allows a second DNA molecule (T-segment) to be transported through the resulting DNA-Top II complex. The transported T-segment is released after passing through the “*gate*” and the energy gained by

hydrolysis of the second ATP molecule to ADP enables religation of broken DNA strands. Subsequently, as a result of the release of ADP molecules, the DNA-Top II complex transforms from a closed clamp form to an open one, which involves the release of DNA from the complex. Enzymes belonging to the Top II group, due to the significant structural changes occurring in them during T-segment transport through created “*gate*”, have the ability to adopt multiple conformational states. In theory, trapping enzymes in either conformational state allows manipulation of Top II activity [84,86,87].

To date, two types of topoisomerase II inhibitors have been identified and described – topoisomerase poisons and catalytic inhibitors.

- Topoisomerase poisons – Top II-DNA-drug complexes formation prevents the DNA strands from religation after the transported T-segment passage through the formed “*gate*”. Consequently, cancer cell death through apoptosis occurs. This means that the drug is used to convert a naturally formed complex into a cell-lethal poison.
- Catalytic inhibitors – include a number of different compounds that interact with Top II at different stages of the catalytic cycle, *i.e.* preventing the formation of a DNA-Top II complex by stabilizing DNA with non-covalent complexes with Top II or blocking ATPase binding sites [84,88].

To date, numerous topoisomerase inhibitors have been identified and described by scientists around the world. However, in many cases, the detailed mechanism of action remains unknown. The use of topoisomerase inhibitors in anticancer therapy leads to irreversible interruption of DNA strands, which in turn leads to programmed cell death [88]. Identification of novel anti-topoisomerase drugs may enable *i.e.* to reduce of the anthracyclines’ cardiotoxic effects or decrease the frequency of drug-induced secondary cancers. In the end, increased significance and rapid development of molecular biology and molecular genetics may allow the application of anti-topoisomerase drugs in personalized anticancer therapy.

A detailed description of known topoisomerase II inhibitors and activators, as well as the latest information on compounds under clinical and preclinical investigation, can be found in the previously mentioned review article [84] that is a part of this doctoral dissertation.

### III. Aim of the work

The aim of the work was to synthesize and evaluate the potential anticancer activity of a series of novel 5-[(Z,2Z)-2-chloro-3-(4-nitrophenyl)-2-propenylidene]-4-thiazolidinones. Chemical structures of the new compounds were confirmed using  $^1\text{H}$  and  $^{13}\text{C}$  NMR, LC-MS, and X-ray analyses. Furthermore, the structure-activity relationship (SAR) analysis of newly synthesized compounds was conducted. To evaluate their anticancer activity, the screening of novel 4-thiazolidinone derivatives toward the NCI60 cell lines panel, gastric cancer (AGS), colon cancer (DLD-1), and breast cancer (MCF-7 and MDA-MB-231) cell lines was performed. Thereafter, an in-depth *in vitro* analysis of the selected compound (Les-3331) was conducted. The molecular docking studies were performed to evaluate the affinity of Les-3331 to topoisomerase II. The influence on apoptosis induction, mitochondrial membrane potential analysis, and the effect on topoisomerase II activity were evaluated. The molecular mechanism study of anticancer activity of Les-3331 including the determination of caspase-9, caspase-8, LC3A, LC3B, Beclin-1, and topoisomerase II concentrations was investigated. Finally, the assessment of the selected ADME-Tox parameters of the Les-3331 allowed for the determination of its permeability, metabolism, and risk of potential drug-drug interactions (DDIs).

## IV. Fulfillment of scientific objectives – materials, methods, and results

### 4.1. Materials and methods

Based on the previous studies conducted by Prof. Lesyk's team, it was found that combining *Ciminalum* and 4-thiazolidinone moiety in a single molecule would be an effective approach in the synthesis of novel hybrid compounds with potential anticancer properties [89,90]. Using Knoevenagel condensation, the new 4-thiazolidinone derivatives were combined with a structural fragment of *Ciminalum*. As a result, a series of novel *Ciminalum*-thiazolidinone hybrid molecules (13 compounds) were obtained. The chemical structures of newly synthesized compounds were confirmed using NMR, LCMS, and crystallography. Moreover, SAR analysis of novel compounds was conducted.

Cytotoxicity and antiproliferative properties of novel 4-thiazolidinones were evaluated after a 24 h incubation of cancer cells (MCF-7 and MDA-MB-231) and human skin fibroblast with the tested compounds. For the determination of cytotoxicity, the MTT assay was used. Subsequently, [<sup>3</sup>H]-thymidine incorporation into the DNA of breast cancer cells was analyzed to evaluate the effect of the newly synthesized compounds on cell proliferation.

The induction of apoptosis and mitochondrial membrane potential analyses were conducted by flow cytometry. The assays were performed using Annexin V binding Apoptosis Detection Kit II and the JC-1 MitoScreen kit according to the manufacturer's protocols.

The ELISA technique was used to determine the concentration of selected proteins: caspase-9, caspase-8, microtubule-associated protein 1A/1B light chain 3A (LC3A), microtubule-associated protein 1A/1B light chain 3B (LC3B), Beclin-1 and topoisomerase II. The tests were carried out according to the manufacturer's protocols.

Molecular docking studies as well as flow cytometric analysis of topoisomerase II $\alpha$  activity were conducted to confirm the inhibitory effect of novel 4-thiazolidinone on topoisomerase II. The 3D structure of Les-3331, obtained from the crystallographic analysis, was used for the *in silico* simulations. The results were visualized and interpreted using Discovery Studio Visualizer®. Topoisomerase II $\alpha$  activity was evaluated using an anti-topoisomerase II $\alpha$  antibody. Analysis of the obtained results was performed using a flow cytometer and FACSDiva software.

Finally, the *in vitro* evaluation of ADME-Tox parameters of a novel 4-thiazolidinone derivative (Les-3331) was conducted. Permeability of the Les-3331 was analyzed using Pre-coated PAMPA Plate System Gentest™ and UPLC-MS analyzer. The obtained data has allowed for the calculation of the permeability coefficient  $P_e$  according to formulas provided

by the manufacturer. The possible metabolic pathways of Les-3331 and its metabolic stability were evaluated using MetaSite 8.0.1. Software (*in silico* prediction) and RLMs (rat liver microsomes) – *in vitro* assay. The UPLC-MS and MS/MS devices were used to analyze the obtained results. Potential DDIs were assessed by CYP3A4 and CYP2D6 P450-Glo luminescence assays and the resulting signals were measured using a microplate reader. The mutagenicity of Les-3331 was determined using the Ames microplate fluctuation (MPF) protocol and *Salmonella Typhimurium* TA100 strain. The medium control baseline (MCB) and the Binomial B-value of the novel 4-thiazolidinone derivative were calculated based on the obtained results, using the protocols and data sheets provided by the manufacturer.

The results of experimental work constituting the doctoral dissertation have been published in high-profile scientific journals – **Molecules** and the **International Journal of Molecular Sciences**. In articles entitled “*Synthesis and Anticancer Activity Evaluation of 5-[2-Chloro-3-(4-nitrophenyl)-2-propenylidene]-4-thiazolidinones*” and “*2-{5-[(Z,Z)-2-Chloro-3-(4-nitrophenyl)-2-propenylidene]-4-oxo-2-thioxothiazolidin-3-yl}-3-methylbutanoic Acid as a Potential Anti-Breast Cancer Molecule*” anticancer potential of novel 4-thiazolidinone derivatives has been demonstrated. It has been found that designing new potential anticancer molecules through the combination of *Ciminalum* fragment and thiazolidinone moiety is an effective approach [89,90].

## 4.2. Summary of results

The scientific cooperation with the Department of Pharmaceutical, Organic and Bioorganic Chemistry at the Danylo Halytsky Lviv National Medical University resulted in obtaining 48 novel 4-thiazolidinone derivatives by organic synthesis. Computational analysis, molecular docking, and *in vitro* studies have allowed for a selection of 13 compounds with potential anticancer activity (**Figure 3**).



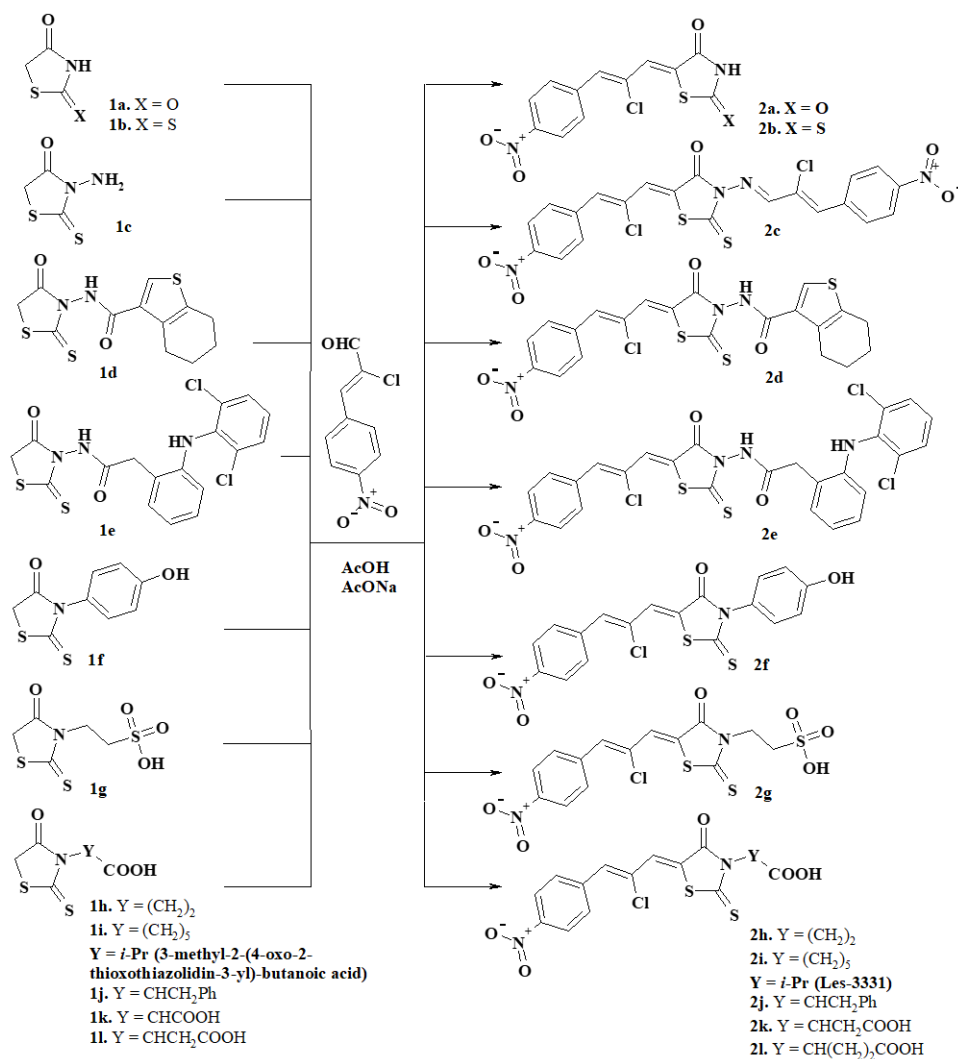


**Figure 3.** Synthesis of 5-[(Z,Z)-2-chloro-3-(4-nitrophenyl)-2-propenylidene]-4-thiazolidinones

(Z,Z)-2-chloro-3-(4-nitrophenyl)prop-2-enal, known as the *Ciminalum*, is an antibacterial agent against Gram (+) and Gram (-) bacteria (**Figure 4**) [91]. *Ciminalum* was used as a drug in medical practice in the former Soviet Union. In previously published papers, the pharmacophore properties of the molecular moiety of *Ciminalum* for thiazolidinone derivatives were established. Thus, 5-[(Z,Z)-2-chloro-3-(4-nitrophenyl)-2-propenylidene]-2-(3-hydroxyphenylamino)-2-thiazolidinone possessed significant anti-inflammatory effect in comparison with diclofenac sodium and aspirin [92]. Subsequent studies of this compound have led to the discovery of a new profile of biological activity, namely anticancer cytotoxicity. This early hit possessed a selectively high effect on leukemia, melanoma, lung, colon, central nervous system, ovarian, renal, prostate, and breast cancer cell lines at micro- and submicromolar levels that is probably associated with the immunosuppressive activity [90].

The in-depth investigation of the anticancer potential of *Ciminalum*-thiazolidinone hybrids has led to the identification of hit compounds and has shown significant prospects in

this direction of anticancer molecule design. The presence of a structural fragment of (2*Z*)-2-chloro-3-(4-nitrophenyl)prop-2-enal in the C5 position of the thiazolidinone ring is essential for the biological activity of *Ciminalum*-thiazolidinone hybrid molecules.

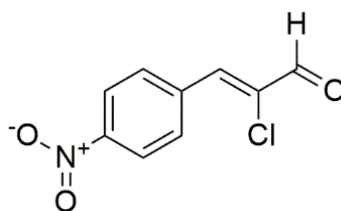


**Figure 4.** *Ciminalum* chemical structure

Based on the SAR analysis, it has been established that the structure of substituent in the N3 position of the thiazolidinone ring affects the anticancer activity of the designed molecule (**Figure 5**). Among the synthesized molecules, compounds with carboxylic acid residues in the N3 position were the most effective in decreasing the viability of MCF-7 and MDA-MB-231 (breast cancers), AGS (gastric cancer), and DLD-1 (colon cancer) cells. The obtained results revealed that the molecules with 3-methylbutanoic acid, propanoic acid, and hexanoic acid substituent in position 3 of the thiazolidinone ring have the highest cytotoxic activity among synthesized hybrid molecules (IC<sub>50</sub> range: 1.73 – 15.24 μM). On the other hand, the introduction of the sulfo group (-SO<sub>3</sub>H) in a position of a carboxyl group (-COOH) or the addition of another carboxylic group results in a significant decrease in the compound's activity (IC<sub>50</sub> range: 9.19 – 21.23 μM). Interestingly, the nature of the substituent in the C2 position of the core heterocycle is also very important in activity against cancer cells. Conducted studies have shown that compounds with the thioxo group at the C2 position were more active (IC<sub>50</sub> range: 1.59 – 21.23 μM) compared to compounds with structurally close 2-thioxo-4-thiazolidinones (rhodanines) with oxo group in the same position (IC<sub>50</sub> range: 16.84 – 27.49 μM). The chemical structure of substituents in the thiazolidinone ring and its influence on anticancer activity of tested compounds are one of the key elements in the design of novel *Ciminalum*-thiazolidinone molecules and should be further investigated.

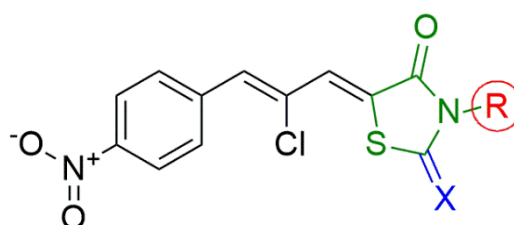


**Figure 5.** The structure of *Ciminalum*-thiazolidinone molecules. The thiazolidinone ring is marked in green.  
 R = H atom, alkyl substituents, heterocyclic compounds, aromatic rings (marked in red).  
 X = O, S (marked in blue)

Given the significant cytotoxic effect of novel 4-thiazolidinone derivatives on human breast cancer cell lines, the 2-{5-[(Z,Z)-2-chloro-3-(4-nitrophenyl)-2-propenylidene]-4-oxo-2-thioxothiazolidin-3-yl}-3-methylbutanoic acid (Les-3331) was selected for in-depth *in vitro* studies. To investigate the molecular mechanism of anticancer activity of Les-3331, cytotoxic and antiproliferative properties tests, assessment of apoptosis induction, mitochondrial membrane potential analysis, determination of selected proteins concentration, and evaluation of ADMETox parameters of the new hybrid molecule were planned.

In biological studies, which aimed to assess the anticancer potential of novel *Ciminalum*-thiazolidinone molecule, etoposide was used as a reference compound. Etoposide is a semi-synthetic derivative of podophyllotoxin obtained from *Podophyllum peltatum* [93]. The mechanism of anticancer activity of etoposide is based on its ability to inhibit topoisomerase II activity. The drug binds covalently to the DNA-topoisomerase II complex, which prevents the religation of breaks in DNA strands. Stabilization of DNA double-strands cleavage indirectly leads to cell death. This process is called “*topoisomerase II poisoning*” and therefore etoposide is referred “*topoisomerase poison*” [94-96].

Cytotoxicity of Les-3331 against MCF-7 and MDA-MB-231 breast cancer cell lines and human skin fibroblasts has been confirmed by MTT assay. The newly synthesized compound inhibited cancer cell viability in a concentration-dependent manner. After 24-hour incubation of MCF-7 and MDA-MB-231 cancer cells, higher cytotoxicity of the newly synthesized compound was observed compared to the etoposide. The half-maximal inhibitory concentration (IC<sub>50</sub>) values of Les-3331 were 5.02 μM and 15.24 μM for MCF-7 and MDA-MB-231 cells, respectively. Etoposide was not as efficient in decreasing cancer cell viability as the new hybrid molecule – in both cases, its IC<sub>50</sub> values exceeded 50 μM. Importantly, it was observed that Les-3331 exhibited lower cytotoxicity against human skin fibroblast with an IC<sub>50</sub> value of 28.52 μM.

Antiproliferative properties of a novel 4-thiazolidinone derivative were investigated by assessing the level of incorporation of radioactive [<sup>3</sup>H]-thymidine into the DNA of selected breast cancer cells. The 24-hours incubation of MCF-7 and MDA-MB-231 cancer cells with Les-3331 caused concentration-dependent inhibition of [<sup>3</sup>H]-thymidine incorporation into the DNA of human breast cancer cells. The obtained results indicate that the novel 4-thiazolidinone derivative is a more potent inhibitor of the DNA biosynthesis process than etoposide. The IC<sub>50</sub> value of Les-3331 was 5.54 μM for MCF-7 cells and 8.01 μM for MDA-MB-231 cells, whereas IC<sub>50</sub> values of etoposide in both cases exceeded 20 μM.

The promising anticancer properties of the new *Ciminalum*-thiazolidinone hybrid molecule may arise from its influence on the programmed cell death induction. The potential proapoptotic effect of Les-3331 on MCF-7 and MDA-MB-231 human breast cancer cells was examined using flow cytometry and Annexin V binding assay. The novel compound and etoposide were tested in two concentrations – 1  $\mu$ M and 5  $\mu$ M. The flow cytometric analysis revealed that both the novel 4-thiazolidinone derivative and reference drug are capable of inducing apoptosis in selected human breast cancer cells. The 24 h exposure of breast cancer cells on 5  $\mu$ M Les-3331 resulted in the detection of 40.4% (MCF-7) and 18.1% (MDA-MB-231) early and late apoptotic cells. The effect of 5  $\mu$ M etoposide on the number of early and late apoptotic cells was almost four times weaker compared with the same concentration of new derivative, with 10.7% of MCF-7 and 7.2% of MDA-MB-231 early and late apoptotic cells detected. The flow cytometric analysis of Les-3331 and etoposide revealed that both compounds are capable of initiating apoptosis in tested human breast cancer cell lines. A significant increase in the apoptotic cell population was observed in both MCF-7 and MDA-MB-231 cancer cells after incubation with Les-3331.

Mitochondria are the crucial elements of PCD and a major checkpoint of this process. One of the characteristic features of early apoptosis is a decrease in the mitochondrial membrane potential caused by exposure of the cell to apoptosis-inducing stimuli [69,97,98]. The results presented in the article entitled “2-{5-[(Z,Z)-2-Chloro-3-(4-nitrophenyl)-2-propenylidene]-4-oxo-2-thioxothiazolidin-3-yl}-3-methylbutanoic Acid as a Potential Anti-Breast Cancer Molecule” clearly indicate that novel *Ciminalum*-thiazolidinone derivative causes a decrease in mitochondrial membrane potential ( $\Delta\Psi_m$ ) of MCF-7 and MDA-MB-231 cancer cells compared to the control group. The greatest percentage of cells with decreased  $\Delta\Psi_m$  was observed after exposition to 5  $\mu$ M Les-3331. A 24-hours incubation of cancer cells with the tested compound caused a reduction of  $\Delta\Psi_m$  in 25.5% of MCF-7 and 36.3% of MDA-MB-231 cells. Incubation with the same concentration of reference compound resulted in an almost twofold lower effect on the percentage of cancer cells with decreased  $\Delta\Psi_m$ . Only 18.5% of MCF-7 and 15.6% of MDA-MB-231 cells had reduced mitochondrial membrane potential after treatment with 5  $\mu$ M etoposide. These results indicate that programmed cell death induced by a novel 4-thiazolidinone derivative may occur through an intrinsic, mitochondrial-dependent pathway.

To confirm the above results, the concentrations of proteins involved in the intrinsic (caspase-9) and extrinsic (caspase-8) apoptotic pathways were assessed. After 24 h incubation of MCF-7 and MDA-MB-231 breast cancer cells with Les-3331, an increase in caspase-9 and

caspase-8 concentrations was shown. Increased concentrations of proteins were observed after the exposition of cancer cells to both tested concentrations (1  $\mu$ M and 5  $\mu$ M) of the novel compound. In contrast to results obtained in the control and reference drug groups, Les-3331 led to a significant increase in caspase-9 and caspase-8 concentrations which may suggest that the novel *Ciminalum*-thiazolidinone derivative induces both intrinsic and extrinsic apoptotic pathways.

In modern studies on new anticancer molecules, increasing interest in the autophagy process has been observed. Numerous scientific papers describing the role of autophagy in the tumorigenesis process and the potential correlation between apoptosis and autophagy have been published in recent years [99-104]. To investigate the influence of Les-3331 on the autophagy process, the concentration of the LC3A, LC3B, and Beclin-1 proteins were checked in MCF-7 and MDA-MB-231 human breast cancer cells. In addition to etoposide, 3-methyladenine (3-MA, a known autophagy inhibitor) was used as a reference compound in the study. The results published in the article entitled “2-{5-[(Z,Z)-2-Chloro-3-(4-nitrophenyl)-2-propenylidene]-4-oxo-2-thioxothiazolidin-3-yl}-3-methylbutanoic Acid as a Potential Anti-Breast Cancer Molecule” have demonstrated that 24-hours incubation of selected cancer cells with a novel 4-thiazolidinone derivative led to a decrease in LC3A, LC3B, and Beclin-1 concentrations. The reference compounds exhibited a weaker inhibitory effect on selected proteins compared with Les-3331. All this indicates that a novel 4-thiazolidinone derivative may inhibit the autophagy process in MCF-7 and MDA-MB-231 cancer cells.

Since 1971, when James C. Wang discovered and described the first Top I ( $\omega$  protein) in *Escherichia Coli*, the rapid development of new topoisomerase inhibitors and activators has been observed. Topoisomerases play an important role in processes that require access to information encoded in DNA helix. Temporary or permanent disruption of DNA strands is essential *i.e.* for transcription, recombination, replication, or the releasement of replicated chromosomes before cell division [105]. Nowadays, many scientists around the world are focused on the search for new, effective topoisomerase II inhibitors with anticancer properties. Molecular docking studies, ELISA and flow cytometric analysis were performed to investigate the effect of the novel *Ciminalum*-thiazolidinone derivative on topoisomerase II. The studies revealed that Les-3331 possesses a good affinity to topoisomerase II and decreases the enzyme concentration and activity in MCF-7 and MDA-MB-231 cancer cells in micromolar concentrations (1  $\mu$ M and 5  $\mu$ M). Moreover, both in the ELISA test and flow cytometric analysis, the inhibitory effect of the new hybrid molecule was notably stronger compared with known topoisomerase II inhibitor – etoposide.

ADME-Tox is an acronym for absorption (A), distribution (D), metabolism (M), excretion (E), and toxicity (Tox). Determining the specific parameters associated with the aforementioned features is one of the key aspects of *in vitro* studies of a new potential therapeutic molecule. To investigate the permeability of the newly synthesized compound, the PAMPA was performed. The permeability coefficient ( $P_e$ ) of Les-3331 was  $0.96 \times 10^{-6}$  cm/s and it was over sixfold lower than the  $P_e$  of highly permeable reference compound – caffeine ( $P_e = 6.58 \times 10^{-6}$  cm/s). Due to the low passive permeability of the novel 4-thiazolidinone derivative, it might be assumed that the intracellular concentration of Les-3331 achieved through passive transport is sufficient to trigger the changes resulting in cell death. On the other hand, the additional active mechanism may be involved in the transport of the compound into the cell, which could explain its high antitumor activity. *In silico* and *in vitro* studies using RLMs allowed investigation of the metabolic stability and the most probable degradation pathway of Les-3331. The obtained results indicate that Les-3331 is a metabolically stable compound with 52% of the compound remaining in the reaction mixture after 120 minutes of incubation. The degradation of 2-thioxo-4-thiazolidinone moiety was indicated as a predicted metabolic pathway of Les-3331. Furthermore, a study of the effect of Les-3331 on CYP3A4 and CYP2D6 activity allowed to exclude or predict potential DDIs. It was observed that the compound activates CYP3A4 in concentrations of 10  $\mu$ M and 25  $\mu$ M. In contrast, slight inhibition of CYP2D6 activity was observed for 25  $\mu$ M Les-3331. Nevertheless, Les-3331 shows a very low risk of DDIs compared with reference CYP3A4 and CYP2D6 inhibitors. Finally, the mutagenicity of the novel 4-thiazolidinone derivative was studied using *Salmonella Typhimurium* TA100 strain and Ames MPF protocol. The known mutagen 4-NQO was used as a reference compound. Whereas Les-3331 was safe at 1  $\mu$ M concentration, a risk of mutagenicity was demonstrated at a higher concentration (5  $\mu$ M). However, based on this, it cannot be concluded that Les-3331 is a mutagenic compound and further in-depth studies are required.

The results obtained in the present dissertation, indicate the potential use of new 4-thiazolidinone derivatives in cancer therapy. Undoubtedly, it is necessary to confirm the anticancer activity of the tested compounds in animal model studies.

## V. Conclusions

1. High cytotoxicity of the new 4-thiazolidinone derivatives against AGS, DLD-1, MCF-7, and MDA-MB-231 cancer cell lines was demonstrated.
2. The SAR analysis revealed the essential role of the *Ciminalum* (2-chloro-3-(4-nitrophenyl)prop-2-enylidene) substituent at the C5 position for the 4-thiazolidinone ring and showed the correlation between the anticancer activity of the synthesized compounds and the nature of substituents at the N3 position of the thiazolidinone ring.
3. Novel *Ciminalum*-thiazolidinone derivative – Les-3331, induces the intrinsic and extrinsic apoptotic pathways. The compound leads to a decrease in mitochondrial membrane potential and increases caspase-9 and caspase-8 concentration in MCF-7 and MDA-MB-231 breast cancer cell lines.
4. Molecular docking studies have shown that Les-3331 possesses a good affinity to topoisomerase II. Additional studies revealed that this compound decreases topoisomerase II concentration and enzyme activity.
5. Les-3331 leads to a decrease in the concentration of autophagy-related proteins: LC3A, LC3B, and Beclin-1, in breast cancer cells.
6. The degradation of the 2-thioxo-4-thiazolidinone moiety was identified as a main metabolic pathway of the newly synthesized derivative in *in silico* and *in vitro* studies.
7. Les-3331 demonstrated a very low risk of DDIs.
8. Les-3331 has shown no mutagenic effect at 1  $\mu$ M concentration.
9. Novel *Ciminalum*-thiazolidinone hybrid molecules, including Les-3331, are promising candidates for new anticancer chemotherapeutic agents.

## VI. References

1. Yabroff, K.R.; Wu, X.-C.; Negoita, S.; Stevens, J.; Coyle, L.; Zhao, J.; Mumphrey, B.J.; Jemal, A.; Ward, K.C. Association of the COVID-19 pandemic with patterns of statewide cancer services. *Journal of the National Cancer Institute* **2021**, 10.1093/jnci/djab122, doi:10.1093/jnci/djab122.
2. Siegel, R.L.; Miller, K.D.; Fuchs, H.E.; Jemal, A. Cancer statistics, 2022. *CA: A Cancer Journal for Clinicians* **2022**, 72, 7-33, doi:10.3322/caac.21708.
3. Tomašić, T.; Peterlin Mašič, L. Rhodanine as a scaffold in drug discovery: A critical review of its biological activities and mechanisms of target modulation. *Expert Opinion on Drug Discovery* **2012**, 7, 549-560, doi:10.1517/17460441.2012.688743.
4. Tripathi, A.C.; Gupta, S.J.; Fatima, G.N.; Sonar, P.K.; Verma, A.; Saraf, S.K. 4-Thiazolidinones: The advances continue.... *European Journal of Medicinal Chemistry* **2014**, 72, 52-77, doi:10.1016/j.ejmech.2013.11.017.
5. Tomasic, T.; Masic, P.L. Rhodanine as a privileged scaffold in drug discovery. *Current Medicinal Chemistry* **2009**, 16, 1596-1629, doi:10.2174/092986709788186200.
6. Lesyk, R.; Zimenkovsky, B. 4-Thiazolidones: Centenarian history, current status and perspectives for modern organic and medicinal chemistry. *Current Organic Chemistry* **2004**, 8, 1547-1577, doi:10.2174/1385272043369773.
7. Lesyk, R.B.; Zimenkovsky, B.S.; Kaminsky, D.V.; Kryshchyshyn, A.P.; Havryluk, D.Y.; Atamanyuk, D.V.; Subtel'na, I.Y.; Khylyuk, D.V. Thiazolidinone motif in anticancer drug discovery. Experience of DH LNMU medicinal chemistry scientific group. *Biopolymers & Cell* **2011**, 27, 107-117, doi:10.7124/bc.000089.
8. Kaminsky, D.; Kryshchyshyn, A.; Lesyk, R. Recent developments with rhodanine as a scaffold for drug discovery. *Expert Opinion on Drug Discovery* **2017**, 12, 1233-1252, doi:10.1080/17460441.2017.1388370.
9. Brown, F.C. 4-Thiazolidinones. *Chemical Reviews* **1961**, 61, 463-521, doi:10.1021/cr60213a002.
10. Newkome, G.R.; Nayak, A. 4-Thiazolidinones. In *Advances in Heterocyclic Chemistry*, Katritzky, A.R., Boulton, A.J., Eds. Academic Press: 1980; Vol. 25, pp. 83-112.
11. Singh, S.P.; Parmar, S.S.; Raman, K.; Stenberg, V.I. Chemistry and biological activity of thiazolidinones. *Chemical Reviews* **1981**, 81, 175-203, doi:10.1021/cr00042a003.
12. Tahmasvand, R.; Bayat, P.; Vahdaniparast, S.M.; Dehghani, S.; Kooshafar, Z.; Khaleghi, S.; Almasirad, A.; Salimi, M. Design and synthesis of novel 4-thiazolidinone



- derivatives with promising anti-breast cancer activity: Synthesis, characterization, *in vitro* and *in vivo* results. *Bioorganic Chemistry* **2020**, *104*, 104276, doi:10.1016/j.bioorg.2020.104276.
13. Jain, A.K.; Vaidya, A.; Ravichandran, V.; Kashaw, S.K.; Agrawal, R.K. Recent developments and biological activities of thiazolidinone derivatives: A review. *Bioorganic & Medicinal Chemistry* **2012**, *20*, 3378-3395, doi:10.1016/j.bmc.2012.03.069.
  14. Molina, D.A.; Ramos, G.A.; Zamora-Vélez, A.; Gallego-López, G.M.; Rocha-Roa, C.; Gómez-Marin, J.E.; Cortes, E. In vitro evaluation of new 4-thiazolidinones on invasion and growth of *Toxoplasma gondii*. *International Journal for Parasitology: Drugs and Drug Resistance* **2021**, *16*, 129-139, doi:10.1016/j.ijpddr.2021.05.004.
  15. Gupta, A.; Singh, R.; Sonar, P.K.; Saraf, S.K. Novel 4-thiazolidinone derivatives as anti-infective agents: Synthesis, characterization, and antimicrobial evaluation. *Biochemistry Research International* **2016**, *2016*, 8086762, doi:10.1155/2016/8086762.
  16. Kaminsky, D.; Kryshchyshyn, A.; Lesyk, R. 5-Ene-4-thiazolidinones - An efficient tool in medicinal chemistry. *European Journal of Medicinal Chemistry* **2017**, *140*, 542-594, doi:10.1016/j.ejmech.2017.09.031.
  17. Lesyk, R. Drug design: 4-thiazolidinones applications. Part 1. Synthetic routes to the drug-like molecules. *Journal of Medical Science* **2020**, *89*, 33-49, doi:10.20883/medical.406.
  18. Lesyk, R. Drug design: 4-thiazolidinones applications. Part 2. Pharmacological profiles. *Journal of Medical Science* **2020**, *89*, 132-141, doi:10.20883/medical.e407.
  19. Charlier, C.; Michaux, C. Dual inhibition of cyclooxygenase-2 (COX-2) and 5-lipoxygenase (5-LOX) as a new strategy to provide safer non-steroidal anti-inflammatory drugs. *European Journal of Medicinal Chemistry* **2003**, *38*, 645-659, doi:10.1016/S0223-5234(03)00115-6.
  20. Ramirez, M.A.; Borja, N.L. Epalrestat: An aldose reductase inhibitor for the treatment of diabetic neuropathy. *Pharmacotherapy* **2008**, *28*, 646-655, doi:10.1592/phco.28.5.646.
  21. Sohda, T.; Momose, Y.; Meguro, K.; Kawamatsu, Y.; Sugiyama, Y.; Ikeda, H. Studies on antidiabetic agents. Synthesis and hypoglycemic activity of 5-[4-(pyridylalkoxy)benzyl]-2,4-thiazolidinediones. *Arzneimittelforschung* **1990**, *40*, 37-42.

22. Havrylyuk, D.; Zimenkovsky, B.; Lesyk, R. Synthesis, biological activity of thiazolidinones bearing indoline moiety and isatin based hybrids. *Mini-Reviews in Organic Chemistry* **2015**, *12*, 66-87, doi:10.2174/1570193X11666141028231910.
23. Havrylyuk, D.; Roman, O.; Lesyk, R. Synthetic approaches, structure activity relationship and biological applications for pharmacologically attractive pyrazole/pyrazoline–thiazolidine-based hybrids. *European Journal of Medicinal Chemistry* **2016**, *113*, 145-166, doi:10.1016/j.ejmech.2016.02.030.
24. Verma, A.; Saraf, S.K. 4-Thiazolidinone – A biologically active scaffold. *European Journal of Medicinal Chemistry* **2008**, *43*, 897-905, doi:10.1016/j.ejmech.2007.07.017.
25. Mendgen, T.; Steuer, C.; Klein, C.D. Privileged scaffolds or promiscuous binders: A comparative study on rhodanines and related heterocycles in medicinal chemistry. *Journal of Medicinal Chemistry* **2012**, *55*, 743-753, doi:10.1021/jm201243p.
26. Baell, J.B.; Holloway, G.A. New substructure filters for removal of Pan Assay Interference Compounds (PAINS) from screening libraries and for their exclusion in bioassays. *Journal of Medicinal Chemistry* **2010**, *53*, 2719-2740, doi:10.1021/jm901137j.
27. Baell, J.B. Observations on screening-based research and some concerning trends in the literature. *Future Medicinal Chemistry* **2010**, *2*, 1529-1546, doi:10.4155/fmc.10.237.
28. Carter, P.H.; Scherle, P.A.; Muckelbauer, J.A.; Voss, M.E.; Liu, R.-Q.; Thompson, L.A.; Tebben, A.J.; Solomon, K.A.; Lo, Y.C.; Li, Z., et al. Photochemically enhanced binding of small molecules to the tumor necrosis factor receptor-1 inhibits the binding of TNF- $\alpha$ . *Proceedings of the National Academy of Sciences* **2001**, *98*, 11879-11884, doi:10.1073/pnas.211178398.
29. Degterev, A.; Lugovskoy, A.; Cardone, M.; Mulley, B.; Wagner, G.; Mitchison, T.; Yuan, J. Identification of small-molecule inhibitors of interaction between the BH3 domain and Bcl-x<sub>L</sub>. *Nature Cell Biology* **2001**, *3*, 173-182, doi:10.1038/35055085.
30. Zheng, W.; Degterev, A.; Hsu, E.; Yuan, J.; Yuan, C. Structure–activity relationship study of a novel necroptosis inhibitor, necrostatin-7. *Bioorganic & Medicinal Chemistry Letters* **2008**, *18*, 4932-4935, doi:10.1016/j.bmcl.2008.08.058.
31. Xia, Z.; Knaak, C.; Ma, J.; Beharry, Z.M.; McInnes, C.; Wang, W.; Kraft, A.S.; Smith, C.D. Synthesis and evaluation of novel inhibitors of Pim-1 and Pim-2 protein kinases. *Journal of Medicinal Chemistry* **2009**, *52*, 74-86, doi:10.1021/jm800937p.

32. Dayam, R.; Aiello, F.; Deng, J.; Wu, Y.; Garofalo, A.; Chen, X.; Neamati, N. Discovery of small molecule integrin  $\alpha_v\beta_3$  antagonists as novel anticancer agents. *Journal of Medicinal Chemistry* **2006**, *49*, 4526-4534, doi:10.1021/jm051296s.
33. Theocharis, S.; Margeli, A.; Kouraklis, G. Peroxisome proliferator activated receptor-gamma ligands as potent antineoplastic agents. *Current Medicinal Chemistry - Anti-Cancer Agents* **2003**, *3*, 239-251, doi:10.2174/1568011033482431.
34. Murphy, G.J.; Holder, J.C. PPAR- $\gamma$  agonists: Therapeutic role in diabetes, inflammation and cancer. *Trends in Pharmacological Sciences* **2000**, *21*, 469-474, doi:10.1016/S0165-6147(00)01559-5.
35. Ottanà, R.; Maccari, R.; Barreca, M.L.; Bruno, G.; Rotondo, A.; Rossi, A.; Chiricosta, G.; Di Paola, R.; Sautebin, L.; Cuzzocrea, S., et al. 5-Arylidene-2-imino-4-thiazolidinones: Design and synthesis of novel anti-inflammatory agents. *Bioorganic & Medicinal Chemistry* **2005**, *13*, 4243-4252, doi:10.1016/j.bmc.2005.04.058.
36. Buzun, K.; Gornowicz, A.; Lesyk, R.; Bielawski, K.; Bielawska, A. Autophagy modulators in cancer therapy. *International Journal of Molecular Sciences* **2021**, *22*, 5804, doi:10.3390/ijms22115804.
37. Kim, R. Recent advances in understanding the cell death pathways activated by anticancer therapy. *Cancer* **2005**, *103*, 1551-1560, doi:10.1002/cncr.20947.
38. Polewska, J. Autophagy – molecular mechanism, apoptosis and cancer. *Postępy Higieny i Medycyny Doświadczalnej (Online)* **2012**, *66*, 921-936, doi:10.5604/17322693.1021109.
39. Dereń-Wagemann, I.; Kielbiński, M.; Kuliczkowski, K. Autophagy – process with two faces. *Acta Haematologica Polonica* **2013**, *44*, 383-391, doi:10.1016/j.achaem.2013.05.003.
40. Galluzzi, L.; Vitale, I.; Aaronson, S.A.; Abrams, J.M.; Adam, D.; Agostinis, P.; Alnemri, E.S.; Altucci, L.; Amelio, I.; Andrews, D.W., et al. Molecular mechanisms of cell death: recommendations of the Nomenclature Committee on Cell Death 2018. *Cell Death & Differentiation* **2018**, *25*, 486-541, doi:10.1038/s41418-017-0012-4.
41. Eskelinen, E.-L.; Saftig, P. Autophagy: A lysosomal degradation pathway with a central role in health and disease. *Biochimica et Biophysica Acta (BBA) - Molecular Cell Research* **2009**, *1793*, 664-673, doi:10.1016/j.bbamcr.2008.07.014.
42. Rabinowitz, J.D.; White, E. Autophagy and metabolism. *Science* **2010**, *330*, 1344-1348, doi:10.1126/science.1193497.

43. Andrade-Tomaz, M.; de Souza, I.; Rocha, C.R.R.; Gomes, L.R. The role of chaperone-mediated autophagy in cell cycle control and its implications in cancer. *Cells* **2020**, *9*, 2140, doi:10.3390/cells9092140.
44. Mizushima, N. Autophagy: Process and function. *Genes & Development* **2007**, *21*, 2861-2873, doi:10.1101/gad.1599207.
45. Kondo, Y.; Kanzawa, T.; Sawaya, R.; Kondo, S. The role of autophagy in cancer development and response to therapy. *Nature Reviews Cancer* **2005**, *5*, 726-734, doi:10.1038/nrc1692.
46. Mehrpour, M.; Esclatine, A.; Beau, I.; Codogno, P. Overview of macroautophagy regulation in mammalian cells. *Cell Research* **2010**, *20*, 748-762, doi:10.1038/cr.2010.82.
47. Yang, Y.; Klionsky, D.J. Autophagy and disease: Unanswered questions. *Cell Death & Differentiation* **2020**, *27*, 858-871, doi:10.1038/s41418-019-0480-9.
48. Birgisdottir, Á.B.; Lamark, T.; Johansen, T. The LIR motif – crucial for selective autophagy. *Journal of Cell Science* **2013**, *126*, 3237-3247, doi:10.1242/jcs.126128.
49. Zaffagnini, G.; Martens, S. Mechanisms of selective autophagy. *Journal of Molecular Biology* **2016**, *428*, 1714-1724, doi:10.1016/j.jmb.2016.02.004.
50. Rogov, V.V.; Stolz, A.; Ravichandran, A.C.; Rios-Szwed, D.O.; Suzuki, H.; Kniss, A.; Löhr, F.; Wakatsuki, S.; Dötsch, V.; Dikic, I., et al. Structural and functional analysis of the GABARAP interaction motif (GIM). *EMBO reports* **2018**, *19*, e47268, doi:10.15252/embr.201847268.
51. Noda, N.N.; Kumeta, H.; Nakatogawa, H.; Satoo, K.; Adachi, W.; Ishii, J.; Fujioka, Y.; Ohsumi, Y.; Inagaki, F. Structural basis of target recognition by Atg8/LC3 during selective autophagy. *Genes to Cells* **2008**, *13*, 1211-1218, doi:10.1111/j.1365-2443.2008.01238.x.
52. Li, W.; He, P.; Huang, Y.; Li, Y.-F.; Lu, J.; Li, M.; Kurihara, H.; Luo, Z.; Meng, T.; Onishi, M., et al. Selective autophagy of intracellular organelles: Recent research advances. *Theranostics* **2021**, *11*, 222-256, doi:10.7150/thno.49860.
53. Lei, Y.; Zhang, D.; Yu, J.; Dong, H.; Zhang, J.; Yang, S. Targeting autophagy in cancer stem cells as an anticancer therapy. *Cancer Letters* **2017**, *393*, 33-39, doi:10.1016/j.canlet.2017.02.012.
54. Guo, J.Y.; White, E. Autophagy, metabolism, and cancer. *Cold Spring Harbor Symposia on Quantitative Biology* **2016**, *81*, 73-78, doi:10.1101/sqb.2016.81.030981.

55. Menzies, F.M.; Fleming, A.; Caricasole, A.; Bento, C.F.; Andrews, S.P.; Ashkenazi, A.; Füllgrabe, J.; Jackson, A.; Jimenez Sanchez, M.; Karabiyik, C., et al. Autophagy and neurodegeneration: Pathogenic mechanisms and therapeutic opportunities. *Neuron* **2017**, *93*, 1015-1034, doi:10.1016/j.neuron.2017.01.022.
56. Plaza-Zabala, A.; Sierra-Torre, V.; Sierra, A. Autophagy and microglia: Novel partners in neurodegeneration and aging. *International Journal of Molecular Sciences* **2017**, *18*, 598, doi:10.3390/ijms18030598.
57. Wang, F.; Jia, J.; Rodrigues, B. Autophagy, metabolic disease, and pathogenesis of heart dysfunction. *Canadian Journal of Cardiology* **2017**, *33*, 850-859, doi:10.1016/j.cjca.2017.01.002.
58. Yim, W.W.-Y.; Mizushima, N. Lysosome biology in autophagy. *Cell Discovery* **2020**, *6*, 6, doi:10.1038/s41421-020-0141-7.
59. Sahu, R.; Kaushik, S.; Clement, C.C.; Cannizzo, E.S.; Scharf, B.; Follenzi, A.; Poticchio, I.; Nieves, E.; Cuervo, A.M.; Santambrogio, L. Microautophagy of cytosolic proteins by late endosomes. *Developmental Cell* **2011**, *20*, 131-139, doi:10.1016/j.devcel.2010.12.003.
60. Uytterhoeven, V.; Lauwers, E.; Maes, I.; Miskiewicz, K.; Melo, Manuel N.; Swerts, J.; Kuenen, S.; Wittoex, R.; Corthout, N.; Marrink, S.-J., et al. Hsc70-4 deforms membranes to promote synaptic protein turnover by endosomal microautophagy. *Neuron* **2015**, *88*, 735-748, doi:10.1016/j.neuron.2015.10.012.
61. Chauhan, A.S.; Kumar, M.; Chaudhary, S.; Dhiman, A.; Patidar, A.; Jakhar, P.; Jaswal, P.; Sharma, K.; Sheokand, N.; Malhotra, H., et al. Trafficking of a multifunctional protein by endosomal microautophagy: Linking two independent unconventional secretory pathways. *The FASEB Journal* **2019**, *33*, 5626-5640, doi:10.1096/fj.201802102R.
62. Liao, Z.; Wang, B.; Liu, W.; Xu, Q.; Hou, L.; Song, J.; Guo, Q.; Li, N. Dysfunction of chaperone-mediated autophagy in human diseases. *Molecular and Cellular Biochemistry* **2021**, 10.1007/s11010-020-04006-z, doi:10.1007/s11010-020-04006-z.
63. Kaushik, S.; Bandyopadhyay, U.; Sridhar, S.; Kiffin, R.; Martinez-Vicente, M.; Kon, M.; Orenstein, S.J.; Wong, E.; Cuervo, A.M. Chaperone-mediated autophagy at a glance. *Journal of Cell Science* **2011**, *124*, 495-499, doi:10.1242/jcs.073874.
64. Mizushima, N.; Levine, B. Autophagy in mammalian development and differentiation. *Nature Cell Biology* **2010**, *12*, 823-830, doi:10.1038/ncb0910-823.

65. Wu, W.K.K.; Coffelt, S.B.; Cho, C.H.; Wang, X.J.; Lee, C.W.; Chan, F.K.L.; Yu, J.; Sung, J.J.Y. The autophagic paradox in cancer therapy. *Oncogene* **2012**, *31*, 939-953, doi:10.1038/onc.2011.295.
66. Roy, S.; Debnath, J. Autophagy and tumorigenesis. *Seminars in Immunopathology* **2010**, *32*, 383-396, doi:10.1007/s00281-010-0213-0.
67. D'Arcy, M.S. Cell death: A review of the major forms of apoptosis, necrosis and autophagy. *Cell Biology International* **2019**, *43*, 582-592, doi:10.1002/cbin.11137.
68. Danial, N.N.; Korsmeyer, S.J. Cell Death: Critical control points. *Cell* **2004**, *116*, 205-219, doi:10.1016/S0092-8674(04)00046-7.
69. Wong, R.S.Y. Apoptosis in cancer: From pathogenesis to treatment. *Journal of Experimental & Clinical Cancer Research* **2011**, *30*, 87, doi:10.1186/1756-9966-30-87.
70. Jan, R.; Chaudhry, G.-E.S. Understanding apoptosis and apoptotic pathways targeted cancer therapeutics. *Advanced Pharmaceutical Bulletin* **2019**, *9*, 205-218, doi:10.15171/apb.2019.024.
71. O'Brien, M.A.; Kirby, R. Apoptosis: A review of pro-apoptotic and anti-apoptotic pathways and dysregulation in disease. *Journal of Veterinary Emergency and Critical Care* **2008**, *18*, 572-585, doi:10.1111/j.1476-4431.2008.00363.x.
72. Hanahan, D.; Weinberg, R.A. The hallmarks of cancer. *Cell* **2000**, *100*, 57-70, doi:10.1016/S0092-8674(00)81683-9.
73. Fulda, S. Targeting apoptosis for anticancer therapy. *Seminars in Cancer Biology* **2015**, *31*, 84-88, doi:10.1016/j.semcancer.2014.05.002.
74. Liang, W.; Cai, A.; Chen, G.; Xi, H.; Wu, X.; Cui, J.; Zhang, K.; Zhao, X.; Yu, J.; Wei, B., et al. Shikonin induces mitochondria-mediated apoptosis and enhances chemotherapeutic sensitivity of gastric cancer through reactive oxygen species. *Scientific Reports* **2016**, *6*, 38267, doi:10.1038/srep38267.
75. Menon, S.; Ks, S.D.; R, S.; S, R.; S, V.K. Selenium nanoparticles: A potent chemotherapeutic agent and an elucidation of its mechanism. *Colloids and Surfaces B: Biointerfaces* **2018**, *170*, 280-292, doi:10.1016/j.colsurfb.2018.06.006.
76. Chen, X.; Wu, Q.; Chen, Y.; Zhang, J.; Li, H.; Yang, Z.; Yang, Y.; Deng, Y.; Zhang, L.; Liu, B. Diosmetin induces apoptosis and enhances the chemotherapeutic efficacy of paclitaxel in non-small cell lung cancer cells via Nrf2 inhibition. *British Journal of Pharmacology* **2019**, *176*, 2079-2094, doi:10.1111/bph.14652.

77. Śliwiński, T.; Sitarek, P.; Skała, E.; M. S. Isca, V.; Synowiec, E.; Kowalczyk, T.; Bijak, M.; Rijo, P. Diterpenoids from *Plectranthus* spp. as potential chemotherapeutic agents via apoptosis. *Pharmaceuticals* **2020**, *13*, 123.
78. Velavan, B.; Divya, T.; Sureshkumar, A.; Sudhandiran, G. Nano-chemotherapeutic efficacy of (–)-epigallocatechin 3-gallate mediating apoptosis in A549 cells: Involvement of reactive oxygen species mediated Nrf2/Keap1 signaling. *Biochemical and Biophysical Research Communications* **2018**, *503*, 1723-1731, doi:10.1016/j.bbrc.2018.07.105.
79. Kedhari Sundaram, M.; Raina, R.; Afroze, N.; Bajbouj, K.; Hamad, M.; Haque, S.; Hussain, A. Quercetin modulates signaling pathways and induces apoptosis in cervical cancer cells. *Bioscience Reports* **2019**, *39*, doi:10.1042/bsr20190720.
80. Kotawong, K.; Chaijaroenkul, W.; Muhamad, P.; Na-Bangchang, K. Cytotoxic activities and effects of atractylodin and  $\beta$ -eudesmol on the cell cycle arrest and apoptosis on cholangiocarcinoma cell line. *Journal of Pharmacological Sciences* **2018**, *136*, 51-56, doi:10.1016/j.jphs.2017.09.033.
81. Yang, J.; Pi, C.; Wang, G. Inhibition of PI3K/Akt/mTOR pathway by apigenin induces apoptosis and autophagy in hepatocellular carcinoma cells. *Biomedicine & Pharmacotherapy* **2018**, *103*, 699-707, doi:10.1016/j.biopha.2018.04.072.
82. Bansal, S.; Bajaj, P.; Pandey, S.; Tandon, V. Topoisomerases: Resistance versus sensitivity, How far we can go? *Medicinal Research Reviews* **2017**, *37*, 404-438, doi:10.1002/med.21417.
83. Wang, J.C. Interaction between DNA and an *Escherichia coli* protein omega. *Journal of Molecular Biology* **1971**, *55*, 523-533, doi:10.1016/0022-2836(71)90334-2.
84. Buzun, K.; Bielawska, A.; Bielawski, K.; Gornowicz, A. DNA topoisomerases as molecular targets for anticancer drugs. *Journal of Enzyme Inhibition and Medicinal Chemistry* **2020**, *35*, 1781-1799, doi:10.1080/14756366.2020.1821676.
85. Mutschler, E.; Geisslinger, G.; Kroemer, H.K.; Menzel, S.; Ruth, P. 22.3. Inhibitory topoizomerazy. In *Farmakologia i toksykologia. 4th ed.*, Drożdżik, M., Kocić, I., Pawlak, D., Eds. MedPharm Polska: Wrocław, 2016; p. 880.
86. Schoeffler, A.J.; Berger, J.M. DNA topoisomerases: Harnessing and constraining energy to govern chromosome topology. *Quarterly Reviews of Biophysics* **2008**, *41*, 41-101, doi:10.1017/S003358350800468X.

87. Corbett, K.D.; Berger, J.M. Structure, molecular mechanisms, and evolutionary relationships in DNA topoisomerases. *Annual Review of Biophysics and Biomolecular Structure* **2004**, *33*, 95-118, doi:10.1146/annurev.biophys.33.110502.140357.
88. Capranico, G.; Binaschi, M.; Borgnetto, M.E.; Zunino, F.; Palumbo, M. A protein-mediated mechanism for the DNA sequence-specific action of topoisomerase II poisons. *Trends in Pharmacological Sciences* **1997**, *18*, 323-329, doi:10.1016/S0165-6147(97)01095-X.
89. Panchuk, R.; Chumak, V.; Fil, M.R.; Havrylyuk, D.; Zimenkovsky, B.S.; Lesyk, R.; Stoika, R.S. Study of molecular mechanisms of proapoptotic action of novel heterocyclic 4-thiazolidone derivatives. *Biopolymers & Cell* **2012**, *28*, 121-128, doi:10.7124/bc.00003D.
90. Subtel'na, I.; Atamanyuk, D.; Szymańska, E.; Kieć-Kononowicz, K.; Zimenkovsky, B.; Vasylenko, O.; Gzella, A.; Lesyk, R. Synthesis of 5-arylidene-2-amino-4-azolones and evaluation of their anticancer activity. *Bioorganic & Medicinal Chemistry* **2010**, *18*, 5090-5102, doi:10.1016/j.bmc.2010.05.073.
91. Antypenko, L.; S., G. Development and validation of UV-spectrophotometric determination of ciminalum in drug. *Recipe* **2017**, *20*, 153-160.
92. Lesyk, R.; Zimenkovsky, B.; Subtelna, I.; Nektgayev, I.; Kazmirchuk, G. Synthesis and antiinflammatory activity of some 2-arylamino-2-thiazoline-4-ones. *Acta Poloniae Pharmaceutica - Drug Research* **2003**, *60*, 457-466.
93. Kuruppu, A.I.; Paranagama, P.; Goonasekara, C.L. Medicinal plants commonly used against cancer in traditional medicine formulae in Sri Lanka. *Saudi Pharmaceutical Journal* **2019**, *27*, 565-573, doi:10.1016/j.jsps.2019.02.004.
94. Montecucco, A.; Zanetta, F.; Biamonti, G. Molecular mechanisms of etoposide. *EXCLI Journal* **2015**, *14*, 95-108, doi:10.17179/excli2015-561.
95. Clark, P.I.; Slevin, M.L. The Clinical Pharmacology of Etoposide and Teniposide. *Clinical Pharmacokinetics* **1987**, *12*, 223-252, doi:10.2165/00003088-198712040-00001.
96. Hande, K.R. Etoposide: four decades of development of a topoisomerase II inhibitor. *European Journal of Cancer* **1998**, *34*, 1514-1521, doi:10.1016/S0959-8049(98)00228-7.
97. Goldar, S.; Khaniani, M.S.; Derakhshan, S.M.; Baradaran, B. Molecular mechanisms of apoptosis and roles in cancer development and treatment. *Asian Pacific Journal of Cancer Prevention* **2015**, *16*, 2129-2144, doi:10.7314/apjcp.2015.16.6.2129.



98. Ly, J.D.; Grubb, D.R.; Lawen, A. The mitochondrial membrane potential ( $\Delta\psi_m$ ) in apoptosis; an update. *Apoptosis* **2003**, *8*, 115-128, doi:10.1023/A:1022945107762.
99. Gordy, C.; He, Y.-W. The crosstalk between autophagy and apoptosis: Where does this lead? *Protein & Cell* **2012**, *3*, 17-27, doi:10.1007/s13238-011-1127-x.
100. Mukhopadhyay, S.; Panda, P.K.; Sinha, N.; Das, D.N.; Bhutia, S.K. Autophagy and apoptosis: Where do they meet? *Apoptosis* **2014**, *19*, 555-566, doi:10.1007/s10495-014-0967-2.
101. Mariño, G.; Niso-Santano, M.; Baehrecke, E.H.; Kroemer, G. Self-consumption: The interplay of autophagy and apoptosis. *Nature Reviews Molecular Cell Biology* **2014**, *15*, 81-94, doi:10.1038/nrm3735.
102. Singh, S.S.; Vats, S.; Chia, A.Y.-Q.; Tan, T.Z.; Deng, S.; Ong, M.S.; Arfuso, F.; Yap, C.T.; Goh, B.C.; Sethi, G., et al. Dual role of autophagy in hallmarks of cancer. *Oncogene* **2018**, *37*, 1142-1158, doi:10.1038/s41388-017-0046-6.
103. Cooper, K.F. Till death do us part: The marriage of autophagy and apoptosis. *Oxidative Medicine and Cellular Longevity* **2018**, *2018*, 4701275, doi:10.1155/2018/4701275.
104. Yun, C.W.; Jeon, J.; Go, G.; Lee, J.H.; Lee, S.H. The dual role of autophagy in cancer development and a therapeutic strategy for cancer by targeting autophagy. *International Journal of Molecular Sciences* **2021**, *22*, 179.
105. Champoux, J.J. DNA topoisomerases: Structure, function, and mechanism. *Annual Review of Biochemistry* **2001**, *70*, 369-413, doi:10.1146/annurev.biochem.70.1.369.

## VII. Abstract

Modern cancer therapeutic strategies are largely based on cytostatic drugs, which target apoptosis induction and mitosis inhibition in cells through cell cycle disruptions. Unfortunately, low therapeutic index and poor drug selectivity, lead to a number of side effects.

The dynamic development of medicinal chemistry, molecular biology, and cancer genetics allow for the search and design of new, highly effective therapeutic strategies. Based on discoveries concerning intracellular signal transduction, designing new small-molecule drugs oriented on the inhibition of signaling pathways in a cancer cell is possible. Novel inhibitors of checkpoint regulatory proteins are increasingly used in anticancer drug research. Numerous scientific teams worldwide aim to develop new treatments for cancer and among the main goals increasing the effectiveness and reducing the toxicity can be distinguished. A particularly interesting group of compounds with potent anticancer properties are novel 4-thiazolidinone derivatives.

In the presented doctoral dissertation, 13 novel 4-thiazolidinone derivatives obtained by organic synthesis were examined for anticancer properties. The preliminary studies allowed to investigate the structure-activity relationship of the new compounds and to select the Les-3331 compound for further in-depth *in vitro* studies. This study aimed to determine the molecular mechanism of action of the compound against MCF-7 and MDA-MB-231 human breast cancer cell lines. The influence of Les-3331 on apoptosis induction, mitochondrial membrane potential changes, caspase-9, and caspase-8 activity, autophagy-related proteins, and topoisomerase II activity were studied. Furthermore, selected ADME-Tox parameters of a new 4-thiazolidinone derivative were evaluated. Etoposide was used as a reference compound.

Based on the obtained results, it may be concluded that novel 4-thiazolidinone derivatives demonstrate high cytotoxic and antiproliferative activity compared to the etoposide in tested cancer cell lines. The selected Les-3331 compound shows potent cytotoxicity and antiproliferative effect against MCF-7 and MDA-MB-231 cancer cells. Moreover, the compound showed lower toxicity against human skin fibroblasts compared with the tested cancer cell lines. The molecular mechanism of activity of Les-3331 is related to topoisomerase II inhibition. Les-3331 induces apoptosis in cancer cells through both the intrinsic and extrinsic pathways. Additionally, a novel 4-thiazolidinone derivative inhibits the autophagy process in MCF-7 and MDA-MB-231 cancer cells. Les-3331 is a metabolically stable compound and shows no risk of drug-drug interactions. Finally, Les-3331 is metabolized in the cell by degradation of the 2-thioxo-4-thiazolidinone ring.

## VIII. Streszczenie w języku polskim

Współczesne strategie terapeutyczne chorób nowotworowych oparte są w znacznej mierze na lekach cytostatycznych, których celem jest indukcja apoptozy oraz zahamowanie mitozy w komórkach nowotworowych poprzez zaburzenie cyklu komórkowego. Niestety, niski współczynnik terapeutyczny oraz niewielka selektywność leków, prowadzą do wystąpienia szeregu efektów ubocznych.

Dynamiczny rozwój chemii medycznej, biologii molekularnej oraz genetyki nowotworów pozwala na poszukiwanie i tworzenie nowych, wysoce skutecznych strategii terapeutycznych. W oparciu o odkrycia dotyczące wewnątrzkomórkowej transmisji sygnałów możliwe jest projektowanie nowych drobnocząsteczkowych leków, których zadaniem jest hamowanie szlaków sygnałowych w komórce nowotworowej. W badaniach nad lekami przeciwnowotworowymi coraz częściej stosuje się związki chemiczne będące inhibitorami białek regulujących punkty kontrolne. Celem pracy wielu zespołów naukowców na całym świecie jest opracowywanie nowych metod leczenia nowotworów a wśród głównych założeń jest zwiększenie skuteczności oraz zmniejszenie toksyczności leków przeciwnowotworowych. Szczególnie interesującą grupę związków o silnych właściwościach przeciwnowotworowych stanowią nowe pochodne 4-tiazolidynonu.

W ramach niniejszej rozprawy doktorskiej, 13 nowych pochodnych 4-tiazolidynonu otrzymanych na drodze syntezy organicznej przebadano pod kątem właściwości przeciwnowotworowych. Badania przesiewowe pozwoliły określić zależności struktura-aktywność nowych związków oraz wyselekcjonować cząsteczkę Les-3331 do dalszych, pogłębionych badań *in vitro*. Celem badań było poznanie molekularnego mechanizmu działania związku wobec komórek raka piersi linii MCF-7 i MDA-MB-231. Zbadano wpływ związku na indukcję procesu apoptozy, zmianę mitochondrialnego potencjału błonowego, aktywność kaspazy-9 i kaspazy-8, białka związane z procesem autofagii oraz aktywność topoizomerazy II. Ponadto, określono wybrane parametry ADME-Tox nowej pochodnej 4-tiazolidynonu. W badaniach biologicznych jako związek referencyjny zastosowano etopozyd.

Na podstawie otrzymanych wyników stwierdzono, że nowe pochodne 4-tiazolidynonu wykazują wysoką aktywność cytotoksyczną wobec wybranych linii komórek nowotworowych w porównaniu z etopozydem. Wyselekcjonowana cząsteczką – Les-3331 – wykazała silny efekt cytotoksyczny wobec komórek raka piersi linii MCF-7 i MDA-MB-231. Ponadto, związek ten charakteryzował się niską toksycznością wobec komórek prawidłowych – fibroblastów skóry ludzkiej, w porównaniu do badanych linii komórek nowotworowych. Wraz ze wzrostem

stężenia Les-3331 obserwowano także zwiększone hamowanie procesu wbudowywania [<sup>3</sup>H]-tymidyny do DNA komórek nowotworowych, co świadczy o właściwościach antyproliferacyjnych związku. Molekularny mechanizm przeciwnowotworowego działania Les-3331 związany jest z inhibicją topoizomerazy II. Les-3331 indukuje apoptozę w komórkach nowotworowych na drodze zewnątrzpochodnej i wewnątrzpochodnej. Co więcej, badania wykazały, że nowa pochodna hamuje proces autofagii w komórkach linii MCF-7 i MDA-MB-231. Les-3331 jest związkiem stabilnym metabolicznie i nie wykazuje ryzyka wystąpienia interakcji lek-lek w przypadku ewentualnego podania go z innymi lekami. Badany związek jest metabolizowany w komórce na drodze degradacji pierścienia 2-tiokso-4-tiazolidynowego.

## DNA topoisomerases as molecular targets for anticancer drugs

Kamila Buzun<sup>a</sup> , Anna Bielawska<sup>a</sup> , Krzysztof Bielawski<sup>b</sup>  and Agnieszka Gornowicz<sup>a</sup> 

<sup>a</sup>Department of Biotechnology, Medical University of Białystok, Białystok, Poland; <sup>b</sup>Department of Synthesis and Technology of Drugs, Medical University of Białystok, Białystok, Poland

### ABSTRACT

The significant role of topoisomerases in the control of DNA chain topology has been confirmed in numerous research conducted worldwide. The prevalence of these enzymes, as well as the key importance of topoisomerase in the proper functioning of cells, have made them the target of many scientific studies conducted all over the world. This article is a comprehensive review of knowledge about topoisomerases and their inhibitors collected over the years. Studies on the structure–activity relationship and molecular docking are one of the key elements driving drug development. In addition to information on molecular targets, this article contains details on the structure–activity relationship of described classes of compounds. Moreover, the work also includes details about the structure of the compounds that drive the mode of action of topoisomerase inhibitors. Finally, selected topoisomerase inhibitors at the stage of clinical trials and their potential application in the chemotherapy of various cancers are described.

### ARTICLE HISTORY

Received 7 July 2020  
Revised 1 September 2020  
Accepted 2 September 2020

### KEYWORDS

DNA topoisomerases;  
topoisomerase inhibitors;  
cancer; anticancer activity;  
anticancer drugs

### Introduction

In 1971 Jim Wang discovered first DNA topoisomerase I (the omega ( $\omega$ ) protein from *Escherichia coli*)<sup>1,2</sup>. At that time, the separation of the supercoiled and relaxed DNA was necessary to perform the activity test. To achieve this, the reaction products were run on a sucrose gradient and then the DNA contained in each fraction taken from the centrifugation tubes were collected and analysed<sup>2</sup>.

In 1975, for the first time, agarose gel electrophoresis was used to differentiate between various DNA topoisomers. The use of this method greatly facilitated work for DNA topologists<sup>3</sup>. For nearly 40 years, many topoisomerases have been discovered and characterised in all three domains of life (bacteria, eukarya and archaea). The first discovery, in 1976, was bacterial DNA gyrase<sup>4</sup> and then in 1980, eukaryotic decatenase was found<sup>5</sup>.

DNA topoisomerases are a group of enzymes that control DNA topology. They are involved in many significant biological processes in all cells (e.g. DNA replication, transcription and recombination or chromosome condensation)<sup>6</sup>. These enzymes bind covalently to the DNA phosphorus group, split the DNA strand or strands and finally reunite them. According to their mechanism of action, there are two main types of topoisomerases: topoisomerases I (Top I) and topoisomerases II (Top II) divided into five subfamilies (see Table 1).

The presence of topoisomerases and their proper functioning is one of the key elements of most processes taking place in the cell. For most of the processes requiring access to the information stored in the DNA duplex, a permanent or temporary separation of the two strands of DNA is necessary (e.g. topoisomerases enable the release of replicated chromosomes before partitioning and cell division)<sup>7</sup>.

The use of cytostatic agents, which inhibit enzyme activity, leads to irreversible interruption of DNA strands (by a stable DNA-

topoisomerase complex), which causes cell death. Increased topoisomerase activity observed in many cancers results in selective action of agents that are topoisomerase inhibitors<sup>8</sup>.



In the beginning, we would like to briefly describe the topoisomerases I and II and their mechanism of action. Then we will present and characterise the topoisomerases I and II inhibitors, in particular compounds in clinical trials.

### Type I topoisomerases

Primarily named  $\omega$  protein, topoisomerase I was discovered by James C. Wang in the 1970s. He identified the first topoisomerase I in *Escherichia coli*<sup>2</sup>. Proteins belonging to the group of topoisomerases I were found in eukaryotic and prokaryotic organisms<sup>9–12</sup>. These enzymes are responsible for relaxing negatively supercoiled DNA and allow for catenation or decatenation of broken DNA<sup>11,13</sup>.

Topoisomerases I can be divided into three subfamilies: topoisomerases IA, topoisomerases IB and topoisomerases IC<sup>14–16</sup>. For all subtypes of topoisomerases I, changing the DNA topology by breaking the phosphodiester bond between DNA strands is based on the same general mechanism. The phosphoryl group of DNA is attacked by tyrosyl group of topoisomerase I. This creates a covalent bond between the tyrosyl group and one side of the broken DNA. At the same time, the free hydroxylated strand is released and rotated. The hydroxyl end of the free strand of DNA attacks the formed phosphotyrosine bond, rebuilds the phosphodiester bond between the two strands and releases the topoisomerase to the next catalytic cycle<sup>1,17</sup>.

In most cases, change the topology of DNA by type I topoisomerases do not require external energy (e.g. ATP hydrolysis). Reverse gyrase is the only enzyme in topoisomerase I subfamily which needs energy from ATP hydrolysis to introduce positively supercoiled DNA. Now, one of the main challenges is to identify

**CONTACT** Kamila Buzun  [kamila.buzun@umb.edu.pl](mailto:kamila.buzun@umb.edu.pl)  Department of Biotechnology, Medical University of Białystok, Jana Kilinskiego 1, Białystok 15-089, Poland  
© 2020 The Author(s). Published by Informa UK Limited, trading as Taylor & Francis Group.  
This is an Open Access article distributed under the terms of the Creative Commons Attribution License (<http://creativecommons.org/licenses/by/4.0/>), which permits unrestricted use, distribution, and reproduction in any medium, provided the original work is properly cited.

**Table 1.** Types and subfamilies of topoisomerases

Type of topoisomerase	Subfamily	Subunit structure	Domains of life
I	IA	Monomer Heterodimer—reverse gyrase isolated from <i>Methanopyrus kandleri</i>	Bacteria, Archaea, Eukarya
	IB	Monomer	Eukarya and some viruses
	IC	Monomer	Archaea ( <i>Methanopyrus</i> genus)
II	IIA	Heterotetramer - prokaryotic Top IIA Homodimer - eukaryotic Top IIA	Eukarya, Bacteria
	IIB	Heterotetramer	Archaea, Bacteria

the way how energy stored in the DNA is converted into protein changes in the course of the reaction. Knowing this mechanism will help to fully understand not only type I topoisomerases but also other enzymes belonging to this class<sup>9</sup>.

### Type IA topoisomerases

Topoisomerases IA (Top IA) are a subfamily of enzymes found in all three domains of life (bacteria, archaea and eukarya). The sequence analysis has shown that all topoisomerases IA are monomeric enzymes (the exception—reverse gyrase isolated from *Methanopyrus kandleri*) composed of two main parts: a core (molecular weight around 67 kDa) with all the conserved domains, especially those creating the active site of the enzyme, and a carboxyl-terminal domain, very diverse in size and sequence<sup>9,10</sup>.

Type IA enzymes are responsible for relaxation only negative supercoils in DNA and a single-stranded region in DNA is required for their activity. The mechanism of action of the topoisomerases IA known as “enzyme-bridged strand passage” was defined based on structural, biochemical and biophysical studies. To change DNA topology type IA enzyme causes splitting of a single strand of DNA. The enzyme attaches tyrosine to the DNA 5'-phosphoryl group with a covalent bond. Released 3'-OH end remains attached Top IA and cannot freely rotate. This result in creating a gap that allows the transport of another DNA strand. After passing the transported segment through the gap, both ends of broken DNA are religated<sup>9,18,19</sup>.

Examples of enzymes belonging to the Top IA subfamily are bacterial topoisomerase I, bacterial topoisomerase III, eukaryotic topoisomerase III and reverse gyrase<sup>1,6,20</sup>.

### Type IB topoisomerases

Type IB topoisomerases (Top IB) are a subfamily of enzymes presented in eukaryotes, some viruses and bacteria but not in archaea<sup>9,12</sup>. As opposed to Top IA, topoisomerases IB can relax both negatively and positively supercoiled DNA with energy accumulated in DNA supercoils<sup>12</sup>. Type IB topoisomerases change DNA topology by “DNA rotation” based on the splitting of a single strand of DNA, covalent attachment of tyrosine to the 3'-phosphoryl group and release a free 5'-OH end. Temporary interruption of a single DNA strand enables the relaxation of supercoiled DNA by rotating the DNA molecule around the breakpoint. The reaction lasts until all torsional strain is removed and DNA is completely relaxed. Type IB enzymes do not require Mg<sup>2+</sup> ions or ATP for relaxation of positive or negative supercoils in DNA (Figure 1)<sup>9,21–23</sup>.

Structures of all topoisomerases IB include a highly conserved pentad of residues creating the active site (Tyr, Arg, Arg, Lys and His/Asn). The only difference in the structure of this region between eukaryotic/viral (Tyr, Arg, Arg, Lys, His) and bacterial type

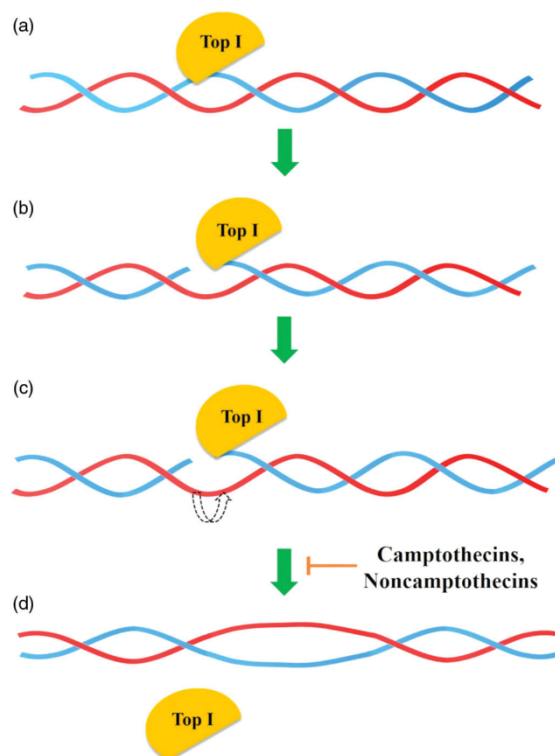


**Figure 1.** General mechanism of action of topoisomerase I (a) Top I binds to the DNA, (b) single-strand DNA (in blue) splitting, (c) controlled rotation of free DNA strand (in red), (d) religation of cleaved DNA strand.

IB enzymes (Tyr, Arg, Arg, Lys, Asn) is a replacement of histidine with asparagine in the bacterial pentad<sup>9</sup>.

The most important example of a type IB topoisomerases is the eukaryotic Top I (including human Top I), which is an important molecular target of anticancer therapies. In addition, Top IB group includes poxvirus topoisomerase and eubacterial Top IB<sup>6,9</sup>.

### Human topoisomerase I

Human topoisomerase I (hTop I) belongs to Top IB subfamily. It is a monomeric enzyme and its molecular weight is 91 kDa<sup>24</sup>. The enzyme consists of 765 amino acids which form four domains: an N-terminal domain, a linker domain, a core domain and a C-terminal domain<sup>25</sup>. The detailed hTop I architecture was determined by X-ray crystallography<sup>26</sup>. There is a correlation between hTop I expression level and cell sensitivity to Top I inhibitors. While in healthy cells lower hTop I expression level has been observed, rapidly dividing cancer cells are observed to express a higher level

of hTop I. Based on these results, we can assume that it is possible to target hTop I inhibitors towards cancer cells, tumours or patients with “overexpression” or increased expression of hTop I<sup>24</sup>.

### Type IC topoisomerases

Topoisomerase V (Top V) is a 110 kDa enzyme originally discovered in the archaeon *Methanopyrus kandleri*. So far, it is the only member of type IC topoisomerases subfamily<sup>27–29</sup>. Topoisomerase V is involved in DNA relaxation<sup>27</sup> and DNA repair<sup>30,31</sup>. Similar to type IB topoisomerases, Top V can relax negatively and positively supercoiled DNA and cleaves single strand of DNA<sup>13</sup>. However, structural analyses showed a novel fold in the crystal structure of topoisomerase V and probably a different location of an active site of tyrosine. This allows us to suppose that the mechanism of DNA relaxation by Top V is different than in the case of type IB topoisomerases<sup>29</sup>. Based on that, topoisomerase V was classified as a member of new topoisomerase I subfamily named type IC topoisomerases<sup>28,32</sup>.

Topoisomerase I inhibitors used in the treatment of many types of cancer include compounds belong to a various class. These compounds will be presented and discussed in a separate chapter titled “Inhibitors of type I topoisomerases”.

### Type II topoisomerases

Type II topoisomerases, divided into two subfamilies (topoisomerases IIA and topoisomerases IIB) are presented in various organisms. Topoisomerases IIA (Top IIA) occur in bacteria, eukaryote and also in few species of archaea, whereas topoisomerases IIB (Top IIB) are present mainly in archaea, plants and certain algae. Based on structural and phylogenetic analyses, significant differences in global architecture and biochemistry between Top IIA and Top IIB were found<sup>14,33</sup>.

General mechanism of changing the topology of DNA by topoisomerases II is based on cleaving both strands of DNA duplex with  $Mg^{2+}$  and energy from ATP hydrolysis. Topoisomerase II covalently attaches tyrosine to the 5' end of broken DNA, release a free 3' end and allows to passing a second DNA duplex (the transported or T-segment) through a gap (the gate or G-segment)<sup>1,33–35</sup>. All enzymes belong to this family can relax both positive and negative supercoils in DNA<sup>1</sup>.

Due to their exceptional ability to untangle double strands of DNA, Top II is involved in many crucial nuclear processes, e.g. transcription, replication or recombination<sup>36,37</sup>. The formation of double-stranded DNA breaks as a result of a loss of activity by Top II leads to cell death. Moreover, disruption of the proper functioning of the enzyme by increasing the level of DNA cleavage (both genetic and drug-induced) leads to e.g. translocations of DNA<sup>38</sup>.

### Type IIA topoisomerases

Type IIA topoisomerases subfamily includes eukaryotic Top II, bacterial DNA gyrase, human topoisomerase II and bacterial Top IV<sup>39</sup>. The sequences of all the enzymes belonging to the family of type IIA topoisomerases (Top IIA) show significant similarity, and the only differences are found in the quaternary structures of these proteins. Gyrase and topoisomerase IV (Top IV) belonging to type IIA bacterial topoisomerases are composed of two subunits: the ParE and ParC which are homologues of the GyrB and GyrA subunits of gyrase. In terms of structure, prokaryotic type IIA topoisomerases are referred to as heterotetramers in contrast to

eukaryotic enzymes which belong to the group of homodimers. The N-terminal half-ends of the eukaryotic Top IIA are homologues of the GyrB/ParE subunits of gyrase and Top IV, and the central parts of the enzymes are homologues of the GyrA/ParC subunits (gyrase/Top IV). The C-terminal half-ends, unlike the N-terminal parts of the eukaryotic topoisomerases type IIA, show significant structural differences between the enzymes of different eukaryotes. Analysis of C-terminal eukaryotic and prokaryotic type IIA topoisomerases did not show similarities in the sequence of these enzymes<sup>40</sup>.

Type IIA topoisomerases perform DNA double-strand cleavage based on the “two-gate” mechanism (Figure 2)<sup>41–43</sup>. Initially, Top IIA binds to the first DNA helix (G-segment), which will be cleaved in the further stage of the catalytic cycle. In the next step, the resulting Top IIA- G-segment complex binds to the second DNA helix (T-segment) which will be transported through the created gap. Two ATP molecules are attached to the Top IIA—G-segment—T-segment complex causing conformational changes in the enzyme. As a result of hydrolysis of one ATP molecule to ADP, in the presence of  $Mg^{2+}$  ions, tyrosine from both Top IIA monomers attacks the phosphodiester bond of the first DNA helix resulting in cleavage of the strand with a shift of 4-bp and becomes covalently attached to the 5' ends of the cleaved DNA (G-segment). Thanks to the transition, it is possible to transport the T-segment through a gap resulting after breaking the G-segment. Due to the hydrolysis of the second ATP molecule, the broken strands of the G-segment are religated. After passing through the gap, the T-segment is released. Then, due to the release of ADP molecules, the DNA-topoisomerase IIA complex is transformed from a closed into an open clamp, which is connected with the release of G-segment. Top IIA is free and ready for the next enzymatic reaction<sup>44–47</sup>.

### Human topoisomerase II

Human topoisomerase II (hTop II) is composed of four domains: two N-terminal domains, a core domain and C-terminal domain. There are two homodimeric isoforms of hTop II:  $\alpha$  (molecular weight around 170 kDa) and  $\beta$  (molecular weight around 180 kDa)<sup>48,49</sup>. Their amino acid sequences are homologous in approximately 70%<sup>50</sup>. Depending on the phases of the cell cycle, changes in human topoisomerase II $\alpha$  (hTop II $\alpha$ ) and human topoisomerase II $\beta$  (hTop II $\beta$ ) expression levels are observed. While the increased expression of hTop II $\alpha$  is mainly observed in proliferating cells (the peak of expression is observed in G<sub>2</sub>-M phases), in case of hTop II $\beta$  level of enzyme expression is constant regardless of the cell cycle stage<sup>51,52</sup>. hTop II $\alpha$  is crucial for cell survival due to its role in chromosome condensation and segregation processes whereas hTop II $\beta$  plays an important role in neurons development<sup>53,54</sup>.

### Type IIB topoisomerases

Commonly found in Archaea (except *Thermoplasma* spp.) type IIB topoisomerases were first discovered in the hyperthermophilic archaeon *Sulfolobus shibatae*<sup>55</sup>. The discovered enzyme was named topoisomerase VI (Top VI) and classified as a different subfamily of type II topoisomerases<sup>56</sup>. Like bacterial type IIA topoisomerases, Top VI is a heterotetramer enzyme composed of two subunits: A and B (A<sub>2</sub>B<sub>2</sub>). Structural and sequence analysis of type IIA and IIB topoisomerases did not reveal any similarities between the A subunits of both enzymes. The A subunit of Top VI shows similarity to eukaryotic Spo11 protein which is responsible for the initiation of meiotic DNA recombination as a result of the splitting

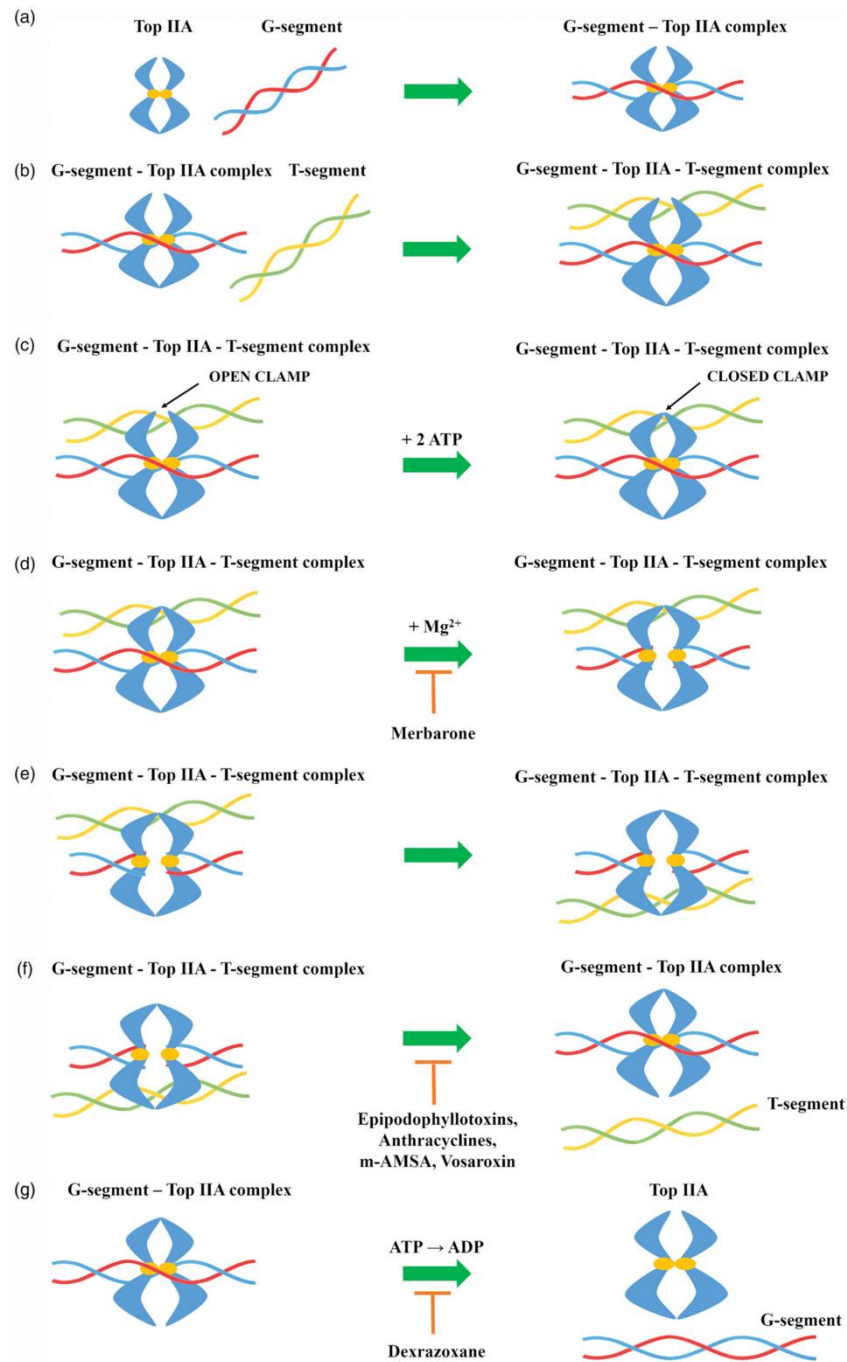


**Figure 2.** General mechanism of action of topoisomerase II (a) topoisomerase binds to the G-segment, (b) Top IIA- G-segment complex binds to T-segment, (c) Two ATP molecules are attached to the resulting complex, (d) G-segment cleavage in presence of  $Mg^{2+}$  ions, (e) T-segment transport through the created gap, (f) T-segment release and religation of G-segment broken strands and (g) hydrolysis of ATP molecules and release of the G-segment.

of double DNA helix<sup>57</sup>. The B subunit of type IIB topoisomerases, responsible for binding and hydrolysis of ATP molecules shows significant structural similarity and slight sequence similarity to the B subunit of Top IIA<sup>58</sup>.

Among Archaea topoisomerase VI causes relaxation of positively and negatively supercoiled DNA and is also involved in DNA replication and transcription. Initiated by the type IIB topoisomerases changes in DNA topology by the formation of breaks in



**Table 2.** Clinically relevant topoisomerases inhibitors

Drug	Class	Molecular target	Date and country of approval	Application
Topotecan	Camptothecins	Top IB	1996–U.S.A.	Treatment of metastatic ovarian cancer, relapsed platinum-SCLC, recurrent or persistent cervical cancer
Irinotecan	Epididophyllotoxins	Top IIA	1994–Japan	Treatment of colon cancer
Belotecan			2003–South Korea	Treatment of NSCLC and ovarian cancer
Etoposide			1983–U.S.A.	Treatment of SCLC, lymphomas (including non-Hodgkin's lymphomas), AML, testicular and ovarian cancer
Teniposide	Anthracyclines		1992–U.S.A.	Treatment of childhood ALL, glioma, central nervous system tumours and bladder cancer
Doxorubicin			1974–U.S.A.	Treatment of various types of cancer i.a. ovarian, lung, gastric and breast cancers, multiple myeloma, thyroid cancer, Hodgkin's and non-Hodgkin's lymphoma, paediatric cancers and sarcoma
Epirubicin			1999–U.S.A.	Mainly in the treatment of advanced breast cancer
Valrubicin			1998–U.S.A.	Intravesical treatment of patients with BCG-refractory carcinoma <i>in situ</i>
Mitoxantrone	Anthracenediones		1987–U.S.A.	Treatment of acute leukaemia, lymphoma, prostate and breast cancer
Amsacrine	Acridines		1983–Canada	Treatment patients with AML and refractory ALL

double-stranded DNA occurs with a shift of 2-bp rather than 4-bp as in type IIA topoisomerases<sup>57</sup>. Recently, topoisomerase VI has been identified in the plant kingdom<sup>55,56,59</sup>, including red and green algae<sup>60</sup>. Occurring in plants, Top VI plays an important role in the DNA endoreduplication process. Proper DNA endoreduplication is essential to maintain the correct size of plant cells and consequently the normal size of the entire plant<sup>61</sup>.

Scientific papers report the identification of new type IIB topoisomerase–topoisomerase VIII (Top VIII). It is the smallest known representative of type IIB subfamily of topoisomerases. The A and B subunits of this enzyme are merged into one single protein, hence the small size of Top VIII. Top VIII occurs in genomes of few bacteria species, two bacterial plasmids and one of the Archaea plasmids. In order to determine the structure and functions Top VIII, further detailed studies of this potential new type IIB topoisomerases subfamily member are necessary<sup>62</sup>.

### Topoisomerase inhibitors

Over the last few decades after discovering that doxorubicin induces DNA double helix cleavage via human topoisomerase II, scientific research based on searching of new compounds with an anticancer activity that are inhibitors of enzymes from the topoisomerases family has been intensified rapidly. To date, a significant number of topoisomerase inhibitors has been discovered and described in the scientific papers, however, in many cases, the detailed mechanism of action of these compounds is still unknown. Drugs classified as topoisomerase inhibitors can be divided into two groups: topoisomerase poisons or catalytic inhibitors. Doxorubicin, quinolones and many other anticancer or antibacterial drugs act as topoisomerases poisons. The mechanism of action of these compounds is based on the stabilisation of the formed enzyme–DNA covalent complex which prevents the religation of the cut strand<sup>63</sup>. The resulting DNA damages lead to cell death through apoptosis<sup>64</sup>. Catalytic inhibitors work by blocking the ability of the topoisomerase to attach to the substrate (DNA strand). Among this group there are two modes of action: the compound is binding to the DNA duplex or the topoisomerase. Regardless of the mode of action, catalytic inhibitors will lead to cell death through apoptosis<sup>65</sup>.

Tables 2 and 3 summarise information on important topoisomerase inhibitors and selected clinically investigated compounds, discussed in detail in this article.

### Inhibitors of type I topoisomerases

Mechanism of action of drugs classified as Top I inhibitors is based on the entrapment of created Top I–DNA covalent complex and prevents its cleavage<sup>66–68</sup>. This leads to permanent disruption of the DNA strands and consequently, to cell cycle arrest and induction of programmed cell death–apoptosis<sup>69,70</sup>.

### Camptothecins (CPTs)

In 1985, it was confirmed that topoisomerase I is the molecular target of camptothecin anticancer activity<sup>71,72</sup>. Isolated in 1966 by Wall et al. from the bark of *Camptotheca acuminata* tree, camptothecin is a pentacyclic ring structure<sup>73</sup>. Structure–activity relationship studies revealed that modifications at C-7, C-9 or C-10 positions at quinolone moiety (A and B rings on Figure 3) increase the anticancer activity of CPTs<sup>74</sup>. The E-ring, interacting with topoisomerase at three sites, is the most important part of the CPTs structure. The –OH group located at C-20 position forms a hydrogen bond with the Asp-533 side chain in the Top I polypeptide chain, and Arg-364 of Top I binds with two hydrogen bonds to the lactone part of the CPTs E-ring. Moreover, the D-ring, responsible for the stabilisation of the covalent Top I–DNA complex, is hydrogen-bonded with +1 cytosine of the uncleaved DNA chain. This H bond is located between the amino group of the +1 cytosine pyrimidine ring and the CPTs carbonyl group on the D-ring C-17 position<sup>75</sup>. The molecular mechanism of action of the drug is based on reversible induction of single-strand breakages which affects the cell replication capacity. Top I–DNA cleavable complex is stabilised by camptothecin but the resulting breaks are non-lethal to the cell due to their full reversibility. The single-stranded breaks are transformed into irreversible double-stranded breaks as a result of the cleavable complex collision with DNA replication fork. Caspase activation leads to cell death by apoptosis<sup>76,77</sup>. As a result of the inhibition of caspase activation, the cells are temporarily arrested in the G<sub>1</sub> cell cycle phase, which leads to necrosis<sup>78</sup>. S-phase-specific camptothecin shows its cytotoxic activity only when the DNA replication process is active. *In vitro* studies have

**Table 3.** Selected topoisomerase inhibitors under clinical investigation

Compound	Study purpose	Clinical trial status	Clinical trial identification number
Namitecan	Determination of the pharmacokinetic profile and dose finding of the compound in treatment of patients with solid tumours	Phase I completed	NCT01748019
CZ-48	Examination the safety of CZ-48 administered orally	Recruitment of patients for the phase I trial	NCT02575638
AR-67	Application of AR-67 in the treatment of patients with refractory or metastatic solid malignancies	Phase I completed	NCT00389480
	AR-67 application in the treatment of patients with recurrence of glioblastoma multiforme or gliosarcoma	Phase I completed	NCT01202370
		Unknown	NCT01124539
Gimatecan	Safety, tolerance and pharmacokinetics study of the compound in fallopian tube cancer, advanced ovarian epithelial cancer or primary peritoneal cancer	Recruitment of patients for the phase I trial	NCT04029909
Edotecarin	Evaluation the effectiveness of edotecarin with cisplatin in the treatment of advanced or metastatic solid tumours	Phase I completed	NCT00072332
	Determination of the effectiveness of treatment of women with chemoresistant locally advanced or metastatic breast cancer	Phase II completed	NCT00070031
LMP400	Application of the LMP400 and LMP776 in the treatment of adults with relapsed solid tumours and lymphomas	Phase I completed	NCT01051635
LMP776			
Genz-644282	Determination of the safety and tolerability of the compound	Phase I completed	NCT00942799
F14512	Evaluation of the maximum tolerated dose and the efficacy of combined therapy (F14512 and cytarabine) in patients ( $\geq 60$ years old) with AML	Phase II completed	2012-005241-20 (EudraCT number)
Amrubicin	Application of amrubicin plus pembrolizumab in the treatment of refractory SCLC	Phase II is ongoing	NCT03253068
	The use of amrubicin for the treatment of relapsed or refractory thymic malignancies	Phase II completed	NCT01364727
	Potent application of the amrubicin in the therapy of HER2-negative metastatic breast cancer	Phase I completed	NCT01033032
Amrubicin	The use of amrubicin in combination therapy with cyclophosphamide for the treatment of advanced solid organ malignancies	Phase I completed	NCT00890955
Aldoxorubicin	Aldoxorubicin application in the treatment of glioblastoma	Phase II completed	NCT02014844
	The use of aldoxorubicin in the therapy of soft tissue sarcomas	Phase III completed	NCT02049905
	Application of combination therapy (aldoxorubicin plus gemcitabine) in the treatment of metastatic solid tumours	Phase I completed	NCT02235688
	Determination of the safety and efficacy of the standard chemotherapy in combination with aldoxorubicin and other drugs compared to standard chemotherapy in patients with locally advanced or metastatic pancreatic cancer	Recruitment of patients for the phase I trial	NCT04390399
Vosaroxin	Application of vosaroxin with azacitidine in treating older patients with AML	Recruitment of patients for the phase II trial	NCT03338348
	The use of vosaroxin in the treatment of patients with myelodysplastic syndromes	Phase I is ongoing	NCT01913951
Vosaroxin	Evaluation of combination therapy (vosaroxin with infusional cytarabine) in therapy of untreated AML	Phase II is ongoing	NCT02658487

shown that S-phase cells are 100–1000 times more sensitive to camptothecin than G<sub>1</sub> or G<sub>2</sub> cells<sup>79</sup>. Selected camptothecin derivatives used in the cancers treatment and compounds in the clinical trials (Figure 4) are discussed below.

#### Clinically important CPTs

Topotecan (9-[(dimethylamino)methyl]-10-hydroxycamptothecin; Hycamtin®) is semisynthetic, water-soluble camptothecin (CPT) derivative and it was the first CPT derivative approved in 1996 by the US Food and Drug Administration (FDA) for clinical use<sup>80</sup>. The studies conducted by Staker et al. allowed to determine the detailed mechanism of antitopoisomerase activity of topotecan (Figure 4(a)). DNA and compound intercalation occurs at the Top I-mediated DNA splitting site and is stabilised by interactions between the topotecan and –1 (upstream) and +1 (downstream)

base pairs of DNA duplex. The rotation of the phosphodiester (OP) bond results in the formation of an intercalation binding pocket. The movement of phosphodiester OP towards the binding pocket simultaneously stimulates energetically the release of +1 and –1 base pairs, which in turn is necessary for OP rotation. The transported OP phosphodiester is stabilised in the binding pocket as a result of the interaction between the two hydrogen bonds and the nitrogens of the main chain Gly-363 and Arg-362<sup>81</sup>. The understanding of the exact method of topotecan intercalation to DNA made it possible to explain the mechanism by which this compound blocks religation of the DNA strand. As a result of binding the topotecan molecule with the DNA, the +1 (downstream) base pair is shifted by 3.6 Å and a 5'-OH of the splitted DNA strand is shifted from the phosphotyrosine by 8 Å. Due to the fact that the topotecan binding pocket is located inside the DNA substrate and, moreover, is formed after the first

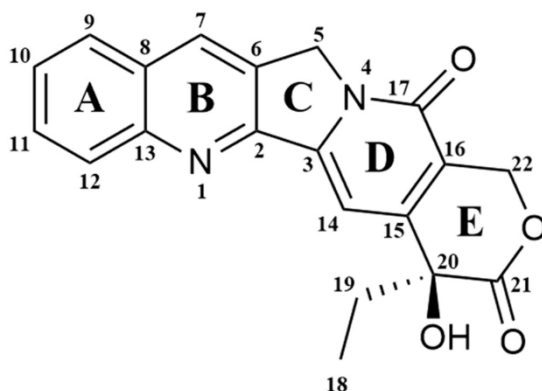


Figure 3. Chemical structure of camptothecin.

transesterification, it becomes understandable why camptothecin and its derivatives interact with the Top I-DNA complex and not with the enzyme itself<sup>82</sup>. Topotecan, a known topoisomerase I inhibitor, has a broad spectrum of anticancer applications. It is successfully used for the second-line treatment of metastatic ovarian cancer in over 70 countries and the treatment of relapsed platinum-sensitive small-cell lung cancer (SCLC) in more than 30 countries around the world<sup>83,84</sup>. In 2006, topotecan was approved by the FDA for use to the treatment of recurrent or persistent cervical cancer not susceptible to surgery and/or radiation therapy<sup>85</sup>.

Irinotecan (7-ethyl-10-[4-(1-piperidino)-1-piperidino]carbonyloxy-camptothecin; CPT-11) as topotecan is a water-soluble, semisynthetic camptothecin derivative (Figure 4(b)). It is a prodrug swiftly converted *in vivo* by human carboxylesterase 2 (hCE2) enzyme (occurs in liver, intestinal mucosa and plasma) to metabolite named SN-38 (7-ethyl-10-hydroxycamptothecin, Figure 4(c)) with high anticancer activity<sup>86</sup>. hCE2 converts CPT-11 into its active metabolite SN-38 by hydrolysis and the metabolite shows a more than 100 times higher *in vitro* cytotoxicity than the parent compound<sup>87</sup>. The ionic strength, pH and protein concentration all influence the rate of hydrolysis of CPT-11 to SN-38. Both irinotecan and SN-38 occur in two forms - lactone and carboxylate. The lactone form with a closed  $\alpha$ -hydroxy- $\delta$ -lactone ring is hydrolysed into a carboxylate form (open-ring hydroxyl acid). Based on the conducted research, it was found that the lactone form, whose antitumor activity is much more potent than the carboxylate form, is crucial for the stabilisation of the covalent Top I - DNA complex<sup>88</sup>. In liver, active SN-38 is metabolised into its inactive  $\beta$ -glucuronide form (SN-38G) by uridine-diphosphate glucuronosyltransferase (UGT)<sup>89</sup>. For the first time, irinotecan was approved in 1994 in Japan for the treatment of SCLC and non-small cell lung cancer (NSCLC), ovarian cancer and cervix cancer<sup>90</sup>. Marketed by Pfizer Inc. and known as Camptosar® it is used for the treatment of colorectal cancer<sup>91</sup>.

#### Promising active CPT derivatives

Belotecan (7-[2-(N-isopropylamino)ethyl]-(20S)-camptothecin; CKD-602, Camtobell®) is a relatively new, semisynthetic and water-soluble CPT derivative (Figure 4(d)). It was approved in 2003 in South Korea for the treatment of patients with NSCLC and ovarian cancer<sup>92</sup>. Belotecan exhibits similar efficacy profile compared to other CPT derivatives. However, its toxicity level is lower than the mentioned agents<sup>93</sup>. In 2018, Chong Kun Dang Pharmaceutical has completed the phase II clinical trial to evaluate the efficacy and safety of belotecan in comparison to topotecan in patients

with relapsed SCLC (NCT01497873). Furthermore, in 2019 Lee et al. conducted *in vitro* and *in vivo* studies on the effects of CKD-602 in selected cervical cancer cell lines (CaSki, HeLa and SiHa). In CaSki-xenografted nude mice treated with CKD-602, a significant reduction of tumour volume was observed<sup>94</sup>.

Namitecan (7-(2-aminoethoxy)iminomethyl-camptothecin; ST1968) is one of the CPT derivatives (Figure 4(e)). Novel topoisomerase I inhibitor was evaluated in several preclinical studies with various tumour models (including resistant to topotecan/irinotecan xenografts, paediatric tumour models and diversified squamous-cell tumour models) and a significant antitumor activity was observed<sup>95</sup>. The conducted studies allowed us to determine the safety and pharmacokinetic profile of the namitecan. Furthermore, during phase I of clinical trials (NCT01748019), the anticancer activity of ST1968 in patients with endometrium and bladder cancer was observed<sup>95,96</sup>.

CZ-48 (camptothecin-20(S)-O-propionate hydrate) is CPT prodrug synthesised by Cao *et al.* in 2009. Researchers examined the anticancer activity of CZ-48 (Figure 4(f)) against 21 human tumour xenografts. Obtained results showed an excellent activity of the tested compound against various cancers (i. a. bladder, breast, colon, melanoma, lung and pancreatic tumour lines). In the case of 19 from 21 tested tumour lines, notable growth inhibition (>50%) or regression was observed<sup>97</sup>. Great anticancer activity and reduced toxicity compared to irinotecan and topotecan resulted in rapid clinical development of CZ-48. Cao Pharmaceuticals Inc. is currently recruiting patients with a solid tumour or malignant lymphoma of extranodal and/or solid organ site for phase I clinical trial to examine the safety of CZ-48 administered orally (NCT02575638).

AR-67 (7-*tert*-butyldimethylsilyl-10-hydroxycamptothecin; formerly DB-67) is a lipophilic CPT analogue synthesised by Bom *et al.* in the 1990s (Figure 4(g)). The scientist has designed a novel compound to improve blood stability and activity of CPT analogues. The conducted studies have shown *in vitro* and *in vivo* anticancer activity of the compound via interaction with topoisomerase I as well as improved stability of AR-67 in blood compared to clinically relevant CPTs<sup>98</sup>. The information provided by Arno Therapeutics and the University of Kentucky shows that phase I of the clinical trials on the potential application of AR-67 in the treatment of patients with refractory or metastatic solid malignancies (NCT00389480 and NCT01202370) has been completed. Furthermore, in 2014 Arno Therapeutics posted information about active phase II trial of AR-67 in patients with recurrence of glioblastoma multiforme or gliosarcoma (NCT01124539) however, the current study status remains unknown.

Gimatecan (7-*tert*-butoxyiminomethyl-camptothecin; ST1481) is novel, semisynthetic and lipophilic CPT analogue with good oral bioavailability (Figure 4(h)). Based on the promising results of the preclinical study, gimatecan was selected for clinical development<sup>99</sup>. Rapid absorption, compound accumulation and prolonged distribution in cancer cells are associated with Top I activity inhibition and stabilisation of the Top I DNA-Top I-gimatecan complex<sup>100</sup>. High efficacy of administered orally gimatecan against a panel of subcutaneous human tumour xenograft models, metastatic and orthotopic tumour models was observed<sup>101</sup>. Lee's Pharmaceutical Limited is currently recruiting patients with fallopian tube cancer, advanced ovarian epithelial cancer or primary peritoneal cancer for phase I clinical trial to investigate the safety, tolerability and pharmacokinetics of gimatecan (NCT04029909).

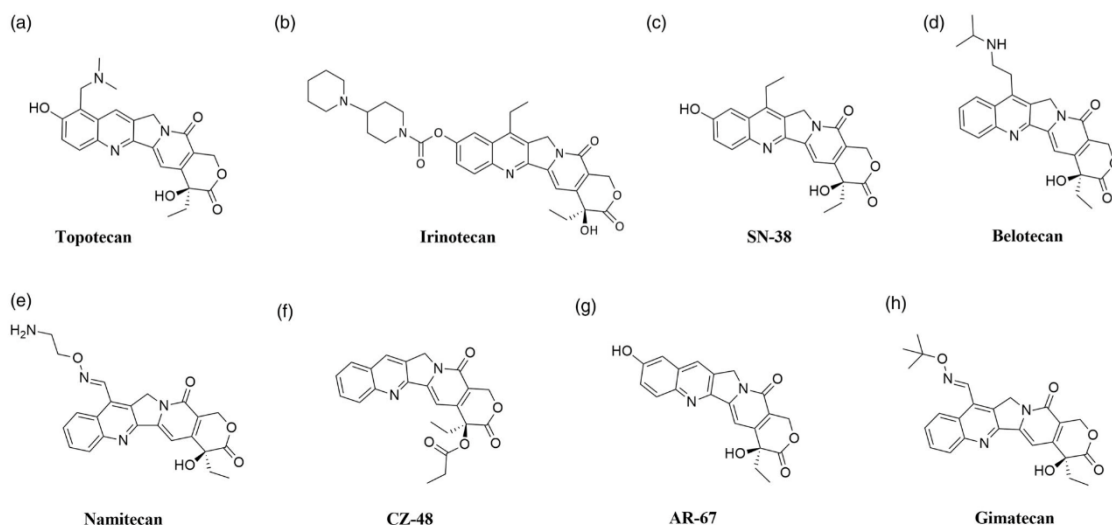


Figure 4. Chemical structures of camptothecins.

#### Noncamptothecins

Nowadays, the only group of Top I inhibitors used in the oncological treatment are camptothecins. The excellent effectiveness of these compounds is accompanied by strong side effects (e.g. diarrhoea or neutropenia) and instability<sup>6,20</sup>. As mentioned above, camptothecins are characterised by chemical instability—compounds are immediately inactivated in the blood to carboxylate. Furthermore, due to the rapid reversal of Top I-DNA covalent complexes after drug removal, long infusions are necessary to ensure the effectiveness of treatment<sup>102</sup>. Described restrictions on the use of camptothecins have prompted scientists to investigate new non-camptothecin Top I inhibitors (Figure 5)<sup>103,104</sup>. Currently, in the clinical trials, there are compounds from indenoisoquinolines<sup>105</sup>, indolocarbazoles<sup>106</sup> and dibenzonaphthyridinones<sup>107</sup> groups.

#### Promising active noncamptothecins

**Indolocarbazoles.** Edotecarin (6-*N*-(1-hydroxymethyl-2-hydroxy)ethylamino-12,13-dihydro-2,10-dihydroxy-13-( $\beta$ -D-glucopyranosyl)-5*H*-indolo[2,3-*a*]-pyrrolo[3,4-*c*]-carbazole-5,7(6*H*)-dione; J-107088) is a synthetic analogue of natural antibiotics isolated from several *Actinomycetes* (Figure 5(a)). It is a derivative of a compound named NB-506. Indolocarbazole NB-506 is an anticancer compound in which mechanism of antitumor activity is based on topoisomerase I or II poisoning. Edotecarin is a strong and specific topoisomerase I inhibitor, which is more effective in inducing single-strand DNA splitting compared to CPT or NB-506<sup>108</sup>. Furthermore, the stability of DNA-topoisomerase I covalent complexes formed as a result of edotecarin activity ensures longer effectiveness of the drug after the end of cell incubation with the compound<sup>106</sup>. Memorial Sloan Kettering Cancer Centre in collaboration with NCI conducted a phase I of clinical trials to evaluate the effectiveness of edotecarin combined with cisplatin in the treatment of patients with advanced or metastatic solid tumours (NCT00072332). In addition, the same collaborators completed phase II trial to study the effectiveness of treatment of women with chemoresistant locally advanced or metastatic breast cancer (NCT00070031).

**Indenoisoquinolines.** Indenoisoquinolines are developed in the 1990s by the NCI and represent a novel group of Top I inhibitors. These synthetic compounds are characterised by good chemical stability and better stabilisation of DNA–enzyme–drug covalent complexes than CPTs<sup>103,109</sup>. Among over 400 synthesised compounds, only two are currently under clinical trials: indotecan (LMP400; NSC 314622, Figure 5(b)) and indimitecan (LMP776; NSC 725776, Figure 5(c))<sup>110</sup>. Both compounds have been studied by scientists from the U.S. NCI in the treatment of adults with relapsed solid tumours and lymphomas (NCT01051635). Based on the information provided by the National Institutes of Health Clinical Centre, it is known that phase I of clinical trials has been completed<sup>111</sup>.

**Dibenzonaphthyridinones.** Next group of non-CPT topoisomerase I inhibitors are dibenzo[*c,h*][1,6]naphthyridinone derivatives. A novel group of compounds identified by LaVoie and his research team showed potent *in vitro* and *in vivo* anticancer activity<sup>112,113</sup>. Mechanism of topoisomerase inhibition by dibenzo[*c,h*][1,6]naphthyridinone derivatives is based on the stabilisation of cleavage DNA–Top I covalent complexes<sup>114–116</sup>.

Topovale (8,9-dimethoxy-5-(2-*N,N*-dimethylaminoethyl)-2,3-methylenedioxy-5*H*-dibenzo[*c,h*][1,6]naphthyridin-6-one; ARC-111) is a synthetic compound and strong Top I inhibitor (Figure 5(d)). The efficacy of topovale was evaluated against seven cancer cell lines and the obtained results showed higher cytotoxicity compared to the SN-38 or topotecan. Furthermore, the high effectiveness of this compound in cells which expressed the efflux pumps was observed<sup>14,107</sup>.

Next dibenzo[*c,h*][1,6]naphthyridinone derivative in clinical trials is Genz-644282 (8,9-dimethoxy-5-(2-*N*-methylaminoethyl)-2,3-methylenedioxy-5*H*-dibenzo[*c,h*][1,6]naphthyridin-6-one). The development of this drug was based on studies of structure-activity relationship in the family of dibenzo[*c,h*][1,6]naphthyridin-6-one compounds<sup>117</sup>. Studies conducted to determine the cytotoxicity of Genz-644282 (Figure 5(e)) using bone marrow cells and cancer cell colony-forming assays have shown favourable cytotoxicity profile of this compound. Furthermore, based on the results obtained from studies of Genz-644282 activity in xenograft models, similar or higher activity of the tested drug was observed compared to the standard drugs<sup>118</sup>. Furthermore, in 2014 the phase I of the clinical trial on safety and

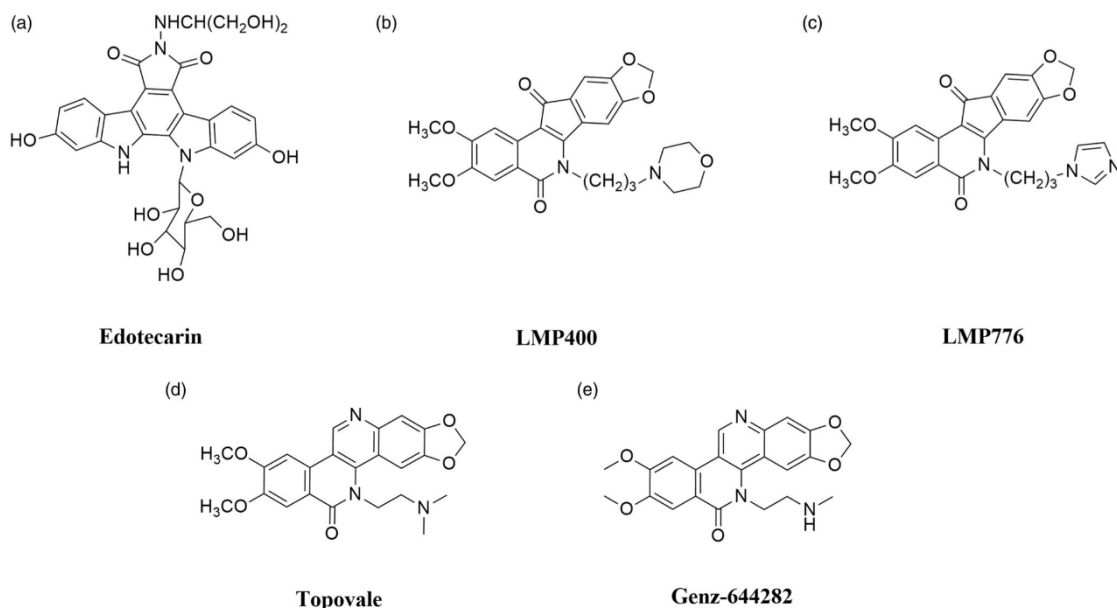


Figure 5. Chemical structures of noncamptothecins.

tolerability of the compound in the therapy of solid tumours was completed (NCT00942799).

#### Inhibitors of type II topoisomerases

The enzymes belonging to topoisomerases II family have the ability to achieve various conformational states as these proteins undergo significant structural changes during T-segment transport through the generated gate. In theory, trapping the enzyme in any conformational state allows manipulating of the topoisomerase II activity. To date, two types of Top II inhibitors have been identified and described: topoisomerase poisons and catalytic inhibitors<sup>119,120</sup>.

#### Topoisomerase poisons

Topoisomerase II poisons (Top II poisons) are the first from two types of Top II inhibitors. They cause inhibition of Top II ability to religation of cleaved DNA strands. Mechanism of action of Top II poisons is based on blocking of broken DNA ends rejoining as a result of slipping Top II poison molecules between splitted nitrogenous bases. This causes DNA double-strand breakage permanent by replicating broken DNA by cells. Moreover, replication of damaged DNA leads to the activation of the DNA damage response pathway and that in turn usually leads to cancer cell death through apoptotic pathway<sup>121–123</sup>.

**Epipodophyllotoxins.** For almost 2000 years, podophyllotoxins have been used in traditional medicine<sup>124</sup>. In the 19th century, podophyllin was identified as an effective drug used topically to treat skin cancers<sup>125</sup>. Despite the moderate anticancer properties of podophyllin and its derivatives selected in clinical trials, the high toxicity of tested drugs was observed<sup>126</sup>. As a result of research initiated in the 1950s by Sandoz Pharmaceuticals aimed at the synthesis of new derivatives with similar to podophyllin

anticancer activity but significantly lower toxicity, in 1966 etoposide and one year later teniposide were synthesised<sup>127</sup>. Both podophyllin derivatives show a negligible affinity for DNA in the absence of Top II. Based on many studies, scientists have unequivocally concluded that drug–enzyme interactions are crucial for the proper functioning of drugs, and also indirectly participate in the formation of the Top II–DNA–compound ternary complex<sup>128–130</sup>.

#### Clinically important epipodophyllotoxins

Etoposide ((8*a**R*,9*R*)-5-[(7,8-dihydroxy-2-methyl-4,4*a*,6,7,8,8*a*-hexahydro-pyrano[3,2-*d*][1,3]dioxin-6-yl)oxy]-9-(4-hydroxy-3,5-dimethoxyphenyl)-5*a*,6,8*a*,9-tetrahydro-5*H*-[2]benzofuro[6,5-*f*][1,3]benzodioxol-8-one; VP-16) is a semisynthetic podophyllotoxin derivative and clinically significant anticancer compound<sup>124,131</sup>. Discovered in 1966, VP-16 was approved by the FDA for cancer treatment in 1983<sup>132</sup>. The anticancer activity of etoposide is based on topoisomerase II poisoning by binding to the Top II–DNA covalent complexes<sup>133</sup>. This prevents religation of DNA strands, changing temporary DNA double-stranded breaks into permanent<sup>134</sup>, which indirectly leads to cell death by apoptosis. The combination of the results of the studies on the binary binding of the enzyme–drug complex, the research on DNA cleavage in the Top II–DNA–compound complex and NMR analysis made it possible to determine the functions of individual structures building the etoposide—the best-known epipodophyllotoxin. Presumably, the binding of etoposide (Figure 6) to Top II occurs through the interaction of the enzyme with the A- and B-ring of the compound, and also through the interaction between the enzyme and the E-ring of the compound. The –OH group and the methoxyl groups on the E-ring are an important element for the proper functioning of the drug. At the same time, both mentioned above groups do not significantly affect the specificity of DNA strands splitting or creating an enzyme–drug bond. The D-ring and the glycoside at position 4 of the C-ring probably interact with DNA found in the Top II–DNA–compound

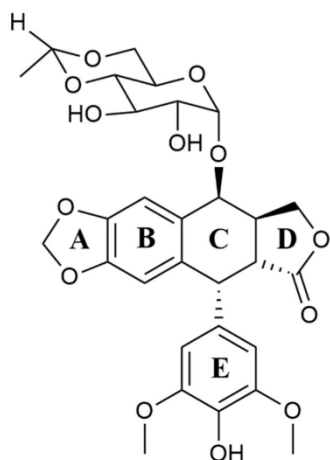


Figure 6. Chemical structure of etoposide.

ternary complex, affecting the specificity of DNA cleavage. Interestingly, both structures do not interact with the enzyme found in the binary enzyme-drug complex<sup>130,135</sup>. Removal of the glycoside group from the compound's structure does not significantly affect the etoposide-induced DNA cleavage process and substituting it with, for example, a spermine fragment (as in the case of the mentioned below compound - F14512) significantly increases the potency of the parent compound<sup>136</sup>. Etoposide is used for the treatment of SCLCs, lymphomas (including non-Hodgkin's lymphomas), acute myeloid leukaemia (AML), testicular and ovarian cancer.<sup>123,137,138</sup>

Teniposide ((5*S*,5*aR*,8*aR*,9*R*)-5-[[[(2*R*,4*aR*,6*R*,7*R*,8*R*,8*aS*)-7,8-dihydroxy-2-thiophen-2-yl-4,4*a*,6,7,8,8*a*-hexahydroprano[3,2-*d*][1,3]dioxin-6-yl]oxy]-9-(4-hydroxy-3,5-dimethoxyphenyl)-5*a*,6,8*a*,9-tetrahydro-5*H*-[2]benzofuro[6,5-*f*][1,3]benzodioxol-8-one; VM-26) is a second, semisynthetic derivative of podophyllotoxin and an analogue of etoposide (Figure 7(a)). Interestingly, VM-26 was discovered and tested in clinical trials before VP-16<sup>124,127</sup>. The mechanism of action of teniposide is similar to etoposide. It causes DNA double-stranded breaks via stabilisation of DNA-Topoisomerase II complexes<sup>139</sup>. Hypersensitivity reactions to teniposide in patients, as well as inappropriate administration of VM-26 using too low doses, caused slower development of the drug compared to etoposide. Consequently, teniposide was approved by the FDA in 1992, nearly 30 years after the first synthesis of the compound<sup>140</sup>. VM-26 is mainly used in the therapy of childhood acute lymphocytic leukaemia (ALL), glioma, central nervous system tumours and bladder cancer<sup>141,142</sup>.

#### Promising active epipodophyllotoxin derivatives

F14512 (*N*-[[[(5*S*,5*aS*,8*aR*,9*R*)-9-(4-hydroxy-3,5-dimethoxyphenyl)-8-oxo-5*a*,6,8*a*,9-tetrahydro-5*H*-[2]benzofuro[5,6-*f*][1,3]benzodioxol-5-yl]-2-[3-[4-(3-aminopropylamino)butylamino]propylamino]acetamide) is a novel etoposide derivative developed by Barret et al. The compound was designed by the replacement of VP-16 carbohydrate group with a polycation spermine moiety (Figure 7(b)). The modification of VP-16 structure resulted in a significant increase in compound solubility, cellular uptake, and cytotoxicity of F14512<sup>136</sup>. The presence of a spermine moiety in the compound molecule led to an increase in the degree of DNA binding and consequently to an enhancement of the inhibition of Top II activity<sup>143</sup>. Moreover, the overexpression of polyamine transport system observed in cancer

tumours was used to intensify selective drug uptake by cancer cells<sup>144,145</sup>. *In vitro* activity of F14512 was evaluated in 29 human cancer cell lines (i.a. leukaemia, sarcoma, myeloma, prostate, pancreatic and ovarian cancer cell lines) and noteworthy cytotoxicity in 21 cell lines was observed<sup>136</sup>. F14512 *in vivo* anticancer activity was investigated using 19 experimental models. In 13 out of 19 investigated models, F14512 exhibited a strong antineoplastic activity<sup>146</sup>. Furthermore, based on the information provided by the EU Clinical Trials Register, it is known that phase I-II study to evaluate the maximum tolerated dose and the efficacy of combined therapy of F14512 and cytarabine in patients ( $\geq 60$  years old) with AML has been completed (EudraCT number: 2012-005241-20).

**Anthracyclines.** Anthracyclines were isolated in the 1950s from *Streptomyces peucetius* which is one of the *Actinomyces* species. Obtained compounds showed antibacterial properties *in vitro*<sup>147</sup>. For over 50 years anthracyclines combined with various cytotoxic agents or targeted agents have been the most commonly used anticancer drugs to the treatment of solid or haematological tumours<sup>148,149</sup>. As topoisomerase poisons, anthracyclines stabilise DNA-topoisomerase II covalent complexes, which indirectly leads to apoptosis via double-stranded DNA breaks and inhibition of DNA transcription and replication processes<sup>150</sup>. A characteristic feature of all anthracycline derivatives is that the structures of individual compounds slightly differ from one another. These slight modifications cause significant changes in compounds activity. For instance, modification of the compound's structure by removing the 3-amino or 4-methoxy substituent significantly increases the activity of the compound. Moreover, the presence and nature of the substituent at position 3 of the sugar moiety is crucial for the selectivity of the anthracyclines DNA cleavage process<sup>151</sup>.

#### Clinically important anthracyclines

Doxorubicin ((7*S*,9*S*)-7-[[[(2*R*,4*S*,5*S*,6*S*)-4-amino-5-hydroxy-6-methyl-oxan-2-yl]oxy]-6,9,11-trihydroxy-9-(2-hydroxyacetyl)-4-methoxy-8,10-dihydro-7*H*-tetracene-5,12-dione; Adriamycin) is a chemotherapeutic drug which belongs to the anthracyclines group. It was first extracted in the 1970s from *Streptomyces peucetius* var. *caesius*<sup>152</sup>. The doxorubicin molecule is composed of sugar and aglycone moieties. The aglycone (doxorubicinone) consists of a tetracyclic ring linked to a hydroquinone and quinone residue, a short side-chain containing a primary alcohol at C-14 atom and a carbonyl group at C-13 position (Figure 8). The aminosugar (daunosamine) is linked by a glycosidic bond with the C-7 carbon located in the A-ring<sup>153</sup>. The molecular docking analyses enabled the researchers to identify the mechanism of interaction between the Top II-DNA complex and DOX. The obtained results showed that the planar DOX molecule is located between the GC base pairs of cleaved DNA strands. Three H bonds are formed between topoisomerase and DOX. The -OH group of Ser-740 Top II combines with the -OH group located in position C-11 in the anthraquinone fragment and Thr-744 forms a bond with DOX carbonyl oxygen located in position C-12. The last hydrogen bond is formed between the side chain Gln-750 and the C-14 atom of DOX<sup>154</sup>. A-ring and the DOX sugar moiety also interact with the DNA itself, forming H bonds between a base complement to the base at the -1 position in DNA and the -OH group in the C-9 position of the DOX A-ring. Scientists speculate that the interaction between C-9 of A-ring of DOX and DNA is crucial to stabilise the drug-molecular target complex. Proper recognition of DNA threads by compound may be associated with the formation of hydrogen bonds

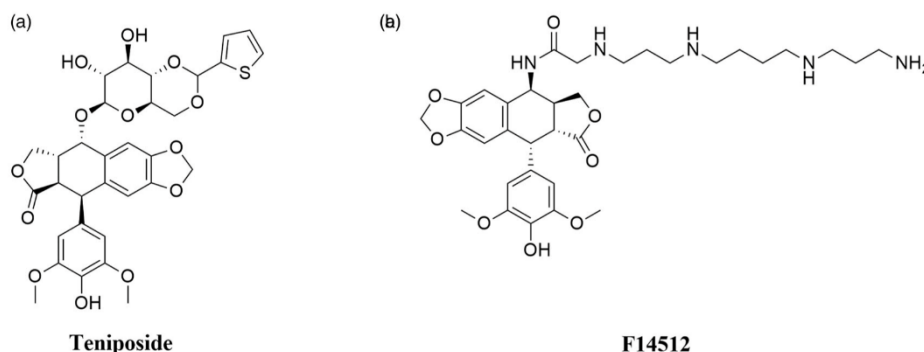


Figure 7. Chemical structures of epipodophyllotoxins.

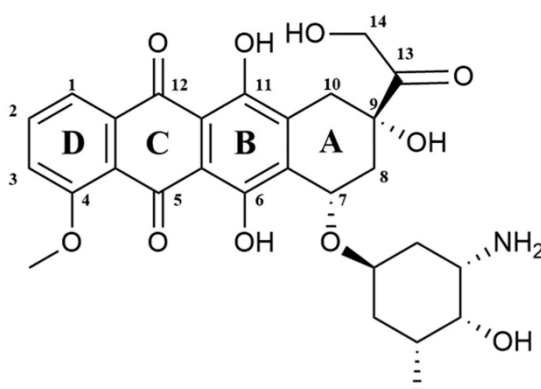


Figure 8. Chemical structures of doxorubicin.

between DNA and daunosamine moiety. G-2 and C-1 of DNA bond with the –OH group in position 4' and the amine group located in position 3' of daunosamine, respectively<sup>155</sup>. There are two main mechanisms of action of doxorubicin (DOX) which lead to the inhibition of the catalytic cycle. At the beginning of the catalytic cycle, doxorubicin can interfere with DNA binding which prevents relaxation or (de)catenation of DNA by Top II. Furthermore, DOX can prevent the religation of G-segment cleaved strands<sup>156</sup>. Despite its anticancer properties doxorubicin is responsible for serious side effect which is dose-dependent cardiotoxicity<sup>157,158</sup>. The exact mechanism of DOX cardiac toxicity is still unclear. However, the most probable pathway is related to the formation of iron-related free radicals<sup>159,160</sup>. Strong evidence, supporting this hypothesis is the fact that dexrazoxane, a known iron chelator, is used as a doxorubicin-induced cardiotoxicity protector<sup>152,161</sup>. Approved by FDA in 1974, it is used in the therapy of various types of cancer i.a. ovarian, lung, gastric and breast cancers, multiple myeloma, thyroid cancer, Hodgkin's and non-Hodgkin's lymphoma, paediatric cancers and sarcoma<sup>152,162</sup>.

Epirubicin ((7S,9S)-7-[(2R,4S,5R,6S)-4-amino-5-hydroxy-6-methoxy-2-yl]oxy-6,9,11-trihydroxy-9-(2-hydroxyacetyl)-4-methoxy-8,10-dihydro-7H-tetracene-5,12-dione; 4'-epidoxorubicin) is anthracycline derivative (Figure 9(a)), epimer of doxorubicin<sup>163</sup>. Epirubicin (EPI) shows activity in all phases of the cell cycle, but the highest activity is observed in the S and G<sub>2</sub> phases. The mechanism of action of EPI is similar to doxorubicin. The drug inhibits the topoisomerase II activity by stabilisation of DNA–topoisomerase II covalent complexes which prevent splitting of DNA strands<sup>164</sup>. In 1999 it

was approved for clinical use in the United States. The anticancer activity of EPI was confirmed against a broad spectrum of cancers but it is mainly used against advanced breast cancer<sup>165</sup>.

Valrubicin (N-trifluoroacetylauramycin-14-valerate; AD-32) is anthracycline derivative and Top II inhibitor obtained by modification of DOX (Figure 9(b)). Substitutions of two side chain of DOX resulted in the formation of a novel molecule with enhanced safety profile and lack skin toxicity, which allows the topical application of the compound<sup>166,167</sup>. The compound developed by Anthra Pharmaceuticals, Inc. (Valstar®) was approved by the FDA in 1998 for intravesical treatment of patients with BCG-refractory carcinoma *in situ*<sup>168</sup>. Currently ongoing clinical trials investigate the application of valrubicin i.a. in the treatment of early-stage bladder cancer (NCT00003129, phase II completed) and upper tract urothelial carcinoma (NCT01606345, phase I completed).

#### Promising active anthracycline derivatives

Amrubicin (9-amino-anthracycline; SM-5887) is a synthetic anthracycline derivative with potent antitumor activity based on the hTop II inhibition (Figure 9(c)). Cytotoxic activity of amrubicin results from the stabilisation of DNA–hTop II cleavable complexes<sup>169,170</sup>. Moreover, amrubicinol, an active amrubicin metabolite, is 5–220 times more cytotoxic than the original compound<sup>171</sup>. In Japan, amrubicin has been approved for the treatment of patients with NSCLC and SCLC<sup>172</sup>. Furthermore, it is used as a therapy option in the chemotherapy of NSCLC after the 3rd-line treatment<sup>170</sup>. Phase II of clinical trials for the use of amrubicin plus pembrolizumab in the treatment of refractory SCLC (NCT03253068) is currently ongoing. In addition, research concerning the use of amrubicin for the treatment of relapsed or refractory thymic malignancies (NCT01364727, phase II completed), HER2-negative metastatic breast cancer (NCT01033032, phase I completed) and in combination with cyclophosphamide for the treatment of advanced solid organ malignancies (NCT00890955, phase I completed) is being conducted.

Aldoxorubicin ((6-maleimidocaproyl)hydrazide of doxorubicin; formerly INNO-206) is doxorubicin prodrug developed by CytRx Corporation (Figure 9(d)). The aldoxorubicin (ALDOX) molecule consists of doxorubicin conjugated with a linker (6-maleimidocaproic acid hydrazide). After intravenous injection, ALDOX is quickly and selectively attached to cysteine-34, which belongs to the group of endogenous amino acids of serum albumin. After binding to albumin, DOX is transported to the tumour. The acidic tumour environment breaks the acid-labile hydrazine bond between the linker and the drug. The release of DOX, intercalation of the drug with DNA and inhibition of topoisomerase II activity

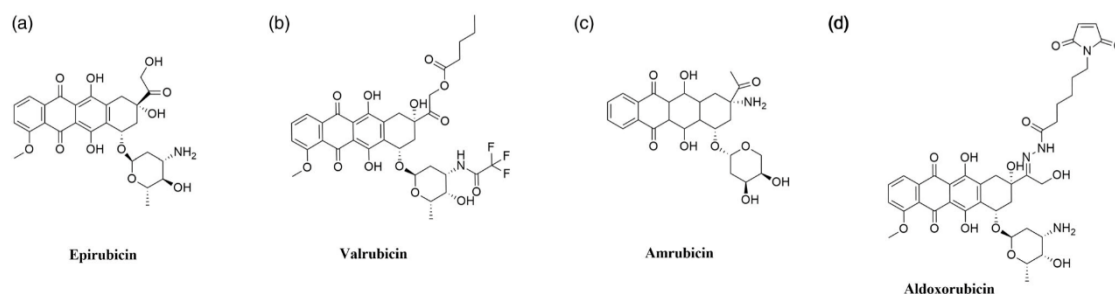


Figure 9. Chemical structure of anthracyclines.

occurs<sup>173,174</sup>. Preclinical studies performed on mouse xenograft tumour models of ovarian, breast, lung and pancreatic cancers have shown higher ALDOX anticancer activity compared to DOX<sup>175,176</sup>. Research conducted by Sanchez et al. demonstrated a significant *in vitro* and *in vivo* ALDOX activity against multiple myeloma cells. Moreover, an enhanced effect of combined ALDOX and bortezomib therapy of multiple myeloma compared to single-agent therapy (ALDOX or bortezomib alone) was observed<sup>177</sup>. Over the last years, numerous clinical trials on the use of ALDOX in the treatment of various cancers have been initiated. Research on the use of ALDOX in the treatment of glioblastoma (NCT02014844, phase II completed), soft tissue sarcomas (NCT02049905, phase III completed) as well as in combination with gemcitabine in the treatment of metastatic solid tumours (NCT02235688, phase I completed) is ongoing. Furthermore, in May 2020 ImmunityBio, Inc. reported the launch of a clinical trial to determine the safety and efficacy of the standard chemotherapy in combination with aldoxorubicin and other drugs compared to standard chemotherapy in patients with locally advanced or metastatic pancreatic cancer (NCT04390399).

**Anthracenediones.** Mitoxantrone (1,4-dihydroxy-5,8-bis[2-(2-hydroxyethylamino)ethylamino]anthracene-9,10-dione; MTX) is a synthetic chemotherapeutic agent belonging to the anthracenedione derivatives (Figure 10)<sup>178</sup>. It was discovered in the 1970s by two independent groups of investigators: the Medical Research Division of the American Cyanamid<sup>179</sup> and the Midwest Research Institute<sup>180</sup>. The search of new antineoplastic drugs began with a study of structure–activity relationships of new anthracenedione derivatives. Based on the obtained results, which revealed that the presence and composition of side-chains have a large impact on the activity of anthracenediones<sup>179,181</sup> MTX was selected for further studies as a potent anticancer compound<sup>182</sup>. Conducted in the 1990s, footprinting studies revealed that mitoxantrone-mediated DNA cleavage occurs at sites having a thymine or cytosine residue in close proximity. Additionally, the location of DNA cleavage is influenced by the presence of guanine located two nucleotides downstream—in the +2 position<sup>183</sup>. X-ray crystallographic analysis enable scientists to build the 3D model of Top II–DNA–MTX complex. A single drug molecule is introduced exactly at both sites of splitted DNA strands. The dihydroxyanthracenedione chromophore of the MTX molecule has a dual function—through intercalation, it docks the MTX molecule in the DNA duplex and allows direct contact between the additional hydrogen bonds and amino acid residues of the protein. Two hydroxyalkylamine side-chains of the MTX molecule “surround” nucleobases located *vis-a-vis* the DNA breakpoint. At the same time, such method of “surrounding” DNA allows interaction with closer amino acid residues of the protein, which are responsible

for further stabilisation of the complex<sup>184</sup>. The anticancer activity of MTX is based on inhibition of topoisomerase II activity by stabilisation of DNA-topoisomerase II covalent complex, which leads to DNA breakages. Splitting of DNA strands results in inhibition of two significant processes: replication of DNA and transcription of RNA<sup>185,186</sup>. MTX was approved by the FDA in 1987 and nowadays it is the only clinically approved drug from the anthracenedione derivatives group<sup>187</sup>. It is used as a chemotherapeutic drug in the treatment of acute leukaemia, lymphoma, prostate cancer and breast cancer<sup>188</sup>. Furthermore, MTX is used in the treatment of multiple sclerosis<sup>189</sup>.

**Acridines.** Amsacrine (*N*-[4-(acridin-9-ylamino)-3-methoxyphenyl]-methanesulfonamide; *m*-AMSA) is hTop II $\beta$  inhibitor belonging to the class of acridines. The amsacrine molecule is composed of two basic elements: the acridine group and the 4'-amino-methanesulfone-*m*-aniside head group (Figure 11). To determine the role of *m*-AMSA-mediated DNA binding in the proper functioning of the compound and to perform a comprehensive structure–activity relationship analysis, scientists analysed different amsacrine derivatives. The compounds were tested for their possibility of DNA intercalation and the ability to increase the intensity of the DNA strand cleavage process with the participation of hTop II $\alpha$  and hTop II $\beta$ . The obtained results indicate that the presence of the methoxy group in the 3' position (*m*-AMSA) has a positive effect on the anti-tumour activity of the drug. In turn, changing the location of the group by placing it in the 2' (*o*-AMSA) position causes inhibition of drug activity. It is probably caused by an increase in the freedom of rotation of the 4'-amino-methanesulfone-*m*-aniside group, which may disrupt, e.g. the intercalation process of the 1' substituent in the Top II–DNA–drug complex<sup>190</sup>. Moro et al. conducted modelling of *m*-AMSA interaction with the Top II–DNA complex. Based on the obtained results, it was found that the CG and GC base pairs of DNA, which form a clamp, are 3.4–6.8 Å away from each other. This arrangement of base pairs allows locating the drug molecule between them. The aniline sulfonamide in position 1' strongly binds with –OH Thr-744 group. The oxygen of Gly-747 carbonyl group and NH of sulfonamide residue form another strong bond. Moreover, hydrophobic interaction was observed between –CH<sub>3</sub> group in position 3' of aniline methoxyl substituent and side-chain Phe-754<sup>155</sup>. The drug was approved in 1983 in Canada<sup>25</sup> and to date is used for the treatment patients with AML and refractory ALL. The inhibitory effect of *m*-AMSA on hTop II $\beta$  activity is based on the topoisomerase poisoning and increasing level of DNA- hTop II $\beta$  covalent complexes in the cell<sup>190,191</sup>. Furthermore, few clinical trials are conducted to evaluate the effectiveness of combination therapy (*m*-AMSA with various compounds) in the treatment of several cancers (NCT03765541, NCT00003436, NCT00002719).



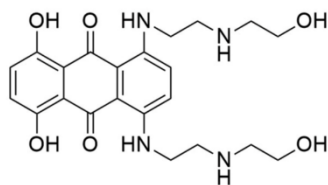


Figure 10. Chemical structure of mitoxantrone.

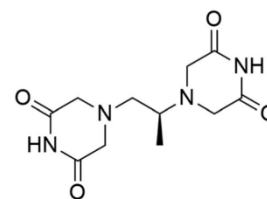


Figure 13. Chemical structure of dexrazoxane.

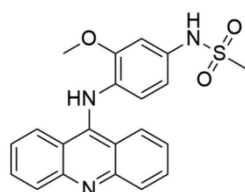


Figure 11. Chemical structure of amsacrine.

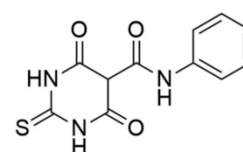


Figure 14. Chemical structure of merbarone.

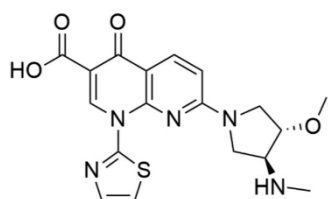


Figure 12. Chemical structure of vosaroxin.

**Quinolones.** Vosaroxin (7-[(3S,4S)-3-methoxy-4-(methylamino)pyrrolidin-1-yl]-4-oxo-1-(1,3-thiazol-2-yl)-1,8-naphthyridine-3-carboxylic acid; formerly AG-7532, SN-595 or voreloxin) was first described in 2002. It is a synthetic, antineoplastic quinolone derivative (Figure 12) developed by Sunesis Pharmaceuticals<sup>192,193</sup>. It is the first anticancer quinolone derivative and its antineoplastic mechanism of action is based on the topoisomerase II poisoning and induction of site-specific breaks in double-stranded DNA<sup>194</sup>. Currently, there are ongoing clinical studies concerning the application of vosaroxin with azacitidine in treating older patients with AML (NCT03338348, University of Ulm is recruiting participants for the phase II trial). Phase I trial in the treatment of patients with myelodysplastic syndromes (NCT01913951) is ongoing. Moreover, combination therapy (vosaroxin with infusional cytarabine) is evaluated in untreated AML therapy (NCT02658487, phase II trial is ongoing).

#### Catalytic inhibitors

Catalytic inhibitors are the second from two types of Top II inhibitors. Their mechanism of action is based on preventing the DNA-Top II A bond formation, stabilisation of DNA by the formation of non-covalent complexes with Top II A or blocking the ATPase enzyme binding site<sup>195-197</sup>.

**Bisdioxopiperazines.** Dexrazoxane (4-[[2(2S)-2-(3,5-dioxopiperazin-1-yl)propyl]piperazine-2,6-dione; ICRF-187) is an ethylenediaminetetraacetic acid (EDTA) derivative and belongs to the group of bisdioxopiperazine compounds<sup>161</sup>. To date, the ICRF-187 (Figure 13) is the only drug approved for the treatment of anthracycline-induced cardiotoxicity. Due to the fact that ICRF-187 is an EDTA derivative, the cardioprotective properties of this compound are attributed to its ability to chelate free iron and iron complexed by anthracyclines—this prevents the formation of cardiotoxic reactive oxygen species<sup>198,199</sup>. The bisdioxopiperazine derivative act by Top II arrestment in a specific point in the catalytic cycle<sup>200</sup>. The dexrazoxane mechanism of action consists of blocking DNA dependent hydrolysis of ATP by Top II which prevents the N-terminal clamp opening and consequently blocks the release of transported DNA segment<sup>201</sup>. The ICRF-187 molecule is comprised of two piperazinedione rings bounded by a monomethyl substituted ethanediyl linker. Interactions between the enzyme and the compound occur between the Top II “tyrosine –dome” and the two ICRF-187 piperazinedione rings. The “tyrosine dome” is located approximately parallel to the piperazinedione rings of ICRF-187. Each of the Gln-365 of the Top II protomer forms a hydrophobic bond with the hydrogen of the imide dexrazoxane moiety. Furthermore, the ICRF-187 methyl side-chain forms an additional hydrophobic  $\pi$ -methyl bond with Tyr-28 of one of the Top II protomers. Losing this hydrophobic interaction by removing the linker group, but also replacing it with a larger side-chain significantly reduces the compound's ability to inhibit Top II activity<sup>202,203</sup>.

**Thiobarbiturates.** Merbarone (5-[N-phenylcarboxamido]-2-thiobarbituric acid; NSC 336628), catalytic topoisomerase II inhibitor, is a thiobarbiturate analogue (Figure 14). In 1998 Fortune and Osheroff conducted biochemical studies and have classified the compound as a hTop II $\alpha$  catalytic inhibitor<sup>204</sup>. Moreover, in 2012 Pastor *et al.* carried out research on AA8 ovary fibroblast Chinese hamster cell line which showed that merbarone is not only a cytotoxic but also genotoxic compound. Besides, studies reported the induction of the endoreduplication process by compound<sup>205</sup>. The detailed mechanism of hTop II $\alpha$  inhibition remains still unknown

and although it is not approved as a therapeutic agent. In the hTop II $\alpha$ -DNA complex, Arg-804 and Tyr-805 are important elements that allow the transesterification reaction and splitting the DNA strand at the phosphate centre. The close proximity of the phosphorus atom of the DNA sugar-phosphate backbone and hydroxyl oxygen located in the Tyr-805 side-chain determines the hTop II $\alpha$  catalysed reaction. Merbarone, creating a hydrogen bond between the oxygen of the amide residue and Tyr-805 of the topoisomerase, increases the distance between the phosphorus in the DNA backbone and the hydroxyl oxygen of the Tyr-805 side-chain. Scientists presume that by increasing the distance between Tyr-805 and the hTop II $\alpha$  reaction site, merbarone prevents the 5'-phosphotyrosyl bond in the hTop II $\alpha$ -DNA complex<sup>206</sup>. Currently, the drug is used as a tool for studies on Top II<sup>191</sup>.

### Conclusions and perspectives

DNA replication, transcription and repair mechanisms are crucial processes occurring in each cell and topoisomerases are one of the key elements of these processes. Due to their significant biological functions, enzyme structure and mechanisms of action, these enzymes have been one of the main molecular targets in the design of new anticancer agents for nearly 30 years. Despite all the collected data about topoisomerases, there are still some elements that are unclear for us. Now, a phenomenon that poses a great challenge to scientists around the world is the developing resistance to anti-topoisomerase drugs. The main challenge is to maintain topoisomerase sensitivity to drugs, e.g. by designing new enzymes or new drug delivery systems. Furthermore, studies on structure-activity relationship or molecular docking play an important role in the drug development process. The application of computational techniques or the use of special programs to study the interactions between individual structures enables scientists to identify the key elements of the compound structure responsible for their activity. Thanks to this it is possible to modify the structures of known compounds to improve their properties or to design and synthesise new derivatives based on computer simulation results. Development of new anti-topoisomerase drugs, e.g. may allow to limit the cardiotoxic effect of anthracyclines or reduce the incidence of drug-induced secondary cancers. After all, the growing importance and rapid development of molecular genetics and molecular biology may enable the use of anti-topoisomerase agents in personalised anticancer therapy.

### Disclosure statement

No potential conflict of interest was reported by the author(s).

### Funding

This work was financed from the European Union funds [project № POWR.03.02.00-00-I051/16-00] under grant [Grant № 02/IMSD/G/2019].

### ORCID

Kamila Buzun  <https://orcid.org/0000-0002-5030-2862>  
 Anna Bielawska  <https://orcid.org/0000-0001-9164-8440>  
 Krzysztof Bielawski  <https://orcid.org/0000-0003-3187-4205>  
 Agnieszka Gornowicz  <https://orcid.org/0000-0002-0945-7870>

### References

1. Forterre P, Gribaldo S, Gabelle D, Serre MC. Origin and evolution of DNA topoisomerases. *Biochimie* 2007;89:427-46.
2. Wang JC. Interaction between DNA and an *Escherichia coli* protein omega. *J Mol Biol* 1971;55:523-33.
3. Keller W. Determination of the number of superhelical turns in simian virus 40 DNA by gel electrophoresis. *Proc Natl Acad Sci USA* 1975;72:4876-80.
4. Gellert M, Mizuuchi K, O'Dea MH, Nash HA. DNA gyrase: an enzyme that introduces superhelical turns into DNA. *Proc Natl Acad Sci USA* 1976;73:3872-6.
5. Baldi MI, Benedetti P, Mattocchia E, Tocchini-Valentini GP. In vitro catenation and decatenation of DNA and a novel eucaryotic ATP-dependent topoisomerase. *Cell* 1980;20:461-7.
6. Bansal S, Bajaj P, Pandey S, Tandon V. Topoisomerases: resistance versus sensitivity, how far we can go? *Med Res Rev* 2017;37:404-38.
7. Champoux JJ. DNA topoisomerases: structure, function, and mechanism. *Annu Rev Biochem* 2001;70:369-413.
8. E. Mutschler G, Geisslinger HK, Kroemer S, Menzel PR, 22.3. Inhibitory topozomerazy. In: Drożdżik M, Kocić I, Pawlak D, editors. *Farmakologia i toksykologia*. 4th ed. Wrocław: MedPharm Polska; 2016. p. 880.
9. Baker NM, Rajan R, Mondragón A. Structural studies of type I topoisomerases. *Nucleic Acids Res* 2009;37:693-701.
10. Viard T, de la Tour CB. Type IA topoisomerases: a simple puzzle?. *Biochimie* 2007;89:456-67.
11. Nagaraja V, Godbole AA, Henderson SR, Maxwell A. DNA topoisomerase I and DNA gyrase as targets for TB therapy. *Drug Discov Today* 2017;22:510-8.
12. Capranico G, Marinello J, Chillemi G. Type I DNA topoisomerases. *J Med Chem* 2017;60:2169-92.
13. Bush NG, Evans-Roberts K, Maxwell A. DNA topoisomerases. *EcoSal Plus* 2015;6.
14. Pommier Y. DNA topoisomerases and cancer. New York: Springer New York; 2012.
15. Kirkegaard K, Wang JC. Bacterial DNA topoisomerase I can relax positively supercoiled DNA containing a single-stranded loop. *J. Mol. Biol* 1985;185:625-37.
16. DiGate RJ, Mariani KJ. Identification of a potent decatenating enzyme from *Escherichia coli*. *J Biol Chem* 1988;263:13366-73.
17. Jain C, Majumder H, Roychoudhury S. Natural compounds as anticancer agents targeting DNA topoisomerases. *Curr Genomics* 2017;18:75-92.
18. Viard T, Cossard R, Duguet M, Bouthier De La Tour C. *Thermotoga maritima*-*Escherichia coli* chimeric topoisomerases. Answers about involvement of the carboxyl-terminal domain in DNA topoisomerase I-mediated catalysis. *J Biol Chem* 2004;279:30073-80.
19. Dekker NH, Rybenkov VV, Duguet M, et al. The mechanism of type IA topoisomerases. *Proc Natl Acad Sci USA* 2002;99:12126-31.
20. Delgado JL, Hsieh C-M, Chan N-L, Hiasa H. Topoisomerases as anticancer targets. *Biochem J* 2018;475:373-98.
21. Redinbo MR, Champoux JJ, Hol WG. Structural insights into the function of type IB topoisomerases. *Curr Opin Struct Biol* 1999;9:29-36.
22. Koster DA, Croquette V, Dekker C, et al. Friction and torque govern the relaxation of DNA supercoils by eukaryotic topoisomerase IB. *Nature* 2005;434:671-4.

23. Krogh BO, Shuman S. Catalytic mechanism of DNA topoisomerase IB. *Mol Cell* 2000;5:1035–41.
24. Cinelli MA. Topoisomerase 1B poisons: Over a half-century of drug leads, clinical candidates, and serendipitous discoveries. *Med Res Rev* 2019;39:1294–337.
25. Hevener KE, Verstak TA, Lutat KE, et al. Recent developments in topoisomerase-targeted cancer chemotherapy. *Acta Pharm Sin B* 2018;8:844–61.
26. Redinbo MR, Stewart L, Kuhn P, et al. Crystal structures of human topoisomerase I in covalent and noncovalent complexes with DNA. *Science* 1998;279:1504–13.
27. Slesarev AI, Stetter KO, Lake JA, et al. DNA topoisomerase V is a relative of eukaryotic topoisomerase I from a hyperthermophilic prokaryote. *Nature* 1993;364:735–7.
28. Taneja B, Schnurr B, Slesarev A, et al. Topoisomerase V relaxes supercoiled DNA by a constrained swiveling mechanism. *Proc Natl Acad Sci USA* 2007;104:14670–5.
29. Taneja B, Patel A, Slesarev A, Mondragón A. Structure of the N-terminal fragment of topoisomerase V reveals a new family of topoisomerases. *Embo J* 2006;25:398–408.
30. Belova GI, Prasad R, Kozyavkin SA, et al. A type IB topoisomerase with DNA repair activities. *Proc Natl Acad Sci USA* 2001;98:6015–20.
31. Belova GI, Prasad R, Nazimov IV, et al. The domain organization and properties of individual domains of DNA topoisomerase V, a type IB topoisomerase with DNA repair activities. *J Biol Chem* 2002;277:4959–65.
32. Rajan R, Taneja B, Mondragón A. Structures of minimal catalytic fragments of topoisomerase V reveals conformational changes relevant for DNA binding. *Structure* 2010;18:829–38.
33. Schoeffler AJ, Berger JM. DNA topoisomerases: harnessing and constraining energy to govern chromosome topology. *Q Rev Biophys* 2008;41:41–101.
34. Corbett KD, Berger JM. Structure, molecular mechanisms, and evolutionary relationships in DNA topoisomerases. *Annu Rev Biophys Biomol Struct* 2004;33:95–118.
35. Zechiedrich EL, Christiansen K, Andersen AH, et al. Double-stranded DNA cleavage/religation reaction of eukaryotic topoisomerase II: evidence for a nicked DNA intermediate. *Biochemistry* 1989;28:6229–36.
36. McClendon AK, Osheroff N. DNA topoisomerase II, genotoxicity, and cancer. *Mutat Res* 2007;623:83–97.
37. Deweese JE, Osheroff N. Coordinating the two protomer active sites of human topoisomerase IIalpha: nicks as topoisomerase II poisons. *Biochemistry* 2009;48:1439–41.
38. Deweese JE, Osheroff N. The DNA cleavage reaction of topoisomerase II: wolf in sheep's clothing. *Nucleic Acids Res* 2009;37:738–48.
39. Chang CC, Wang YR, Chen SF, et al. New insights into DNA-binding by type IIA topoisomerases. *Curr Opin Struct Biol* 2013;23:125–33.
40. Gadelle D, Filée J, Buhler C, Forterre P. Phylogenomics of type II DNA topoisomerases. *BioEssays* 2003;25:232–42.
41. Roca J, Wang JC. DNA transport by a type II DNA topoisomerase: evidence in favor of a two-gate mechanism. *Cell* 1994;77:609–16.
42. Lima CD, Mondragón A. Mechanism of type II DNA topoisomerases: a tale of two gates. *Structure* 1994;2:559–60.
43. Berger JM, Gamblin SJ, Harrison SC, Wang JC. Structure and mechanism of DNA topoisomerase II. *Nature* 1996;379:225–32.
44. Schmidt BH, Burgin AB, Deweese JE, et al. A novel and unified two-metal mechanism for DNA cleavage by type II and IA topoisomerases. *Nature* 2010;465:641–4.
45. Laponogov I, Pan XS, Veselkov DA, et al. Structural basis of gate-DNA breakage and resealing by type II topoisomerases. *PLoS One* 2010;5: 1–8.
46. Osheroff N. Eukaryotic topoisomerase II. Characterization of enzyme turnover. *J Biol Chem* 1986;261:9944–50.
47. Pommier Y, Leo E, Zhang H, Marchand C. DNA topoisomerases and their poisoning by anticancer and antibacterial drugs. *Chem Biol* 2010;17:421–33.
48. Kellner U, Sehested M, Jensen PB, et al. Culprit and victim - DNA topoisomerase II. *Lancet Oncol* 2002;3:235–43.
49. Nitiss JL. DNA topoisomerase II and its growing repertoire of biological functions. *Nat Rev Cancer* 2009;9:327–37.
50. Kaur P, Kaur V, Kaur S. DNA Topoisomerase II: promising target for anticancer drugs. In: Gandhi V, Grover R, Pathak SAB, editor. *Multi-targeted approach to treatment of cancer*. Springer International Publishing; 2015:323–38.
51. Lepiarczyk M, Bielawska A, Sosnowska K, Bielawski K. Ludzka topoisomeraza typu II jako molekularny punkt uchwytu leków przeciwnowotworowych. *Gaz Farm* 2011;20:24–6.
52. Linka RM, Porter ACG, Volkov A, et al. C-Terminal regions of topoisomerase IIalpha and IIbeta determine isoform-specific functioning of the enzymes in vivo. *Nucleic Acids Res* 2007;35:3810–22.
53. Farr CJ, Antoniou-Kourouniotti M, Mimmack ML, et al. The  $\alpha$  isoform of topoisomerase II is required for hypercompaction of mitotic chromosomes in human cells. *Nucleic Acids Res* 2014;42:4414–26.
54. Tiwari VK, Burger L, Nikolettou V, et al. Target genes of topoisomerase II $\beta$  regulate neuronal survival and are defined by their chromatin state. *Proc Natl Acad Sci USA* 2012;109:934–43.
55. Bergerat A, Gadelle D, Forterre P. Purification of a DNA topoisomerase II from the hyperthermophilic archaeon *Sulfolobus shibatae*. A thermostable enzyme with both bacterial and eucaryal features. *J Biol Chem* 1994;269:27663–9.
56. Bergerat A, De Massy B, Gadelle D, et al. An atypical topoisomerase II from archaea with implications for meiotic recombination. *Nature* 1997;386:414–7.
57. Buhler C, Lebbink JHG, Bocs C, et al. DNA Topoisomerase VI generates ATP-dependent double-strand breaks with two-nucleotide overhangs. *J Biol Chem* 2001;276:37215–22.
58. Corbett KD, Berger JM. Structure of the topoisomerase VI-B subunit: implications for type II topoisomerase mechanism and evolution. *Embo J* 2003;22:151–63.
59. Hartung F, Puchta H. Molecular characterisation of two paralogous SPO11 homologues in *Arabidopsis thaliana*. *Nucleic Acids Res* 2000;28:1548–54.
60. Malik S-B, Ramesh MA, Hulstrand AM, Logsdon JM. Protist homologs of the meiotic Spo11 gene and topoisomerase VI reveal an evolutionary history of gene duplication and lineage-specific loss. *Mol Biol Evol* 2007;24:2827–41.
61. Sugimoto-Shirasu K, Stacey NJ, Corsar J, et al. DNA topoisomerase VI is essential for endoreduplication in *Arabidopsis*. *Curr Biol* 2002;12:1782–6.
62. Gadelle D, Krupovic M, Raymann K, et al. DNA topoisomerase VIII: a novel subfamily of type IIB topoisomerases encoded by free or integrated plasmids in archaea and bacteria. *Nucleic Acids Res* 2014;42:8578–91.

63. Drwal MN, Marinello J, Manzo SG, et al. Novel DNA topoisomerase II $\alpha$  inhibitors from combined ligand- and structure- based virtual screening. *PLoS One* 2014;9:1–16.
64. Pourquier P, Pommier Y, Topoisomerase I-mediated DNA damage. In: Pourquier P, Pommier Y, editors. *Advances in cancer research*. Vol. 80. Elsevier; 2001. p. 189–216.
65. Capranico G, Binaschi M, Borgnetto ME, et al. A protein-mediated mechanism for the DNA sequence-specific action of topoisomerase II poisons. *Trends Pharmacol. Sci* 1997;18:323–9.
66. Chen SH, Chan N-L, Hsieh T. New mechanistic and functional insights into DNA topoisomerases. *Annu Rev Biochem* 2013;82:139–70.
67. Pommier Y. Drugging topoisomerases: lessons and challenges. *ACS Chem Biol* 2013;8:82–95.
68. Pommier Y, Kiselev E, Marchand C. Interfacial inhibitors. *Bioorg Med Chem Lett* 2015;25:3961–5.
69. Zhang C, Li S, Ji L, et al. Design, synthesis and antitumor activity of non-camptothecin topoisomerase I inhibitors. *Bioorg Med Chem Lett* 2015;25:4693–6.
70. Kümler I, Brünner N, Stenvang J, et al. A systematic review on topoisomerase I inhibition in the treatment of metastatic breast cancer. *Breast Cancer Res Treat* 2013;138:347–58.
71. Hsiang YH, Hertzberg R, Hecht S, Liu LF. Camptothecin induces protein-linked DNA breaks via mammalian DNA topoisomerase I. *J Biol Chem* 1985;260:14873–8.
72. Hsiang YH, Liu LF. Identification of mammalian DNA topoisomerase I as an intracellular target of the anticancer drug camptothecin. *Cancer Res* 1988;48:1722–6.
73. Wall ME, Wani MC, Cook CE, et al. Plant antitumor agents. I. The isolation and structure of camptothecin, a novel alkaloidal leukemia and tumor inhibitor from *Camptotheca acuminata*. *J Am Chem Soc* 1966;88:3888–90.
74. Kacprzak KM, Chemistry and biology of camptothecin and its derivatives. In: *Natural products: phytochemistry, botany and metabolism of alkaloids, phenolics and terpenes*. Berlin Heidelberg: Springer; 2013. p. 643–682.
75. Muqet W, Bano Q. Camptothecin and its analogs antitumor activity by poisoning topoisomerase I, their structure activity relationship and clinical development perspective of analogs. *J App Pharm* 2014;6:386–95.
76. Pizzolato JF, Saltz LB. The camptothecins. *Lancet* 2003;361:2235–42.
77. Strumberg D, Pilon AA, Smith M, et al. Conversion of topoisomerase I cleavage complexes on the leading strand of ribosomal DNA into 5'-phosphorylated DNA double-strand breaks by replication runoff. *Mol Cell Biol* 2000;20:3977–87.
78. Sané AT, Bertrand R. Caspase inhibition in camptothecin-treated U-937 cells is coupled with a shift from apoptosis to transient G1 arrest followed by necrotic cell death. *Cancer Res* 1999;59:3565–9.
79. Li LH, Fraser TJ, Olin EJ, Bhuyan BK. Action of camptothecin on mammalian cells in culture. *Cancer Res* 1972;32:2643–50.
80. Pommier Y. DNA topoisomerase I inhibitors: chemistry, biology, and interfacial inhibition. *Chem Rev* 2009;109:2894–902.
81. Staker BL, Hjerrild K, Feese MD, et al. The mechanism of topoisomerase I poisoning by a camptothecin analog. *Proc Natl Acad Sci USA* 2002;99:15387–92.
82. Hertzberg RP, Caranfa MJ, Hecht SM. On the mechanism of topoisomerase I inhibition by camptothecin: evidence for binding to an enzyme-DNA complex. *Biochemistry* 1989;28:4629–38.
83. Garst J. Topotecan: An evolving option in the treatment of relapsed small cell lung cancer. *Ther Clin Risk Manag* 2007;3:1087–95.
84. Armstrong DK, Spriggs D, Levin Y, et al. Hematologic safety and tolerability of topotecan in recurrent ovarian cancer and small cell lung cancer: an integrated analysis. *Oncologist* 2005;10:686–94.
85. Brave M, Dagher R, Farrell A, et al. Topotecan in combination with cisplatin for the treatment of stage IVB, recurrent, or persistent cervical cancer. *Oncology (Williston Park, N.Y.)* 2006;20:1401–10.
86. Fuchs C, Mitchell EP, Hoff PM. Irinotecan in the treatment of colorectal cancer. *Cancer Treat. Rev* 2006;32:491–503.
87. Ohtsuka K, Inoue S, Kameyama M, et al. Intracellular conversion of irinotecan to its active form, SN-38, by native carboxylesterase in human non-small cell lung cancer. *Lung Cancer* 2003;41:187–98.
88. Mullangi R, Ahlawat P, Srinivas NR. Irinotecan and its active metabolite, SN-38: review of bioanalytical methods and recent update from clinical pharmacology perspectives. *Biomed Chromatogr* 2010;24:104–23.
89. Haaz MC, Rivory L, Jantet S, et al. Glucuronidation of SN-38, the active metabolite of irinotecan, by human hepatic microsomes. *Pharmacol Toxicol* 1997;80:91–6.
90. Tadokoro JI, Kakahata K, Shimazaki M, et al. Post-marketing surveillance (PMS) of all patients treated with irinotecan in Japan: clinical experience and ADR profile of 13,935 patients. *Jpn J Clin Oncol* 2011;41:1101–11.
91. Martino E, Della Volpe S, Terribile E, et al. The long story of camptothecin: from traditional medicine to drugs. *Bioorg Med Chem Lett* 2017;27:701–7.
92. Crul M. CKD-602 Chong Kun Dang. *Curr Opin Investig Drugs* 2003;4:1455–9.
93. Park YH, Chung CU, Park BM, et al. Lesser toxicities of belotecan in patients with small cell lung cancer: a retrospective single-center study of camptothecin analogs. *Can Respir J* 2016;2016:1–8.
94. Lee S, Ho JY, Liu JJ, et al. CKD-602, a topoisomerase I inhibitor, induces apoptosis and cell-cycle arrest and inhibits invasion in cervical cancer. *Mol. Med* 2019;25:23.
95. Joerger M, Hess D, Delmonte A, et al. Phase-I dose finding and pharmacokinetic study of the novel hydrophilic camptothecin ST-1968 (namitecan) in patients with solid tumors. *Invest New Drugs* 2015;33:472–9.
96. Joerger M, Hess D, Delmonte A, et al. Integrative population pharmacokinetic and pharmacodynamic dose finding approach of the new camptothecin compound namitecan (ST1968). *Br J Clin Pharmacol* 2015;80:128–38.
97. Cao Z, Kozielski A, Liu X, et al. Crystalline camptothecin-20(S)-O-propionate hydrate: a novel anticancer agent with strong activity against 19 human tumor xenografts. *Cancer Res* 2009;69:4742–9.
98. Bom D, Curran DP, Kruszewski S, et al. The novel silatecan 7-tert-butylidimethylsilyl-10-hydroxycamptothecin displays high lipophilicity, improved human blood stability, and potent anticancer activity. *J Med Chem* 2000;43:3970–80.
99. Pratesi G, Beretta GL, Zunino F. Gimatecan, a novel camptothecin with a promising preclinical profile. *Anticancer Drugs* 2004;15:545–52.
100. De Cesare M, Pratesi G, Perego P, et al. Potent antitumor activity and improved pharmacological profile of ST1481, a

- novel 7-substituted camptothecin. *Cancer Res* 2001;61:7189–95.
101. De Cesare M. High efficacy of intravenous gimatecan on human tumor xenografts. *Anticancer Res* 2018;38:5783–90.
  102. Sheng C, Miao Z, Zhang W. New strategies in the discovery of novel non-camptothecin topoisomerase I inhibitors. *Curr Med Chem* 2011;18:4389–409.
  103. Teicher BA. Next generation topoisomerase I inhibitors: rationale and biomarker strategies. *Biochem Pharmacol* 2008;75:1262–71.
  104. Pommier Y. Topoisomerase I inhibitors: camptothecins and beyond. *Nat Rev Cancer* 2006;6:789–802.
  105. Kummar S, Chen A, Gutierrez M, et al. Clinical and pharmacologic evaluation of two dosing schedules of indotecan (LMP400), a novel indenoisoquinoline, in patients with advanced solid tumors. *Cancer Chemother Pharmacol* 2016;78:73–81.
  106. Saif MW, Diasio RB. Edotecarin: a novel topoisomerase I inhibitor. *Clin Colorectal Cancer* 2005;5:27–36.
  107. Li TK, Houghton PJ, Desai SD, et al. Characterization of ARC-111 as a novel topoisomerase I-targeting anticancer drug. *Cancer Res* 2003;63:8400–7.
  108. Yoshinari T, Ohkubo M, Fukasawa K, et al. Mode of action of a new indolocarbazole anticancer agent, J-107088, targeting topoisomerase I. *Cancer Res* 1999;59:4271–5.
  109. Pommier Y, Cushman M. The indenoisoquinoline noncamptothecin topoisomerase I inhibitors: update and perspectives. *Mol. Cancer Ther* 2009;8:1008–14.
  110. Cuya SM, Bjornsti M-A, van Waardenburg RCAM. DNA topoisomerase-targeting chemotherapeutics: what's new? *Cancer Chemother Pharmacol* 2017;80:1–14.
  111. A phase I study of indenoisoquinolines LMP400 and LMP776 in adults with relapsed solid tumors and lymphomas - full text view - ClinicalTrials.gov. [accessed 2020 Jun 1]. <https://clinicaltrials.gov/ct2/show/NCT01051635>
  112. Ruchelman AL, Singh SK, Ray A, et al. 5*H*-dibenzo[*c,h*]1,6-naphthyridin-6-ones: novel topoisomerase I-targeting anticancer agents with potent cytotoxic activity. *Bioorg Med Chem* 2003;11:2061–73.
  113. Ruchelman AL, Singh SK, Wu X, et al. Diaza- and triazachrysenes: potent topoisomerase-targeting agents with exceptional antitumor activity against the human tumor xenograft, MDA-MB-435. *Bioorg Med Chem Lett* 2002;12:3333–6.
  114. Zhu S, Ruchelman AL, Zhou N, et al. Esters and amides of 2,3-dimethoxy-8,9-methylenedioxy-benzo[*i*]phenanthridine-12-carboxylic acid: potent cytotoxic and topoisomerase I-targeting agents. *Bioorg Med Chem* 2005;13:6782–94.
  115. Satyanarayana M, Feng W, Cheng L, et al. Syntheses and biological evaluation of topoisomerase I-targeting agents related to 11-[2-(*N,N*-dimethylamino)ethyl]-2,3-dimethoxy-8,9-methylenedioxy-11*H*-isoquino[4,3-*c*]cinnolin-12-one (ARC-31). *Bioorg Med Chem* 2008;16:7824–31.
  116. Feng W, Satyanarayana M, Tsai YC, et al. 12-Substituted 2,3-dimethoxy-8,9-methylenedioxybenzo[*i*]phenanthridines as novel topoisomerase I-targeting antitumor agents. *Bioorg Med Chem* 2009;17:2877–85.
  117. Zhu S, Ruchelman AL, Zhou N, et al. 6-Substituted 6*H*-dibenzo[*c,h*][2,6]naphthyridin-5-ones: reversed lactam analogues of ARC-111 with potent topoisomerase I-targeting activity and cytotoxicity. *Bioorg Med Chem* 2006;14:3131–43.
  118. Sooryakumar D, Dexheimer TS, Teicher BA, Pommier Y. Molecular and cellular pharmacology of the novel non-camptothecin topoisomerase I inhibitor Genz-644282. *Mol Cancer Ther* 2011;10:1490–9.
  119. Pogorelčnik B, Brvar M, Žegura B, et al. Discovery of mono- and disubstituted 1*H*-pyrazolo[3,4]pyrimidines and 9*H*-purines as catalytic inhibitors of human DNA topoisomerase II $\alpha$ . *ChemMedChem* 2015;10:345–59.
  120. Vos SM, Tretter EM, Schmidt BH, Berger JM. All tangled up: how cells direct, manage and exploit topoisomerase function. *Nat Rev Mol Cell Biol* 2011;12:827–41.
  121. de Almeida SMV, Ribeiro AG, de Lima Silva GC, et al. Alves de Lima M do C. DNA binding and topoisomerase inhibition: how can these mechanisms be explored to design more specific anticancer agents? *Biomed. Pharmacother* 2017;96:1538–56.
  122. Nitiss JL. Targeting DNA topoisomerase II in cancer chemotherapy. *Nat Rev Cancer* 2009;9:338–50.
  123. Bailly C. Contemporary challenges in the design of topoisomerase II inhibitors for cancer chemotherapy. *Chem Rev* 2012;112:3611–40.
  124. Clark PI, Slevin ML. The clinical pharmacology of etoposide and teniposide. *Clin Pharmacokinet* 1987;12:223–52.
  125. King LS, Sullivan M. The similarity of the effect of podophyllin and colchicine and their use in the treatment of condylomata acuminata. *Science* 1946;104:244–5.
  126. Greenspan EM, Leiter J, Shear MJ. Effect of alpha-peltatin, beta-peltatin, and podophyllotoxin on lymphomas and other transplanted tumors. *J Natl Cancer Inst* 1950;10:1295–333.
  127. Hande KR. Etoposide: four decades of development of a topoisomerase II inhibitor. *Eur J Cancer* 1998;34:1514–21.
  128. Kingma PS, Burden DA, Osheroff N. Binding of etoposide to topoisomerase II in the absence of DNA: Decreased affinity as a mechanism of drug resistance. *Biochemistry* 1999;38:3457–61.
  129. Burden DA, Kingma PS, Froelich-Ammon SJ, et al. Topoisomerase II/etoposide interactions direct the formation of drug-induced enzyme-DNA cleavage complexes. *J Biol Chem* 1996;271:29238–44.
  130. Wilstermann AM, Bender RP, Godfrey M, et al. Topoisomerase II - drug interaction domains: identification of substituents on etoposide that interact with the enzyme. *Biochemistry* 2007;46:8217–25.
  131. Baldwin EL, Osheroff N. Etoposide, topoisomerase II and cancer. *Curr Med Chem Anticancer Agents* 2005;5:363–72.
  132. Stähelin HF, von Wartburg A. The chemical and biological route from podophyllotoxin glucoside to etoposide: ninth cain memorial award lecture. *Cancer Res* 1991;51:5–15.
  133. Montecucco A, Zanetta F, Biamonti G. Molecular mechanisms of etoposide. *Excli J* 2015;14:95–108.
  134. Kuruppu AI, Paranagama P, Goonasekara CL. Medicinal plants commonly used against cancer in traditional medicine formulae in Sri Lanka. *Saudi Pharm J* 2019;27:565–73.
  135. Bender RP, Osheroff N. DNA topoisomerases as targets for the chemotherapeutic treatment of cancer. In: Dai W, editor. Checkpoint responses in cancer therapy. Totowa: Humana Press; 2008. p. 57–91.
  136. Barret JM, Kruczynski A, Vispé S, et al. F14512, a potent antitumor agent targeting topoisomerase II vectored into cancer cells via the polyamine transport system. *Cancer Res* 2008;68:9845–53.

137. Thakur D. Topoisomerase II Inhibitors in cancer treatment. *Int J Pharm Sci Nanotechnol* 2011;3:1173–81.
138. Najjar IA, Johri RK. Pharmaceutical and pharmacological approaches for bioavailability enhancement of etoposide. *J Biosci* 2014;39:139–44.
139. Li J, Chen W, Zhang P, Li N. Topoisomerase II trapping agent teniposide induces apoptosis and G2/M or S phase arrest of oral squamous cell carcinoma. *World J Surg Oncol* 2006;4:41.
140. Sun J, Wei Q, Zhou Y, et al. A systematic analysis of FDA-approved anticancer drugs. *BMC Syst Biol* 2017;11:87.
141. Guerram M, Jiang ZZ, Zhang LY. Podophyllotoxin, a medicinal agent of plant origin: past, present and future. *Chin J Nat Med* 2012;10:161–9.
142. Hartmann JT, Lipp HP. Camptothecin and podophyllotoxin derivatives: inhibitors of topoisomerase I and II - mechanisms of action, pharmacokinetics and toxicity profile. *Drug Saf* 2006;29:209–30.
143. Gentry AC, Pitts SL, Jablonsky MJ, et al. Interactions between the etoposide derivative F14512 and human type II topoisomerases: implications for the C4 spermine moiety in promoting enzyme-mediated DNA cleavage. *Biochemistry* 2011;50:3240–9.
144. Casero RA, Marton LJ. Targeting polyamine metabolism and function in cancer and other hyperproliferative diseases. *Nat Rev Drug Discov* 2007;6:373–90.
145. Bombarde O, Larminat F, Gomez D, et al. The DNA-binding polyamine moiety in the vectorized DNA topoisomerase II inhibitor F14512 alters reparability of the consequent enzyme-linked DNA double-strand breaks. *Mol Cancer Ther* 2017;16:2166–77.
146. Kruczynski A, Vandenberghe I, Pillon A, et al. Preclinical activity of F14512, designed to target tumors expressing an active polyamine transport system. *Invest New Drugs* 2011;29:9–21.
147. Jasra S, Anampa J. Anthracycline use for early stage breast cancer in the modern era: a review. *Curr Treat Options Oncol* 2018;19:30.
148. Nebigil CG, Désaubry L. Updates in anthracycline-mediated cardiotoxicity. *Front Pharmacol* 2018;9:1262.
149. Aleman BMP, Moser EC, Nuver J, et al. Cardiovascular disease after cancer therapy. *EJC Suppl* 2014;12:18–28.
150. Zunino F, Capranico G. DNA topoisomerase II as the primary target of anti-tumor anthracyclines. *Anticancer Drug Des* 1990;5:307–17.
151. Binaschi M, Bigioni M, Cipollone A, et al. Anthracyclines: selected new developments. *Curr Med Chem Anticancer Agents* 2001;1:113–30.
152. Thorn CF, Oshiro C, Marsh S, et al. Doxorubicin pathways: pharmacodynamics and adverse effects. *Pharmacogenet Genomics* 2011;21:440–6.
153. Menna P, Minotti G, Salvatorelli E. In vitro modeling of the structure-activity determinants of anthracycline cardiotoxicity. *Cell Biol Toxicol* 2007;23:49–62.
154. Pogorelnik B, Perdih A, Solmajer T. Recent developments of DNA poisons-human DNA topoisomerase II $\alpha$  inhibitors-as anticancer agents. *Curr Pharm Des* 2013;19:2474–88.
155. Moro S, Beretta GL, Dal Ben D, et al. Interaction model for anthracycline activity against DNA topoisomerase II. *Biochemistry* 2004;43:7503–13.
156. Lyu YL, Liu LF. 13- Doxorubicin cardiotoxicity revisited: ROS versus Top2. In: Liu X-Y, Pestka S, Shi Y-F, editors. *Recent advances in cancer research and therapy*. Elsevier Inc; 2012. p. 351–369.
157. Carvalho C, Santos R, Cardoso S, et al. Doxorubicin: the good, the bad and the ugly effect. *Curr Med Chem* 2009; 16:3267–85.
158. Zhang S, Liu X, Bawa-Khalfe T, et al. Identification of the molecular basis of doxorubicin-induced cardiotoxicity. *Nat Med* 2012;18:1639–42.
159. Pugazhendhi A, Edison TNJL, Velmurugan BK, et al. Toxicity of doxorubicin (Dox) to different experimental organ systems. *Life Sci* 2018;200:26–30.
160. Zhao L, Zhang B. Doxorubicin induces cardiotoxicity through upregulation of death receptors mediated apoptosis in cardiomyocytes. *Sci Rep* 2017;7:44735.
161. Langer SW. Dexrazoxane for the treatment of chemotherapy-related side effects. *Cancer Manag Res* 2014;6:357–63.
162. Drugs@FDA: FDA-Approved Drugs–Doxorubicin. [accessed 2020 Jun 19]. <https://www.accessdata.fda.gov/scripts/cder/daf/index.cfm?event=overview.process&ApplNo=050467>
163. Robert J. Epirubicin: clinical pharmacology and dose-effect relationship. *Drugs* 1993;45:20–30.
164. Coukell AJ, Faulds D. Epirubicin. An updated review of its pharmacodynamic and pharmacokinetic properties and therapeutic efficacy in the management of breast cancer. *Drugs* 1997;53:453–82.
165. Singh Z, Kaur H. Toxicological aspects of antineoplastic drugs doxorubicin and epirubicin. *J Clin Mol Med* 2019;2: 1–5.
166. Israel M, Potti PG, Seshadri R. Adriamycin analogues. Rationale, synthesis, and preliminary antitumor evaluation of highly active DNA-nonbinding N-(trifluoroacetyl)adriamycin 14-O-hemiester derivatives<sup>1</sup>, 2. *J Med Chem* 1985;28: 1223–8.
167. Onrust SV, Lamb HM. Valrubicin. *Drugs Aging* 1999;15: 69–75.
168. Drug Approval Package: Valstar (Valrubicin) NDA# 20-892. [accessed 2020 Jun 9]. [https://www.accessdata.fda.gov/drugsatfda\\_docs/nda/98/20892.cfm](https://www.accessdata.fda.gov/drugsatfda_docs/nda/98/20892.cfm)
169. Hanada M, Mizuno S, Fukushima A, et al. A new antitumor agent amrubicin induces cell growth inhibition by stabilizing topoisomerase II-DNA complex. *Jpn J Cancer Res* 1998; 89:1229–38.
170. Sakurai R, Kaira K, Miura Y, et al. Clinical significance of topoisomerase-II expression in patients with advanced non-small cell lung cancer treated with amrubicin. *Thorac Cancer* 2020;11:426–35.
171. Yamaoka T, Hanada M, Ichii S, et al. Cytotoxicity of amrubicin, a novel 9-aminoanthracycline, and its active metabolite amrubicinol on human tumor cells. *Jpn J Cancer Res* 1998; 89:1067–73.
172. Kurata T, Okamoto I, Tamura K, Fukuoka M. Amrubicin for non-small-cell lung cancer and small-cell lung cancer. *Invest New Drugs* 2007;25:499–504.
173. Marrero L, Wyczzechowska D, Musto AE, et al. Therapeutic efficacy of aldodoxorubicin in an intracranial xenograft mouse model of human glioblastoma. *Neoplasia* 2014;16:874–82.
174. Kratz F, Warnecke A, Scheuermann K, et al. Probing the cysteine-34 position of endogenous serum albumin with thiol-binding doxorubicin derivatives. Improved efficacy of an acid-sensitive doxorubicin derivative with specific albumin-binding properties compared to that of the parent compound. *J Med Chem* 2002;45:5523–33.

175. Graeser R, Esser N, Unger H, et al. INNO-206, the (6-maleimidocaproyl hydrazone derivative of doxorubicin), shows superior antitumor efficacy compared to doxorubicin in different tumor xenograft models and in an orthotopic pancreas carcinoma model. *Invest New Drugs* 2010;28:14–9.
176. Kratz F, Fichtner I, Graeser R. Combination therapy with the albumin-binding prodrug of doxorubicin (INNO-206) and doxorubicin achieves complete remissions and improves tolerability in an ovarian A2780 xenograft model. *Invest New Drugs* 2012;30:1743–9.
177. Sanchez E, Li M, Wang C, et al. Anti-myeloma effects of the novel anthracycline derivative INNO-206. *Clin Cancer Res* 2012;18:3856–67.
178. White RJ, Durr FE. Development of mitoxantrone. *Invest New Drugs* 1985;3:85–93.
179. Murdock KC, Child RG, Fabio PF, et al. Antitumor agents. 1. 1,4-bis[(aminoalkyl)amino]-9,10-anthracenediones. *J Med Chem* 1979;22:1024–30.
180. Johnson RK, Zee-Cheng RK, Lee WW, et al. Experimental antitumor activity of aminoanthraquinones. *Cancer Treat Rep* 1979;63:425–39.
181. Zee-Cheng RKY, Cheng CC. Antineoplastic agents. Structure-activity relationship study of bis(substituted aminoalkylamino)anthraquinones. *J Med Chem* 1978;21:291–4.
182. Halterman P, Vogelzang NJ, Farabishahadel A, Goodman OB, Mitoxantrone. In: *Drug management of prostate cancer*. New York: Springer; 2010. p. 125–131.
183. Capranico G, De Isabella P, Tinelli S, et al. Similar sequence specificity of mitoxantrone and VM-26 stimulation of *in vitro* DNA cleavage by mammalian DNA topoisomerase II. *Biochemistry* 1993;32:3038–46.
184. Wu CC, Li YC, Wang YR, et al. On the structural basis and design guidelines for type II topoisomerase-targeting anticancer drugs. *Nucleic Acids Res* 2013;41:10630–40.
185. Damiani RM, Moura DJ, Viau CM, et al. Pathways of cardiac toxicity: comparison between chemotherapeutic drugs doxorubicin and mitoxantrone. *Arch Toxicol* 2016;90:2063–76.
186. Rossato LG, Costa VM, De Pinho PG, et al. The metabolic profile of mitoxantrone and its relation with mitoxantrone-induced cardiotoxicity. *Arch Toxicol* 2013;87:1809–20.
187. Drugs@FDA: FDA-Approved Drugs–Mitoxantrone. [accessed 2020 Jun 19]. <https://www.accessdata.fda.gov/scripts/cder/daf/index.cfm?event=overview.process&ApplNo=019297>
188. Enache M, Toader AM, Enache MI. Mitoxantrone-surfactant interactions: a physicochemical overview. *Molecules* 2016; 21:1356.
189. Patel KJ, Trédan O, Tannock IF. Distribution of the anticancer drugs doxorubicin, mitoxantrone and topotecan in tumors and normal tissues. *Cancer Chemother. Pharmacol* 2013;72:127–38.
190. Ketron AC, Denny WA, Graves DE, Osheroff N. Amsacrine as a topoisomerase II poison: importance of drug-DNA interactions. *Biochemistry* 2012;51:1730–9.
191. Murphy MB, Mercer SL, Dewese JE. Inhibitors and poisons of mammalian type II topoisomerases. In: *Advances in molecular toxicology*. Vol. 11. Elsevier B.V.; 2017. p. 203–240.
192. Tomita K, Tsuzuki Y, Shibamori K, et al. Synthesis and structure-activity relationships of novel 7-substituted 1,4-dihydro-4-oxo-1-(2-thiazolyl)-1,8-naphthyridine-3-carboxylic acids as antitumor agents. Part 1. *J. Med. Chem* 2002;45: 5564–75.
193. Abbas JA, Stuart RK. Vosaroxin : a novel antineoplastic quinolone. *Expert Opin Investig Drugs* 2012;21:1223–33.
194. Paubelle E, Zylbersztejn F, Thomas X. The preclinical discovery of vosaroxin for the treatment of acute myeloid leukemia. *Expert Opin Drug Discov* 2017;12:747–53.
195. Li PH, Zeng P, Chen SB, et al. Synthesis and mechanism studies of 1,3-benzoxazolyl substituted pyrrolo[2,3-b]pyrazine derivatives as nonintercalative topoisomerase II catalytic inhibitors. *J Med Chem* 2016;59:238–52.
196. Deng S, Yan T, Nikolova T, et al. The catalytic topoisomerase II inhibitor dexrazoxane induces DNA breaks, ATF3 and the DNA damage response in cancer cells. *Br J Pharmacol* 2015;172:2246–57.
197. Vann KR, Ergün Y, Zencir S, et al. Inhibition of human DNA topoisomerase II $\alpha$  by two novel ellipticine derivatives. *Bioorg Med Chem Lett* 2016;26:1809–12.
198. Jones RL. Utility of dexrazoxane for the reduction of anthracycline-induced cardiotoxicity. *Expert Rev Cardiovasc Ther* 2008;6:1311–7.
199. Cvetković RS, Scott LJ. Dexrazoxane: a review of its use for cardioprotection during anthracycline chemotherapy. *Drugs* 2005;65:1005–24.
200. Roca J, Ishida R, Berger JM, et al. Antitumor bisdioxopiperazines inhibit yeast DNA topoisomerase II by trapping the enzyme in the form of a closed protein clamp. *Proc Natl Acad Sci USA* 1994;91:1781–5.
201. Jensen LH, Nitiss KC, Rose A, et al. A novel mechanism of cell killing by anti-topoisomerase II bisdioxopiperazines. *J Biol Chem* 2000;275:2137–46.
202. Classen S, Olland S, Berger JM. Structure of the topoisomerase II ATPase region and its mechanism of inhibition by the chemotherapeutic agent ICRF-187. *Proc Natl Acad Sci USA* 2003;100:10629–34.
203. Hasinoff BB, Patel D, Wu X. A QSAR study that compares the ability of bisdioxopiperazine analogs of the doxorubicin cardioprotective agent dexrazoxane (ICRF-187) to protect myocytes with DNA topoisomerase II inhibition. *Toxicol Appl Pharmacol* 2020;399:115038.
204. Fortune JM, Osheroff N. Merbarone inhibits the catalytic activity of human topoisomerase II $\alpha$  by blocking DNA cleavage. *J Biol Chem* 1998;273:17643–50.
205. Pastor N, Domínguez I, Orta ML, et al. The DNA topoisomerase II catalytic inhibitor merbarone is genotoxic and induces endoreduplication. *Mutat Res* 2012;738-739: 45–51.
206. Tripathi N, Guchhait SK, Bharatam PV. Pharmacoinformatics analysis of merbarone binding site in human topoisomerase II $\alpha$ . *J Mol Graph Model* 2019;86:1–18.



Review

# Autophagy Modulators in Cancer Therapy

Kamila Buzun <sup>1</sup>, Agnieszka Gornowicz <sup>1,\*</sup>, Roman Lesyk <sup>2</sup>, Krzysztof Bielawski <sup>3</sup> and Anna Bielawska <sup>1</sup>

<sup>1</sup> Department of Biotechnology, Faculty of Pharmacy, Medical University of Białystok, 15-089 Białystok, Poland; kamila.buzun@umb.edu.pl (K.B.); anna.bielawska@umb.edu.pl (A.B.)

<sup>2</sup> Department of Public Health, Dietetics and Lifestyle Disorders, Faculty of Medicine, University of Information Technology and Management in Rzeszów, 35-225 Rzeszów, Poland; dr\_r\_lesyk@org.lviv.net

<sup>3</sup> Department of Synthesis and Technology of Drugs, Faculty of Pharmacy, Medical University of Białystok, 15-089 Białystok, Poland; kbiel@umb.edu.pl

\* Correspondence: agnieszka.gornowicz@umb.edu.pl; Tel.: +48-(85)-748-5742

**Abstract:** Autophagy is a process of self-degradation that plays an important role in removing damaged proteins, organelles or cellular fragments from the cell. Under stressful conditions such as hypoxia, nutrient deficiency or chemotherapy, this process can also become the strategy for cell survival. Autophagy can be nonselective or selective in removing specific organelles, ribosomes, and protein aggregates, although the complete mechanisms that regulate aspects of selective autophagy are not fully understood. This review summarizes the most recent research into understanding the different types and mechanisms of autophagy. The relationship between apoptosis and autophagy on the level of molecular regulation of the expression of selected proteins such as p53, Bcl-2/Beclin 1, p62, Atg proteins, and caspases was discussed. Intensive studies have revealed a whole range of novel compounds with an anticancer activity that inhibit or activate regulatory pathways involved in autophagy. We focused on the presentation of compounds strongly affecting the autophagy process, with particular emphasis on those that are undergoing clinical and preclinical cancer research. Moreover, the target points, adverse effects and therapeutic schemes of autophagy inhibitors and activators are presented.

**Keywords:** autophagy; autophagy inhibitors; autophagy activators; cancer; cancer therapy



**Citation:** Buzun, K.; Gornowicz, A.; Lesyk, R.; Bielawski, K.; Bielawska, A. Autophagy Modulators in Cancer Therapy. *Int. J. Mol. Sci.* **2021**, *22*, 5804. <https://doi.org/10.3390/ijms22115804>

Academic Editor:  
Daniela Trisciuoglio

Received: 14 May 2021  
Accepted: 24 May 2021  
Published: 28 May 2021

**Publisher's Note:** MDPI stays neutral with regard to jurisdictional claims in published maps and institutional affiliations.



**Copyright:** © 2021 by the authors. Licensee MDPI, Basel, Switzerland. This article is an open access article distributed under the terms and conditions of the Creative Commons Attribution (CC BY) license (<https://creativecommons.org/licenses/by/4.0/>).

## 1. Introduction

Autophagy, directly translated as ‘self-eating’, is an evolutionary conservative process, found in all eukaryotic cells—from single-cell yeasts to much more complex multicellular mammalian organisms [1]. The introduction of the term ‘autophagy’ was proposed in February 1963 during the conference titled ‘Ciba Foundation Symposium on Lysosomes’ which took place in London [2]. This process participates in intracellular degradation of damaged or redundant proteins with a long half-life as well as other unnecessary cytoplasm components [3,4]. Autophagy provides an organism’s homeostasis and prevent it from redundant components accumulation inside the cell [5].

Moreover, this process is involved in surfactant formation or red blood cells ripening [3]. Following the Nomenclature Committee on Cell Death, in 2018 the term ‘autophagy-dependent cell death (ADCD)’ was introduced. ADCD is a type of regulated cell death in which functional autophagic markers such as increased degradation of autophagosomal substrates or LC3 (Light Chain protein 3) lipidization occurs [6]. Interestingly, unlike necrosis or apoptosis, autophagy-dependent cell death is not synonymous exclusively with cell death. Under stressful condition such as hypoxia, nutrient deficiency or chemotherapy, this process can become the strategy for cell survival [5]. ADCD occurs in all eukaryotic cells performing important functions, for example, it is an adaptation mechanism to stressful conditions, as it provides cells with a constant supply of nutrients essential for sustaining key life processes. Additionally, through the elimination of redundant cytoplasm components and the adjustment of the endoplasmic reticulum size, ADCD participates



in maintaining the intracellular homeostasis. Furthermore, ADCD is involved in tissue-specific processes, such as erythrocyte ripening or intracellular surfactant formation [3] and also protects the organism from viruses or bacteria multiplication [7,8].

Autophagy-dependent cell death, through its selective and non-selective mechanisms of degradation of pathogens, organelles and various biomolecules (nucleic acids, lipids, carbohydrates and proteins) constitutes the main catabolic system of eukaryotic cells [9,10]. As one of the key elements in maintaining cell homeostasis and health, this process also plays an important role in tumor suppression or genome integrity [11].

The first part of the following paper will provide a brief description of the different types of autophagy. Thereafter, we will focus primarily on the classification and characterization of compounds whose molecular target is autophagy—those undergoing clinical and preclinical trials. Moreover, the target points, adverse effects and therapeutic schemes of autophagy inhibitors and activators are presented in tables.

## 2. Types of Autophagy

Based on the differences in the mechanism of delivery of redundant cytoplasm components to lysosomes, four basic types of autophagy can be distinguished: macroautophagy, selective autophagy, microautophagy and chaperone-mediated autophagy (CMA). The term 'autophagy', commonly used in various papers, refers to macroautophagy—this will apply to the following publication as well.

### 2.1. Macroautophagy

Macroautophagy is the most widespread type of autophagy which is controlled by autophagy-related (*ATG*) genes. The first *ATG* genes were identified in yeast. Interestingly, 14 from 32 of described *Atg* yeast proteins are homologous to those proteins found in mammals [12,13]. This process is regulated by several pathways sensitive to the presence or deficiency of nutrients. Substances such as insulin, amino acids or AMPK (5' adenosine monophosphate-activated protein kinase) act through the protein serine-threonine kinase mTOR (mammalian target of rapamycin). When the natural cellular environment is rich in essential nutrients, the regulatory mTOR pathway is activated, which in turn leads to the inhibition of autophagy and stimulates cells to proliferation [14]. *ATG* genes are responsible for the regulation of the autophagosomes production [15]. During the autophagy process (Figure 1), the cytoplasm fragment is surrounded by a forming C-shaped double membrane. Both ends of the membrane (known as phagophore) extend and close inside the fragment of cytoplasm with whole organelles or proteins with a long half-life. This results in the formation of 300–900 nm bubble (autophagosome), which then undergoes a maturation process. During the maturation autophagosomes and lysosomes merge to form autolysosomes (autophagolysosomes). Inside the autolysosomes, using hydrolytic lysosomal enzymes, the degradation of the macromolecular substrates to fatty acids and amino acids occurs [16,17].

Macroautophagy may play a dual role in tumorigenesis. Depending on the tumor type, its genetic background, developmental stage or tumor microenvironment, it can inhibit or stimulate tumor cell growth. Elimination of damaged organelles, aggregated or unformed proteins and oncogenic proteins prevent tumor initiation and therefore constitutes a tumor suppressor effect of autophagy. On the other hand, autophagy may also promote tumorigenesis through, for example, cytoprotective effects in response to used chemotherapeutics or metabolite recycling that promotes tumorigenesis, proliferation, or tumor metastasis [18]. With the identification of *Beclin 1*, a key gene involved in the autophagy process, it became possible to discover the connection between autophagy and various human cancers. Monoallelic deletion of *Beclin 1*, a tumor suppressor, is observed in hepatocellular carcinoma, ovarian and breast cancer [19–22]. Reduced expression of *Beclin 1* in tumor tissues was observed in 44 patients with hepatocellular carcinoma. Based on these observations, it was concluded that autophagy may lead to inhibition of tumorigenesis [22].

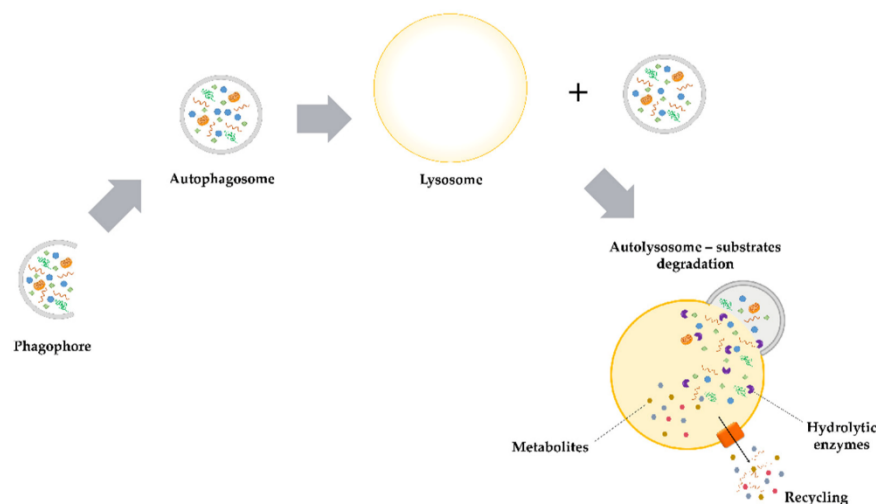


**Figure 1.** Macroautophagy. The C-shaped expansion of the double membrane results in the formation of an autophagosome. This small ‘vesicle’ contains redundant or damaged organelles, cellular fragments or proteins. In the next step, the formed autophagosome fuses with the lysosome and an autolysosome is formed. Inside the created structure, all components are degraded by hydrolytic enzymes.

## 2.2. Selective Autophagy

As mentioned in the introduction, we can distinguish between the selective and non-selective form of autophagy. The mechanism of selective autophagy is based on the degradation of specific organelles, such as endoplasmic reticulum (ER), mitochondria, proteasomes, ribosomes, peroxisomes, lipid droplets (LDs), lysosomes and nuclei. Selective autophagy’s mechanism of action is related to the binding of cargoes by autophagy receptors and thereafter its degradation in lysosomes/vacuoles. A distinguishing feature of autophagy receptors is the presence of AIM (Atg8-Interacting Motif) or LIR (LC3-Interacting Region) on their surface. Both of these fragments allow binding of receptors and proteins from Atg8/LC3/GABARAP family selectively [23–26]. Mentioned proteins are a kind of link between the core autophagic machinery and transported cargo. This enables the selective and efficient recognition of the cargo and its subsequent sequestration in autophagosomes [27]. Based on the types of removed organelles, we distinguish the following subtypes of selective autophagy: ER-phagy (endoplasmic reticulum), mitophagy (mitochondria), proteaphagy (proteasomes), ribophagy (ribosomes), pexophagy (peroxisomes), lipophagy (LDs), lysophagy (lysosomes) and nucleophagy (nuclei) (Figure 2).

The selective autophagy’s ability to remove organelles makes this process a key element in cellular homeostasis maintenance [28]. Disruption of the selective autophagy functions may lead to the occurrence of various disorders, such as cancer [29,30], heart failure [31], metabolic abnormalities [32] and inflammatory [33] or neurodegenerative diseases [34,35].

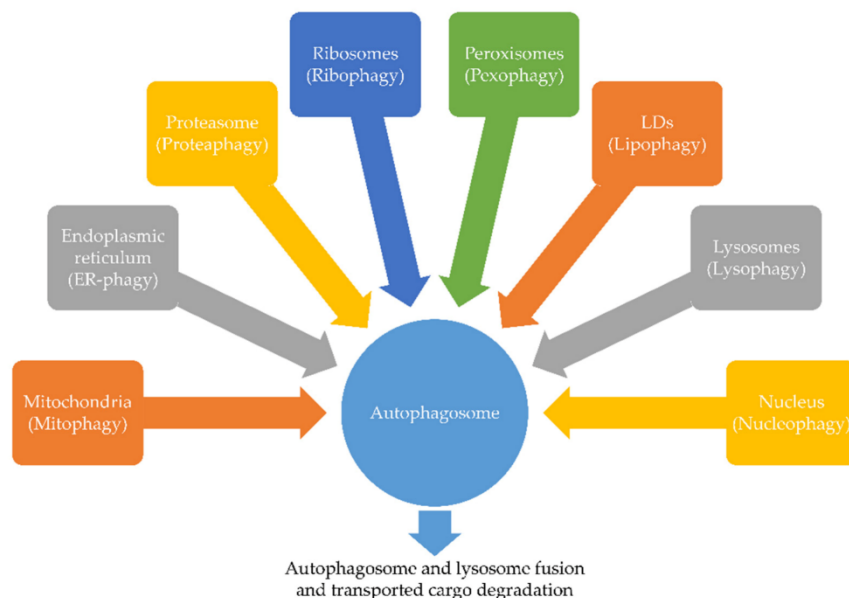


**Figure 2.** Selective forms of autophagy. Depending on the degraded organelle we can distinguish: mitophagy, ER-phagy, proteaphagy, ribophagy, pexophagy, lipophagy, lysophagy and nucleophagy.

### 2.2.1. ER-Phagy

Post-translationally or co-translationally introduced into the endoplasmic reticulum, plasma membrane proteins and secretory proteins inside the ER adopt the native structure. During this process, the newly synthesized polypeptides are often misfolded [36]. Moreover, when mutations occur in the protein-coding sequence, the frequency of this phenomenon increases. To prevent the accumulation of misfolded polypeptides in the ER, they can be transported back to the cytosol and then degraded using the ubiquitin-proteasome system [37,38]. However, proteins may be the only substrates of the mentioned degradation process. In contrast, the autophagy-lysosome system can degrade both protein aggregates and ER membrane lipids. This process is referred to as ER-phagy. There are two basic pathways of ER-phagy: micro-ER-phagy and macro-ER-phagy. In the process of micro-ER-phagy, lysosomal membranes involute and part of the reticulum is “cut off” from the lysosome lumen [39,40].

In contrast, in the macro-ER-phagy process, ER fragments are surrounded by autophagosomes, followed by the fusion of autophagosomes and lysosomes, which results in the formation of autolysosomes where material previously transported by autophagosomes is degraded [41]. Mutations that occurred in *SEC62* and *FAM134B* genes are involved in cancer progression and development, i.e., *FAM134B* mutations in esophageal squamous cell carcinoma promotes tumor development while in colon cancer, it leads to tumor suppression [42,43].

### 2.2.2. Mitophagy

Mitophagy is the second subtype of selective autophagy. Autophagy machinery recognizes the dysfunctional, obsolete or damaged mitochondria, ultimately leading to the degradation of redundant organelles in lysosomes [44]. Those redundant mitochondria are incapable of efficient oxidative phosphorylation due to their transmembrane potential dissipation. The consequence of this is the reactive oxygen species accumulation and the subsequent increase in oxidative stress level throughout the cell. Specific mitophagy receptors recognize isolated damaged organelles, combine with the core autophagy machinery

and leads to the mitochondria-induced ADCD [44,45]. It has been observed that in cancer patients, many proteins involved in mitophagy such as BNIP3, NIX, MFN1 and MFN2 or PINK1 and PINK2 are dysregulated. However, how these proteins interact with cells to act as a tumor promoter (i.e., BNIP3 receptor in pancreatic cancer, melanoma or renal cell carcinoma) or suppressor (i.e., BNIP3 receptor in breast cancer) appears to depend largely on the context and subtype of cancer present in the patient [46].

### 2.2.3. Proteaphagy

The eukaryotic proteasome, composed of two subunits, regulatory (RP) and core (CP), has an important function in proteostasis maintenance, and by removing e.g., signaling molecules, significantly influences various cellular processes [47]. The role of the RP subunit is to recognize and degrade substrate molecules. The goal of this action is to deliver a target protein to the CP subunit to be degraded [48]. Proteasomes are among the highly mobile complexes, allowing them to move between the cell nucleus and the cytoplasm depending on the phase of the cell cycle, stress conditions or cellular growth [48,49]. In 1995, proteasomes were first observed within lysosomes and autophagic vesicles located in liver cells of starved rats [50]. Twenty years later, in 2015, the term 'proteaphagy' was introduced confirming the existence of a proteasome-selective autophagy process [51]. In mammalian cells, the proteasome undergoes amino acid starvation-induced ubiquitination. p62, the autophagy receptor, recognizes these proteasomes, and through the receptor's concomitant interaction with LC3, they are delivered to the phagophore. In the expanding phagophore, ultimate degradation of the organelles occurs [52]. Despite extensive research, the biological consequences of proteaphagy remain largely unknown. Continued research is needed to determine what role proteaphagy plays in maintaining a population of healthy proteasomes in cells [53].

### 2.2.4. Ribophagy

Ribosomes represent 10% of the mass of all proteins located in a cell. Their degradation by autophagy is called 'ribophagy'. In cells in the basal state, the activity of this process is very low, whereas mTOR 1 inhibition or starvation causes an enhancement of ribophagy. Inhibition of mTOR 1 causes transport of NUFIP 1 (Nuclear FMR1 Interacting Protein 1), from the cell nucleus to lysosomes and autophagosomes. Subsequently, NUFIP1 is bound by ribosomes. The degradation of these organelles is initiated by autophagy. Following the interaction between NUFIP1 and ribosomes, LC3 recruits autophagosomes [54,55]. By direct interaction of autophagosomes with LC3, ribosomes are transported to autophagosomes for degradation. To date, little is known about the effects of ribophagy on tumorigenesis. However, the high levels of nucleotides and amino acids in ribosomes suggest that they may provide some sort of nutrient store in the tumor environment [56].

### 2.2.5. Pexophagy

Peroxisomes are small organelles that degrade lipids in the cytoplasm. Because the estimated half-life of these structures is approximately 2 days, both biogenesis and degradation of peroxisomes are probably dynamic processes [57]. Degradation of peroxisomes by autophagy called 'pexophagy', requires the participation of specific autophagy receptors. In the case of pexophagy, these are *NBR1* (a gene adjacent to the *BRCA 1* gene) and sequestosome 1 (*SQSTM1* or *p62*). Overexpression of the above factors induces clustering and subsequent degradation of peroxisomes in mammalian cells [58,59]. As a result of overexpression of ubiquitin molecule-linked PMPs (Peroxisomal Membrane Proteins), such as PEX3 or PMP34, *SQSTM1*-dependent induction of pexophagy in mammalian cells occurs [60]. Unfortunately, an appropriate answer to the following question remains unknown: "If a PMP is ubiquitinated under pexophagy-inducing conditions and whether subsequent interaction with *NBR1* and/or *SQSTM1* links ubiquitinated peroxisomes to the autophagic machinery?" [61].

### 2.2.6. Lipophagy

Lipophagy is the degradation of lipid molecules by autophagy. At the surface of the autophagosome, the interaction of MAP1LC3 (Microtubule-Associated Protein 1 Light Chain 3) with the autophagosomal membrane results in cargo recognition [62]. Lipophagy initiation is usually enabled by the presence of one or more autophagy receptors, e.g., NBR1 or p62, linking the membrane of organelles and LC3 [63]. Depending on the size of the degraded LDs, we distinguish between fragmented microautophagy and macroautophagy. In fragmentary microautophagy, only part of a large lipid droplet is sequestered by autophagosomes. The droplet is then detached as a double-membrane vesicle enriched with LC3 and the contained material is gradually degraded by lysosomes. In contrast, macroautophagy results in the entrapment of the entire lipid droplet inside the autophagosome. After fusion with the lysosome, complete degradation of the droplet occurs in the autolysosome [62,64]. Conducted studies have shown that lipophagy can contribute to both inhibition and stimulation of cancer cell growth. The anti-tumor effect of lipophagy depends on the level of LAL (Lysosomal Acid Lipase), which is a tumor suppressor. Zhao et al. demonstrated that abnormal levels of LAL, specifically a deficiency of this enzyme, enables the growth and metastasis of cancer cells [65]. On the other hand, the carcinogenic effect of lipophagy is related to the possibility of using stored LDs as specific energy resources in the tumorigenesis process, which may contribute to cancer development [66].

### 2.2.7. Lysophagy

Lysosomes are small, acidic organelles that break down redundant intracellular materials. They contain a large number of hydrolytic enzymes and various membrane proteins. Destabilization of the lysosome leads to the release of significant amounts of hydrolases from its interior into the cytosol, a detrimental phenomenon for the cell [67,68]. Furthermore, lysosome rupture results in the release of calcium ions and protons from the lysosomal compartment into the cytosol, leading to impairment of cellular function [69]. Damaged lysosomes can be degraded by selective autophagy, termed 'lysophagy'. Following the damage of lysosomal membrane induced by various factors e.g., viral or bacterial toxins,  $\beta$ -amyloid, mineral crystals or lysosomotropic factors the induction of lysophagy occurs [70]. Galectins localized in the cytosol receive signals about the damage that has occurred and induce the ubiquitination of proteins located in the lysosomal membrane. Protein ubiquitination leads to the recruitment of additional adaptors such as SQSTM1. This triggers the core autophagy machinery, engulfment of the damaged organelle by the phagophore, and downstream fusion of normal lysosomes with autophagosomes to degrade damaged lysosomes [71].

### 2.2.8. Nucleophagy

The last subtype of selective autophagy is degradation of nuclear components, such as RNA, DNA, nuclear proteins or nucleolus, called 'nucleophagy'. We can distinguish between two types of nucleophagy: macronucleophagy (in mammals) and micronucleophagy (in yeast). Macronucleophagy is based on the degradation of redundant nuclear components via engulfing the material by autophagosomes. Next, autophagosomes merge with lysosomes, where degradation of the redundant material occurs [72,73]. Nucleophagy has a dual function in tumorigenesis—it can both induce and inhibit cancer cells. The carcinogenic effect of nucleophagy, observed in the later stages of tumor growth, is based on the providing of nutrients that allow tumor cells to survive and metastasize in a nutrient-poor environment. In contrast, the anti-cancer effect of this process is based on the removal of damaged DNA or nuclear structures. As a result, it is possible to preserve the normal integrity of nuclear structures and consequently prevent the development of cancer [74].

## 2.3. Microautophagy

The term 'microautophagy' was introduced by lysosome discoverer—Christian de Duve. One of the hypotheses put forward by a Belgian scientist, regarding the process of

multivesicular lysosomes formation, was “internalization by ‘microautophagy’ of small cytoplasmic buds in shrinking lysosomes” [75]. Microautophagy, a process of non-invasive engulfment of cytoplasmic material through membrane invaginations, occurring directly in lysosomes. Although more than 50 years have passed since the Christian de Duve’s discovery, we still know relatively little about the molecular mechanism of microautophagy as well as how this process is regulated [76].

Mammals’ inability to distinguish between lysosomes and late endosomes results from the complexity of the endocytic system. Furthermore, these structures have the same diameter (about 500 nm) and are significantly smaller compared to autophagosomes found in macroautophagy [77]. All of these aspects make the size of the microautophagic load limited and also the process itself more difficult to detect than macroautophagy [78].

Sahu and co-authors found that in mammalian organisms microautophagy occurs on late endosomes (Figure 3). The substrates of this process are randomly or selectively collected and transported to endosomes in vesicles. Similar to the CMA described above, endosomal microphagy (eMI) substrates have a KFERQ-like motif and are delivered to endosomes by Hsc70 (Heat shock cognate protein 70). However, in contrast to the CMA, eMI process do not require either substrates unfolding or LAMP2A (Lysosome-Associated Membrane Protein type 2A) involvement [79]. Due to the fact that eMI does not require the involvement of LAMP2A, which is found only in avian and mammalian genomes, this mechanism may also occur in other organisms carrying proteins with the KFERQ-like motif [80]. In the eMI process, endosomal membrane invagination occurs with the help of the ESCRT (Endosomal Sorting Complex Required for Transport) machinery [79,81]. Furthermore, another structure which is partially involved in that process is Hsc70, which may cause membrane deformation when bound to phosphatidylserine [79,82]. eMI substrates, integrated into intraluminal vesicles may be degraded in lysosomes/endosomes or can be secreted outside the cell [83].

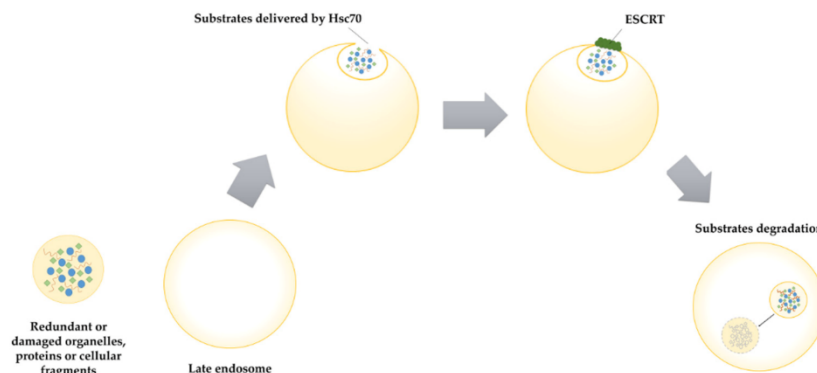


**Figure 3.** Microautophagy. Redundant or damaged organelles, proteins or cellular fragments are transported inside the formed vesicle to the late endosome by Hsc70. Subsequently, endosomal membrane invagination occurs with the involvement of ESCRT (Endosomal Sorting Complex Required for Transport). The final stage of microautophagy process is the degradation of substrates inside the endosome.

Mejlvang et al. conducted a study investigating the effect of amino acid starvation on the induction of autophagy. The results showed that starvation leads to immediate activation of autophagic response based on macroautophagy and subsequent eMI. Degradation of autophagy receptors via eMI ensures rapid decomposition of supplied substrates. This enables the maintenance of the initiated anabolic processes and, subsequently, the introduction of appropriate adaptive mechanisms allowing cells to survive a period of prolonged starvation. This phenomenon may be important in the survival and development of cancer cells [84]. To date, endosomal microautophagy is the least studied and described type of autophagy. Its exact role in tumorigenesis remains unclear and requires further studies.

#### 2.4. Chaperone-Mediated Autophagy

The last of described type of autophagy is chaperone-mediated autophagy (CMA). It is one of the intracellular proteins degradation pathways occurring in lysosomes (Figure 4). Unlike microautophagy, which requires the presence of multilamellar vesicle bodies that capture redundant fragments of cellular organelles [85], in the case of CMA, substrate proteins are identified individually by a cytosolic chaperone, Hsc70. Moreover, the microautophagy process does not require the presence of LAMP2A during cargo transport to the late endosome [85]. CMA selectivity is based on a specific sequence (KFERQ-like motifs) found in all proteins constituting the substrate of that process [86]. Furthermore, in certain cases where the specific motif is incomplete, it is possible to obtain recognizable sequence thanks to post-translational acetylation or phosphorylation [87]. Only the recognized proteins are further transported to the lysosome surface by Hsc70 and its co-chaperones. This mechanism is completely different from that which occurs in microautophagy and macroautophagy processes, where substrates are transported to lysosomes inside the vesicles [11,88]. In the next step, proteins delivered on lysosome surface bind to lysosome-associated membrane protein type 2A. The formation of the protein-lysosomal receptor complex (mass 700 kDa) allows further transport of substrate proteins into the lumen of the lysosome, where hydrolytic enzymes subsequently degrade them [86].

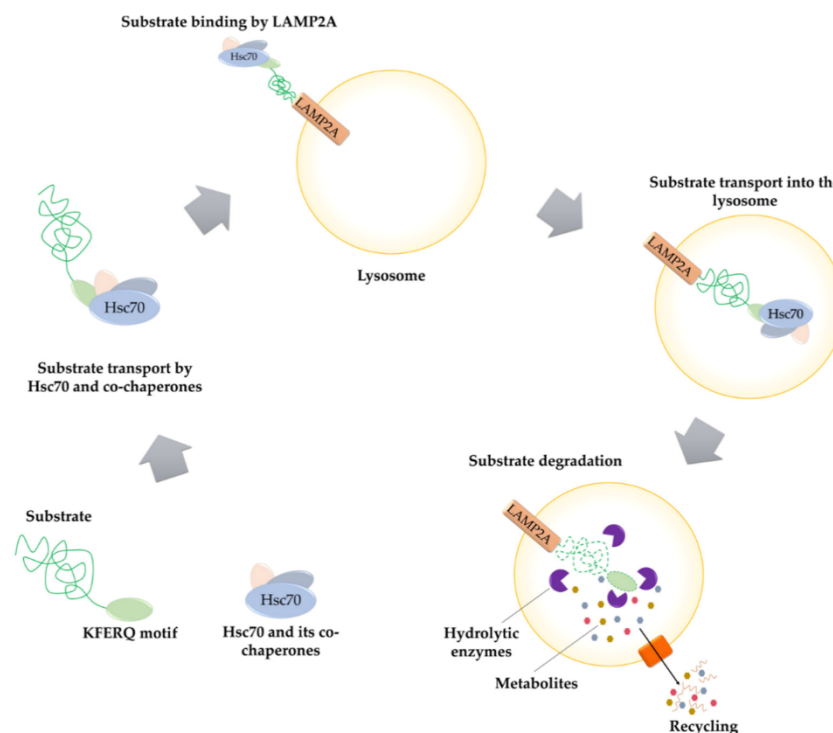


**Figure 4.** Chaperone-mediated autophagy. Substrate proteins with KFERQ motif are identified by Hsc70 (Heat Shock Cognate protein 70). Next, the recognized substrates are transported by Hsc70 and its co-chaperones on the lysosome surface. Delivered proteins bind to the LAMP2A (Lysosome-Associated Membrane Protein type 2A) and LAMP2A-protein complex is formed. At the final stage of the CMA process, substrate proteins are transported into the lysosome lumen and their degradation by hydrolytic enzyme occurs.

CMA selectivity allows to control the level of many specific proteins in the cell, including proto-oncogenic proteins [11]. The occurrence of CMA dysfunction could lead to the adverse phenomenon of oncogenic protein accumulation inside the cell. One of the

important transcription factors is MYC, which level is indirectly regulated by CMA [89]. In CMA-deficient cells, higher levels of MYC are observed. This leads to tumor-beneficial metabolic changes and an increase in the intensity of cell proliferation. Therefore, a normal CMA pathway prevents the malignant transformation of normal cells [89]. Unfortunately, in cancer cells, the anticancer properties of CMA promote tumorigenesis. After transformation, an increase in CMA activity is observed to enable the maintenance of important pro-oncogenic functions [90]. A perfect example of this action is the effect of CMA on hexokinase II, which is a glycolytic enzyme essential for tumorigenesis [91]. As a result of phosphorylation of the enzyme at the Thr473 position, the degradation process of hexokinase II by CMA does not occur, thereby increasing the protein stability. This leads to enhanced glycolysis and stimulates cell growth of HEK293T, MCF-7, MDA-MB-231, and SW480 (breast cancer) lines in vitro and in vivo [92].

### 3. Autophagy and Programmed Cell Death—Double-Edged Sword Relationship

Autophagy and apoptosis are regulated in the cell by different mechanisms. However, it happens that both processes overlap. Under the influence of stress, sequential or simultaneous activation of the apoptotic and autophagy pathways can occur in a cell. There are potential pathways of the relationship between apoptosis and autophagy: activation of autophagy and subsequent inhibition of apoptosis, activation of autophagy leading to activation of the apoptotic pathway, autophagy suppression and induction of apoptosis or activation of autophagy and apoptosis simultaneously, leading to cell death on apoptotic and autophagy-dependent pathway (Figure 5) [93–95]. In the former case, the cell activates autophagy in response to a stress signal. As a defense mechanism, autophagy leads to the removal of damaged fragments, preventing the activation of the apoptotic pathway. The second possibility is a situation in which the cell is no longer able to defend itself against the resulting damage, and the activated autophagy subsequently leads to activation of apoptosis and cell death. In the last case, a stress signal triggers both processes, resulting in cell death via two pathways [93]. Key factors connecting apoptosis and autophagy include, for example: p53, Bcl-2/Beclin 1, Atg proteins, p62 or caspases.

#### 3.1. p53 in Apoptosis and Autophagy

p53, a protein which binds specific DNA sequences, is involved in many cellular processes including repair of damaged DNA and induction of apoptosis. Due to its ability to regulate the cell cycle, p53 is called the guardian of the genome [96]. Activation of this factor can occur, for example, as a result of DNA damage, hypoxia, or nutritional stress [97–99]. p53 can affect both the extrinsic and intrinsic pathway of apoptosis. DNA damage causes mitochondrial translocation of p53. The protein promotes cytoplasmically localized Fas and TRAIL receptors, leading to induction of the extrinsic apoptotic pathway [100,101]. However, in the cell nucleus, p53 promotes many proapoptotic proteins, such as Bid, PUMA or Bax. In addition, it leads to inhibition of Bcl-2 expression, and both of these actions trigger the intrinsic apoptosis pathway [101].

The p53 protein is also involved in the regulation of autophagy. Based on their study, Crighton and co-authors found that genotoxic stress results in transcriptional activation of DRAM (Damage-Regulated Autophagy Modulator), a direct target gene of p53, which causes induction of autophagy. The DRAM signaling cascade promotes the fusion of autophagosomes and lysosomes, resulting in the formation of autolysosomes. This p53 target gene is an essential factor in the proper functioning of the apoptosis regulatory network and p53-dependent autophagy [102]. Furthermore, Tasdemir et al. demonstrated that cytoplasmically localized p53 through inactivation of AMPK and subsequent activation of the mTOR signaling pathway leads to inhibition of autophagy in the cell [103].

Scherz-Shouval and co-authors detected a relationship between autophagy and apoptosis processes. They revealed that under starvation conditions, p53 post-translationally inhibits the regulation of LC3 level, which leads to its accumulation in cells and decreases the rate of the autophagy process. The consequence is cell death by apoptosis [104].



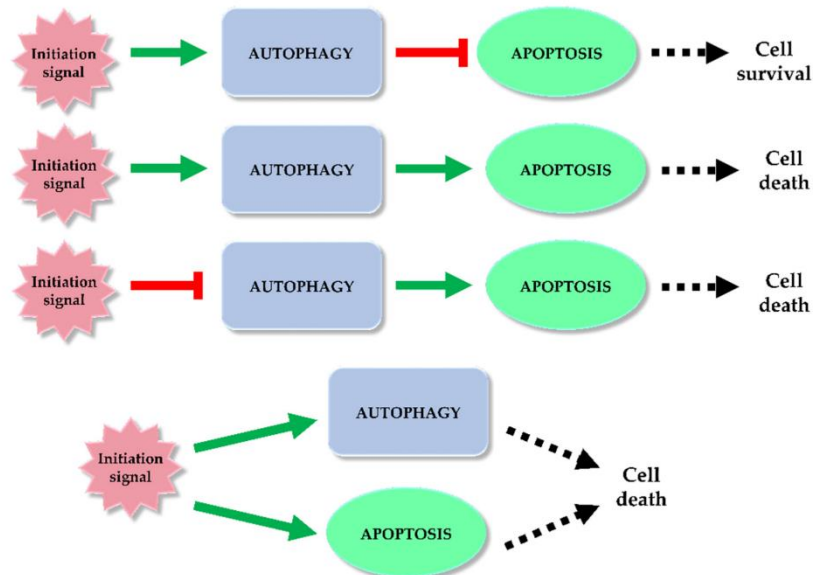


**Figure 5.** Autophagy and apoptosis relationship. Among the potential correlation pathways between autophagy and programmed cell death we can distinguish: activation of autophagy and apoptosis inhibition, activation of autophagy and activation of the apoptotic pathway, autophagy suppression and induction of apoptosis or simultaneous activation of autophagy and apoptosis leading to ADCD and apoptosis. The inhibitory effect of each process (red mark) and inducing effect (green mark) is indicated on the scheme.

### 3.2. Bcl-2/Beclin 1 in Apoptosis and Autophagy

Bcl-2, members of the B-cell lymphoma family of proteins, inhibits the release of cytochrome c from the mitochondrial interior, thereby playing a key role in the intrinsic apoptotic pathway [105]. Beclin 1 is a key element involved in autophagosome formation and is also an important component of the PI3K/Vps34 class III complex [106]. Bcl-2 binding to Beclin 1 leads to dissociation of Beclin 1 from PI3K class III, which results in inhibition of autophagy [107]. However, the occurrence of mutation in the BH3 receptor domain of Bcl-2 or Beclin 1 domain leads to dysfunction of Bcl-2/Beclin 1 complex, intensification of autophagy and promotion of cell survival [108,109].

Under nutrient-deficient conditions, autophagy is an essential element for cell survival. Activation of JNK1 (C-Jun N-terminal protein Kinase 1) and phosphorylation of residues involved in the Bcl-2's regulatory loop lead to the destruction of the Bcl-2/Beclin 1 complex and consequently to initiation of autophagy [110]. Under standard conditions the phosphorylated Bcl-2 molecule binds to Bax, leading to inhibition of apoptosis. Due to the normal phosphorylation of Bcl-2, it is possible to maintain the integrity of the mitochondrial membrane, which in turn protects cells from death by the intrinsic apoptotic pathway. Sustaining the integrity of the mitochondrial membrane prevents the release of proapoptotic proteins from within the organelle into the cytoplasm [111]. However, in the situation of long-term nutrient deficiency, autophagy is not able to alleviate cellular damages. Intensification of Bcl-2 phosphorylation (hyperphosphorylation) promoted by JNK1 occurs [112]. This results in dissociation of the Bcl-2 molecule from Bax and apoptotic cell death. When the cell receives adequate amounts of nutrients, Bax/Bak and Beclin 1 bind to Bcl-X<sub>L</sub> or Bcl-2, leading to the inhibition of activation of both processes, apoptosis and autophagy [109,113].

### 3.3. Atg Proteins in Apoptosis and Autophagy

The level of autophagy-related proteins in a cell is regulated by the availability of growth factors and nutrients essential for proper cell functioning. Among Atg proteins we can distinguish the Atg12–Atg5 complex, which is important in both autophagy and apoptosis [114].

The Atg12–Atg5 complex, essential for autophagosome formation, also participates in the apoptotic pathway in an unconjugated form. Atg12 binding through a BH3-like motif to Bcl-2 and Mcl-1 (Myeloid Cell Leukemia 1) increases the intensity of the intrinsic apoptotic pathway. Interestingly, the anti-apoptotic properties of Mcl-1 can be inhibited in the cell as a result of abnormal Atg12 expression. Moreover, silencing Atg12 in an apoptotic cell will result in the inhibition of Bax induction and the arrest of cytochrome c release from the mitochondrion [115]. Cleaved by cell stress-activated cysteine proteases (caplains), Atg5 plays a significant role in the initiation of the intrinsic apoptosis pathway. As a consequence of cleavage, translocation of the N-terminal part of the Atg5 protein into the mitochondrion occurs. Inside the organelle, this fragment interacts with Bcl-X<sub>L</sub> allowing Atg-5 to be involved in the release of cytochrome c from the mitochondrion and indirectly participating in apoptosis promotion [116]. Taken together, Atg5 and Atg12 proteins may be involved in both autophagy and apoptosis, depending on the cellular conditions.

### 3.4. p62 in Apoptosis and Autophagy

p62, also known as SQSTM1, is a multi-domain adaptor protein that controls cell viability by regulating both autophagy and apoptosis [117]. By polymerizing with other p62 molecules, this protein has the ability to accumulate ubiquitin-tagged proteins. Aggregates of p62 (called p62 speckles), through their storage properties and ability to bind to the LC3 molecule, recognize, gather, and most importantly transport cargo to the autophagosomes [96]. p62, through its ability to activate caspase-8 on the autophagosome membrane also plays an important role in the induction of apoptosis. The autophagy-dependent mechanism of caspase-8 activation involves simultaneous induction of autophagy and activation of caspase-8. The autophagosomal membrane provides some kind of platform on which the caspase cascade leading to cell death by apoptosis is initiated. Depletion of Atg3 or Atg5 leads to the suppression of autophagosome formation, which in turn results in the inhibition of caspase-8 activation and subsequent suppression of apoptosis [118].

### 3.5. Caspases in Apoptosis and Autophagy

Caspases, enzymes belonging to the group of cysteine proteases, have been known to science for a long time. Their participation and the exact mechanism of action in the process of apoptosis have been widely studied and described in many scientific articles [119–121]. These enzymes are involved in both intrinsic and extrinsic pathways of apoptosis, acting as initiators (caspases-2, -8, -9 and -10) or effectors (3, -6 and -7) [122]. Caspases under standard conditions occurring in the form of inactive zymogenic precursors can be activated under the influence of various external or internal stimuli that initiate apoptosis. Activated enzymes may participate in the apoptotic pathway [123]. Despite the significant differences between the autophagy and apoptosis processes, the conducted studies indicate that caspases also affect the autophagy process. Oral and co-authors have shown that overexpression of caspase-8 leads to degradation of Atg3 protein and thus prevents its pro-autophagic activity [124]. Furthermore, Wirawan et al. showed that two key components of the autophagy-inducing complex (class III PI3K and Beclin 1) are direct substrates of caspases. It was observed that in response to different signals inducing the two apoptotic pathways, these enzymes cause cleavage of the complex components. Thus, the researchers confirmed that class III PI3K and Beclin 1 are substrates of caspases [125]. In contrast, Han and co-authors showed that caspase-9, by promoting Atg7-dependent LC3-II transformation, facilitates autophagosome formation. Moreover, the authors showed that depending on the cellular conditions, Atg7 can also form a complex with caspase-9 and directly inhibit

the proapoptotic activity of the enzyme [126]. All of these studies indicate there is a mutual correlation between autophagy and apoptosis processes.

#### 4. Autophagy Inhibitors and Activators

In a cancer therapy context, autophagy is a dichotomous process—it may inhibit or induce tumor growth (Figure 6) [127]. As a mechanism that promotes cancer cells development, autophagy protects cells from the negative impact of various forms of cellular stress. In anti-cancer therapy, that process is referred to as ‘adaptive autophagy’. It sustains cancer cells growth, increasing chances of tumor survival despite the use of toxic chemotherapeutics or ionizing radiation. However, intentional inhibition of adaptive autophagy leads to reversal of this phenomenon, causing cells re-sensitization to ionizing radiation or used chemotherapeutic agents [128,129]. On the other hand, autophagy can promote genomic stability and inhibits inflammation at the early stage of carcinogenesis process. Interestingly, in animals disruption of *ATG* genes results in accelerated cancer development [128].

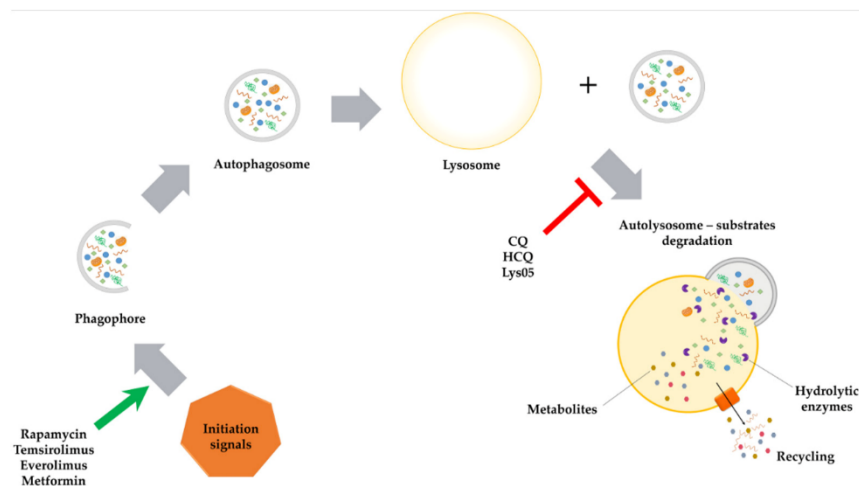


**Figure 6.** The influence of selected inhibitors or activators on autophagy process. Rapamycin, temsirolimus, everolimus and metformin via inhibition of initiation signals, stimulates autophagy process (marked with green arrow on the scheme). Chloroquine (CQ), hydroxychloroquine (HCQ) and Lys05 through blocking of autophagosome and lysosome fusion inhibits the autophagy (marked with red T-shaped sign on the scheme).

#### 4.1. Autophagy Inhibitors Undergoing Clinical Trials

##### 4.1.1. Chloroquine

Chloroquine (CQ) is a compound known for many years. This aminoquinolone derivative was first approved by the U.S. Food and Drug Administration (FDA) in October 1949 as an antimalarial agent [130]. Although more than 70 years have passed since the CQ was discovered, the detailed mechanism of the antimalarial effect of this agent remains unknown. Presumably, CQ as a weak base, acting as a lysosomotropic compound, inhibits lysosome activity [131]. Chloroquine is protonated after entering the lysosome, due to low pH inside the organelle. Protonated CQ accumulation inside the lysosome leads to inhibition of autophagic cargo degradation and consequently blocked autophagic flux [132]. Inhibition of cargo degradation located inside the lysosome stops the last autophagy stage. As a consequence, the ability to provide energy to the cell through the autophagy process is blocked. CQ’s ability to inhibit autophagy is being used by scientists e.g., in the investigation of new cancer therapy methods.

Erkisa et al. [35] published an article describing the combination therapy of metastatic prostate cancer using the palladium(II) barbiturate complex and CQ. The author's study showed increased efficacy of combined therapy: CQ and palladium(II) barbiturate complex compared to single-agent (CQ or palladium(II) barbiturate complex alone) treatment. The use of CQ resulted in inhibition of prosurvival autophagy function and consequently increased the sensitivity of tumor cells to the tested complex [133]. A paper recently published by Lopiccio and co-authors describes in vitro and in vivo studies using chloroquine and nelfinavir as a combination therapy in non-small cell lung cancer (NSCLC) treatment. The obtained results indicate that both in vitro and in vivo, combination therapy was effective in NSCLC treatment. The combined administration of CQ and nelfinavir resulted in increased inhibition of NSCLC cell growth while enhancing apoptosis and ER stress induction [134]. Next interesting, this year's paper is an article published by Wei et al. describing the use of cyanidin-3-O-glucoside (C3G) combined with CQ in *Drosophila* malignant  $Raf^{GOF}$ scrib<sup>-/-</sup> model to determine the antitumor activity of C3G. Results presented in the paper revealed that CQ and C3G combined therapy is more effective against *Drosophila* malignant  $Raf^{GOF}$ scrib<sup>-/-</sup> model than CQ or C3G used alone [135]. All papers and results mentioned above suggest that the combination of CQ with the different compound may be more effective than single-agent therapy.

#### 4.1.2. Hydroxychloroquine

Hydroxychloroquine (HCQ), belonging to the 4-aminocholine class, is a CQ analogue. The original CQ molecule has been enriched with a hydroxyl group, thus forming HCQ, which compared to the parent compound is three times less toxic [136]. In 1955, HCQ was approved by the FDA and, like CQ, registered as an antimalarial agent [137]. Hydroxychloroquine as an inhibitor of autophagy process blocks autolysosomes formation by preventing lysosomes and autophagosomes fusion [138,139]. Both HCQ and described above CQ have been used as standard autophagy inhibitors in many clinical and preclinical studies. Only right now (May 2021) there are at least a dozen active clinical trials on the use of HCQ in the treatment of various cancers ([ClinicalTrials.gov](https://ClinicalTrials.gov), accessed on 27 May 2021). The Emory University is actively recruiting patients for a trial investigating the use of HCQ in combined therapy (HCQ + paricalcitol with standard chemotherapeutics: gemcitabine + nab-paclitaxel) of metastatic or advanced pancreatic cancer (NCT04524702). As another example, M.D. Anderson Cancer Center is investigating the use of HCQ with letrozole and palbociclib in patients with estrogen receptor-positive, HER2 negative breast cancer before they undergo surgery. This study aims to enhance the efficacy of the provided treatment (NCT03774472). Finally, it is also worth mentioning that there are many ongoing clinical trials on the use of CQ and HCQ in the treatment of patients with COVID-19 ([ClinicalTrials.gov](https://ClinicalTrials.gov)).

#### 4.1.3. Verteporfin

Verteporfin is benzoporphyrin derivative consisting of two regioisomers (I and II). This compound was approved by the FDA in 2002 for photodynamic therapy of patients with age-related macular degeneration [140,141]. To find new autophagosomes accumulation inhibitors, scientists decided to screen the databases of off-patents agents and libraries of compounds with known pharmacological activity. Among  $\approx 3500$  of screened compounds, only verteporfin (VP) was selected for further investigation. Donohue et al. examined the ability of verteporfin to inhibit autophagy process by pre-treating MCF-7 cells with CQ. Autophagosomes accumulation induced by CQ was subsequently inhibited by verteporfin. Furthermore, inhibition of accumulation of autophagosomes occurred in the dark. Based on this, the authors concluded that the ability of verteporfin autophagy inhibition is not associated with its photodynamic properties [141]. Researchers are investigating the use of verteporfin in the treatment of various cancers. The increased efficacy of gemcitabine in combination with verteporfin in the treatment of pancreatic ductal adenocarcinoma model, the improved effectiveness of sorafenib therapy with VP against hepatocellular

carcinoma or the increased sensitivity of osteosarcoma cells to treatment caused by the use of VP have been demonstrated [142–144]. In addition, currently ongoing clinical trials are investigating the use of VP, e.g., for the treatment of recurrent prostate cancer (NCT03067051) or pancreatic cancer therapy (NCT03033225).

#### 4.1.4. Clarithromycin

Clarithromycin (CAM) is well-known medicine, belonging to the class of macrolide antibiotics. Approved in 2000 by the FDA [145], CAM is commonly used in therapy of various bacterial infections, treatment of *Helicobacter pylori*-induced gastric infections or Lyme disease therapy. Data collected from the extensive clinical and preclinical studies on CAM indicate that the drug, combined with conventional therapeutics, could be used to treat various cancers. CAM's anticancer properties are based on its ability to anti-angiogenesis, pro-inflammatory cytokines reduction and autophagy inhibition [146]. After the fusion of autophagosomes and lysosomes, autophagy is blocked by inhibition of lysosomes function [147]. Ongoing clinical trials are investigating the CAM's application in the treatment of: multiple myeloma (NCT04302324, NCT04063189, NCT02542657), mucosa-associated lymphoid tissue lymphoma (NCT03031483) and previously untreated, advanced-stage indolent lymphoma (NCT00461084).

Information regarding the compounds undergoing clinical trials is collected in Table 1. Target points, adverse effects and selected therapeutic schemes of described autophagy inhibitors are presented in Table 2.

**Table 1.** Selected autophagy inhibitors under clinical investigation.

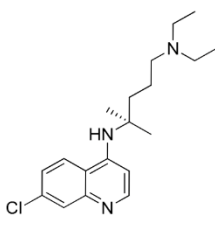
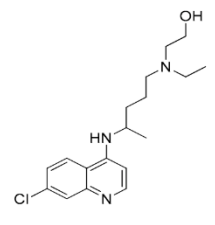
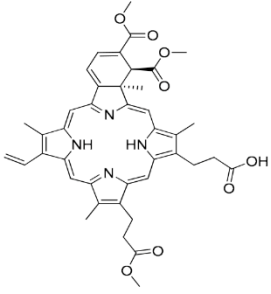
Autophagy Inhibitor	Chemical Structure	Study Type	References
Chloroquine		<b>Preclinical studies:</b> metastatic prostate cancer, NSCLC treatment	[133–135]
Hydroxychloroquine		<b>Clinical trials:</b> therapy of metastatic or advanced pancreatic cancer or HER2 negative breast cancer	NCT04524702, NCT03774472
Verteporfin		<b>Preclinical studies:</b> treatment of pancreatic ductal adenocarcinoma, hepatocellular carcinoma or osteosarcoma <b>Clinical trials:</b> recurrent prostate cancer or pancreatic cancer treatment	[141–144] NCT03067051, NCT03033225

Table 1. Cont.

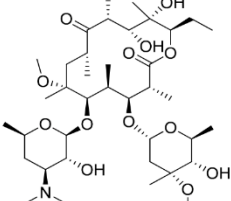
Autophagy Inhibitor	Chemical Structure	Study Type	References
Clarithromycin		<b>Clinical trials:</b> multiple myeloma, mucosa-associated lymphoid tissue lymphoma or previously untreated, advanced-stage indolent lymphoma therapy	NCT04302324, NCT04063189, NCT02542657, NCT03031483, NCT00461084

Table 2. Target points, adverse effects and selected therapeutic schemes of autophagy inhibitors.

Autophagy Inhibitor	Target Point	Adverse Effects	Therapeutic Combination or Single-Agent Treatment	Tumor Type	References
Chloroquine	lysosomes	headache, visual disturbances, pruritus or gastrointestinal upset, the risk of acute kidney injury due to kidney cells sensitization to chemotherapy [148]	CQ + temozolomide + radiation therapy	glioblastoma, gliosarcoma and astrocytoma (grade IV)	NCT04397679, NCT02432417
			CQ + taxane after anthracycline failure	advanced or metastatic breast cancer	NCT01446016
Hydroxychloroquine	lysosomes	no adverse effects observed	HCQ + paclitaxel + carboplatin	advanced or recurrent NSCLC	NCT01649947
			HCQ + capecitabine, oxaliplatin and bevacizumab	metastatic colorectal cancer	NCT01006369
Verteporfin	autophagy formation	no adverse effects observed	verteporfin photodynamic therapy	advanced pancreatic cancer	[149]
Clarithromycin	autophagy flux	anemia, gastrointestinal disorders, dyspnea	clarithromycin + abemaciclib	neoplasm	NCT02117648
		upper respiratory infections, sinus/acute otitis	clarithromycin, dexamethasone, lenalidomide therapy after stem cell transplant	multiple myeloma	NCT00445692
Clarithromycin	autophagy flux	anemia, neutropenia, diarrhea, vomiting, fever, lung infection, renal insufficiency, dehydration, dyspnea	clarithromycin, dexamethasone, pomalidomide	relapsed or refractory myeloma	NCT01159574

## 4.2. Autophagy Inhibitors Undergoing Preclinical Trials

### 4.2.1. 3-Methyladenine

3-Methyladenine (3-MA) was discovered in 1982 by Seglen & Gordon. The scientists through screening of a large number of N6-methylated adenosine derivatives selected the most promising compound, which appeared to be 3-MA [150]. Nowadays, 3-MA is one of the most commonly used autophagy inhibitor [151]. This compound affects two molecular targets involved in the autophagy process: phosphoinositide 3-kinase (PI3K) and Vps34. The duality of the compound's action means that it affects autophagy with increased potency [152,153]. Wu et al. in their work described the duality of 3-MA action. Based on the obtained results scientists concluded that the compound, when administered over a prolonged period, in nutrient-rich conditions, promotes autophagic flux. However, under nutrient-deficiency conditions, it inhibits autophagy [154].

Scientists around the world are conducting research on the use of 3-MA combined with different drugs in the therapy of various cancers. Wang et al. showed in their *in vitro* studies that resveratrol used alone against human ovarian serous papillary cystadenocarcinoma cell line SK-OV-3 can inhibit apoptosis by inducing autophagy. Furthermore, results obtained from combined therapy (resveratrol with 3-MA) revealed that simultaneous application of autophagy inhibitor and chemotherapeutic drug in SK-OV-3 tumor could improve the drug efficiency and also protect normal cells from tumorigenesis [155]. In a recently published paper, Zhao et al. investigated the effect of 3-MA on the treatment of hepatocellular carcinoma cells (HepG2 cell line). They showed that 3-MA (used in combined therapy with sorafenib), by inhibiting the autophagosome formation, leads to a reduction of acquired sorafenib resistance of HepG2 cells [156].

### 4.2.2. SAR405

SAR405, Vps34 and Vps18 inhibitor with low molecular mass, was first described in 2014 by Ronan et al. [157]. Research published a year after by Pasquier revealed that inhibition of Vps34 by SAR405 leads to the impairment of lysosome function and inhibition of autophagy process [158]. In 2020, Janji et al. published an article describing the usage of Vps34 inhibitors (SAR405 and SB02024) in the therapy of colorectal and melanoma tumor cells. Based on the obtained results, scientists concluded that the use of these compounds enhances the therapeutic effect of the applied anti-PD-1/PD-L1 immunotherapy [159].

### 4.2.3. Lys05

Lys05 is a water-soluble bisaminoquinoline inhibitor of autophagy. The enhanced autophagy inhibition by Lys05 compared to CQ and HCQ is attributed to the presence of C-7 chlorine, triamine linker and two aminoquinolone rings in the Lys05 structure. A study conducted by McAfee and co-workers compared the efficacy of HCQ and Lys05 in treatment of C8161, PC-9, LN-229 cell lines and 1205Lu xenograft model. Obtained *in vivo* results revealed 34-fold higher Lys05 concentration in tumor cells compared to HCQ. Moreover, a Lys05 application-related double accumulation of autophagy vesicles compared with HCQ therapy in a used xenograft model was observed [160].

DeVorkin et al. published an article in which they showed that the administration of Lys05 together with sunitinib (receptor tyrosine kinase inhibitor) improve the therapeutic effect of this drug. In used clear cell ovarian carcinoma xenograft models, inhibition of autophagy process by Lys05 resulted in enhancing the anti-cancer activity of sunitinib compared with single-agent treatment (sunitinib or Lys05 alone) [161]. In an article titled, "Targeting quiescent leukemic stem cells using second generation autophagy inhibitors," Baquero et al. investigated the potential application of Lys05 with tyrosine kinase inhibitors in the treatment of chronic myeloid leukemia (CML). The obtained results showed that Lys05-mediated inhibition of autophagy process affects tumor cells via reduction of quiescence of leukemic stem cells and increasing the expansion of myeloid cells [162].

#### 4.2.4. ROC-325

ROC-325 is a compound developed by applying a logical medicinal chemistry approach to drug design. To create a more effective, well-tolerated and more potent autophagy inhibitor, scientists generated new dimeric compounds based on the modified CQ, HCQ and lucanthone (antischistosomal drug) elements. Carew et al., based on the obtained results, concluded that ROC-325 (with lucanthone and HCQ motifs) exhibited significantly greater anti-cancer activity against various types of cancer than the parent compounds. Moreover, they found that ROC-325 used at much lower doses inhibited autophagy more effectively than HCQ.

Based on in vitro studies using renal cell carcinoma models, it was possible to determine the ROC-325 effect on the autophagy process. ROC-325 was shown to inhibit autophagic flux as well as lead to the autophagosomes accumulation and lysosomes deacidification. Under in vivo conditions, the compound administered orally to mice at low doses inhibited tumor growth more effectively than HCQ administered at high doses. Furthermore, by analyzing of tumor samples from ROC-325 treated mice, autophagy was inhibited and apoptosis and proliferation of tumor cells were reduced [163]. In 2019, Nawrocki et al. conducted preclinical in vitro and in vivo studies on the use of ROC-325 in acute myeloid leukemia (AML). The in vitro studies examined the efficacy of ROC-325 (single-agent treatment or in combination with azacitidine) against four tumor cell lines: MV4-11, MOLM-13, KG-1 and HL-60. During in vivo studies, mice were treated with azacitidine (AZA), ROC-325 or AZA + ROC-325 combination. The results obtained in vitro as well as in vivo indicated that combination therapy is more effective and significantly extended the overall survival time. In addition to this, the combined agents were well tolerated [164].

#### 4.2.5. Spautin-1

Spautin-1 was originally identified as a selective and strong phosphodiesterase type 5 inhibitor [165,166]. During preclinical studies, the researchers discovered that spautin-1 is also an autophagy inhibitor. The obtained results revealed that by promoting the degradation of Vps34 complexes, spautin-1 inhibits two ubiquitin-specific peptidases (USP10 and USP13), which consequently leads to inhibition of the autophagy process [167]. The collected data suggest that spautin-1 could be used in the treatment of ovarian cancers [168], CML [169] or prostate cancer [170].

#### 4.2.6. MM124 and MM137

MM124 and MM137 are compounds belonging to a group of 7-methyl-5-phenyl-pyrazolo[4,3-*e*]tetrazolo[4,5-*b*][1,2,4]triazine sulfonamide derivatives. In a study conducted by Gornowicz et al., the anticancer effects of new derivatives on colorectal cancer cells were investigated. The obtained results showed that MM124 and MM137 decrease the concentration of LC3A, LC3B and Beclin 1 in the tested cell lines (DLD-1 and HT-29). Based on this, the researchers concluded that MM124 and MM137 could inhibit the autophagy process at the autophagosome formation level. Nevertheless, further in vivo studies are required to confirm the autophagy-inhibiting effect of the novel derivatives [171].

Table 3 summarizes information about autophagy inhibitors undergoing preclinical investigation.



**Table 3.** Selected autophagy inhibitor under preclinical investigation.

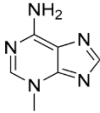
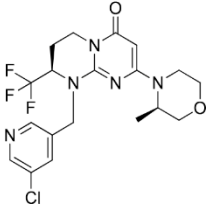
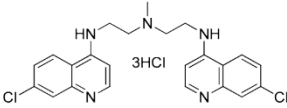
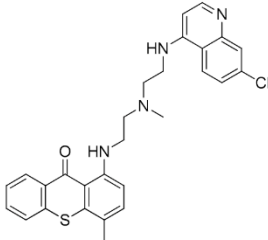
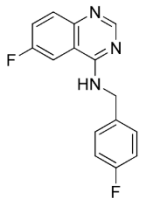
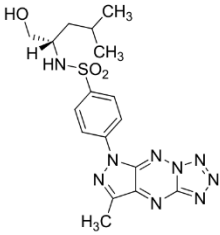
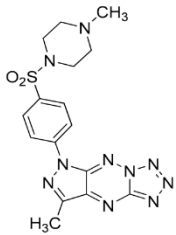
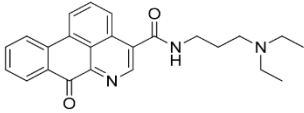
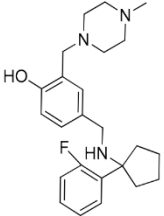
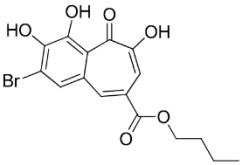
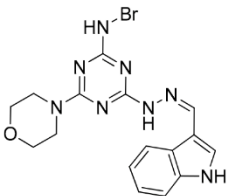
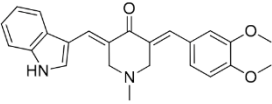
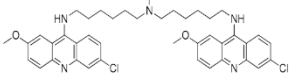
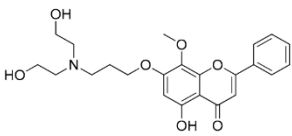
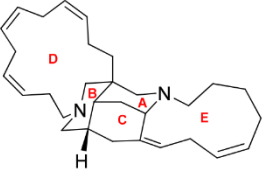
Autophagy Inhibitor	Chemical Structure	Preclinical Studies	References
3-Methyladenine		therapy of human ovarian serous papillary cystadenocarcinoma or hepatocellular carcinoma	[155,156]
SAR405		colorectal and melanoma tumors treatment	[159]
Lys05		ovarian carcinoma or CML therapy	[160–162]
ROC-325		treatment of AML	[164]
Spautin-1		ovarian cancers, CML or prostate cancer treatment	[168–170]
MM124		in vitro studies on colon cancer cells	[171]
MM137		in vitro studies on colon cancer cells	[171]

Table 3. Cont.

Autophagy Inhibitor	Chemical Structure	Preclinical Studies	References
S130		colorectal cancer therapy	[172]
ARN5187		breast cancer treatment	[173,174]
UAMC-2526		human colon adenocarcinoma treatment	[175]
DCZ5248		colon cancer therapy	[176]
CA-5f		NSCLC therapy	[177]
DQ661		melanoma, colon cancer or pancreatic cancer therapy	[178]
FV-429		gastric cancers or T-cell malignancies treatment	[179,180]
Madangamine A		human cervical carcinoma, human fibrosarcoma and human melanoma therapy	[181]

### 4.3. Autophagy Activators Undergoing Clinical Trials

#### 4.3.1. Rapamycin

Rapamycin (RAPA, Sirolimus) is a 31-membered macrocyclic antifungal antibiotic produced by *Streptomyces hygroscopicus* [182]. This naturally occurring mTOR inhibitor was first approved by the FDA in 1999 as Sirolimus [183]. RAPA is the compound with a broad spectrum of pharmacological and biological activity. In addition to its antifungal activity, this compound exhibits e.g., neuroprotective [184], antitumor [185], anti-ageing [186] and immunosuppressive properties [187]. mTOR signaling plays a crucial role in autophagy occurring in cancer cells by increasing their growth and enhancing proliferation. Inhibition of mTOR activity induced by RAPA may cause an increase in autophagy flux in tumor cells and consequently contribute to a reduction in tumor growth. Furthermore, conducted studies revealed that RAPA induces autophagosomes formation and, at the later stage, lysosomes and autophagosomes fusion [188–190]. Ongoing clinical trials, concerning the application of RAPA in the treatment of, e.g., kaposiform hemangioendothelioma in children (NCT04077515), bladder cancer (NCT02753309, NCT04375813), HER2+ metastatic breast cancer (NCT04736589) and refractory solid tumors (NCT02688881). There are also ongoing studies investigating the use of sirolimus in combination with durvalumab for the treatment of NSCLC (NCT04348292) and sirolimus with metronomic therapy for the treatment of pediatric relapsed or refractory tumors (NCT02574728).

#### 4.3.2. Temsirolimus

Temsirolimus (CCI-779, TEM, Torisel®) is a known analogue of RAPA. This water-soluble RAPA's prodrug was first developed by Wyeth Pharmaceuticals and it was approved by the FDA in the treatment of advanced renal cell carcinoma (RCC) [191] in 2007. TEM is produced via RAPA and 2,2-dihydroxymethylpropionic acid esterification [192]. However, due to the ease of the degradation of orally administered esters, this drug must be administered intravenously [193]. Studies on the potential use of TEM in the therapy of colorectal cancer [194], prostate cancer [195], human papillomavirus-related oropharyngeal squamous cell carcinoma [196] or advanced solid tumors [197] have been conducted. Furthermore, there are at least several dozen ongoing clinical trials on the use of temsirolimus for the treatment of advanced or metastatic malignancies (NCT01552434), advanced gynecological malignancies (NCT01065662), advanced rare tumors (NCT01396408), diffuse intrinsic pontine glioma (NCT02420613) or solid tumors in adults (NCT01375829) are under investigations.

#### 4.3.3. Everolimus

Everolimus (RAD001) is a next RAPA water-soluble analogue, developed by Novartis. The drug is produced via the esterification (ethylene glycol plus RAPA) process. Compounds esterification results in the formation of a new derivative (RAD001) with improved solubility in water and stability [93]. Everolimus was first approved by the FDA in 2009 as a therapeutic agent in the treatment of advanced renal carcinoma [198]. Since then, the new therapeutic applications of the drug in the treatment of various cancers have been continuously developed. In the past year alone, the possibility of using RAD001 in various cancer therapies has been investigated, e.g., in combination therapy (everolimus plus bevacizumab) for advanced papillary variant renal cell carcinoma [199], in the treatment of triple-negative breast cancer (everolimus in combination with gefitinib) [200] or in the treatment of advanced solid tumors (everolimus plus vatalanib) [201]. Moreover, there are current, ongoing clinical trials concerning the application of RAD001 on the treatment of, e.g., recurrent or progressive ependymoma in children (NCT02155920), Hodgkin lymphoma (NCT03697408), metastatic transitional cell carcinoma of the urothelium (NCT00805129), advanced gynecologic malignancies and breast cancers (NCT03154281) or recurrent low grade gliomas in young adults and pediatric patients (NCT04485559).

#### 4.3.4. Metformin

Metformin was discovered in 1922 as a by-product of the synthesis of N,N-dimethylguanidine [202]. As a result of numerous studies, the hypoglycemic effect of metformin was discovered, and it was first used in the treatment of diabetes in 1957 [203]. Nowadays, this compound, approved by the FDA in 1998, is the most commonly prescribed antidiabetic drug and is used in the treatment of type 2 diabetes, especially in obese diabetics [204–206]. Based on the conducted studies, Tomic et al. were found that metformin significantly affects melanoma cells proliferation by inhibiting tumor growth. Moreover, based on the tumor samples analysis the drug was found to increase the level of apoptosis markers in cancer cells and induce the autophagy process [207]. In 2014, Takahashi and co-authors obtained similar results during a study with endometrial cancer cells [208]. Recently, intensive studies exploring new properties of this compound were conducted. The potential use of metformin, for example in the treatment of PCOS [209,210], in cancer therapy [211], as a cardiovascular protector [212] or as an inhibitor of the ageing process [213,214], has been investigated. There are many ongoing studies on the use of metformin in cancer treatment. Currently, clinical studies are being conducted on the use of the compound in the treatment of, for example, breast cancer (NCT04559308, NCT04387630, NCT01980823, NCT04741204), colon cancer (NCT03359681), thoracic neoplasm (NCT03477162) or prostate cancer (NCT02176161, NCT02339168).

Described autophagy activators undergoing clinical trials and their target points, adverse effects or selected therapeutic schemes are listed in Tables 4 and 5.

#### 4.4. Autophagy Activators Undergoing Preclinical Trials

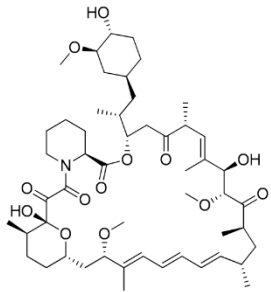
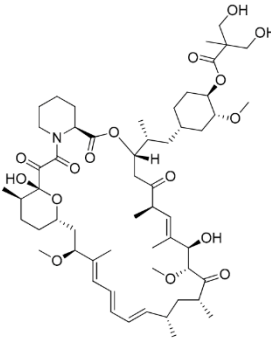
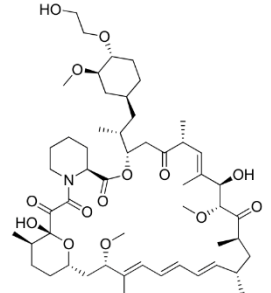
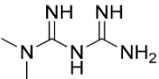
##### 4.4.1. Miconazole

Miconazole (MCZ), an imidazole derivative, is a known antifungal drug originally approved by the FDA for the treatment of vaginal candidiasis in 1974 [215]. Moreover, this drug is used also in the treatment of athlete's foot [216] or tinea versicolor [217]. Interestingly, in recent decades MCZ has attracted scientist as a potential drug with anticancer properties. Conducted studies have shown, that MCZ inhibits the growth of various human tumors, e.g., breast cancer and glioma [218,219] or osteosarcoma [220]. Jung et al. have been investigated the effect of MCZ on the autophagy process. Conducted studies revealed that MCZ induces autophagy in glioblastoma cells. The authors presumed, that MCZ-induced autophagy-mediated cell death might be activated via reactive oxygen species-mediated endoplasmic reticulum stress [221]. In published recently paper, Ho et al. have shown that MCZ induces autophagy process in bladder cancer cells. The authors demonstrated that miconazole increases the autophagic flux and promotes the expression of LC3 in the tested cancer cells. They revealed that combination therapy (MCZ with autophagy inhibitor) enhanced the anticancer properties of miconazole [222].

##### 4.4.2. CRO15

CRO15 is a new compound derived from metformin, recently identified by Jaune and co-authors. The research aimed to develop a new molecule with a better pharmacological profile, enhanced potency and improved effect in patients compared to its parent drug, metformin. The initial screening and structure-activity relationship studies revealed a new potential drug—CRO15. Extensive *in vitro*, *in vivo* studies and studies in melanoma xenograft models have shown that CRO15 reduces tumor cell viability. The molecular mechanism of action of the compound is based on effects on two main processes—autophagy and apoptosis. The results obtained, both *in vitro* and *in vivo*, showed that CRO15 induces autophagy by accumulating LC3 in melanoma cancer cells. Moreover, the performed *in vivo* studies did not show strong toxicity of the tested compound in mice. All of this data suggests that CRO15 should be further evaluated as a potential anticancer drug [223].

**Table 4.** Selected autophagy activators under clinical investigation.

Autophagy Activator	Chemical Structure	Study Type	References
Rapamycin		<b>Clinical trials:</b> therapy of kaposiform hemangioendothelioma in children, bladder cancer, HER2+ metastatic breast cancer, refractory solid tumors, NSCLC and pediatric relapsed or refractory tumors	NCT04077515, NCT02753309, NCT04375813, NCT04736589, NCT02688881, NCT04348292, NCT02574728
Temsirolimus		<b>Preclinical studies:</b> colorectal cancer, prostate cancer, human papillomavirus-related oropharyngeal squamous cell carcinoma or advanced solid tumors treatment <b>Clinical trials:</b> advanced/metastatic malignancies, gynecological malignancies, rare tumors, diffuse intrinsic pontine glioma or solid tumors therapy	[194–197] NCT01552434, NCT01065662, NCT01396408, NCT02420613, NCT01375829
Everolimus		<b>Preclinical studies:</b> treatment of advanced papillary variant renal cell carcinoma, triple-negative breast cancer or advanced solid tumors <b>Clinical trials:</b> recurrent or progressive ependymoma in children, Hodgkin lymphoma, metastatic transitional cell carcinoma of the urothelium, advanced gynecologic malignancies and breast cancers or recurrent low grade gliomas in young adults and pediatric patients	[199–201] NCT02155920, NCT03697408, NCT00805129, NCT03154281, NCT04485559
Metformin		<b>Clinical trials:</b> breast cancer, colon cancer, thoracic neoplasm or prostate cancer therapy	NCT04559308, NCT04387630, NCT01980823, NCT04741204, NCT03359681, NCT03477162, NCT02176161, NCT02339168

**Table 5.** Target points, adverse effects and selected therapeutic schemes of autophagy activators.

Autophagy Activator	Target Point	Adverse Effects	Therapeutic Combination or Single-Agent Treatment	Tumor Type	References
Rapamycin	mTOR	blood and lymphatic system disorders e.g., anemia or leukopenia, nausea, fatigue, mucositis, rash after treatment with high-dose RAPA (6 mg): neutropenia, diarrhea, fever, stomatitis	rapamycin + trastuzumab	HER2 receptor positive metastatic breast cancer	NCT00411788
		anemia, abdominal pain, diarrhea, nausea, fever, non-cardiac chest pain, dyspnea, headache, cough, metabolism and nutrition disorders	rapamycin + radical prostatectomy	advanced localized prostate cancer	NCT00311623
Temsirolimus	mTOR	blood and lymphatic system disorders, gastrointestinal disorders, back pain, dizziness, dry skin, pruritus, rash mucositis oral, fatigue, dehydration, dyspnea	temsirolimus + sorafenib	thyroid cancer	NCT01025453
		no adverse effects observed	temsirolimus + bevacizumab	prostate cancer	NCT01083368
Temsirolimus	mTOR	fatigue, dehydration, dyspnea	temsirolimus + cixutumumab	breast cancer	NCT00699491
Everolimus	mTOR	anemia, vomiting, lower respiratory tract infection, hypercalcemia, confusional state	everolimus and pasireotide	thyroid cancer	NCT01270321
		anemia, abdominal pain, diarrhea, mucositis oral, nausea, vomiting, fatigue, rash xerostomia, dysphagia, fatigue, dysgeusia	everolimus + exemestane	estrogen receptor positive advanced breast cancer	NCT01743560
Metformin	Beclin 1/mTOR	anemia, abdominal pain, diarrhea, mucositis oral, nausea, vomiting, fatigue, rash xerostomia, dysphagia, fatigue, dysgeusia	everolimus + pazopanib	solid tumor, kidney cancer	NCT01184326
		anemia, tinnitus, diarrhea, vomiting, nausea, white blood cell decreased	external beam radiation therapy + metformin	head and neck cancer	NCT03109873
			metformin + cisplatin and radiation therapy	locally advanced head and neck squamous cell carcinoma	NCT02325401

#### 4.4.3. $\alpha$ -Hederin

$\alpha$ -Hederin ( $\alpha$ -HN) is a molecule belonging to the wide group of monodesmosidic triterpenoid saponins. This compound is the main component isolated from *Hedera helix L.* leaves. It is also found in *Nigella sativa*, *Kalopanax pictus* and *Chenopodium quinoa* plants [224]. Studies conducted by Li et al. revealed that  $\alpha$ -HN may act through increasing the ROS concentration, consequently leading to the activation of the intrinsic apoptotic pathway [225]. This finding prompted Li and co-workers to investigate the influence of  $\alpha$ -HN on the autophagy process in colorectal cancer cells. Obtained results have shown that  $\alpha$ -HN induces autophagy-mediated cell death through the activation of the ROS-dependent AMPK/mTOR signaling pathway. Nevertheless, the potential use of  $\alpha$ -HN as an anticancer agent requires further investigation due to its toxicity, hemolytic effect and protein absorption [226].

#### 4.4.4. MJ-33

MJ-33 is a novel quinazolinone derivative synthesized by Ha and co-authors. A recently published paper revealed the anti-cancer properties of this compound in 5-fluorouracil-resistant (5FUR) colon cancer cells (HT-29/5FUR). Furthermore, the molecular mechanism of MJ-33 activity was also investigated. Based on the obtained results, MJ-33 was found to induce the autophagy process in HT-29/5FUR cells through inhibition of mTOR phosphorylation and subsequent upregulation of ATG proteins expression. Additionally, combined therapy with MJ-33 and known autophagy inhibitor, 3-MA, has shown significant enhancement in effector caspases (caspase-3 and caspase-7) activity compared with single-agent therapy with MJ-33. Obtained results suggest that the autophagy process plays a cytoprotective role in tested HT-29/5FUR cells [227]. Nowadays, scientists around the world investigate the effect of combined therapies, autophagy inhibitors together with autophagy activators, as a novel strategy in cancers treatment [228]. The authors of the aforementioned paper suggest that further studies on new quinazolinone derivative should examine the effect of combined therapy with MJ-33 and autophagy inhibitors [227].

Table 6 summarizes information about all described autophagy activators undergoing preclinical investigation.

**Table 6.** Selected autophagy activators under preclinical investigation.

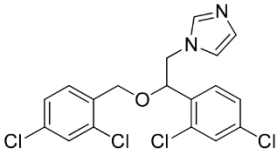
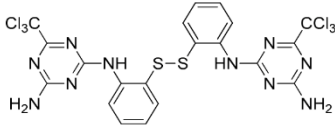
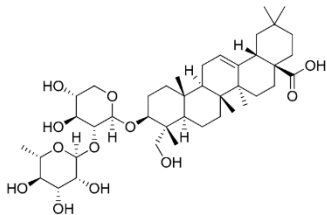
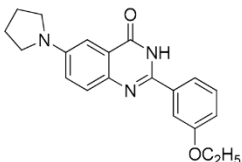
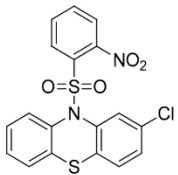
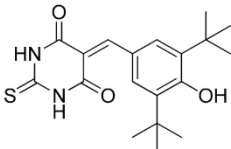
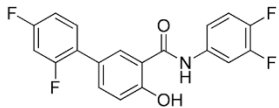
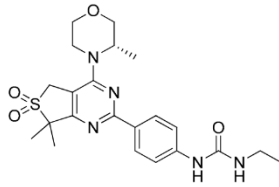
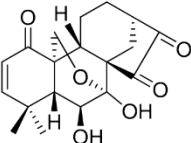
Autophagy Activator	Chemical Structure	Preclinical Studies	References
Miconazole		glioblastoma and bladder cancer therapy	[221,222]
CRO15		treatment of melanoma	[223]
$\alpha$ -Hederin		in vitro and in vivo studies on colorectal cancer cells	[226]

Table 6. Cont.

Autophagy Activator	Chemical Structure	Preclinical Studies	References
MJ-33		in vitro study on HT-29/5FUR cells	[227,229]
DS00329		in vitro study on malignant glioblastoma cells	[230]
MHY2256		endometrial and colorectal cancer treatment	[231,232]
LCC03		in vitro and in vivo study on castration-resistant prostate cancer	[233]
CZ415		in vitro and in vivo study on human papillary thyroid carcinoma cells	[234]
Eriocalyxin B		in vitro and in vivo study on breast cancer	[235]

## 5. Conclusions

Neoplastic transformation requires significant changes in biological processes as part of increased demand and consumption of energy under stressful conditions. It leads to intracellular adaptation that ensures survival in conditions with a limited amount of nutrients and oxygen. There is a change in metabolism, protein and organelle turnover, and bioenergy functions. These neoplastic signaling pathways cross with autophagy at many levels. Autophagy is a dichotomous process—it may inhibit or induce tumor growth. These observations suggest that autophagy plays a dynamic and complex role play in cancer, which may, in fact, explain the duplicity of autophagy in carcinogenesis. While targeting autophagy pathways appears to be a promising tool in developing new anti-cancer therapies, recent findings suggest that the underlying molecular mechanisms and specific targets of autophagy in cancer need to be well defined before it can be used effectively in pharmaceutical and medical research.



Despite the fact that the most well-known inhibitors (such as chloroquine, hydroxychloroquine, clarithromycin or verteporfin) and activators (rapamycin, metformin, temsirolimus or everolimus) of autophagy are recognized in the scientific and medical world for years, they have not been used in medicinal practice. As presented in this paper, a number of clinical and preclinical studies are conducted, the aim of which is to discover new possibilities in oncological therapy, including the use of autophagy modulators in combination with anticancer drugs. Recent studies have identified new classes of inhibitors and activators of autophagy that are currently in preclinical research. Among them, the most promising are 3-Methyladenine, SAR405, Lys05, 7-methyl-5-phenylpyrazolo[4,3-*e*]tetrazolo[4,5-*b*][1,2,4]triazine sulfonamide derivatives, miconazole, CRO15 or  $\alpha$ -Hederin. These compounds have different target points in the autophagy process and further detailed studies are needed to determine their potential use in the practical treatment of cancer.

**Funding:** This work was supported by European Union funds (project NO. POWR.03.02.00-00-I051/16-00), grant NO. 02/IMSD/G/2019.

**Institutional Review Board Statement:** Not applicable.

**Informed Consent Statement:** Not applicable.

**Data Availability Statement:** Not applicable.

**Conflicts of Interest:** The authors declare no conflict of interest. The funders had no role in the design of the manuscript, in the writing of the manuscript, or in the decision to publish.

### Abbreviations

3-MA	3-Methyladenine
5FUR	5-fluorouracil-resistant
ADCD	autophagy-dependent cell death
AML	acute myeloid leukemia
AMPK	5' adenosine monophosphate-activated protein kinase
ATG	autophagy-related
AZA	azacitidine
C3G	cyaniding-3-O-glucoside
CAM	clarithromycin
CMA	chaperone-mediated autophagy
CML	chronic myeloid leukemia
CQ	chloroquine
DRAM	damage-regulated autophagy modulator
eMI	endosomal microphagy
ER	endoplasmic reticulum
ESCRT	endosomal sorting complex required for transport
FDA	Food and Drug Administration
HCQ	hydroxychloroquine
Hsc70	heat shock cognate protein 70
JNK-1	C-Jun N-terminal protein kinase 1
LAL	lysosomal acid lipase
LAMP2A	lysosome associated membrane protein type 2A
LC3	light chain protein 3

LDs	lipid droplets
Mcl-1	myeloid cell leukemia 1
MCZ	miconazole
mTOR	mammalian target of rapamycin
NSCLC	non-small cell lung cancer
NUFIP 1	nuclear FMR1 interacting protein 1
PIK3K	phosphoinositide 3-kinase
PMPs	peroxisomal membrane proteins
RAD001	everolimus
RAPA	rapamycin
SQSTM1	sequestosome 1
TEM	temsirolimus
VP	verteporfin
$\alpha$ -HN	$\alpha$ -Hederin

## References

- Levine, B.; Klionsky, D.J. Development by self-digestion: Molecular mechanisms and biological functions of autophagy. *Dev. Cell* **2004**, *6*, 463–477. [[CrossRef](#)]
- Kroemer, G.; Galluzzi, L.; Vandenabeele, P.; Abrams, J.; Alnemri, E.S.; Baehrecke, E.H.; Blagosklonny, M.V.; El-Deiry, W.S.; Golstein, P.; Green, D.R.; et al. Classification of cell death: Recommendations of the Nomenclature Committee on Cell Death 2009. *Cell Death Differ.* **2009**, *16*, 3–11. [[CrossRef](#)] [[PubMed](#)]
- Kim, R. Recent advances in understanding the cell death pathways activated by anticancer therapy. *Cancer* **2005**, *103*, 1551–1560. [[CrossRef](#)] [[PubMed](#)]
- Polewska, J. Autophagy—molecular mechanism, apoptosis and cancer. *Postepy Hig. Med. Dosw.* **2012**, *66*, 921–936. [[CrossRef](#)] [[PubMed](#)]
- Dereń-Wagemann, I.; Kielbiński, M.; Kuliczowski, K. Autofagia—Proces o dwóch obliczach. *Acta Haematol. Pol.* **2013**, *44*, 383–391. [[CrossRef](#)]
- Galluzzi, L.; Vitale, I.; Aaronson, S.A.; Abrams, J.M.; Adam, D.; Agostinis, P.; Alnemri, E.S.; Altucci, L.; Amelio, I.; Andrews, D.W.; et al. Molecular mechanisms of cell death: Recommendations of the Nomenclature Committee on Cell Death 2018. *Cell Death Differ.* **2018**, *25*, 486–541. [[CrossRef](#)]
- Klionsky, D.J. The molecular machinery of autophagy: Unanswered questions. *J. Cell Sci.* **2005**, *118*, 7–18. [[CrossRef](#)]
- Yang, Y.-P.; Liang, Z.-Q.; Gu, Z.-L.; Qin, Z.-H. Molecular mechanism and regulation of autophagy. *Acta Pharmacol. Sin.* **2005**, *26*, 1421–1434. [[CrossRef](#)]
- Rabinowitz, J.D.; White, E. Autophagy and metabolism. *Science* **2010**, *330*, 1344–1348. [[CrossRef](#)]
- Eskelinen, E.-L.; Saftig, P. Autophagy: A lysosomal degradation pathway with a central role in health and disease. *Biochim. Et Biophys. Acta (BBA) Mol. Cell Res.* **2009**, *1793*, 664–673. [[CrossRef](#)]
- Andrade-Tomaz, M.; de Souza, I.; Rocha, C.R.R.; Gomes, L.R. The role of chaperone-mediated autophagy in cell cycle control and its implications in cancer. *Cells* **2020**, *9*, 2140. [[CrossRef](#)]
- Kon, M.; Kiffin, R.; Koga, H.; Chapochnik, J.; Macian, F.; Varticovski, L.; Cuervo, A.M. Chaperone-mediated autophagy is required for tumor growth. *Sci. Transl. Med.* **2011**, *3*, 109ra117. [[CrossRef](#)]
- Glick, D.; Barth, S.; Macleod, K.F. Autophagy: Cellular and molecular mechanisms. *J. Pathol.* **2010**, *221*, 3–12. [[CrossRef](#)] [[PubMed](#)]
- Mizushima, N. Autophagy: Process and function. *Genes Dev.* **2007**, *21*, 2861–2873. [[CrossRef](#)] [[PubMed](#)]
- Mizushima, N.; Yoshimori, T.; Ohsumi, Y. The role of Atg proteins in autophagosome formation. *Annu. Rev. Cell Dev. Biol.* **2011**, *27*, 107–132. [[CrossRef](#)]
- Kondo, Y.; Kanzawa, T.; Sawaya, R.; Kondo, S. The role of autophagy in cancer development and response to therapy. *Nat. Rev. Cancer* **2005**, *5*, 726–734. [[CrossRef](#)]
- Mehrpour, M.; Esclatine, A.; Beau, I.; Codogno, P. Overview of macroautophagy regulation in mammalian cells. *Cell Res.* **2010**, *20*, 748–762. [[CrossRef](#)]
- Yang, Y.; Klionsky, D.J. Autophagy and disease: Unanswered questions. *Cell Death Differ.* **2020**, *27*, 858–871. [[CrossRef](#)] [[PubMed](#)]
- Li, X.; He, S.; Ma, B. Autophagy and autophagy-related proteins in cancer. *Mol. Cancer* **2020**, *19*, 12. [[CrossRef](#)] [[PubMed](#)]
- Liang, X.H.; Jackson, S.; Seaman, M.; Brown, K.; Kempkes, B.; Hibshoosh, H.; Levine, B. Induction of autophagy and inhibition of tumorigenesis by beclin 1. *Nature* **1999**, *402*, 672–676. [[CrossRef](#)]
- Jin, S.; White, E. Role of autophagy in cancer: Management of metabolic stress. *Autophagy* **2007**, *3*, 28–31. [[CrossRef](#)]
- Ding, Z.-B.; Shi, Y.-H.; Zhou, J.; Qiu, S.-J.; Xu, Y.; Dai, Z.; Shi, G.-M.; Wang, X.-Y.; Ke, A.-W.; Wu, B.; et al. Association of autophagy defect with a malignant phenotype and poor prognosis of hepatocellular carcinoma. *Cancer Res.* **2008**, *68*, 9167–9175. [[CrossRef](#)]
- Birgisdottir, Å.B.; Lamark, T.; Johansen, T. The LIR motif—Crucial for selective autophagy. *J. Cell Sci.* **2013**, *126*, 3237–3247. [[CrossRef](#)]
- Zaffagnini, G.; Martens, S. Mechanisms of selective autophagy. *J. Mol. Biol.* **2016**, *428*, 1714–1724. [[CrossRef](#)]

25. Rogov, V.V.; Stolz, A.; Ravichandran, A.C.; Rios-Szwed, D.O.; Suzuki, H.; Kniss, A.; Löhr, F.; Wakatsuki, S.; Dötsch, V.; Dikic, I.; et al. Structural and functional analysis of the GABARAP interaction motif (GIM). *EMBO Rep.* **2018**, *19*, e47268. [[CrossRef](#)]
26. Noda, N.N.; Kumeta, H.; Nakatogawa, H.; Satoo, K.; Adachi, W.; Ishii, J.; Fujioka, Y.; Ohsumi, Y.; Inagaki, F. Structural basis of target recognition by Atg8/LC3 during selective autophagy. *Genes Cells* **2008**, *13*, 1211–1218. [[CrossRef](#)] [[PubMed](#)]
27. Johansen, T.; Lamark, T. Selective autophagy mediated by autophagic adapter proteins. *Autophagy* **2011**, *7*, 279–296. [[CrossRef](#)] [[PubMed](#)]
28. Li, W.; He, P.; Huang, Y.; Li, Y.-F.; Lu, J.; Li, M.; Kurihara, H.; Luo, Z.; Meng, T.; Onishi, M.; et al. Selective autophagy of intracellular organelles: Recent research advances. *Theranostics* **2021**, *11*, 222–256. [[CrossRef](#)] [[PubMed](#)]
29. Lei, Y.; Zhang, D.; Yu, J.; Dong, H.; Zhang, J.; Yang, S. Targeting autophagy in cancer stem cells as an anticancer therapy. *Cancer Lett.* **2017**, *393*, 33–39. [[CrossRef](#)]
30. Guo, J.Y.; White, E. Autophagy, metabolism, and cancer. *Cold Spring Harb. Symp. Quant. Biol.* **2016**, *81*, 73–78. [[CrossRef](#)]
31. Wang, F.; Jia, J.; Rodrigues, B. Autophagy, metabolic disease, and pathogenesis of heart dysfunction. *Can. J. Cardiol.* **2017**, *33*, 850–859. [[CrossRef](#)]
32. Miettinen, T.P.; Björklund, M. The mevalonate pathway as a metabolic requirement for autophagy—implications for growth control, proteostasis, and disease. *Mol. Cell. Oncol.* **2016**, *3*, e1143546. [[CrossRef](#)] [[PubMed](#)]
33. Zhong, Z.; Sanchez-Lopez, E.; Karin, M. Autophagy, NLRP3 inflammasome and auto-inflammatory/immune diseases. *Clin. Exp. Rheumatol* **2016**, *34*, 12–16.
34. Menzies, F.M.; Fleming, A.; Caricasole, A.; Bento, C.F.; Andrews, S.P.; Ashkenazi, A.; Füllgrabe, J.; Jackson, A.; Jimenez Sanchez, M.; Karabiyik, C.; et al. Autophagy and neurodegeneration: Pathogenic mechanisms and therapeutic opportunities. *Neuron* **2017**, *93*, 1015–1034. [[CrossRef](#)] [[PubMed](#)]
35. Plaza-Zabala, A.; Sierra-Torre, V.; Sierra, A. Autophagy and microglia: Novel partners in neurodegeneration and aging. *Int. J. Mol. Sci.* **2017**, *18*, 598. [[CrossRef](#)]
36. Chino, H.; Mizushima, N. ER-Phagy: Quality control and turnover of endoplasmic reticulum. *Trends Cell Biol.* **2020**, *30*, 384–398. [[CrossRef](#)]
37. Ruggiano, A.; Foresti, O.; Carvalho, P. ER-associated degradation: Protein quality control and beyond. *J. Cell Biol.* **2014**, *204*, 869–879. [[CrossRef](#)] [[PubMed](#)]
38. Oikonomou, C.; Hendershot, L.M. Disposing of misfolded ER proteins: A troubled substrate's way out of the ER. *Mol. Cell. Endocrinol.* **2020**, *500*, 110630. [[CrossRef](#)] [[PubMed](#)]
39. Wilkinson, S. ER-phagy: Shaping up and destressing the endoplasmic reticulum. *FEBS J.* **2019**, *286*, 2645–2663. [[CrossRef](#)]
40. Schuck, S.; Gallagher, C.M.; Walter, P. ER-phagy mediates selective degradation of endoplasmic reticulum independently of the core autophagy machinery. *J. Cell Sci.* **2014**, *127*, 4078–4088. [[CrossRef](#)]
41. De Leonibus, C.; Cinque, L.; Settembre, C. Emerging lysosomal pathways for quality control at the endoplasmic reticulum. *Febs Lett.* **2019**, *593*, 2319–2329. [[CrossRef](#)]
42. Islam, F.; Gopalan, V.; Law, S.; Tang, J.C.-o.; Lam, A.K.-y. FAM134B promotes esophageal squamous cell carcinoma in vitro and its correlations with clinicopathologic features. *Hum. Pathol.* **2019**, *87*, 1–10. [[CrossRef](#)]
43. Islam, F.; Gopalan, V.; Wahab, R.; Smith, R.A.; Qiao, B.; Lam, A.K.-Y. Stage dependent expression and tumor suppressive function of FAM134B (JK1) in colon cancer. *Mol. Carcinog.* **2017**, *56*, 238–249. [[CrossRef](#)] [[PubMed](#)]
44. Vara-Perez, M.; Felipe-Abrio, B.; Agostinis, P. Mitophagy in cancer: A tale of adaptation. *Cells* **2019**, *8*, 493. [[CrossRef](#)]
45. Sorrentino, V.; Menzies, K.J.; Auwerx, J. Repairing mitochondrial dysfunction in disease. *Annu. Rev. Pharmacol. Toxicol.* **2018**, *58*, 353–389. [[CrossRef](#)] [[PubMed](#)]
46. Kulikov, A.V.; Luchkina, E.A.; Gogvadze, V.; Zhivotovsky, B. Mitophagy: Link to cancer development and therapy. *Biochem. Biophys. Res. Commun.* **2017**, *482*, 432–439. [[CrossRef](#)] [[PubMed](#)]
47. Bard, J.A.M.; Goodall, E.A.; Greene, E.R.; Jonsson, E.; Dong, K.C.; Martin, A. Structure and function of the 26S proteasome. *Annu. Rev. Biochem.* **2018**, *87*, 697–724. [[CrossRef](#)] [[PubMed](#)]
48. Livneh, I.; Cohen-Kaplan, V.; Cohen-Rosenzweig, C.; Avni, N.; Ciechanover, A. The life cycle of the 26S proteasome: From birth, through regulation and function, and onto its death. *Cell Res.* **2016**, *26*, 869–885. [[CrossRef](#)]
49. Grice, G.L.; Nathan, J.A. The recognition of ubiquitinated proteins by the proteasome. *Cell. Mol. Life Sci.* **2016**, *73*, 3497–3506. [[CrossRef](#)] [[PubMed](#)]
50. Cuervo, A.M.; Palmer, A.; Rivett, A.J.; Knecht, E. Degradation of proteasomes by lysosomes in rat liver. *Eur. J. Biochem.* **1995**, *227*, 792–800. [[CrossRef](#)] [[PubMed](#)]
51. Marshall, R.S.; Li, F.; Gemperline, D.C.; Book, A.J.; Vierstra, R.D. Autophagic degradation of the 26S proteasome is mediated by the dual ATG8/ubiquitin receptor RPN10 in *Arabidopsis*. *Mol. Cell* **2015**, *58*, 1053–1066. [[CrossRef](#)]
52. Cohen-Kaplan, V.; Livneh, I.; Avni, N.; Fabre, B.; Ziv, T.; Kwon, Y.T.; Ciechanover, A. p62- and ubiquitin-dependent stress-induced autophagy of the mammalian 26S proteasome. *Proc. Natl. Acad. Sci. USA* **2016**, *113*, E7490–E7499. [[CrossRef](#)] [[PubMed](#)]
53. Beese, C.J.; Brynjólfssdóttir, S.H.; Frankel, L.B. Selective autophagy of the protein homeostasis machinery: Ribophagy, proteaphagy and ER-phagy. *Front. Cell Dev. Biol.* **2020**, *7*, 373. [[CrossRef](#)] [[PubMed](#)]
54. An, H.; Harper, J.W. Systematic analysis of ribophagy in human cells reveals bystander flux during selective autophagy. *Nat. Cell Biol.* **2018**, *20*, 135–143. [[CrossRef](#)] [[PubMed](#)]

55. Wyant, G.A.; Abu-Remaileh, M.; Frenkel, E.M.; Laqtom, N.N.; Dharamdasani, V.; Lewis, C.A.; Chan, S.H.; Heinze, I.; Ori, A.; Sabatini, D.M. NUFIP1 is a ribosome receptor for starvation-induced ribophagy. *Science* **2018**, *360*, 751–758. [[CrossRef](#)] [[PubMed](#)]
56. Devenport, S.N.; Shah, Y.M. Functions and implications of autophagy in colon cancer. *Cells* **2019**, *8*, 1349. [[CrossRef](#)]
57. Huybrechts, S.J.; Van Veldhoven, P.P.; Brees, C.; Mannaerts, G.P.; Los, G.V.; Fransen, M. Peroxisome dynamics in cultured mammalian cells. *Traffic* **2009**, *10*, 1722–1733. [[CrossRef](#)]
58. Mancias, J.D.; Kimmelman, A.C. Mechanisms of selective autophagy in normal physiology and cancer. *J. Mol. Biol.* **2016**, *428*, 1659–1680. [[CrossRef](#)]
59. Deosaran, E.; Larsen, K.B.; Hua, R.; Sargent, G.; Wang, Y.; Kim, S.; Lamark, T.; Jauregui, M.; Law, K.; Lippincott-Schwartz, J.; et al. NBR1 acts as an autophagy receptor for peroxisomes. *J. Cell Sci.* **2013**, *126*, 939–952. [[CrossRef](#)]
60. Kim, P.K.; Hailey, D.W.; Mullen, R.T.; Lippincott-Schwartz, J. Ubiquitin signals autophagic degradation of cytosolic proteins and peroxisomes. *Proc. Natl. Acad. Sci. USA* **2008**, *105*, 20567–20574. [[CrossRef](#)]
61. Eberhart, T.; Kovacs, W.J. Pexophagy in yeast and mammals: An update on mysteries. *Histochem. Cell Biol.* **2018**, *150*, 473–488. [[CrossRef](#)] [[PubMed](#)]
62. Kounakis, K.; Chaniotakis, M.; Markaki, M.; Tavernarakis, N. Emerging roles of lipophagy in health and disease. *Front. Cell Dev. Biol.* **2019**, *7*. [[CrossRef](#)]
63. Rogov, V.; Dötsch, V.; Johansen, T.; Kirkin, V. Interactions between autophagy receptors and ubiquitin-like proteins form the molecular basis for selective autophagy. *Mol. Cell* **2014**, *53*, 167–178. [[CrossRef](#)]
64. Singh, R.; Kaushik, S.; Wang, Y.; Xiang, Y.; Novak, I.; Komatsu, M.; Tanaka, K.; Cuervo, A.M.; Czaja, M.J. Autophagy regulates lipid metabolism. *Nature* **2009**, *458*, 1131–1135. [[CrossRef](#)] [[PubMed](#)]
65. Zhao, T.; Du, H.; Ding, X.; Walls, K.; Yan, C. Activation of mTOR pathway in myeloid-derived suppressor cells stimulates cancer cell proliferation and metastasis in *lal*<sup>-/-</sup> mice. *Oncogene* **2015**, *34*, 1938–1948. [[CrossRef](#)] [[PubMed](#)]
66. Gómez de Cedrón, M.; Ramírez de Molina, A. Microtargeting cancer metabolism: Opening new therapeutic windows based on lipid metabolism. *J. Lipid Res.* **2016**, *57*, 193–206. [[CrossRef](#)] [[PubMed](#)]
67. Saftig, P.; Klumperman, J. Lysosome biogenesis and lysosomal membrane proteins: Trafficking meets function. *Nat. Rev. Mol. Cell Biol.* **2009**, *10*, 623–635. [[CrossRef](#)] [[PubMed](#)]
68. Aits, S.; Jäättelä, M. Lysosomal cell death at a glance. *J. Cell Sci.* **2013**, *126*, 1905–1912. [[CrossRef](#)]
69. Boya, P.; Kroemer, G. Lysosomal membrane permeabilization in cell death. *Oncogene* **2008**, *27*, 6434–6451. [[CrossRef](#)]
70. Maejima, I.; Takahashi, A.; Omori, H.; Kimura, T.; Takabatake, Y.; Saitoh, T.; Yamamoto, A.; Hamasaki, M.; Noda, T.; Isaka, Y.; et al. Autophagy sequesters damaged lysosomes to control lysosomal biogenesis and kidney injury. *Embo J.* **2013**, *32*, 2336–2347. [[CrossRef](#)]
71. Papadopoulos, C.; Kravic, B.; Meyer, H. Repair or lysophagy: Dealing with damaged lysosomes. *J. Mol. Biol.* **2020**, *432*, 231–239. [[CrossRef](#)] [[PubMed](#)]
72. Bo Otto, F.; Thumm, M. Nucleophagy—implications for microautophagy and health. *Int. J. Mol. Sci.* **2020**, *21*, 4506. [[CrossRef](#)]
73. Park, Y.-E.; Hayashi, Y.K.; Bonne, G.; Arimura, T.; Noguchi, S.; Nonaka, I.; Nishino, I. Autophagic degradation of nuclear components in mammalian cells. *Autophagy* **2009**, *5*, 795–804. [[CrossRef](#)] [[PubMed](#)]
74. Zhao, L.; Li, W.; Luo, X.; Sheng, S. The multifaceted roles of nucleophagy in cancer development and therapy. *Cell Biol. Int.* **2021**, *45*, 246–257. [[CrossRef](#)] [[PubMed](#)]
75. Duve, C.d.; Wattiaux, R. Functions of lysosomes. *Annu. Rev. Physiol.* **1966**, *28*, 435–492. [[CrossRef](#)] [[PubMed](#)]
76. Yim, W.W.-Y.; Mizushima, N. Lysosome biology in autophagy. *Cell Discov.* **2020**, *6*, 6. [[CrossRef](#)]
77. Klionsky, D.J.; Eskelinen, E.L. The vacuole versus the lysosome: When size matters. *Autophagy* **2014**, *10*, 185–187. [[CrossRef](#)]
78. Schuck, S. Microautophagy—distinct molecular mechanisms handle cargoes of many sizes. *J. Cell Sci.* **2020**, *133*, jcs246322. [[CrossRef](#)]
79. Sahu, R.; Kaushik, S.; Clement, C.C.; Cannizzo, E.S.; Scharf, B.; Follenzi, A.; Potolicchio, I.; Nieves, E.; Cuervo, A.M.; Santambrogio, L. Microautophagy of cytosolic proteins by late endosomes. *Dev. Cell* **2011**, *20*, 131–139. [[CrossRef](#)]
80. Mukherjee, A.; Patel, B.; Koga, H.; Cuervo, A.M.; Jenny, A. Selective endosomal microautophagy is starvation-inducible in *Drosophila*. *Autophagy* **2016**, *12*, 1984–1999. [[CrossRef](#)]
81. Uytterhoeven, V.; Lauwers, E.; Maes, I.; Miskiewicz, K.; Melo, M.N.; Swerts, J.; Kuenen, S.; Wittocx, R.; Corthout, N.; Marrink, S.-J.; et al. Hsc70-4 deforms membranes to promote synaptic protein turnover by endosomal microautophagy. *Neuron* **2015**, *88*, 735–748. [[CrossRef](#)]
82. Morozova, K.; Clement, C.C.; Kaushik, S.; Stiller, B.; Arias, E.; Ahmad, A.; Rauch, J.N.; Chatterjee, V.; Melis, C.; Scharf, B.; et al. Structural and biological interaction of hsc-70 protein with phosphatidylserine in endosomal microautophagy. *J. Biol. Chem.* **2016**, *291*, 18096–18106. [[CrossRef](#)] [[PubMed](#)]
83. Chauhan, A.S.; Kumar, M.; Chaudhary, S.; Dhiman, A.; Patidar, A.; Jakhar, P.; Jaswal, P.; Sharma, K.; Sheokand, N.; Malhotra, H.; et al. Trafficking of a multifunctional protein by endosomal microautophagy: Linking two independent unconventional secretory pathways. *FASEB J.* **2019**, *33*, 5626–5640. [[CrossRef](#)] [[PubMed](#)]
84. Mejlvang, J.; Olsvik, H.; Svenning, S.; Bruun, J.-A.; Abudu, Y.P.; Larsen, K.B.; Brech, A.; Hansen, T.E.; Brenne, H.; Hansen, T.; et al. Starvation induces rapid degradation of selective autophagy receptors by endosomal microautophagy. *J. Cell Biol.* **2018**, *217*, 3640–3655. [[CrossRef](#)]

85. Rios, J.; Sequeira, A.; Albornoz, A.; Budini, M. Chaperone mediated autophagy substrates and components in cancer. *Front. Oncol.* **2021**, *10*. [[CrossRef](#)]
86. Liao, Z.; Wang, B.; Liu, W.; Xu, Q.; Hou, L.; Song, J.; Guo, Q.; Li, N. Dysfunction of chaperone-mediated autophagy in human diseases. *Mol. Cell. Biochem.* **2021**. [[CrossRef](#)]
87. Cuervo, A.M.; Wong, E. Chaperone-mediated autophagy: Roles in disease and aging. *Cell Res.* **2014**, *24*, 92–104. [[CrossRef](#)]
88. Kaushik, S.; Bandyopadhyay, U.; Sridhar, S.; Kiffin, R.; Martinez-Vicente, M.; Kon, M.; Orenstein, S.J.; Wong, E.; Cuervo, A.M. Chaperone-mediated autophagy at a glance. *J. Cell Sci.* **2011**, *124*, 495–499. [[CrossRef](#)]
89. Gomes, L.R.; Menck, C.F.M.; Cuervo, A.M. Chaperone-mediated autophagy prevents cellular transformation by regulating MYC proteasomal degradation. *Autophagy* **2017**, *13*, 928–940. [[CrossRef](#)]
90. Arias, E.; Cuervo, A.M. Pros and cons of chaperone-mediated autophagy in cancer biology. *Trends Endocrinol. Metab.* **2020**, *31*, 53–66. [[CrossRef](#)]
91. Xia, H.-g.; Najafov, A.; Geng, J.; Galan-Acosta, L.; Han, X.; Guo, Y.; Shan, B.; Zhang, Y.; Norberg, E.; Zhang, T.; et al. Degradation of HK2 by chaperone-mediated autophagy promotes metabolic catastrophe and cell death. *J. Cell Biol.* **2015**, *210*, 705–716. [[CrossRef](#)] [[PubMed](#)]
92. Yang, T.; Ren, C.; Qiao, P.; Han, X.; Wang, L.; Lv, S.; Sun, Y.; Liu, Z.; Du, Y.; Yu, Z. PIM2-mediated phosphorylation of hexokinase 2 is critical for tumor growth and paclitaxel resistance in breast cancer. *Oncogene* **2018**, *37*, 5997–6009. [[CrossRef](#)] [[PubMed](#)]
93. Condello, M.; Pellegrini, E.; Caraglia, M.; Meschini, S. Targeting autophagy to overcome human diseases. *Int. J. Mol. Sci.* **2019**, *20*, 725. [[CrossRef](#)] [[PubMed](#)]
94. Chen, Q.; Kang, J.; Fu, C. The independence of and associations among apoptosis, autophagy, and necrosis. *Signal. Transduct. Target. Ther.* **2018**, *3*, 18. [[CrossRef](#)] [[PubMed](#)]
95. Mariño, G.; Niso-Santano, M.; Baehrecke, E.H.; Kroemer, G. Self-consumption: The interplay of autophagy and apoptosis. *Nat. Rev. Mol. Cell Biol.* **2014**, *15*, 81–94. [[CrossRef](#)] [[PubMed](#)]
96. Hu, C.-A.A.; White, K.; Torres, S.; Ishak, M.-A.; Sillerud, L.; Miao, Y.; Liu, Z.; Wu, Z.; Sklar, L.; Berwick, M. Chapter 10—Apoptosis and autophagy: The yin–yang of homeostasis in cell death in cancer. In *Autophagy: Cancer, Other Pathologies, Inflammation, Immunity, Infection, and Aging*; Hayat, M.A., Ed.; Academic Press: Amsterdam, The Netherlands, 2015; pp. 161–181.
97. Gaglia, G.; Lahav, G. Constant rate of p53 tetramerization in response to DNA damage controls the p53 response. *Mol. Syst. Biol.* **2014**, *10*, 753. [[CrossRef](#)] [[PubMed](#)]
98. Leszczynska, K.B.; Foskolou, I.P.; Abraham, A.G.; Anbalagan, S.; Tellier, C.; Haider, S.; Span, P.N.; O'Neill, E.E.; Buffa, F.M.; Hammond, E.M. Hypoxia-induced p53 modulates both apoptosis and radiosensitivity via AKT. *J. Clin. Investig.* **2015**, *125*, 2385–2398. [[CrossRef](#)]
99. Reid, M.A.; Wang, W.I.; Rosales, K.R.; Welliver, M.X.; Pan, M.; Kong, M. The B55 $\alpha$  subunit of PP2A drives a p53-dependent metabolic adaptation to glutamine deprivation. *Mol. Cell* **2013**, *50*, 200–211. [[CrossRef](#)]
100. Li, M.; Gao, P.; Zhang, J. Crosstalk between autophagy and apoptosis: Potential and emerging therapeutic targets for cardiac diseases. *Int. J. Mol. Sci.* **2016**, *17*, 332. [[CrossRef](#)]
101. Fridman, J.S.; Lowe, S.W. Control of apoptosis by p53. *Oncogene* **2003**, *22*, 9030–9040. [[CrossRef](#)]
102. Crighton, D.; Wilkinson, S.; O'Prey, J.; Syed, N.; Smith, P.; Harrison, P.R.; Gasco, M.; Garrone, O.; Crook, T.; Ryan, K.M. DRAM, a p53-induced modulator of autophagy, is critical for apoptosis. *Cell* **2006**, *126*, 121–134. [[CrossRef](#)] [[PubMed](#)]
103. Tasdemir, E.; Maiuri, M.C.; Galluzzi, L.; Vitale, I.; Djavaheri-Mergny, M.; D'Amelio, M.; Criollo, A.; Morselli, E.; Zhu, C.; Harper, F.; et al. Regulation of autophagy by cytoplasmic p53. *Nat. Cell Biol.* **2008**, *10*, 676–687. [[CrossRef](#)]
104. Scherz-Shouval, R.; Weidberg, H.; Gonen, C.; Wilder, S.; Elazar, Z.; Oren, M. p53-dependent regulation of autophagy protein LC3 supports cancer cell survival under prolonged starvation. *Proc. Natl. Acad. Sci. USA* **2010**, *107*, 18511–18516. [[CrossRef](#)] [[PubMed](#)]
105. Kilbride, S.M.; Prehn, J.H.M. Central roles of apoptotic proteins in mitochondrial function. *Oncogene* **2013**, *32*, 2703–2711. [[CrossRef](#)]
106. McKnight, N.C.; Yue, Z. Beclin 1, an essential component and master regulator of PI3K-III in health and disease. *Curr. Pathobiol. Rep.* **2013**, *1*, 231–238. [[CrossRef](#)] [[PubMed](#)]
107. Decuyper, J.-P.; Parys, J.B.; Bultynck, G. Regulation of the autophagic Bcl-2/Beclin 1 interaction. *Cells* **2012**, *1*, 284–312. [[CrossRef](#)] [[PubMed](#)]
108. Kang, R.; Zeh, H.J.; Lotze, M.T.; Tang, D. The Beclin 1 network regulates autophagy and apoptosis. *Cell Death Differ.* **2011**, *18*, 571–580. [[CrossRef](#)]
109. Maiuri, M.C.; Criollo, A.; Tasdemir, E.; Vicencio, J.M.; Tajeddine, N.; Hickman, J.A.; Geneste, O.; Kroemer, G. BH3-only proteins and BH3 mimetics induce autophagy by competitively disrupting the interaction between Beclin 1 and Bcl-2/Bcl-X<sub>L</sub>. *Autophagy* **2007**, *3*, 374–376. [[CrossRef](#)]
110. Wei, Y.; Pattingre, S.; Sinha, S.; Bassik, M.; Levine, B. JNK1-mediated phosphorylation of Bcl-2 regulates starvation-induced autophagy. *Mol. Cell* **2008**, *30*, 678–688. [[CrossRef](#)]
111. Ruvolo, P.P.; Deng, X.; May, W.S. Phosphorylation of Bcl2 and regulation of apoptosis. *Leukemia* **2001**, *15*, 515–522. [[CrossRef](#)]
112. Wei, Y.; Sinha, S.C.; Levine, B. Dual role of JNK1-mediated phosphorylation of Bcl-2 in autophagy and apoptosis regulation. *Autophagy* **2008**, *4*, 949–951. [[CrossRef](#)]
113. van Delft, M.F.; Huang, D.C.S. How the Bcl-2 family of proteins interact to regulate apoptosis. *Cell Res.* **2006**, *16*, 203–213. [[CrossRef](#)] [[PubMed](#)]

114. Cooper, K.F. Till death do us part: The marriage of autophagy and apoptosis. *Oxidative Med. Cell. Longev.* **2018**, *2018*, 4701275. [CrossRef] [PubMed]
115. Rubinstein, A.D.; Eisenstein, M.; Ber, Y.; Bialik, S.; Kimchi, A. The autophagy protein Atg12 associates with antiapoptotic Bcl-2 family members to promote mitochondrial apoptosis. *Mol. Cell* **2011**, *44*, 698–709. [CrossRef]
116. Yousefi, S.; Perozzo, R.; Schmid, I.; Ziemiecki, A.; Schaffner, T.; Scapozza, L.; Brunner, T.; Simon, H.-U. Calpain-mediated cleavage of Atg5 switches autophagy to apoptosis. *Nat. Cell Biol.* **2006**, *8*, 1124–1132. [CrossRef] [PubMed]
117. Huang, S.; Okamoto, K.; Yu, C.; Sinicrope, F.A. p62/sequestosome-1 up-regulation promotes ABT-263-induced caspase-8 aggregation/activation on the autophagosome\*. *J. Biol. Chem.* **2013**, *288*, 33654–33666. [CrossRef] [PubMed]
118. Young, M.M.; Takahashi, Y.; Khan, O.; Park, S.; Hori, T.; Yun, J.; Sharma, A.K.; Amin, S.; Hu, C.-D.; Zhang, J.; et al. Autophagosomal membrane serves as platform for intracellular Death-inducing Signaling Complex (iDISC)-mediated caspase-8 activation and apoptosis\*. *J. Biol. Chem.* **2012**, *287*, 12455–12468. [CrossRef] [PubMed]
119. Gornowicz, A.; Bielawska, A.; Szymanowski, W.; Gabryel-Porowska, H.; Czarnomysy, R.; Bielawski, K. Mechanism of anticancer action of novel berenil complex of platinum(II) combined with anti-MUC1 in MCF-7 breast cancer cells. *Oncol. Lett.* **2018**, *15*, 2340–2348. [CrossRef]
120. Pawłowska, N.; Gornowicz, A.; Bielawska, A.; Surażyński, A.; Szymanowska, A.; Czarnomysy, R.; Bielawski, K. The molecular mechanism of anticancer action of novel octahydropyrazino[2,1-a:5,4-a']diisoquinoline derivatives in human gastric cancer cells. *Investig. New Drugs* **2018**, *36*, 970–984. [CrossRef]
121. Gornowicz, A.; Pawłowska, N.; Czajkowska, A.; Czarnomysy, R.; Bielawska, A.; Bielawski, K.; Michalak, O.; Staszewska-Krajewska, O.; Kuzu, Z. Biological evaluation of octahydropyrazino[2,1-a:5,4-a']diisoquinoline derivatives as potent anticancer agents. *Tumor Biol.* **2017**, *39*, 1010428317701641. [CrossRef] [PubMed]
122. Wu, H.; Che, X.; Zheng, Q.; Wu, A.; Pan, K.; Shao, A.; Wu, Q.; Zhang, J.; Hong, Y. Caspases: A molecular switch node in the crosstalk between autophagy and apoptosis. *Int. J. Biol. Sci.* **2014**, *10*, 1072–1083. [CrossRef]
123. Parrish, A.B.; Freil, C.D.; Kornbluth, S. Cellular mechanisms controlling caspase activation and function. *Cold Spring Harb. Perspect Biol.* **2013**, *5*. [CrossRef] [PubMed]
124. Oral, O.; Oz-Arslan, D.; Itah, Z.; Naghavi, A.; Deveci, R.; Karacali, S.; Gozuacik, D. Cleavage of Atg3 protein by caspase-8 regulates autophagy during receptor-activated cell death. *Apoptosis* **2012**, *17*, 810–820. [CrossRef]
125. Wirawan, E.; Vande Walle, L.; Kersse, K.; Cornelis, S.; Claerhout, S.; Vanoverberghe, I.; Roelandt, R.; De Rycke, R.; Verspurten, J.; Declercq, W.; et al. Caspase-mediated cleavage of Beclin-1 inactivates Beclin-1-induced autophagy and enhances apoptosis by promoting the release of proapoptotic factors from mitochondria. *Cell Death Dis.* **2010**, *1*, e18. [CrossRef] [PubMed]
126. Han, J.; Hou, W.; Goldstein, L.A.; Stolz, D.B.; Watkins, S.C.; Rabinowich, H. A complex between Atg7 and caspase-9: A novel mechanism of cross-regulation between autophagy and apoptosis\*. *J. Biol. Chem.* **2014**, *289*, 6485–6497. [CrossRef]
127. Mizushima, N.; Levine, B. Autophagy in mammalian development and differentiation. *Nat. Cell Biol.* **2010**, *12*, 823–830. [CrossRef]
128. Wu, W.K.K.; Coffelt, S.B.; Cho, C.H.; Wang, X.J.; Lee, C.W.; Chan, F.K.L.; Yu, J.; Sung, J.J.Y. The autophagic paradox in cancer therapy. *Oncogene* **2012**, *31*, 939–953. [CrossRef] [PubMed]
129. Roy, S.; Debnath, J. Autophagy and tumorigenesis. *Semin. Immunopathol.* **2010**, *32*, 383–396. [CrossRef] [PubMed]
130. Drugs@FDA: FDA-Approved Drugs (Chloroquine). Available online: <https://www.accessdata.fda.gov/scripts/cder/daf/index.cfm?event=overview.process&ApplNo=006002> (accessed on 1 March 2021).
131. Solomon, V.R.; Lee, H. Chloroquine and its analogs: A new promise of an old drug for effective and safe cancer therapies. *Eur. J. Pharm.* **2009**, *625*, 220–233. [CrossRef] [PubMed]
132. Pellegrini, P.; Strambi, A.; Zipoli, C.; Hägg-Olofsson, M.; Buoncervello, M.; Linder, S.; De Milito, A. Acidic extracellular pH neutralizes the autophagy-inhibiting activity of chloroquine. *Autophagy* **2014**, *10*, 562–571. [CrossRef]
133. Erkisa, M.; Aydinlik, S.; Cevatemre, B.; Aztopal, N.; Akar, R.O.; Celikler, S.; Yilmaz, V.T.; Ari, F.; Ulukaya, E. A promising therapeutic combination for metastatic prostate cancer: Chloroquine as autophagy inhibitor and palladium(II) barbiturate complex. *Biochimie* **2020**, *175*, 159–172. [CrossRef] [PubMed]
134. Lopiccolo, J.; Kawabata, S.; Gills, J.J.; Dennis, P.A. Combining nelfinavir with chloroquine inhibits in vivo growth of human lung cancer xenograft tumors. *Vivo* **2021**, *35*, 141–145. [CrossRef]
135. Wei, T.; Ji, X.; Xue, J.; Gao, Y.; Zhu, X.; Xiao, G. Cyanidin-3-O-glucoside represses tumor growth and invasion in vivo by suppressing autophagy via inhibition of the JNK signaling pathways. *Food Funct.* **2021**, *12*, 387–396. [CrossRef] [PubMed]
136. Wolf, R.; Wolf, D.; Ruocco, V. Antimalarials: Unapproved uses or indications. *Clin. Dermatol.* **2000**, *18*, 17–35. [CrossRef]
137. Drugs@FDA: FDA-Approved Drugs (Hydroxychloroquine). Available online: <https://www.accessdata.fda.gov/scripts/cder/daf/index.cfm?event=overview.process&ApplNo=009768> (accessed on 1 March 2021).
138. Shi, T.-T.; Yu, X.-X.; Yan, L.-J.; Xiao, H.-T. Research progress of hydroxychloroquine and autophagy inhibitors on cancer. *Cancer Chemother. Pharmacol.* **2017**, *79*, 287–294. [CrossRef]
139. White, E. Deconvoluting the context-dependent role for autophagy in cancer. *Nat. Rev. Cancer* **2012**, *12*, 401–410. [CrossRef]
140. Drug Approval Package (Verteporfin). Available online: [https://www.accessdata.fda.gov/drugsatfda\\_docs/nda/2002/21-119s04\\_Visudyne.cfm](https://www.accessdata.fda.gov/drugsatfda_docs/nda/2002/21-119s04_Visudyne.cfm) (accessed on 5 March 2021).
141. Donohue, E.; Tovey, A.; Vogl, A.W.; Arns, S.; Sternberg, E.; Young, R.N.; Roberge, M. Inhibition of autophagosome formation by the benzoporphyrin derivative verteporfin. *J. Biol. Chem.* **2011**, *286*, 7290–7300. [CrossRef]

142. Donohue, E.; Thomas, A.; Maurer, N.; Manisali, I.; Zeisser-Labouebe, M.; Zisman, N.; Anderson, H.J.; Ng, S.S.W.; Webb, M.; Bally, M.; et al. The autophagy inhibitor verteporfin moderately enhances the antitumor activity of gemcitabine in a pancreatic ductal adenocarcinoma model. *J. Cancer* **2013**, *4*, 585–596. [CrossRef]
143. Gavini, J.; Dommann, N.; Jakob, M.O.; Keogh, A.; Bouchez, L.C.; Karkampouna, S.; Julio, M.K.-d.; Medova, M.; Zimmer, Y.; Schläfli, A.M.; et al. Verteporfin-induced lysosomal compartment dysregulation potentiates the effect of sorafenib in hepatocellular carcinoma. *Cell Death Dis.* **2019**, *10*, 749. [CrossRef]
144. Saini, H.; Sharma, H.; Mukherjee, S.; Chowdhury, R. Verteporfin disrupts multiple steps of autophagy and regulates p53 to sensitize osteosarcoma cells. *Cancer Cell Int.* **2021**, *21*, 52. [CrossRef]
145. Drug Approval Package (Clarithromycin). Available online: [https://www.accessdata.fda.gov/drugsatfda\\_docs/nda/2000/50775S1\\_Biaxin.cfm](https://www.accessdata.fda.gov/drugsatfda_docs/nda/2000/50775S1_Biaxin.cfm) (accessed on 1 March 2021).
146. Van Nuffel, A.M.; Sukhatme, V.; Pantziarka, P.; Meheus, L.; Sukhatme, V.P.; Bouche, G. Repurposing Drugs in Oncology (ReDO)-clarithromycin as an anti-cancer agent. *Ecancermedicalscience* **2015**, *9*, 513. [CrossRef] [PubMed]
147. Nakamura, M.; Kikukawa, Y.; Takeya, M.; Mitsuya, H.; Hata, H. Clarithromycin attenuates autophagy in myeloma cells. *Int. J. Oncol.* **2010**, *37*, 815–820. [CrossRef] [PubMed]
148. Kimura, T.; Takabatake, Y.; Takahashi, A.; Isaka, Y. Chloroquine in cancer therapy: A double-edged sword of autophagy. *Cancer Res.* **2013**, *73*, 3–7. [CrossRef] [PubMed]
149. Huggett, M.T.; Jermyn, M.; Gillams, A.; Illing, R.; Mosse, S.; Novelli, M.; Kent, E.; Bown, S.G.; Hasan, T.; Pogue, B.W.; et al. Phase I/II study of verteporfin photodynamic therapy in locally advanced pancreatic cancer. *Br. J. Cancer* **2014**, *110*, 1698–1704. [CrossRef]
150. Seglen, P.O.; Gordon, P.B. 3-Methyladenine: Specific inhibitor of autophagic/lysosomal protein degradation in isolated rat hepatocytes. *Proc. Natl. Acad. Sci. USA* **1982**, *79*, 1889–1892. [CrossRef]
151. Vinod, V.; Padmakrishnan, C.J.; Vijayan, B.; Gopala, S. 'How can I halt thee?' The puzzles involved in autophagic inhibition. *Pharmacol. Res.* **2014**, *82*, 1–8. [CrossRef] [PubMed]
152. Petiot, A.; Ogier-Denis, E.; Blommaert, E.F.C.; Meijer, A.J.; Codogno, P. Distinct classes of phosphatidylinositol 3'-kinases are involved in signaling pathways that control macroautophagy in HT-29 cells. *J. Biol. Chem.* **2000**, *275*, 992–998. [CrossRef] [PubMed]
153. Pasquier, B. Autophagy inhibitors. *Cell. Mol. Life Sci.* **2016**, *73*, 985–1001. [CrossRef]
154. Wu, Y.-T.; Tan, H.-L.; Shui, G.; Bauvy, C.; Huang, Q.; Wenk, M.R.; Ong, C.-N.; Codogno, P.; Shen, H.-M. Dual role of 3-methyladenine in modulation of autophagy via different temporal patterns of inhibition on class I and III phosphoinositide 3-kinase. *J. Biol. Chem.* **2010**, *285*, 10850–10861. [CrossRef]
155. Wang, H.; Peng, Y.; Wang, J.; Gu, A.; Li, Q.; Mao, D.; Guo, L. Effect of autophagy on the resveratrol-induced apoptosis of ovarian cancer SKOV3 cells. *J. Cell. Biochem.* **2019**, *120*, 7788–7793. [CrossRef]
156. Zhao, F.; Feng, G.; Zhu, J.; Su, Z.; Guo, R.; Liu, J.; Zhang, H.; Zhai, Y. 3-Methyladenine-enhanced susceptibility to sorafenib in hepatocellular carcinoma cells by inhibiting autophagy. *Anti Cancer Drugs* **2021**. Publish Ahead of Print. [CrossRef]
157. Ronan, B.; Flamand, O.; Vescovi, L.; Dureuil, C.; Durand, L.; Fassy, F.; Bachelot, M.-F.; Lambertson, A.; Mathieu, M.; Bertrand, T.; et al. A highly potent and selective Vps34 inhibitor alters vesicle trafficking and autophagy. *Nat. Chem. Biol.* **2014**, *10*, 1013–1019. [CrossRef]
158. Pasquier, B. SAR405, a PIK3C3/Vps34 inhibitor that prevents autophagy and synergizes with mTOR inhibition in tumor cells. *Autophagy* **2015**, *11*, 725–726. [CrossRef] [PubMed]
159. Janji, B.; Hasmim, M.; Parpal, S.; De Milito, A.; Berchem, G.; Noman, M.Z. Lighting up the fire in cold tumors to improve cancer immunotherapy by blocking the activity of the autophagy-related protein PIK3C3/VPS34. *Autophagy* **2020**, *16*, 2110–2111. [CrossRef] [PubMed]
160. McAfee, Q.; Zhang, Z.; Samanta, A.; Levi, S.M.; Ma, X.-H.; Piao, S.; Lynch, J.P.; Uehara, T.; Sepulveda, A.R.; Davis, L.E.; et al. Autophagy inhibitor Lys05 has single-agent antitumor activity and reproduces the phenotype of a genetic autophagy deficiency. *Proc. Natl. Acad. Sci. USA* **2012**, *109*, 8253–8258. [CrossRef] [PubMed]
161. DeVorkin, L.; Hattersley, M.; Kim, P.; Ries, J.; Spowart, J.; Anglesio, M.S.; Levi, S.M.; Huntsman, D.G.; Amaravadi, R.K.; Winkler, J.D.; et al. Autophagy inhibition enhances sunitinib efficacy in clear cell ovarian carcinoma. *Mol. Cancer Res.* **2017**, *15*, 250–258. [CrossRef] [PubMed]
162. Baquero, P.; Dawson, A.; Mukhopadhyay, A.; Kuntz, E.M.; Mitchell, R.; Olivares, O.; Ianniciello, A.; Scott, M.T.; Dunn, K.; Nicastri, M.C.; et al. Targeting quiescent leukemic stem cells using second generation autophagy inhibitors. *Leukemia* **2019**, *33*, 981–994. [CrossRef]
163. Carew, J.S.; Espitia, C.M.; Zhao, W.; Han, Y.; Visconte, V.; Phillips, J.; Nawrocki, S.T. Disruption of autophagic degradation with ROC-325 antagonizes renal cell carcinoma pathogenesis. *Clin. Cancer Res.* **2017**, *23*, 2869–2879. [CrossRef]
164. Nawrocki, S.T.; Han, Y.; Visconte, V.; Przychodzen, B.; Espitia, C.M.; Phillips, J.; Anwer, F.; Advani, A.; Carraway, H.E.; Kelly, K.R.; et al. The novel autophagy inhibitor ROC-325 augments the antileukemic activity of azacitidine. *Leukemia* **2019**, *33*, 2971–2974. [CrossRef]
165. Takase, Y.; Saeki, T.; Watanabe, N.; Adachi, H.; Souda, S.; Saito, I. Cyclic GMP phosphodiesterase inhibitors. 2. Requirement of 6-substitution of quinazoline derivatives for potent and selective inhibitory activity. *J. Med. Chem.* **1994**, *37*, 2106–2111. [CrossRef] [PubMed]

166. MacPherson, J.D.; Gillespie, T.D.; Dunkerley, H.A.; Maurice, D.H.; Bennett, B.M. Inhibition of phosphodiesterase 5 selectively reverses nitrate tolerance in the venous circulation. *J. Pharmacol. Exp. Ther.* **2006**, *317*, 188–195. [CrossRef]
167. Liu, J.; Xia, H.; Kim, M.; Xu, L.; Li, Y.; Zhang, L.; Cai, Y.; Norberg, H.V.; Zhang, T.; Furuya, T.; et al. Beclin1 controls the levels of p53 by regulating the deubiquitination activity of USP10 and USP13. *Cell* **2011**, *147*, 223–234. [CrossRef]
168. Correa, R.J.M.; Valdes, Y.R.; Peart, T.M.; Fazio, E.N.; Bertrand, M.; McGee, J.; Préfontaine, M.; Sugimoto, A.; DiMattia, G.E.; Shepherd, T.G. Combination of AKT inhibition with autophagy blockade effectively reduces ascites-derived ovarian cancer cell viability. *Carcinogenesis* **2014**, *35*, 1951–1961. [CrossRef]
169. Shao, S.; Li, S.; Qin, Y.; Wang, X.; Yang, Y.; Bai, H.; Zhou, L.; Zhao, C.; Wang, C. Spautin-1, a novel autophagy inhibitor, enhances imatinib-induced apoptosis in chronic myeloid leukemia. *Int. J. Oncol.* **2014**, *44*, 1661–1668. [CrossRef]
170. Liao, Y.; Guo, Z.; Xia, X.; Liu, Y.; Huang, C.; Jiang, L.; Wang, X.; Liu, J.; Huang, H. Inhibition of EGFR signaling with Spautin-1 represents a novel therapeutics for prostate cancer. *J. Exp. Clin. Cancer Res.* **2019**, *38*, 157. [CrossRef]
171. Gornowicz, A.; Szymanowska, A.; Mojzycz, M.; Bielawski, K.; Bielawska, A. The effect of novel 7-methyl-5-phenyl-pyrazolo[4,3-*e*]tetrazolo[4,5-*b*]1,2,4-triazine sulfonamide derivatives on apoptosis and autophagy in DLD-1 and HT-29 colon cancer cells. *Int. J. Mol. Sci.* **2020**, *21*, 5221. [CrossRef]
172. Fu, Y.; Hong, L.; Xu, J.; Zhong, G.; Gu, Q.; Gu, Q.; Guan, Y.; Zheng, X.; Dai, Q.; Luo, X.; et al. Discovery of a small molecule targeting autophagy via ATG4B inhibition and cell death of colorectal cancer cells in vitro and in vivo. *Autophagy* **2019**, *15*, 295–311. [CrossRef]
173. Das, C.K.; Banerjee, I.; Mandal, M. Pro-survival autophagy: An emerging candidate of tumor progression through maintaining hallmarks of cancer. *Semin. Cancer Biol.* **2020**, *66*, 59–74. [CrossRef]
174. De Mei, C.; Ercolani, L.; Parodi, C.; Veronesi, M.; Vecchio, C.L.; Bottegoni, G.; Torrente, E.; Scarpelli, R.; Marotta, R.; Ruffili, R.; et al. Dual inhibition of REV-ERB $\beta$  and autophagy as a novel pharmacological approach to induce cytotoxicity in cancer cells. *Oncogene* **2015**, *34*, 2597–2608. [CrossRef]
175. Kurdi, A.; Cleenerwerck, M.; Vangestel, C.; Lyssens, S.; Declercq, W.; Timmermans, J.-P.; Stroobants, S.; Augustyns, K.; De Meyer, G.R.Y.; Van Der Veken, P.; et al. ATG4B inhibitors with a benzotropolone core structure block autophagy and augment efficiency of chemotherapy in mice. *Biochem. Pharmacol.* **2017**, *138*, 150–162. [CrossRef]
176. Chen, X.-L.; Liu, P.; Zhu, W.-L.; Lou, L.-g. DCZ5248, a novel dual inhibitor of Hsp90 and autophagy, exerts antitumor activity against colon cancer. *Acta Pharmacol. Sin.* **2021**, *42*, 132–141. [CrossRef]
177. Zhang, L.; Qiang, P.; Yu, J.; Miao, Y.; Chen, Z.; Qu, J.; Zhao, Q.; Chen, Z.; Liu, Y.; Yao, X.; et al. Identification of compound CA-5f as a novel late-stage autophagy inhibitor with potent anti-tumor effect against non-small cell lung cancer. *Autophagy* **2019**, *15*, 391–406. [CrossRef]
178. Rebecca, V.W.; Nicastrì, M.C.; McLaughlin, N.; Fennelly, C.; McAfee, Q.; Ronghe, A.; Nofal, M.; Lim, C.-Y.; Witze, E.; Chude, C.I.; et al. A unified approach to targeting the lysosome's degradative and growth signaling roles. *Cancer Discov.* **2017**, *7*, 1266–1283. [CrossRef]
179. Hu, P.; Wang, J.; Qing, Y.; Li, H.; Sun, W.; Yu, X.; Hui, H.; Guo, Q.; Xu, J. FV-429 induces autophagy blockage and lysosome-dependent cell death of T-cell malignancies via lysosomal dysregulation. *Cell Death Dis.* **2021**, *12*, 80. [CrossRef] [PubMed]
180. Zhou, Y.; Wei, L.; Zhang, H.; Dai, Q.; Li, Z.; Yu, B.; Guo, Q.; Lu, N. FV-429 induced apoptosis through ROS-mediated ERK2 nuclear translocation and p53 activation in gastric cancer cells. *J. Cell. Biochem.* **2015**, *116*, 1624–1637. [CrossRef]
181. Miura, K.; Kawano, S.; Suto, T.; Sato, T.; Chida, N.; Simizu, S. Identification of madangamine A as a novel lysosomotropic agent to inhibit autophagy. *Bioorganic Med. Chem.* **2021**, *34*, 116041. [CrossRef]
182. Park, S.R.; Yoo, Y.J.; Ban, Y.-H.; Yoon, Y.J. Biosynthesis of rapamycin and its regulation: Past achievements and recent progress. *J. Antibiot.* **2010**, *63*, 434–441. [CrossRef]
183. Drug Approval Package (Rapamycin). Available online: [https://www.accessdata.fda.gov/drugsatfda\\_docs/nda/99/21083A.cfm](https://www.accessdata.fda.gov/drugsatfda_docs/nda/99/21083A.cfm) (accessed on 1 March 2021).
184. Steiner, J.P.; Connolly, M.A.; Valentine, H.L.; Hamilton, G.S.; Dawson, T.M.; Hester, L.; Snyder, S.H. Neurotrophic actions of nonimmunosuppressive analogues of immunosuppressive drugs FK506, rapamycin and cyclosporin A. *Nat. Med.* **1997**, *3*, 421–428. [CrossRef] [PubMed]
185. Douros, J.; Suffness, M. New antitumor substances of natural origin. *Cancer Treat. Rev.* **1981**, *8*, 63–87. [CrossRef]
186. Harrison, D.E.; Strong, R.; Sharp, Z.D.; Nelson, J.F.; Astle, C.M.; Flurkey, K.; Nadon, N.L.; Wilkinson, J.E.; Frenkel, K.; Carter, C.S.; et al. Rapamycin fed late in life extends lifespan in genetically heterogeneous mice. *Nature* **2009**, *460*, 392–395. [CrossRef]
187. Calne, R.Y.; Lim, S.; Samaan, A.; Collier, D.S.J.; Pollard, S.G.; White, D.J.G.; Thiru, S. Rapamycin for immunosuppression in organ allografting. *Lancet* **1989**, *334*, 227. [CrossRef]
188. Demain, A.L. Importance of microbial natural products and the need to revitalize their discovery. *J. Ind. Microbiol. Biotechnol.* **2014**, *41*, 185–201. [CrossRef]
189. Chiarini, F.; Evangelisti, C.; McCubrey, J.A.; Martelli, A.M. Current treatment strategies for inhibiting mTOR in cancer. *Trends Pharmacol. Sci.* **2015**, *36*, 124–135. [CrossRef]
190. Zhou, C.; Zhong, W.; Zhou, J.; Sheng, F.; Fang, Z.; Wei, Y.; Chen, Y.; Deng, X.; Xia, B.; Lin, J. Monitoring autophagic flux by an improved tandem fluorescent-tagged LC3 (mTagRFP-mWasabi-LC3) reveals that high-dose rapamycin impairs autophagic flux in cancer cells. *Autophagy* **2012**, *8*, 1215–1226. [CrossRef]





191. Drug Approval Package (Temsirolimus). Available online: [https://www.accessdata.fda.gov/drugsatfda\\_docs/nda/2007/022088s000TOC.cfm](https://www.accessdata.fda.gov/drugsatfda_docs/nda/2007/022088s000TOC.cfm) (accessed on 9 March 2021).
192. Meng, L.-h.; Zheng, X.F.S. Toward rapamycin analog (rapalog)-based precision cancer therapy. *Acta Pharmacol. Sin.* **2015**, *36*, 1163–1169. [CrossRef] [PubMed]
193. Raymond, E.; Alexandre, J.; Faivre, S.; Vera, K.; Maternan, E.; Boni, J.; Leister, C.; Korth-Bradley, J.; Hanauske, A.; Armand, J.-P. Safety and pharmacokinetics of escalated doses of weekly intravenous infusion of CCI-779, a novel mTOR inhibitor, in patients with cancer. *J. Clin. Oncol.* **2004**, *22*, 2336–2347. [CrossRef]
194. Shiratori, H.; Kawai, K.; Hata, K.; Tanaka, T.; Nishikawa, T.; Otani, K.; Sasaki, K.; Kaneko, M.; Muro, K.; Emoto, S.; et al. The combination of temsirolimus and chloroquine increases radiosensitivity in colorectal cancer cells. *Oncol. Rep.* **2019**, *42*, 377–385. [CrossRef]
195. Inamura, S.; Ito, H.; Taga, M.; Tsuchiyama, K.; Hoshino, H.; Kobayashi, M.; Yokoyama, O. Low-dose docetaxel enhanced the anticancer effect of temsirolimus by overcoming autophagy in prostate cancer cells. *Anticancer Res.* **2019**, *39*, 5417–5425. [CrossRef] [PubMed]
196. Kondo, S.; Hirakawa, H.; Ikegami, T.; Uehara, T.; Agha, S.; Uezato, J.; Kinjyo, H.; Kise, N.; Yamashita, Y.; Tanaka, K.; et al. Raptor and rictor expression in patients with human papillomavirus-related oropharyngeal squamous cell carcinoma. *Bmc Cancer* **2021**, *21*, 87. [CrossRef]
197. Trivedi, N.D.; Armstrong, S.; Wang, H.; Hartley, M.; Deeken, J.; Ruth He, A.; Subramaniam, D.; Melville, H.; Albanese, C.; Marshall, J.L.; et al. A phase I trial of the mTOR inhibitor temsirolimus in combination with capecitabine in patients with advanced malignancies. *Cancer Med.* **2021**, *10*, 1944–1954. [CrossRef] [PubMed]
198. Drugs@FDA: FDA-Approved Drugs (Everolimus). Available online: <https://www.accessdata.fda.gov/scripts/cder/daf/index.cfm?event=overview.process&varApplNo=022334> (accessed on 10 March 2021).
199. Feldman, D.R.; Ged, Y.; Lee, C.-H.; Knezevic, A.; Molina, A.M.; Chen, Y.-B.; Chaim, J.; Coskey, D.T.; Murray, S.; Tickoo, S.K.; et al. Everolimus plus bevacizumab is an effective first-line treatment for patients with advanced papillary variant renal cell carcinoma: Final results from a phase II trial. *Cancer* **2020**, *126*, 5247–5255. [CrossRef]
200. El Guerrab, A.; Bamdad, M.; Bignon, Y.-J.; Penault-Llorca, F.; Aubeil, C. Co-targeting EGFR and mTOR with gefitinib and everolimus in triple-negative breast cancer cells. *Sci. Rep.* **2020**, *10*, 6367. [CrossRef]
201. Zhu, M.; Molina, J.R.; Dy, G.K.; Croghan, G.A.; Qi, Y.; Glockner, J.; Hanson, L.J.; Roos, M.M.; Tan, A.D.; Adjei, A.A. A phase I study of the VEGFR kinase inhibitor vatalanib in combination with the mTOR inhibitor, everolimus, in patients with advanced solid tumors. *Investig. New Drugs* **2020**, *38*, 1755–1762. [CrossRef] [PubMed]
202. Werner, E.A.; Bell, J. CCXIV.—The preparation of methylguanidine, and of  $\beta\beta$ -dimethylguanidine by the interaction of dicyanodiamide, and methylammonium and dimethylammonium chlorides respectively. *J. Chem. Soc. Trans.* **1922**, *121*, 1790–1794. [CrossRef]
203. Bailey, C.J. Metformin: Historical overview. *Diabetologia* **2017**, *60*, 1566–1576. [CrossRef] [PubMed]
204. Drug Approval Package (Metformin). Available online: [https://www.accessdata.fda.gov/drugsatfda\\_docs/nda/98/020357s010.cfm](https://www.accessdata.fda.gov/drugsatfda_docs/nda/98/020357s010.cfm) (accessed on 1 March 2021).
205. Pernicova, I.; Korbonits, M. Metformin—mode of action and clinical implications for diabetes and cancer. *Nat. Rev. Endocrinol.* **2014**, *10*, 143–156. [CrossRef] [PubMed]
206. Lu, G.; Wu, Z.; Shang, J.; Xie, Z.; Chen, C.; Zhang, C. The effects of metformin on autophagy. *Biomed. Pharmacother.* **2021**, *137*, 111286. [CrossRef]
207. Tomic, T.; Botton, T.; Cerezo, M.; Robert, G.; Luciano, F.; Puissant, A.; Gounon, P.; Allegra, M.; Bertolotto, C.; Bereder, J.M.; et al. Metformin inhibits melanoma development through autophagy and apoptosis mechanisms. *Cell Death Dis.* **2011**, *2*, e199. [CrossRef] [PubMed]
208. Takahashi, A.; Kimura, F.; Yamanaka, A.; Takebayashi, A.; Kita, N.; Takahashi, K.; Murakami, T. Metformin impairs growth of endometrial cancer cells via cell cycle arrest and concomitant autophagy and apoptosis. *Cancer Cell Int.* **2014**, *14*, 53. [CrossRef]
209. Diamanti-Kandarakis, E.; Economou, F.; Palimeri, S.; Christakou, C. Metformin in polycystic ovary syndrome. *Ann. N.Y. Acad. Sci.* **2010**, *1205*, 192–198. [CrossRef] [PubMed]
210. Patel, R.; Shah, G. Effect of metformin on clinical, metabolic and endocrine outcomes in women with polycystic ovary syndrome: A meta-analysis of randomized controlled trials. *Curr. Med. Res. Opin.* **2017**, *33*, 1545–1557. [CrossRef]
211. Gandini, S.; Puntoni, M.; Heckman-Stoddard, B.M.; Dunn, B.K.; Ford, L.; DeCensi, A.; Szabo, E. Metformin and cancer risk and mortality: A systematic review and meta-analysis taking into account biases and confounders. *Cancer Prev. Res.* **2014**, *7*, 867–885. [CrossRef]
212. Hong, J.; Zhang, Y.; Lai, S.; Lv, A.; Su, Q.; Dong, Y.; Zhou, Z.; Tang, W.; Zhao, J.; Cui, L.; et al. Effects of metformin versus glipizide on cardiovascular outcomes in patients with type 2 diabetes and coronary artery disease. *Diabetes Care* **2013**, *36*, 1304–1311. [CrossRef]
213. Piskovatska, V.; Stefanyshyn, N.; Storey, K.B.; Vaiserman, A.M.; Lushchak, O. Metformin as a geroprotector: Experimental and clinical evidence. *Biogerontology* **2019**, *20*, 33–48. [CrossRef]
214. Bannister, C.A.; Holden, S.E.; Jenkins-Jones, S.; Morgan, C.L.; Halcox, J.P.; Scherthaner, G.; Mukherjee, J.; Currie, C.J. Can people with type 2 diabetes live longer than those without? A comparison of mortality in people initiated with metformin or sulphonylurea monotherapy and matched, non-diabetic controls. *Diabetes Obes. Metab.* **2014**, *16*, 1165–1173. [CrossRef]

215. Drugs@FDA: FDA-Approved Drugs (Miconazole). Available online: <https://www.accessdata.fda.gov/scripts/cder/daf/index.cfm?event=overview.process&ApplNo=017450> (accessed on 15 March 2021).
216. Piérard, G.E.; Wallace, R.; De Doncker, P. Biometrological assessment of the preventive effect of a miconazole spray powder on athlete's foot. *Clin. Exp. Derm.* **1996**, *21*, 344–346. [[CrossRef](#)]
217. Tanenbaum, L.; Anderson, C.; Rosenberg, M.J.; Akers, W. 1% Sulconazole Cream v 2% Miconazole Cream in the Treatment of Tinea Versicolor: A Double-blind, Multicenter Study. *Arch. Dermatol.* **1984**, *120*, 216–219. [[CrossRef](#)] [[PubMed](#)]
218. Park, J.-Y.; Jung, H.-J.; Seo, I.; Jha, B.K.; Suh, S.-I.; Suh, M.-H.; Baek, W.-K. Translational suppression of HIF-1 $\alpha$  by miconazole through the mTOR signaling pathway. *Cell. Oncol.* **2014**, *37*, 269–279. [[CrossRef](#)] [[PubMed](#)]
219. Shahbazfar, A.; Zare, P.; Ranjbaran, M.; Tayefi-Nasrabadi, H.; Fakhri, O.; Farshi, Y.; Shadi, S.; Khoshkardar, A. A survey on anticancer effects of artemisinin, iron, miconazole, and butyric acid on 5637 (bladder cancer) and 4T1 (Breast cancer) cell lines. *J. Cancer Res. Ther.* **2014**, *10*, 1057–1062. [[CrossRef](#)]
220. Chang, H.-T.; Chen, W.-C.; Chen, J.-S.; Lu, Y.-C.; Hsu, S.-S.; Wang, J.-L.; Cheng, H.-H.; Cheng, J.-S.; Jiann, B.-P.; Chiang, A.-J.; et al. Effect of miconazole on intracellular Ca<sup>2+</sup> levels and proliferation in human osteosarcoma cells. *Life Sci.* **2005**, *76*, 2091–2101. [[CrossRef](#)]
221. Jung, H.-J.; Seo, I.; Jha, B.K.; Suh, S.-I.; Baek, W.-K. Miconazole induces autophagic death in glioblastoma cells via reactive oxygen species-mediated endoplasmic reticulum stress. *Oncol. Lett.* **2021**, *21*, 335. [[CrossRef](#)]
222. Ho, C.-Y.; Chang, A.-C.; Hsu, C.-H.; Tsai, T.-F.; Lin, Y.-C.; Chou, K.-Y.; Chen, H.-E.; Lin, J.-F.; Chen, P.-C.; Hwang, T.I.-S. Miconazole induces protective autophagy in bladder cancer cells. *Environ. Toxicol.* **2021**, *36*, 185–193. [[CrossRef](#)]
223. Jaune, E.; Cavazza, E.; Ronco, C.; Grytsai, O.; Abbe, P.; Tekaya, N.; Zerhouni, M.; Beranger, G.; Kaminski, L.; Bost, F.; et al. Discovery of a new molecule inducing melanoma cell death: Dual AMPK/MELK targeting for novel melanoma therapies. *Cell Death Dis.* **2021**, *12*, 64. [[CrossRef](#)]
224. Adamska, A.; Stefanowicz-Hajduk, J.; Ochocka, J.R. Alpha-hederin, the active saponin of *Nigella sativa*, as an anticancer agent inducing apoptosis in the SKOV-3 cell line. *Molecules* **2019**, *24*, 2958. [[CrossRef](#)]
225. Li, J.; Wu, D.-D.; Zhang, J.-X.; Wang, J.; Ma, J.-J.; Hu, X.; Dong, W.-G. Mitochondrial pathway mediated by reactive oxygen species involvement in  $\alpha$ -hederin-induced apoptosis in hepatocellular carcinoma cells. *World J. Gastroenterol.* **2018**, *24*, 1901–1910. [[CrossRef](#)] [[PubMed](#)]
226. Sun, J.; Feng, Y.; Wang, Y.; Ji, Q.; Cai, G.; Shi, L.; Wang, Y.; Huang, Y.; Zhang, J.; Li, Q.  $\alpha$ -hederin induces autophagic cell death in colorectal cancer cells through reactive oxygen species dependent AMPK/mTOR signaling pathway activation. *Int. J. Oncol.* **2019**, *54*, 1601–1612. [[CrossRef](#)]
227. Ha, H.A.; Chiang, J.H.; Tsai, F.J.; Bau, D.T.; Juan, Y.N.; Lo, Y.H.; Hour, M.J.; Yang, J.S. Novel quinazolinone MJ-33 induces AKT/mTOR-mediated autophagy-associated apoptosis in 5FU-resistant colorectal cancer cells. *Oncol. Rep.* **2021**, *45*, 680–692. [[CrossRef](#)] [[PubMed](#)]
228. Liu, T.; Zhang, J.; Li, K.; Deng, L.; Wang, H. Combination of an autophagy inducer and an autophagy inhibitor: A smarter strategy emerging in cancer therapy. *Front. Pharm.* **2020**, *11*, 408. [[CrossRef](#)]
229. Hour, M.-J.; Tsai, S.-C.; Wu, H.-C.; Lin, M.-W.; Chung, J.G.; Wu, J.-B.; Chiang, J.-H.; Tsuzuki, M.; Yang, J.-S. Antitumor effects of the novel quinazolinone MJ-33: Inhibition of metastasis through the MAPK, AKT, NF- $\kappa$ B and AP-1 signaling pathways in DU145 human prostate cancer cells. *Int. J. Oncol.* **2012**, *41*, 1513–1519. [[CrossRef](#)]
230. Omoruyi, S.I.; Ekpo, O.E.; Semanya, D.M.; Jardine, A.; Prince, S. Exploitation of a novel phenothiazine derivative for its anti-cancer activities in malignant glioblastoma. *Apoptosis* **2020**, *25*, 261–274. [[CrossRef](#)]
231. De, U.; Son, J.Y.; Sachan, R.; Park, Y.J.; Kang, D.; Yoon, K.; Lee, B.M.; Kim, I.S.; Moon, H.R.; Kim, H.S. A new synthetic histone deacetylase inhibitor, MHY2256, induces apoptosis and autophagy cell death in endometrial cancer cells via p53 acetylation. *Int. J. Mol. Sci.* **2018**, *19*, 2743. [[CrossRef](#)]
232. Kim, M.J.; Kang, Y.J.; Sung, B.; Jang, J.Y.; Ahn, Y.R.; Oh, H.J.; Choi, H.; Choi, I.; Im, E.; Moon, H.R.; et al. Novel SIRT inhibitor, MHY2256, induces cell cycle arrest, apoptosis, and autophagic cell death in HCT116 human colorectal cancer cells. *Biomol. Ther.* **2020**, *28*, 561–568. [[CrossRef](#)] [[PubMed](#)]
233. Hsieh, C.-L.; Huang, H.-S.; Chen, K.-C.; Saka, T.; Chiang, C.-Y.; Chung, L.W.K.; Sung, S.-Y. A novel salicylanilide derivative induces autophagy cell death in castration-resistant prostate cancer via ER stress-activated PERK signaling pathway. *Mol. Cancer Ther.* **2020**, *19*, 101–111. [[CrossRef](#)] [[PubMed](#)]
234. Li, X.; Li, Z.; Song, Y.; Liu, W.; Liu, Z. The mTOR kinase inhibitor CZ415 inhibits human papillary thyroid carcinoma cell growth. *Cell. Physiol. Biochem.* **2018**, *46*, 579–590. [[CrossRef](#)]
235. Zhou, X.; Yue, G.G.-L.; Chan, A.M.-L.; Tsui, S.K.-W.; Fung, K.-P.; Sun, H.; Pu, J.; Lau, C.B.-S. Eriocalyxin B, a novel autophagy inducer, exerts anti-tumor activity through the suppression of Akt/mTOR/p70S6K signaling pathway in breast cancer. *Biochem. Pharmacol.* **2017**, *142*, 58–70. [[CrossRef](#)]

Article

# Synthesis and Anticancer Activity Evaluation of 5-[2-Chloro-3-(4-nitrophenyl)-2-propenylidene]-4-thiazolidinones

Kamila Buzun <sup>1</sup>, Anna Kryshchshyn-Dylevych <sup>2</sup>, Julia Senkiv <sup>3</sup>, Olexandra Roman <sup>2</sup>, Andrzej Gzella <sup>4</sup>, Krzysztof Bielawski <sup>5</sup>, Anna Bielawska <sup>1</sup> and Roman Lesyk <sup>2,6,\*</sup>

<sup>1</sup> Department of Biotechnology, Medical University of Białystok, Jana Kilińskiego 1, 15-089 Białystok, Poland; kamila.buzun@umb.edu.pl (K.B.); anna.bielawska@umb.edu.pl (A.B.)

<sup>2</sup> Department of Pharmaceutical, Organic and Bioorganic Chemistry, Danylo Halytsky Lviv National Medical University, Pekarska 69, 79010 Lviv, Ukraine; kryshchshyn.a@gmail.com (A.K.-D.); lesia\_roman@ukr.net (O.R.)

<sup>3</sup> Institute of Cell Biology of National Academy of Sciences of Ukraine, 14/16 Drahomanov Str., 79005 Lviv, Ukraine; yu.senkiv@gmail.com

<sup>4</sup> Department of Organic Chemistry, Poznan University of Medical Sciences, Grunwaldzka 6, 60-780 Poznan, Poland; akgzella@ump.edu.pl

<sup>5</sup> Department of Synthesis and Technology of Drugs, Medical University of Białystok, 15-089 Białystok, Poland; kbiel@umb.edu.pl

<sup>6</sup> Department of Public Health, Dietetics and Lifestyle Disorders, Faculty of Medicine, University of Information Technology and Management in Rzeszow, 35-225 Rzeszow, Poland

\* Correspondence: dr\_r\_lesyk@org.lviv.net; Tel.: +38-032-275-5966



**Citation:** Buzun, K.; Kryshchshyn-Dylevych, A.; Senkiv, J.; Roman, O.; Gzella, A.; Bielawski, K.; Bielawska, A.; Lesyk, R. Synthesis and Anticancer Activity Evaluation of 5-[2-Chloro-3-(4-nitrophenyl)-2-propenylidene]-4-thiazolidinones. *Molecules* **2021**, *26*, 3057. <https://doi.org/10.3390/molecules26103057>

Academic Editor: Fabio Marchetti

Received: 18 April 2021

Accepted: 16 May 2021

Published: 20 May 2021

**Publisher's Note:** MDPI stays neutral with regard to jurisdictional claims in published maps and institutional affiliations.



**Copyright:** © 2021 by the authors. Licensee MDPI, Basel, Switzerland. This article is an open access article distributed under the terms and conditions of the Creative Commons Attribution (CC BY) license (<https://creativecommons.org/licenses/by/4.0/>).

**Abstract:** A series of novel 5-[(Z,Z)-2-chloro-3-(4-nitrophenyl)-2-propenylidene]-thiazolidinones (Ciminalum–thiazolidinone hybrid molecules) have been synthesized. Anticancer activity screening toward the NCI60 cell lines panel, gastric cancer (AGS), human colon cancer (DLD-1), and breast cancer (MCF-7 and MDA-MB-231) cell lines allowed the identification of 3-[5-[(Z,Z)-2-chloro-3-(4-nitrophenyl)-2-propenylidene]-4-oxo-2-thioxothiazolidin-3-yl]propanoic acid (**2h**) with the highest level of antimitotic activity with mean GI<sub>50</sub>/TGI values of 1.57/13.3 μM and a certain sensitivity profile against leukemia (MOLT-4, SR), colon cancer (SW-620), CNS cancer (SF-539), melanoma (SK-MEL-5), gastric cancer (AGS), human colon cancer (DLD-1), and breast cancers (MCF-7 and MDA-MB-231) cell lines. The hit compounds **2f**, **2i**, **2j**, and **2h** have been found to have low toxicity toward normal human blood lymphocytes and a fairly wide therapeutic range. The significant role of the 2-chloro-3-(4-nitrophenyl)prop-2-enylidene (Ciminalum) substituent in the 5 position and the substituent's nature in the position 3 of core heterocycle in the anticancer cytotoxicity levels of 4-thiazolidinone derivatives have been established

**Keywords:** synthesis; 4-thiazolidinones; Ciminalum; anticancer activity; SAR analysis

## 1. Introduction

In recent years, one of successful directions in the structure design of “drug-like” molecules is the “hybrid-pharmacophore” approach that involves combining different fragments in one molecule that can be parts, biomimetics, and/or bioisosteres of biologically active molecules or drugs. This strategy allows potentiating the desired action or appearance of new effects [1–3] and can be relevant for the search for new highly active compounds based on 4-thiazolidinones as effective biophores. Thus, modern studies of the pharmacological potential of thiazolidinones have significantly expanded the range of their activity, including anticancer, antibacterial, antifungal, antiviral, antiparasitic, and anti-tuberculosis. Along with this, there is indisputable evidence of the affinity of these derivatives for biotargets involved in the biochemical processes of tumor cell growth (TNF-α-TNFRc-1, JSP-1, antiapoptotic complex Bcl-XL-BH3), the microorganisms life cycle

(UDP-NMurNA/L-Ala-ligase), the development of inflammatory conditions (COX-2/5-LOX), and the development of type II diabetes mellitus (PPAR $\gamma$ ) [4,5].

Based on our previous research, we have established that the combination of a thiazolidinone moiety and a structural fragment of the *Ciminalum* in one hybrid molecule is an effective approach for the design of potential anticancer agents [6,7]. *Ciminalum* (*p*-nitro- $\alpha$ -chlorocinnamic aldehyde or (2*Z*)-2-chloro-3-(4-nitrophenyl)prop-2-enal, CAS 3626-97-9) is an active antimicrobial agent against Gram-positive and Gram-negative microorganisms. *Ciminalum* was used as a drug in medical practice in the former Soviet Union (Figure 1) [8]. *Ciminalum*-thiazolidinone hybrid molecules (namely 5-[(*Z,Z*)-2-chloro-3-(4-nitrophenyl)-2-propenylidene]-4-thiazolidinones) showed a significant cytotoxic effect on tumor cells. It is important to note that the presence of a *Ciminalum* moiety in position 5 of the thiazolidinone ring is key to the manifestation of biological activity. Thus, early hits **I** and **II** (Figure 1) possessed a selectively high effect on leukemia, melanoma, lung, colon, CNS, ovarian, renal, prostate, and breast cancers cell lines at micro- and submicromolar levels that is probably associated with the immunosuppressive activity [7]. Early anticancer hit **III** has induced and activated specific signaling apoptotic pathways in tumor cells [6]. Thus, compound **III** leads to weak caspase-7 activation and a weak cleavage of PARP-1 and DFF45 in the Jurkat T-cells. However, this *Ciminalum*-thiazolidinone hybrid may be involved in the caspase-independent, AIF-mediated apoptosis. AIF (apoptosis-inducing factor) is known to induce the mitochondria-mediated caspase-independent apoptosis. Derivative **III** leads to the activation of intrinsic apoptotic pathways, mediated by mitochondria, and caspases seem to play a minor role here.

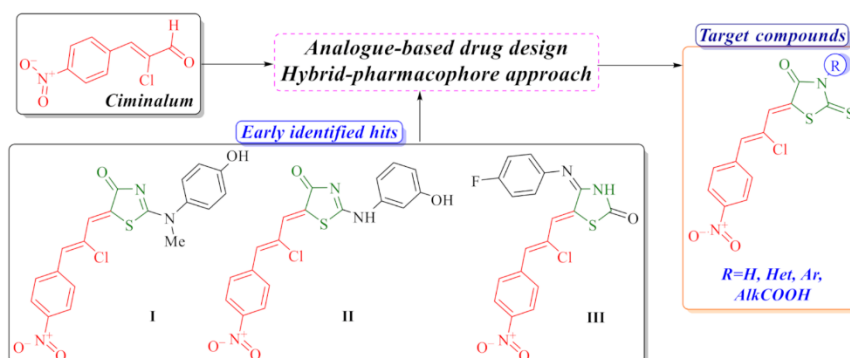


**Figure 1.** Background of the target compounds design.

Our research was aimed at optimization of anticancer activity profile of 5-[(*Z,Z*)-2-chloro-3-(4-nitrophenyl)-2-propenylidene]-4-thiazolidinones and SAR analysis within these series in accordance with our systematic study of anticancer activity of thiazolidinone-related derivatives [9,10].

## 2. Results and Discussion

### 2.1. Chemistry

The synthetic approach to target compounds design was based on 4-thiazolidinone derivatives as active methylene heterocycles in Knoevenagel reaction with (2*Z*)-2-chloro-3-(4-nitrophenyl)prop-2-enal (*Ciminalum*) as an oxo-compound (Figure 2).

The starting 2,4-thiazolidinedione **1a** and 2-thioxo-4-thiazolidinone (rhodanine) derivatives **1b-1** were obtained according to described procedures. We used three synthetic approaches to this end: (1) [2+3]-cyclocondensation of chloroacetic acid with thiourea (**1a** [11]) or ammonium thiocyanate (**1b** [12]); (2) dithiocarbamate method of 3-substituted 2-thioxo-4-thiazolidinone (rhodanine) derivatives synthesis (**1c** [13], **1g-1** [14–19]); (3) the reaction of trithiocarbonyl diglycolic acid with amino compounds (**1d-f** [20,21]).

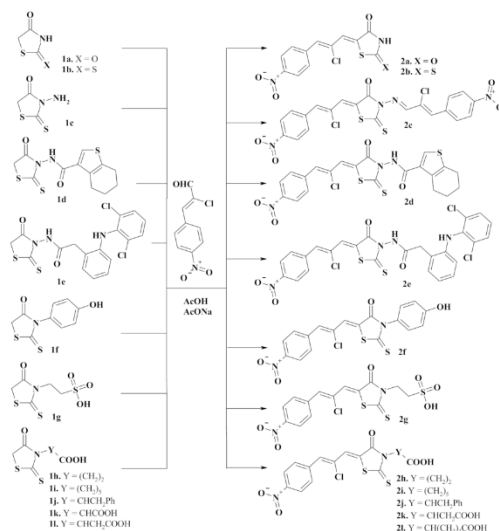


**Figure 2.** Synthesis of 5-[(Z,Z)-2-chloro-3-(4-nitrophenyl)-2-propenylidene]-4-thiazolidinones **2a–m**. Reagents and conditions: appropriate 4-thiazolidinone **1a–f** (0.01 mol), (Z,Z)-2-chloro-3-(4-nitrophenyl)prop-2-enal (0.010 mol, in the case of 3-aminorhodanine **1e** 0.02 mol), AcONa (0.01 mol), AcOH (20 mL), reflux, 3 h, 68–83%.

Target *Ciminalum*-thiazolidinone hybrid molecules **2a–l** were synthesized via the Knoevenagel condensation of (Z,Z)-2-chloro-3-(4-nitrophenyl)prop-2-enal and appropriate 4-thiazolidinone in the presence of sodium acetate under reflux in acetic acid (Figure 2). In the case of 3-aminorhodanine **1c**, in parallel with the Knoevenagel condensation, the reaction with amino group and formation of appropriate azomethine derivative **2c** was observed. The data characterizing synthesized novel 4-thiazolidinones are presented in the experimental part. Analytical and spectral data ( $^1\text{H}$  and  $^{13}\text{C}$ -NMR, LCMS) confirmed the structure of the synthesized compounds. The  $^1\text{H}$ -NMR spectra of the synthesized compounds are characterized by the signals of the *Ciminalum* residue in the form of two singlets at 7.55–8.01 and 7.88–8.07 ppm for the  $\text{CH}=\text{CCl}-\text{CH}=\text{}$  group as well as two doublets of the *p*-nitrophenyl substituent at 8.00 and 8.30 ppm. For compound **2g**, these signals were slightly shifted into a strong magnetic field and appeared as two singlets at 6.89 and 7.19 ppm and two doublets at 7.23 and 7.51 ppm. In the  $^{13}\text{C}$ -NMR spectra of rhodanine derivatives signals of  $\text{C}=\text{O}$  and  $\text{C}=\text{S}$  groups of the core heterocycle were characteristic and appeared at 158.7–174.4 and 193.5–199.3 ppm, respectively.

Structural features of the synthesized *Ciminalum*-thiazolidinone hybrid molecules were confirmed by single-crystal X-ray diffraction study of compound **2i**. As follows from the X-ray analysis, the investigated compound has the structure of 6-[5-[(Z,Z)-2-chloro-3-(4-nitrophenyl)-2-propenylidene]-4-oxo-2-thioxothiazolidin-3-yl]hexanoic acid (**2i**) and crystallizes as dimethylformamide solvate in a molar ratio of 1:1 (Figure 3). 5-Carboxypentyl group located at N-3 atom adopts anticlinal conformation with respect to C2–N3 bond belonging to 2-thioxo-4-thiazolidinone moiety. This arrangement is confirmed by the torsion angle C2–N3–C7–C12 [ $-101.19(15)^\circ$ ]. The 3-(4-nitrophenyl)-2-chloroprop-2-en-1-ylidene residue at the C-5 atom assumes *Z* configuration with respect to the S1–C5 bond. The torsion angle S1–C5–C16–C17 has the value of  $2.0(3)^\circ$ . The system formed by the named residue and 2-thioxo-1,3-thiazolidin-4-one system is approximately planar [r.m.s.d. = 0.0949 Å].

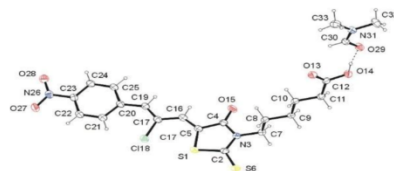


**Figure 3.** ORTEP view of **2i**-DMF showing the atomic labeling scheme. Non-H atoms are drawn as 30% probability displacement ellipsoids and H atoms are drawn as spheres of an arbitrary radius.

The conformation of the molecule of **2i** is stabilized by the intermolecular hydrogen bonding. The hydrogen bonds C22–H···S6<sup>iii</sup> and C25–H25···O29<sup>iv</sup> (Table 1) stabilize the almost coplanar arrangement of the 3-(4-nitrophenyl)-2-chloroprop-2-en-1-ylidene and 2-thioxo-4-thiazolidinone moieties. Moreover, the hydrogen bonds O14–H14···O29, C11–H11A···O13<sup>i</sup>, and C11–H11B···O15<sup>ii</sup> (Table 1) stabilize the spatial arrangement of the 5-carboxypentyl group. The C5=C16 [1.345(2) Å] and C17=C19 [1.351(2) Å] bond lengths confirmed the occurrence of a double bonds between these carbon atoms (Figure 3).

**Table 1.** Hydrogen-bond geometry (Å, °) for **2i**-DMF.

D—H···A	D—H	H···A	D···A	D—H···A
O14—H14···O29	0.95 (3)	1.63 (3)	2.5758 (16)	171 (3)
C11—H11A···O13 <sup>i</sup>	0.99	2.55	3.5287 (19)	172
C11—H11A···O15 <sup>ii</sup>	0.99	2.47	3.135 (2)	125
C21—H22···C118	0.95	2.51	3.2049 (15)	130
C22—H22···S6 <sup>iii</sup>	0.95	2.75	3.6734 (16)	164
C25—H25···O29 <sup>iv</sup>	0.95	2.50	3.4332 (18)	169

Symmetry codes: (i)  $x, 1 + y, z$ ; (ii)  $1/2 - x, 1/2 + y, 1/2 - z$ ; (iii)  $1 - x, 2 - y, 1 - z$ ; (iv)  $1/2 - x, -1/2 + y, 1/2 - z$ .

## 2.2. In Vitro Evaluation of the Anticancer Activity

At the first stage of biological activity study, the antitumor activity screening of the selected compounds **2b**, **2c**, **2f**, **2h**, and **2j** was performed according to the NCI DTP (USA) standard protocol at the concentrations ranging from  $10^{-4}$  to  $10^{-8}$  M toward 60 tumor cell lines [22–25]. The percentage of growth was evaluated spectrophotometrically versus controls not treated with test agents after 48 h exposure and using SRB protein assay to estimate cell viability or growth. Dose–response parameters were calculated for each cell line: GI<sub>50</sub>—molar concentration of the compound that inhibits 50% net cell growth; TGI—molar concentration of the compound leading to the total inhibition; and LC<sub>50</sub>—molar concentration of the compound leading to 50% net cell death. Furthermore, mean graph midpoints (MG\_MID) were calculated for each of the parameters, giving an average activity parameter over all cell lines for the tested compound. For the MG\_MID calculation, insensitive cell lines were included with the highest concentration tested.

The obtained results of screening evaluation of *Ciminalum*–thiazolidinone hybrids confirmed their significant anticancer activity (Table 2). Thus, compounds **2f** and **2h** inhibited the growth of all tested cancer cell lines at submicromolar and micromolar concentrations. The average meanings of three dose–response parameters GI<sub>50</sub>, TGI, and LC<sub>50</sub> were 2.80/32.3/80.8 μM (**2f**) and 1.57/13.3/65.0 μM (**2h**), respectively. It is important to note that the most active compound **2h** was active in the GI<sub>50</sub> concentration range of < 0.01–0.02 μM toward the following cell lines: MOLT-4, SR (Leukemia); SW-620 (Colon cancer); SF-539 (CNS cancer); SK-MEL-5 (Melanoma). Regarding the preliminary SAR analysis, it is worth mentioning that the presence of the (*Z,Z*)-2-chloro-3-(4-nitrophenyl)-2-propenyldiene moiety turned out to be a necessary requirement for achieving the anticancer effects. Moreover, the substituent nature at position 3 of the 4-thiazolidinone ring is important. Derivatives with carboxylic acids residues (**2h**, **2j**) and *p*-hydroxyphenyl substituent (**2f**) proved to be the most effective. The absence of a substituent in position 3 (**2b**) or an additional fragment of the *Ciminalum* (**2c**) leads to the weakening of anticancer cytotoxicity.

Table 2. Influence of compounds 2b, 2c, 2f, 2h, and 2j on the growth of individual tumor cell lines.

Cell line/comp.	2b	2c	2f	2h	2j
	GI <sub>50</sub> /TGI/LC <sub>50</sub> , μM	GI <sub>50</sub> /TGI/LC <sub>50</sub> , μM	GI <sub>50</sub> /TGI/LC <sub>50</sub> , μM	GI <sub>50</sub> /TGI/LC <sub>50</sub> , μM	GI <sub>50</sub> /TGI/LC <sub>50</sub> , μM
<b>Leukemia</b>					
CCRF-CEM	1.97/21.5/>50	4.42/35.3/>100			2.92/>100/>100
HL-60(TB)	1.21/14.4/>50	5.32/23.3/87.2	0.485/4.48/>100	0.347/1.87/>100	
K-562	1.44/42.5/>50	3.98/25.5/>100	0.521/>100/>100	0.212/2.83/>100	3.01/>100/>100
MOLT-4	1.74/14.2/>50	3.20/8.95/52.5	0.389/>100/>100	0.016/19.7/>100	3.14/>100/>100
RPMI-8226	1.54/20.6/>50	2.38/6.32/>100	<0.01/0.264/>100	0.138/1.30/>100	3.22/>100/>100
SR	1.18/7.96/>50	3.67/12.0/>100	0.01/0.138/>100	<0.01/1.41/>100	2.45/>100/>100
<b>Non-Small Cell Lung Cancer</b>					
A549/ATCC	8.18/>50/>50	18.9/42.6/96.1	2.25/6.47/>100	1.76/7.62/>100	3.46/>100/>100
EKVX	2.76/>50/>50	23.7/47.7/96.1	2.37/16.2/>100	0.334/4.01/55.6	2.59/7.29/>100
HOP-62	15.4/33.1/>50	17.2/39.7/91.9	2.61/5.22/11.6	6.54/19.9/52.8	2.31/6.75/>100
HOP-92	8.48/>50/>50		8.53/39.4/>100	4.81/18.3/50.7	2.36/5.71/>100
NCI-H226	6.28/20.0/>50	12.0/31.8/84.2			1.58/3.27/6.76
NCI-H23	3.27/13.4/45.5	16.6/31.6/60.3	1.48/3.11/6.52	1.44/3.22/7.19	2.13/4.86/>100
NCI-322M	6.51/18.8/>50	87.6/>100/>100	2.49/9.02/>100	2.83/10.9/63.4	>100/>100/>100
NCI-H460	3.95/18.6/>50	15.0/32.3/69.5	0.754/>100/>100	0.804/3.32/>100	2.19/>100/>100
NCI-H522	3.19/13.1/42.3	16.3/32.9/66.2			1.72/4.47/29.5
<b>Colon Cancer</b>					
Colo 205	4.04/17.4/>50	56.2/>100/>100	4.34/>100/>100	0.350/>100/>100	2.45/>100/>100
HCC-2998	5.43/11.7/25.0				1.96/3.50/6.27
HCT-116	2.93/11.0/33.7	2.73/6.51/23.3	1.27/2.96/6.92	0.270/1.19/>100	2.01/5.47/56.7
HCT-15	1.79/8.81/25.4	16.6/33.0/65.7	0.409/>100/>100	0.230/2.96/>100	1.92/4.58/>100
HT-29	1.48/9.48/>50		2.14/>100/>100	1.25/2.77/>100	2.84/8.47/>100
KM12	5.27/14.6/40.4	20.6/59.1/>100	2.85/>100/>100	0.639/29.5/>100	2.06/4.35/9.16
SW-620	1.94/7.62/23.5	7.24/>100/>100	0.037/1.52/>100	<0.01/3.25/>100	2.10/4.39/>100
<b>CNS Cancer</b>					
SF-268	5.24/18.9/>50	17.0/41.3/>100	2.55/34.5/>100	2.12/9.74/>100	2.21/>100/>100
SF-295	8.46/37.9/>50	18.0/37.3/77.1	2.26/13.8/>100	3.36/21.6/>100	2.59/7.85/>100
SF-539	9.39/23.1/>50	25.9/57.4/>100	0.0252/0.242/28.1	<0.01/0.267/25.8	2.74/>100/>100
SNB-19	8.10/21.4/>50	48.3/>100/>100	10.0/32.0/97.5	0.658/26.3/83.7	1.85/>100/>100
SNB-75	7.59/23.5/>50		25.1/>100/>100	12.5/46.0/>100	1.96/5.37/>100
U251	3.09/9.73/22.1	8.03/24.5/65.8	0.368/3.06/38.9	0.149/2.00/>100	1.72/3.52/7.21
<b>Melanoma</b>					
LOX IMVI	6.60/15.4/36.0	13.0/28.8/63.8	1.17/3.70/>100	0.161/0.515/>100	1.64/3.26/6.46
MALME-3M	4.93/14.9/44.6	25.0/60.4/>100	6.53/27.6/94.5	9.70/61.9/>100	2.13/4.82/>100
M14	8.87/32.2/>50	16.2/35.7/78.5	1.90/3.73/7.32	1.66/3.58/7.74	2.53/>100/>100
SK-MEL-2	8.07/26.9/>50	19.0/36.4/69.8		0.802/4.93/65.1	1.87/4.50/>100
SK-MEL-28	5.87/12.3/25.9		4.49/47.7/>100	3.59/23.6/89.5	2.16/4.68/11.6
SK-MEL-5	3.82/10.6/24.0	19.4/38.3/75.6	<0.01/<0.01/3.41	0.0193/0.0849/1.88	1.68/3.06/5.60
UACC-62	5.75/12.5/27.2	13.6/28.1/58.0	1.69/3.85/8.78	1.23/2.97/7.18	2.00/4.85/30.2
<b>Ovarian Cancer</b>					
IGROV1	7.28/21.1/>50	13.3/28.0/58.9	1.63/6.13/>100	0.794/3.68/43.1	2.99/>100/>100
OVCAR-3	1.65/8.08/26.6	0.821/12.7/41.1	0.977/41.8/>100	0.135/6.05/66.6	1.76/3.51/6.98
OVCAR-4	1.95/11.7/>50		2.63/>100/>100	2.66/14.9/56.2	3.21/>100/>100
OVCAR-5	11.1/19.5/32.4	15.1/36.2/86.6			2.82/7.91/>100
OVCAR-8	5.08/15.6/47.9	1.98/4.08/8.38	1.14/22.9/>100	0.244/11.5/>100	3.13/>100/>100
SK-OV-3	13.0/>50/>50	59.6/>100/>100	10.2/41.5/>100	6.83/27.4/77.6	4.13/>100/>100

Table 2. Cont.

Cell line/comp.	2b	2c	2f	2h	2j
	GI <sub>50</sub> /TGI/LC <sub>50</sub> , μM	GI <sub>50</sub> /TGI/LC <sub>50</sub> , μM	GI <sub>50</sub> /TGI/LC <sub>50</sub> , μM	GI <sub>50</sub> /TGI/LC <sub>50</sub> , μM	GI <sub>50</sub> /TGI/LC <sub>50</sub> , μM
<b>Renal Cancer</b>					
786-0	9.40/18.8/37.6	12.1/30.7/77.8	2.04/3.83/7.18	1.13/2.47/5.42	2.10/5.01/>100
A498	4.57/12.2/30.9	13.0/29.6/67.3			1.65/3.24/6.37
ACHN	3.64/11.8/31.7	15.6/29.7/56.4	1.70/3.51/7.27	1.02/2.42/5.76	1.80/3.30/6.04
CAKI-1	7.14/25.2/>50	3.11/11.2/>100	4.44/>100/>100	0.485/6.14/47.1	2.28/5.09/16.7
RXF 393				0.105/0.341/1.73	1.54/3.02/5.93
SN12C	4.11/18.0/>50	29.0/>100/>100	1.98/4.41/>100	1.05/2.99/8.48	2.84/>100/>100
TK-10	10.6/23.2/>50	28.0/69.6/>100	4.87/29.0/>100	2.33/16.9/92.0	2.43/>100/>100
UO-31	4.12/21.8/>50	17.5/32.2/59.1	2.08/3.98/>100	0.812/2.43/6.31	1.59/3.10/6.05
<b>Prostate Cancer</b>					
PC-3	4.68/>50/>50	8.10/45.8/>100	2.29/84.8/>100	0.712/13.7/41.9	2.53/7.98/>100
DU-145	7.09/14.2/28.4	21.7/52.8/>100	0.666/5.81/50.1	0.421/3.48/52.3	2.06/4.56/11.7
<b>Breast Cancer</b>					
MCF-7	2.14/38.0/>50	4.08/19.8/83.7	0.401/28.0/>100	0.239/14.4/>100	2.38/10.7/>100
NCI/ADR-Res	5.71/18.3/>50	6.55/20.8/61.7	2.17/6.13/>100	0.407/2.11/6.43	
MDA-MB-231/ATCC	8.16/28.1/>50	10.0/35.4/>100	2.18/12.2/92.1	1.08/4.86/25.9	3.35/>100/>100
HS 578T	1.42/12.1/>50	29.5/>100/>100			4.37/>100/>100
MDA-MB-435	8.57/47.9/>50	20.3/41.9/86.3	3.50/7.71/>100	1.25/4.12/29.3	
BT-549	1.47/4.74/27.2	27.3/76.0/>100	1.55/7.71/>100	0.247/0.920/36.3	1.79/4.17/>100
T-47D	3.21/>50/>50	24.5/65.3/>100	1.55/7.71/>100	0.363/>100/>100	1.50/3.71/>100
MDA-MB-468					1.39/3.28/7.71

The selectivity index (SI) obtained by dividing the full panel MG-MID (mM) of the tested compound by their individual subpanel MG-MID (mM) was considered as a measure of selectivity of anticancer activity (Table 3). Ratios between 3 and 6 mean moderate selectivity, ratios greater than 6 indicate high selectivity toward the corresponding cell line, while compounds not meeting either of these criteria are rated nonselective [26]. The most active compounds 2f and 2h in the present study were found to be high selective toward the leukemia subpanel at GI<sub>50</sub> levels (selectivity indices 9.89 and 10.73, respectively). Compound 2j possessed high selectivity toward the CNS cancer subpanel at both the TGI and LC<sub>50</sub> levels (selectivity index 11.53 and 10.25, respectively). In general, it is worth noting the selectivity of action against leukemia cell lines for the studied class of heterocyclic compounds.

In the second stage of the research, *Ciminalum*-thiazolidinone hybrids were investigated for antitumor activity on the lines of gastric cancer (AGS), human colon cancer (DLD-1), and breast cancers (MCF-7 and MDA-MB-231). The study was performed in the MTT assay according to the method described previously [27]. The studied cancer line was sensitive to the action of the studied compounds that inhibited its growth in micromolar ranges of GI<sub>50</sub>. The hit compounds that inhibited the growth of all four cancer lines with the lowest GI<sub>50</sub> values were [5-[2-chloro-3-(4-nitrophenyl)prop-2-enylidene]-rhodanines 2c, 2d, 2h, and 2i (Table 4). Moreover, it is important to note the high cytotoxic effect of rhodanine-3-carboxylic acid derivatives 2h and 2i toward breast cancer lines MCF-7 and MDA-MB-231 at the GI<sub>50</sub> level of 0.95–1.74 μM, which is consistent with previous data obtained according to DTP NCI protocol (Table 2).



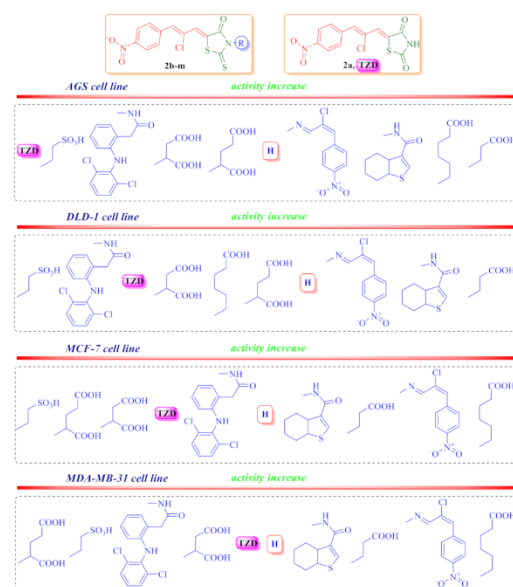
Table 3. Influence of 2b, 2c, 2f, 2h, and 2j on the growth of tumor panels (GI<sub>50</sub>, TGI, LC<sub>50</sub>) and selectivity index (SI) values.

Compound/Disease		2b		2c		2f		2h		2j	
		MG_MID, μM	SI	MG_MID, μM	SI	MG_MID, μM	SI	MG_MID, μM	SI	MG_MID, μM	SI
Leukemia	GI <sub>50</sub>	1.51	3.17	3.83	4.70	0.283	<b>9.89</b>	0.145	<b>10.83</b>	2.95	1.39
	TGI	20.2	1.00	18.6	2.32	41.0	0.78	5.42	2.45	>100	<0.41
	LC <sub>50</sub>	>50	<0.87	90	0.91	>100	<0.81	>100	<0.65	>100	<0.74
Non-Small Cell Lung Cancer	GI <sub>50</sub>	3.79	1.26	25.9	0.69	2.93	0.96	2.65	0.59	13.1	0.31
	TGI	29.7	0.68	44.8	0.96	26.6	1.21	9.61	1.38	36.9	1.10
	LC <sub>50</sub>	48.6	0.90	83.0	0.98	74.0	1.09	61.4	1.06	92.9	0.80
Colon Cancer	GI <sub>50</sub>	3.27	1.46	20.7	0.87	1.84	1.52	0.458	3.43	2.19	1.87
	TGI	11.5	1.77	59.7	0.72	67.4	0.48	23.3	0.57	18.7	2.17
	LC <sub>50</sub>	35.4	1.23	77.8	1.05	84.5	0.96	>100	<0.65	67.4	1.10
CNS Cancer	GI <sub>50</sub>	6.98	0.69	23.4	0.77	6.72	0.42	3.13	0.50	2.18	1.88
	TGI	22.4	0.91	52.1	0.83	30.6	1.05	17.7	0.75	3.52	<b>11.53</b>
	LC <sub>50</sub>	45.4	0.96	88.6	0.92	77.4	1.04	84.9	0.77	7.21	<b>10.25</b>
Melanoma	GI <sub>50</sub>	5.57	0.86	17.7	1.02	2.63	1.06	2.45	0.64	2.00	2.05
	TGI	16.1	1.26	38.0	1.13	14.4	2.23	13.9	0.96	17.9	2.27
	LC <sub>50</sub>	36.8	1.18	74.3	1.10	52.3	1.54	53.1	1.22	50.6	1.46
Ovarian Cancer	GI <sub>50</sub>	6.68	0.72	18.2	0.99	3.32	0.84	2.13	0.74	3.00	1.36
	TGI	21.0	0.97	36.2	1.19	42.5	0.76	12.7	1.05	68.6	0.59
	LC <sub>50</sub>	42.8	1.02	59.0	1.38	>100	<0.81	68.7	0.95	84.5	0.87
Renal Cancer	GI <sub>50</sub>	6.23	0.77	16.9	1.07	2.85	0.98	0.99	1.59	2.03	2.01
	TGI	18.7	1.09	43.3	1.00	24.1	1.34	4.81	2.77	27.8	1.46
	LC <sub>50</sub>	42.9	1.01	80.1	1.02	69.1	1.17	23.8	2.73	42.6	1.73
Prostate Cancer	GI <sub>50</sub>	5.89	0.81	14.9	1.21	1.48	1.89	0.567	2.77	2.30	1.78
	TGI	32.1	0.63	45.3	0.95	45.3	0.71	8.59	1.55	6.27	6.48
	LC <sub>50</sub>	39.2	1.11	75.1	1.09	75.1	1.08	47.1	1.38	55.9	1.32
Breast Cancer	GI <sub>50</sub>	4.38	1.09	17.5	1.03	1.89	1.48	0.598	2.63	24.6	0.17
	TGI	28.4	0.71	51.3	0.84	11.6	2.78	21.1	0.63	37.0	1.10
	LC <sub>50</sub>	46.7	0.93	90.2	0.91	98.7	0.82	49.6	1.31	84.6	0.87
60 lines	GI <sub>50</sub>	<b>4.79</b>		<b>18.0</b>		<b>2.80</b>		<b>1.57</b>		<b>4.09</b>	
	TGI	<b>20.3</b>		<b>43.1</b>		<b>32.2</b>		<b>13.3</b>		<b>40.6</b>	
	LC <sub>50</sub>	<b>43.5</b>		<b>81.7</b>		<b>80.8</b>		<b>65.0</b>		<b>73.9</b>	

**Table 4.** Influence of compounds **2a–e**, **2g**, **2h**, **2k**, and **2l** on the growth of AGS, DLD-1, MCF-7, and MDA-MB-231 cell lines.

Compound	AGS	Cell line, GI <sub>50</sub> , μM		
		DLD-1	MCF-7	MDA-MB-231
<b>2a</b>	18.71	13.98	18.03	13.89
<b>2b</b>	7.86	8.39	4.79	10.56
<b>2c</b>	4.43	6.34	3.60	1.59
<b>2d</b>	4.08	5.47	4.45	3.11
<b>2e</b>	17.05	16.00	17.92	15.83
<b>2g</b>	17.99	27.49	26.40	16.84
<b>2h</b>	2.69	3.67	3.62	1.63
<b>2i</b>	3.20	9.22	1.73	0.95
<b>2k</b>	13.05	10.00	18.08	15.30
<b>2l</b>	12.57	9.19	21.23	17.50

Regarding the SAR analysis (Figure 4), the significant role of the 5-[2-chloro-3-(4-nitrophenyl)prop-2-enylidene]rhodanine (*Ciminalum*) substituent in the anticancer cytotoxicity appearance was confirmed. Moreover, the presence of a thioxo group in position 2 of the core heterocycle is more important than the oxo group, as evidenced by the lower activity of the thiazolidinedione **2b** compared to a structurally close rhodanine derivative **2a**. The role of the substituents nature in position 3 of the rhodanine core on the level of anticancer cytotoxicity level is interesting and important for further in-depth research and the design of drug-like molecules. Thus, the most effective is the presence of carboxylic acids residues, among which fragments of propanoic (**2h**) and hexanoic (**2i**) acids are considered to be important for cytotoxicity toward AGS, DLD-1, MCF-7, and MDA-MB-231 cell lines. The introduction of an additional carboxylic group reduced the effect of derivatives by about 10 times (compounds **2k** and **2l**). Replacing the carboxyl group with a sulfo group had reduced the activity more significantly (compound **2g**). In addition to the carboxylic acid residues, an additional *Ciminalum* fragment (**2c**) or 4,5,6,7-tetrahydrobenzo[*b*]thiophen-3-ylcarboxamide moiety (**2d**) at position 3 of the rhodanine cycle were also important for the anticancer activity.

**Figure 4.** Impact of different substituents in N3 position of the rhodanine core on the anticancer activity levels.

Another part of our study was to determine the influence of compounds **2f**, **2i**, **2j**, and **2h** on normal human blood lymphocytes (Figure 5). GI<sub>50</sub> values for compounds **2j** and **2h** were 48.97  $\mu$ M and 54.54  $\mu$ M correspondingly. Compounds **2i** and **2f** do not reach GI<sub>50</sub> up to 100  $\mu$ M after 48 h incubation. The pure *Ciminalum* has the lowest IC<sub>50</sub> value (GI<sub>50</sub> = 10.4  $\mu$ M) for human normal lymphocytes. Thus, normal blood lymphocytes are blood cells, as well as cells of leukemia cell lines, therapeutic index (TI) of compounds **2f**, **2h**, and **2j** was calculated as GI<sub>50</sub> (normal blood lymphocyte)/GI<sub>50</sub> (leukemia cell line) (Table 5).

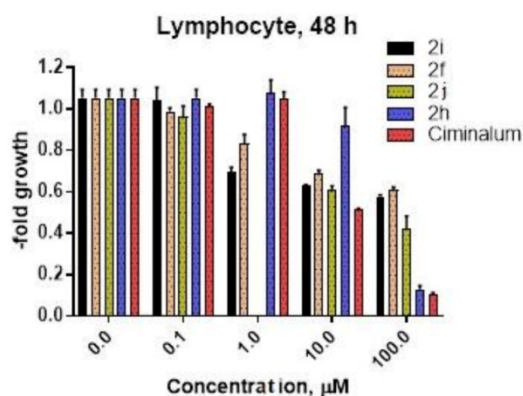


**Figure 5.** Human lymphocyte viability after 48 h of **2f**, **2i**, **2j**, **2h**, and *Ciminalum* drug exposure was estimated by MTT assay.

**Table 5.** Therapeutic index (TI) for compounds **2f**, **2h**, and **2j** regarding diversity leukemia cell lines.

Compound	HL-60(TB)	Leukemia Cell Line TI (Therapeutic Index)				SR	Leukemia Panel
		K-562	MOLT-4	RPMI-8226			
<b>2f</b>	>206.19	>191.94	>257.07	>10,000	>10,000	>353.36	
<b>2h</b>	157.18	257.26	3408.75	395.22	5454	<b>376.14</b>	
<b>2j</b>	n/a	16.27	15.59	15.21	19.99	<b>16.60</b>	

### 3. Materials and Methods

#### 3.1. General Information

All reagents and solvents were purchased from commercial suppliers and were used directly without further purification. NMR spectra were determined with Varian Unity Plus 400 (400 MHz) and Bruker 170 Avance 500 (500 MHz) spectrometers, in DMSO-*d*<sub>6</sub> using tetramethylsilane (TMS) as an internal standard. Melting points were measured on a Kofler hot-stage and are uncorrected. LC-MS was performed using a system with an Agilent 1100 Series HPLC equipped with diode-array detector and Agilent LC\MSD SL mass-selective detector using chemical ionization at atmospheric pressure (APCI). The NMR and LCMS spectra of compounds **2a–l** are presented in Figures S1–S32.

#### 3.2. Synthesis of 5-[(Z,2Z)-2-chloro-3-(4-nitrophenyl)-2-propenylidene]-thiazolidinone derivatives (**2a–l**)

A mixture of (Z,Z)-2-chloro-3-(4-nitrophenyl)prop-2-enal (0.01 mol) and appropriate 4-thiazolidinone (0.01 mol) in the medium of acetic acid (20 mL) and the presence of sodium acetate (0.01 mol) was refluxed for 3 h. Obtained solid product was collected after cooling by filtration and recrystallized from the mixture DMF-ethanol (1:2).

5-[(Z,2Z)-2-Chloro-3-(4-nitrophenyl)-2-propenylidene]-2,4-thiazolidinedione (**2a**). Yield: 78%, mp >270 °C. <sup>1</sup>H-NMR (400 MHz, DMSO-*d*<sub>6</sub>): δ (ppm) 7.70 (s, 1H, CH=), 7.88 (s, 1H, CH=), 8.00 (d, 2H, J = 7.5 Hz, arom.), 8.31 (d, 2H, J = 8.0 Hz, arom.), 12.70 (br.s, 1H, NH).

LCMS (ESI):  $m/z$  309.9/312.0 (95.58%,  $[M + H]^+$ ). Anal. Calc. for  $C_{12}H_7ClN_2O_4S$ : C 46.39%; H 2.27%; N 9.02%. Found: C 46.50%; H 2.40%; N 8.90%.

5-[(Z,Z)-2-Chloro-3-(4-nitrophenyl)-2-propenylidene]-2-thioxo-4-thiazolidinone (**2b**). Yield: 81%, mp 251–253 °C.  $^1H$ -NMR (400 MHz, DMSO- $d_6$ ):  $\delta$  (ppm) 7.55 (s, 1H, CH=), 7.94 (s, 1H, CH=), 8.01 (d, 2H,  $J$  = 8.5 Hz, arom.), 8.31 (d, 2H,  $J$  = 8.2 Hz, arom.), 13.91 (br.s, 1H, NH). LCMS (ESI):  $m/z$  324.9/326.9 (100%,  $[M + H]^+$ ). Anal. Calc. for  $C_{12}H_7ClN_2O_3S_2$ : C 44.11%; H 2.16%; N 8.57%. Found: C 44.00%; H 2.25%; N 8.70%.

5-[(Z,Z)-2-Chloro-3-(4-nitrophenyl)-2-propenylidene]-3-[(Z,Z)-2-chloro-3-(4-nitrophenyl)-2-propenylideneamino]-2-thioxo-4-thiazolidinone (**2c**). Yield: 74%, mp >260 °C.  $^1H$ -NMR (400 MHz, DMSO- $d_6$ ):  $\delta$  (ppm) 7.79 (s, 1H, =CH), 8.01 (s, 1H, =CH), 8.06 (d, 2H,  $J$  = 8.1 Hz, arom.), 8.06 (s, 1H, =CH), 8.07 (s, 1H, =CH), 8.18 (d, 2H,  $J$  = 8.8 Hz, arom.), 8.33 (d, 2H,  $J$  = 8.8 Hz, arom.), 8.37 (d, 2H,  $J$  = 8.1 Hz, arom.), 8.98 (s, 1H, CH=N). LCMS (ESI):  $m/z$  535.0 (95.05%,  $[M + H]^+$ ). Anal. Calc. for  $C_{21}H_{12}Cl_2N_4O_5S_2$ : C 47.11%; H 2.26%; N 10.46%. Found: C 47.00%; H 2.15%; N 10.65%.

5-[(Z,Z)-2-Chloro-3-(4-nitrophenyl)-2-propenylidene]-4-oxo-3-(4,5,6,7-tetrahydrobenzothio-phen-3-ylcarboxamido)-2-thioxo-4-thiazolidinone (**2d**). Yield: 80%, mp >230 °C.  $^1H$ -NMR (400 MHz, DMSO- $d_6$ ):  $\delta$  (ppm) 1.68–1.74 (m, 4H, 2\*CH<sub>2</sub>), 2.67–2.78 (m, 4H, 2\*CH<sub>2</sub>), 7.87 (s, 1H, s, 1H, CH=), 8.03–8.09 (m, 3H, arom., CH=), 8.10 (s, 1H, s, 1H, thiophene), 8.33 (d, 2H,  $J$  = 8.3 Hz, arom.), 11.46 (s, 1H, NH).  $^{13}C$ -NMR (100 MHz, DMSO- $d_6$ ):  $\delta$  (ppm) 27.2, 27.8, 29.8, 30.4, 128.2, 129.1, 134.8, 136.2, 137.9, 140.3, 142.5, 144.3, 144.8, 145.0, 152.7, 168.7 (C=O), 177.9 (C=O), 196.4 (C=S). LCMS (ESI):  $m/z$  504.0/506.0 (100%,  $[M-H]^+$ ). Anal. Calc. for  $C_{21}H_{16}ClN_3O_4S_3$ : C 49.85%; H 3.19%; N 8.30%. Found: C 50.00%; H 3.15%; N 8.35%.

$N^1$ -[5-[(Z,Z)-2-Chloro-3-(4-nitrophenyl)-2-propenylidene]-4-oxo-2-thioxothiazolidin-3-yl]-2-[2-(2,6-dichloroanilino)phenyl]acetamide (**2e**). Yield: 74%, mp 257–258 °C.  $^1H$ -NMR (400 MHz, DMSO- $d_6$ ):  $\delta$  (ppm) 3.85 (d, 1H,  $J$  = 14.8 Hz, CH<sub>2</sub>), 3.90 (d, 1H,  $J$  = 14.8 Hz, CH<sub>2</sub>), 6.30 (d, 1H,  $J$  = 7.6 Hz, arom.), 7.08 (t, 1H,  $J$  = 7.5 Hz, arom.), 7.19 (t, 1H,  $J$  = 8.0 Hz, arom.) 7.29 (s, 1H, NH), 7.34 (d, 1H,  $J$  = 7.3 Hz, arom.), 7.53 (d, 2H,  $J$  = 8.0 Hz, arom.), 7.83 (s, 1H, =CH), 8.05 (d, 2H,  $J$  = 7.7 Hz, arom.), 8.06 (s, 1H, =CH), 8.33 (2H, arom.,  $J$  = 8.4 Hz, arom.), 11.68 (s, 1H, NH).  $^{13}C$ -NMR (100 MHz, DMSO- $d_6$ ):  $\delta$  (ppm) 41.6 (CH<sub>2</sub>), 121.4, 121.5, 126.1, 126.2, 129.1, 129.2, 130.8, 132.9, 134.4, 134.8, 135.3, 135.6, 136.2, 137.7, 142.3, 144.8, 152.7, 168.3 (C=O), 177.0 (C=O), 195.9 (C=S). LCMS (ESI):  $m/z$  618.8/621.6 (96.2%,  $[M - H]^+$ ). Anal. Calc. for  $C_{27}H_{16}Cl_3N_4O_4S_2$ : C 50.37%; H 2.76%; N 9.04%. Found: C 50.20%; H 2.85%; N 9.15%.

5-[(Z,Z)-2-Chloro-3-(4-nitrophenyl)-2-propenylidene]-3-(4-hydroxyphenyl)-2-thioxo-4-thiazolidinone (**2f**). Yield: 76%, mp >260 °C.  $^1H$ -NMR (400 MHz, DMSO- $d_6$ ):  $\delta$  (ppm) 6.89 (d, 2H,  $J$  = 8.4 Hz, arom.), 7.16 (d, 2H,  $J$  = 8.4 Hz, arom.), 7.72 (s, 1H, =CH), 8.02 (s, 1H, =CH), 8.05 (d, 2H,  $J$  = 8.5 Hz, arom.), 8.32 (d, 2H,  $J$  = 8.5 Hz, arom.), 9.89 (s, 1H, OH).  $^{13}C$ -NMR (100 MHz, DMSO- $d_6$ ):  $\delta$  (ppm) 116.3, 119.5, 122.9, 124.4, 127.8, 130.2, 130.4, 131.37, 131.4, 138.2, 149.2, 152.9, 158.7 (C=O), 199.3 (C=S). LCMS (ESI):  $m/z$  419.0/421.0 (97.1%,  $[M + H]^+$ ). Anal. Calc. for  $C_{18}H_{11}ClN_2O_4S_2$ : C 51.61%; H 2.65%; N 6.69%. Found: C 51.80%; H 2.85%; N 6.80%.

2-[5-[(Z,Z)-2-Chloro-3-(4-nitrophenyl)-2-propenylidene]-4-oxo-2-thioxothiazolidin-3-yl]-1-ethanesulfonic acid (**2g**). Yield: 83%, mp >260 °C.  $^1H$ -NMR (400 MHz, DMSO- $d_6$ ):  $\delta$  (ppm) 1.95 (t, 2H,  $J$  = 7.9 Hz, CH<sub>2</sub>), 3.47 (t, 2H,  $J$  = 7.9 Hz, CH<sub>2</sub>), 6.89 (s, 1H, CH=), 7.19 (s, 1H, CH=), 7.23 (d, 2H,  $J$  = 8.9 Hz, arom.), 7.51 (d, 2H,  $J$  = 8.8 Hz, arom.).  $^{13}C$ -NMR (100 MHz, DMSO- $d_6$ ):  $\delta$  (ppm) 41.7 (CH<sub>2</sub>), 47.6 (CH<sub>2</sub>), 124.3, 127.1, 130.3, 130.9, 131.3, 138.2, 140.3, 147.7, 167.1 (C=O), 194.3 (C=S). LCMS (ESI):  $m/z$  432.8/435.0 (100%,  $[M + H]^+$ ). Anal. Calc. for  $C_{14}H_{11}ClN_2O_6S_3$ : C 38.67%; H 2.55%; N 6.44%. Found: C 38.80%; H 2.45%; N 6.60%.

3-[5-[(Z,Z)-2-Chloro-3-(4-nitrophenyl)-2-propenylidene]-4-oxo-2-thioxothiazolidin-3-yl]propanoic acid (**2h**). Yield: 75%, mp 254–256 °C.  $^1H$ -NMR (400 MHz, DMSO- $d_6$ ):  $\delta$  (ppm) 2.63 (t, 2H,  $J$  = 6.8 Hz, CH<sub>2</sub>), 4.22 (t, 2H,  $J$  = 6.8 Hz, CH<sub>2</sub>), 7.73 (s, 1H, CH=), 8.02 (s, 1H, CH=), 8.04 (d, 2H,  $J$  = 8.9 Hz, arom.), 8.32 (d, 2H,  $J$  = 8.9 Hz, arom.), 12.29 (br.s, 1H, COOH).

LCMS (ESI):  $m/z$  399.0/401.0/402.0 (100%, [M + H]<sup>+</sup>). Anal. Calc. for C<sub>15</sub>H<sub>11</sub>ClN<sub>2</sub>O<sub>5</sub>S<sub>2</sub>: C 45.17%; H 2.78%; N 7.02%. Found: C 45.00%; H 2.65%; N 6.90%.

6-[5-[(Z,Z)-2-Chloro-3-(4-nitrophenyl)-2-propenylidene]-4-oxo-2-thioxothiazolidin-3-yl]hexanoic acid (**2i**). Yield: 75%, mp >220 °C. <sup>1</sup>H-NMR (400 MHz, DMSO-*d*<sub>6</sub>): δ (ppm) 1.30 (quint, 2H, *J* = 6.7 Hz, CH<sub>2</sub>), 1.52 (quint, 2H, *J* = 7.1 Hz, CH<sub>2</sub>), 1.62 (quint, 2H, *J* = 6.7 Hz, CH<sub>2</sub>), 2.20 (quint, 2H, *J* = 7.0 Hz, CH<sub>2</sub>), 3.99 (quint, 2H, *J* = 6.9 Hz, CH<sub>2</sub>), 7.69 (s, 1H, CH=), 7.98 (s, 1H, CH=), 8.02 (d, 2H, *J* = 8.5 Hz, arom.), 8.30 (d, 2H, *J* = 8.5 Hz, arom.), 12.00 (s, 1H, COOH). <sup>13</sup>C-NMR (100 MHz, DMSO-*d*<sub>6</sub>): δ (ppm) 24.5 (CH<sub>2</sub>), 26.1 (CH<sub>2</sub>), 26.5 (CH<sub>2</sub>), 33.8 (CH<sub>2</sub>), 44.5 (CH<sub>2</sub>), 124.3, 126.8, 130.2, 131.2, 131.3, 138.4, 140.2, 147.8, 167.4, 174.7 (C=O), 194.6 (C=S). LCMS (ESI):  $m/z$  441.0/443.1 (100%, [M + H]<sup>+</sup>). Anal. Calc. for C<sub>18</sub>H<sub>17</sub>ClN<sub>2</sub>O<sub>5</sub>S<sub>2</sub>: C 49.03%; H 3.89%; N 6.35%. Found: C 49.10%; H 3.85%; N 6.40%.

2-[5-[(Z,Z)-2-Chloro-3-(4-nitrophenyl)-2-propenylidene]-4-oxo-2-thioxothiazolidin-3-yl]-3-phenylpropanoic acid (**2j**). Yield: 70%, mp >220 °C. <sup>1</sup>H-NMR (400 MHz, DMSO-*d*<sub>6</sub>): δ (ppm) 3.49 (t, 2H, CH<sub>2</sub>), 5.87 (br.s, 1H, CH), 7.10–7.25 (m, 5H, arom.), 7.71 (s, 1H, s, 1H, CH=), 8.00 (s, 1H, s, 1H, CH=), 8.02 (d, 2H, *J* = 8.0 Hz, arom.), 8.31 (d, 2H, *J* = 8.0 Hz, arom.), 13.59 (br.s, 1H, COOH). <sup>13</sup>C-NMR (100 MHz, DMSO-*d*<sub>6</sub>): δ (ppm) 38.2 (CH<sub>2</sub>), 63.3 (CH), 129.1, 132.0, 133.5, 134.2, 134.7, 136.2, 137.1, 137.2, 141.6, 144.1, 152.6, 171.6 (C=O), 173.7 (C=O), 198.7 (C=S). LCMS (ESI):  $m/z$  324.9/326.9 (100%, [M + H]<sup>+</sup>). Anal. Calc. for C<sub>21</sub>H<sub>15</sub>ClN<sub>2</sub>O<sub>5</sub>S<sub>2</sub>: C 53.11%; H 3.18%; N 5.90%. Found: C 53.00%; H 3.15%; N 5.80%.

2-[5-[(Z,Z)-2-Chloro-3-(4-nitrophenyl)-2-propenylidene]-4-oxo-2-thioxothiazolidin-3-yl]succinic acid (**2k**). Yield: 68%, mp 220–222 °C. <sup>1</sup>H-NMR (400 MHz, DMSO-*d*<sub>6</sub>): δ (ppm) 2.89 (d, 1H, *J* = 15.5 Hz, CH<sub>2</sub>), 3.23 (dd, *J* = 7.6, 15.6 Hz, 1H, CH<sub>2</sub>), 5.94 (br.s, 1H, CH), 7.75 (s, 1H, CH=), 8.02 (s, 1H, CH=), 8.04 (d, 2H, *J* = 8.9 Hz, arom.), 8.32 (d, 2H, *J* = 8.8 Hz, arom.), 12.68 (br.s, 2H, 2\*COOH). <sup>13</sup>C-NMR (100 MHz, DMSO-*d*<sub>6</sub>): δ (ppm) 33.0 (CH<sub>2</sub>), 53.2 (CH), 115.1 (C-Cl), 123.9, 129.6 (=CH), 131.0, 131.7 (=CH), 138.6, 139.7, 147.4, 166.5 (C=O), 168.6 (COOH), 171.2 (COOH), 193.5 (C=S). LCMS (ESI):  $m/z$  442.8/444.7 (100%, [M + H]<sup>+</sup>). Anal. Calc. for C<sub>16</sub>H<sub>11</sub>ClN<sub>2</sub>O<sub>7</sub>S<sub>2</sub>: C 43.40%; H 2.50%; N 6.33%. Found: C 43.54%; H 2.48%; N 6.45%.

2-[5-[(Z,Z)-2-Chloro-3-(4-nitrophenyl)-2-propenylidene]-4-oxo-2-thioxothiazolidin-3-yl]pentanedioic acid (**2l**). Yield: 72%, mp 205–207 °C. <sup>1</sup>H-NMR (400 MHz, DMSO-*d*<sub>6</sub>): δ (ppm) 2.25–2.45 (m, 4H, CH<sub>2</sub>CH<sub>2</sub>), 5.59 (br.s, 1H, CH), 7.72 (s, 1H, CH=), 8.01 (s, 1H, CH=), 8.04 (d, 2H, *J* = 8.9 Hz, arom.), 8.32 (d, 2H, *J* = 8.9 Hz, arom.), 12.59 (br.s, 2H, 2\*COOH). <sup>13</sup>C-NMR (100 MHz, DMSO-*d*<sub>6</sub>): δ (ppm) 23.3 (CH<sub>2</sub>), 30.7 (CH<sub>2</sub>), 57.2 (CH), 119.3 (C-Cl), 124.3, 125.7 (=CH), 131.4, 131.8 (=CH), 138.8, 140.2, 147.8, 162.5 (C=O), 169.3 (COOH), 174.1 (COOH), 194.8 (C=S). LCMS (ESI):  $m/z$  455.0/456.9 (100%, [M + H]<sup>+</sup>). Anal. Calc. for C<sub>17</sub>H<sub>13</sub>ClN<sub>2</sub>O<sub>7</sub>S<sub>2</sub>: C 44.69%; H 2.87%; N 6.13%. Found: C 44.56%; H 2.78%; N 6.05%.

### 3.3. Crystal Structure Determination of 6-[5-[(Z,Z)-2-chloro-3-(4-nitrophenyl)-2-propenylidene]-4-oxo-2-thioxothiazolidin-3-yl]hexanoic Acid Dimethylaminoformamide Solvate (**2i**·DMF)

Compound **2i** was recrystallized from DMF by slow evaporation at room temperature.

Crystal data. C<sub>18</sub>H<sub>17</sub>ClN<sub>2</sub>O<sub>5</sub>S<sub>2</sub>, C<sub>3</sub>H<sub>7</sub>NO<sub>2</sub>, Mr = 514.00, monoclinic, space group P2<sub>1</sub>/n, *a* = 13.20068(11), *b* = 5.12876(4), *c* = 35.3537(3) Å, β = 94.7348(6)°, *V* = 2385.39(3) Å<sup>3</sup>, *Z* = 4 (*Z'* = 1), *D*<sub>calc</sub> = 1.431 g/cm<sup>3</sup>, μ = 3.425 mm<sup>−1</sup>, *T* = 130.0(1) K.

Data collection. An orange lath crystal (DMF) of 0.40 × 0.10 × 0.07 mm was used to record 18,412 (Cu Kα-radiation, θ<sub>max</sub> = 76.22°) intensities on a Rigaku SuperNova Dual Atlas diffractometer [28] using mirror monochromatized Cu Kα-radiation from a high-flux microfocus source (λ = 1.54178 Å). Accurate unit cell parameters were determined by least-squares techniques from the θ values of 12,519 reflections, θ range 3.47–76.02°. The data were corrected for Lorentz, polarization and for absorption effects [28]. The 4955 total unique reflections (*R*<sub>int</sub> = 0.0175) were used for structure determination.

Structure solution and refinement. The structure was solved by a dual space algorithm (SHELXT) [29] and refined against *F*<sup>2</sup> for all data (SHELXL) [30]. The position of the H atom bonded to the O atom was obtained from the difference Fourier map and was refined freely. The remaining H atoms were positioned geometrically and were refined within the riding model approximation: C–H = 0.98 Å (CH<sub>3</sub>), 0.99 Å (CH<sub>2</sub>), 0.95 Å (*C*<sub>sp<sup>2</sup>H), and</sub>

$U_{\text{iso}}(\text{H}) = 1.2U_{\text{eq}}(\text{C})$  or  $1.5U_{\text{eq}}(\text{C})$  for methyl H atoms. The methyl groups were refined as a rigid group, which were allowed to rotate. Final refinement converged with  $R = 0.0319$  (for 4729 data with  $F^2 > 4\sigma(F^2)$ ),  $wR = 0.0864$  (on  $F^2$  for all data), and  $S = 1.052$  (on  $F^2$  for all data). The largest difference peak and hole was 0.281 and  $-0.275 \text{ e}\text{\AA}^3$ .

The molecular illustration was drawn using ORTEP-3 for Windows [31]. Software used to prepare material for publication was WINGX [31], OLEX2 [32], and PLATON [33].

The supplementary crystallographic data are deposited at the Cambridge Crystallographic Data Centre (CCDC), 12 Union ROAD, Cambridge CB2 1EZ (UK) [phone, (+44) 1223/336-408; fax, (+44) 1223/336-033; e-mail, deposit@ccdc.cam.ac.uk; World Wide Web, <http://www.ccdc.cam.ac.uk>, accessed on 18 April 2021 (deposition no. CCDC 2082064)].

### 3.4. In Vitro Evaluation of the Anticancer Activity According DTP NCI Protocol

Primary anticancer assay was performed on a panel of approximately sixty human tumor cell lines derived from nine neoplastic diseases, in accordance with the protocol of the Drug Evaluation Branch, National Cancer Institute, Bethesda [22–25]. Tested compounds were added to the culture at a single concentration ( $10^{-5} \text{ M}$ ) and the cultures were incubated for 48 h. End point determinations were made with a protein binding dye, sulforhodamine B (SRB). Results for each tested compound were reported as the percent of growth of the treated cells when compared to the untreated control cells. The percentage growth was evaluated spectrophotometrically versus controls not treated with test agents. The cytotoxic and/or growth inhibitory effects of the most active selected compounds were tested in vitro against the full panel of human tumor cell lines at concentrations ranging from  $10^{-4}$  to  $10^{-8} \text{ M}$ . A 48 h continuous drug exposure protocol was followed, and an SRB protein assay was used to estimate cell viability or growth.

Using absorbance measurements (time zero (Tz), control growth in the absence of drug (C), and test growth in the presence of drug (Ti)), the percentage growth was calculated for each drug concentration. Percentage growth inhibition was calculated as:

$$[(\text{Ti} - \text{Tz})/(\text{C} - \text{Tz})] \times 100 \text{ for concentrations for which } \text{Ti} \geq \text{Tz} \quad (1)$$

$$[(\text{Ti} - \text{Tz})/\text{Tz}] \times 100 \text{ for concentrations for which } \text{Ti} < \text{Tz}. \quad (2)$$

Dose–response parameters ( $\text{GI}_{50}$ , TGI,  $\text{LC}_{50}$ ) were calculated for each compound. Growth inhibition of 50% ( $\text{GI}_{50}$ ) was calculated from  $[(\text{Ti} - \text{Tz})/(\text{C} - \text{Tz})] \times 100 = 50$  (1), which is the drug concentration resulting in a 50% lower net protein increase in the treated cells (measured by SRB staining) as compared to the net protein increase seen in the control cells. The drug concentration resulting in total growth inhibition (TGI) was calculated from  $\text{Ti} = \text{Tz}$ . The  $\text{LC}_{50}$  (concentration of drug resulting in a 50% reduction in the measured protein at the end of the drug treatment as compared to that at the beginning) indicating a net loss of cells following treatment was calculated from  $[(\text{Ti} - \text{Tz})/\text{Tz}] \times 100 = -50$  (2). Values were calculated for each of these parameters if the level of activity was reached; however, if the effect was not reached or was excessive, the value for that parameter was expressed as more or less than the maximum or minimum concentration tested. The lowest values were obtained with the most sensitive cell lines. Compounds having  $\text{GI}_{50}$  values  $\leq 100 \mu\text{M}$  were declared to be active.

### 3.5. Cell Viability Assay (AGS, DLD-1, MCF-7 and MDA-MB-231 Cell Lines; Human Blood Lymphocytes)

The assay was performed by using 3-(4,5-dimethylthiazole-2-yl)-2,5-diphenyltetrazolium bromide (MTT). Confluent cells, cultured for 24 h with 0.1, 1, 5, 10, 20, 30, and  $100 \mu\text{M}$  concentrations of studied compounds in 24-well plates were washed with PBS. MTT was dissolved in PBS, and  $25 \mu\text{L}$  were added to each well. Plates were incubated for 4 h at  $37^\circ\text{C}$  in 5%  $\text{CO}_2$  in an incubator. The medium with MTT was removed, and 1 mL of DMSO was added to the attached cells. Furthermore, cells were incubated for 5–10 min in RT and then  $10 \mu\text{L}$  of Sorensen buffer was added to each well. The absorbance of converted dye in living

cells was measured at a wavelength of 570 nm. The cell viability of breast cancer cells, gastric cancer cells, and human colon cancer cells cultured in the presence of ligands was calculated as percent of control cells.

### 3.6. Isolation of Human Blood Lymphocytes and Their Activation

First, 20 mL of venous blood was taken from volunteers (Ethical protocol number 2, 27 January 2019) and collected in the presence of 200  $\mu$ L of undiluted fresh heparin (1/100). Sterile blood was diluted 2 times with 0.9% NaCl under the sterile conditions. Isolation of lymphocytes was performed in a density gradient of ficol-verografin using the protocol of the manufacturer (Lymphoprep, NYCOMED PHARMA AS, Oslo Norway). The resulting lymphocytes were resuspended in the RPMI-1640 medium and cultured for several days (up to 10 days). To separate the lymphocytes from the monocytes, cell suspension was left for 24 h. After 24 h of culture, monocytes were attached, while lymphocytes were transferred to a fresh Falcon tube (15 mL). To stimulate the proliferation of lymphocytes, they were cultured on CD3+ antibody-coated plastic plate in the RPMI-1640 medium supplemented with 20% FBS.

## 4. Conclusions

In the presented paper, new 5-[(Z,Z)-2-chloro-3-(4-nitrophenyl)-2-propenylidene]-4-thiazolidinones (*Ciminalum*-thiazolidinone hybrid molecules) are described. NCI 60-Cell-line antitumor activity assay allowed identifying a highly active compound **2h** with the mean GI<sub>50</sub> 1.57  $\mu$ M and TGI 13.3  $\mu$ M with a certain sensitivity profile in the GI<sub>50</sub> concentration range of < 0.01–0.02  $\mu$ M toward leukemia (MOLT-4, SR), colon cancer (SW-620), CNS cancer (SF-539) and melanoma (SK-MEL-5) cell lines. High cytotoxicity of 5-[(Z,Z)-2-chloro-3-(4-nitrophenyl)-2-propenylidene]-2-thioxo-4-thiazolidinone-3-carboxylic acids against cell lines of gastric cancer (AGS), human colon cancer (DLD-1), and breast cancers (MCF-7 and MDA-MB-231) was established. The hit compounds **2f**, **2i**, **2g**, and **2h** have been found to have low toxicity toward normal human blood lymphocytes and a fairly wide therapeutic range—TI for leukemia panel > 353.36 (**2f**), 376.14 (**2h**) and 16.60 (**2j**). The SAR analysis allowed confirming the crucial role of 2-chloro-3-(4-nitrophenyl)prop-2-enylidene (*Ciminalum*) substituent in position 5 for 4-thiazolidinones and establish the dependence of the anticancer activity of the synthesized compounds on the nature of the substituents in N3 position of the core heterocycle. Further investigations on the *Ciminalum*-thiazolidinone hybrid molecules could lead to more potent compounds as promising candidates for the development of new anticancer chemotherapy. The levels of their anticancer activity cause the need for the in-depth study of their mechanisms of action.

**Supplementary Materials:** The following are available online, Figures S1–S32: Copies of NMR and LCMS spectra of compounds **2a–l**.

**Author Contributions:** Conceptualization, A.B., K.B. (Krzysztof Bielawski) and R.L.; methodology, A.B. and R.L.; validation, K.B. (Krzysztof Bielawski), A.K.-D. and O.R.; formal analysis, K.B. (Krzysztof Bielawski) and A.G.; investigation, K.B. (Kamila Buzun), A.K.-D., J.S. and A.G.; resources, R.L.; data curation, K.B. (Krzysztof Bielawski) and J.S.; writing—original draft preparation, R.L.; writing—review and editing, A.B. and R.L.; visualization, J.S.; supervision, A.B. and R.L.; project administration, A.B. and R.L. All authors have read and agreed to the published version of the manuscript.

**Funding:** This work was financially supported by Grant of Ministry of Healthcare of Ukraine 0121U100690 and the National Research Foundation of Ukraine, under the project number: 2020.02/0035.

**Institutional Review Board Statement:** The study was conducted according to the guidelines of the Declaration of Helsinki, and approved by the Ethics Committee of Institute of Cell Biology of National Academy of Sciences of Ukraine (protocol number 2, 27 January 2019).

**Informed Consent Statement:** Informed consent was obtained from all subjects involved in the study.

**Data Availability Statement:** Data available in a publicly accessible repository.

**Acknowledgments:** We are grateful to G. Morris from Drug Synthesis and Chemistry Branch, National Cancer Institute, Bethesda, MD, USA, for in vitro evaluation of anticancer activity.

**Conflicts of Interest:** The authors declare no conflict of interest.

**Sample Availability:** Samples of the compounds 2a–l are available from the authors.

## References

- Fortin, S.; Berube, G. Advances in the development of hybrid anticancer drugs. *Expert Opin. Drug Discov.* **2013**, *8*, 1547–1577. [[CrossRef](#)] [[PubMed](#)]
- Gediya, L.K.; Njar, V.C. Promise and challenges in drug discovery and development of hybrid anticancer drugs. *Expert Opin. Drug Discov.* **2009**, *4*, 1099–1111. [[CrossRef](#)]
- Nepali, K.; Sharma, S.; Sharma, M.; Bedi, P.M.S.; Dhar, K.L. Rational approaches, design strategies, structure activity relationship and mechanistic insights for anticancer hybrids. *Eur. J. Med. Chem.* **2014**, *77*, 422–487. [[CrossRef](#)] [[PubMed](#)]
- Kaminsky, D.; Kryshchshyn, A.; Lesyk, R. 5-Ene-4-thiazolidinones—An efficient tool in medicinal chemistry. *Eur. J. Med. Chem.* **2017**, *140*, 542–594. [[CrossRef](#)] [[PubMed](#)]
- Kaminsky, D.; Kryshchshyn, A.; Lesyk, R. Recent developments with rhodanine as a scaffold for drug discovery. *Expert Opin. Drug Discov.* **2017**, *12*, 1233–1252. [[CrossRef](#)]
- Panchuk, R.R.; Chumak, V.V.; Fil', M.R.; Havrylyuk, D.Y.; Zimenkovsky, B.S.; Lesyk, R.B.; Stoika, R.S. Study of molecular mechanisms of proapoptotic action of novel heterocyclic 4-thiazolidone derivatives. *Biopolym. Cell* **2012**, *28*, 121–128. [[CrossRef](#)]
- Subtelna, I.; Atamanyuk, D.; Szymańska, E.; Kieć-Kononowicz, K.; Zimenkovsky, B.; Vasylenko, O.; Gzella, A.; Lesyk, R. Synthesis of 5-arylidene-2-amino-4-azolones and evaluation of their anticancer activity. *Bioorg. Med. Chem.* **2010**, *18*, 5089–5101. [[CrossRef](#)]
- Antypenko, L.; Gladysheva, S. Development and validation of UV-spectrophotometric determination of ciminalum in drug. *Recipe* **2017**, *20*, 153–160.
- Lesyk, R. Drug design: 4-thiazolidinones applications. Part 1. Synthetic routes to the drug-like molecules. *JMS* **2020**, *89*, e406. [[CrossRef](#)]
- Lesyk, R. Drug design: 4-thiazolidinones applications. Part 2. Pharmacological profiles. *JMS* **2020**, *89*, e407. [[CrossRef](#)]
- Turkevych, N.M.; Vvedenskij, V.M.; Petlichnaya, L.P. Method of obtaining pseudothiohydantoin and thiazolidinedione-2,4. *Ukr. Khim. Zh. (Russ. Ed.)* **1961**, *27*, 680–681.
- Nencki, M. Ueber die Einwirkung der Monochloressigsäure auf Sulfoacylsäure und ihre Salze. *J. Prakt. Chem.* **1877**, *16*, 1–17. [[CrossRef](#)]
- Petlichnaya, L.I.; Turkevich, N.M. Synthesis of new arylidene derivatives of 3-aminorhodanine. *Chem. Heterocycl. Compd.* **1970**, *4*, 57–59. [[CrossRef](#)]
- Langhals, E.; Balli, H. Novel dimethine merocyanine dyes undergoing J-aggregation in highly dilute solution. *Helv. Chim. Acta* **1985**, *68*, 1782–1797. [[CrossRef](#)]
- Stawoska, I.; Tejchman, W.; Mazuryk, O.; Lyčka, A.; Nowak-Sliwinska, P.; Żesławska, E.; Nitek, W.; Kania, A. Spectral Characteristic and Preliminary Anticancer Activity in vitro of Selected Rhodanine-3-carboxylic Acids Derivatives. *J. Heterocycl. Chem.* **2017**, *54*, 2889–2897. [[CrossRef](#)]
- Horishny, V.; Kartsev, V.; Geronikaki, A.; Matychuk, V.; Petrou, A.; Glamoclija, J.; Ciric, A.; Sokovic, M. 5-(1H-Indol-3-ylmethylene)-4-oxo-2-thioxothiazolidin-3-yl)alkancarboxylic acids as antimicrobial agents: Synthesis, biological evaluation and molecular docking studies. *Molecules* **2020**, *25*, 1964. [[CrossRef](#)]
- Nitsche, C.; Schreier, V.N.; Behnam, M.A.M.; Kumar, A.; Bartenschlager, R.; Klein, C.D. Thiazolidinone-Peptide Hybrids as Dengue Virus Protease Inhibitors with Antiviral Activity in Cell Culture. *J. Med. Chem.* **2013**, *56*, 8389–8403. [[CrossRef](#)]
- Ali Muhammad, S.; Ravi, S.; Thangamani, A. Synthesis and evaluation of some novel N-substituted rhodanines for their anticancer activity. *Med. Chem. Res.* **2016**, *25*, 994–1004. [[CrossRef](#)]
- Brahmbhatt, H.; Molnar, M.; Pavić, V.; Vesna Rastija, V. Synthesis, Characterization, Antibacterial and Antioxidant Potency of N-Substituted-2-Sulfanylidene-1,3-Thiazolidin-4-one Derivatives and QSAR Study. *Med. Chem.* **2019**, *15*, 840–849. [[CrossRef](#)]
- Liu, K.; Lu, H.; Hou, L.; Qi, Z.; Teixeira, C.; Barbault, F.; Fan, B.-T.; Liu, S.; Jiang, S.; Xie, L. Design, Synthesis, and Biological Evaluation of N-Carboxyphenylpyrrole Derivatives as Potent HIV Fusion Inhibitors Targeting gp41. *J. Med. Chem.* **2008**, *51*, 7843–7854. [[CrossRef](#)]
- Shepeta, Y.L.; Lelyukh, M.I.; Zimenkovsky, B.S.; Nektagayev, I.O.; Lesyk, R.B. Synthesis and anti-inflammatory activity evaluation of rhodanine derivatives with 2-(2,6-dichlorophenylamino)-phenylacetamide fragment in molecules. *Pharm. Rev.* **2018**, *1*, 6–15. (In Ukrainian) [[CrossRef](#)]
- Monks, A.; Scudiero, D.; Skehan, P.; Shoemaker, R.; Paull, K.; Vistica, D.; Hose, C.; Langley, J.; Cronise, P.; Vaigro-Wolff, A.; et al. Feasibility of a high-flux anticancer drug screen using a diverse panel of cultured human tumor cell lines. *J. Nat. Cancer Inst.* **1991**, *83*, 757–766. [[CrossRef](#)] [[PubMed](#)]
- Boyd, M.R.; Paull, K.D. Some practical considerations and applications of the national cancer institute in vitro anticancer drug discovery screen. *Drug Dev. Res.* **1995**, *34*, 91–109. [[CrossRef](#)]
- Boyd, M.R. *Cancer Drug Discovery and Development*; Teicher, B.A., Ed.; Humana Press: Totowa, NJ, USA, 1997; Volume 2, pp. 23–43.



25. Shoemaker, R.H. The NCI60 human tumour cell line anticancer drug screen. *Nat. Rev. Cancer* **2006**, *6*, 813–823. [[CrossRef](#)] [[PubMed](#)]
26. Rostom, S.A.F. Synthesis and in vitro antitumor evaluation of some indeno [1,2-c]pyrazol(in)es substituted with sulfonamide, sulfonylurea(-thiourea) pharmacophores, and some derived thiazole ring systems. *Bioorg. Med. Chem.* **2006**, *14*, 6475–6485. [[CrossRef](#)] [[PubMed](#)]
27. Carmichael, J.; DeGraff, W.G.; Gazdar, A.F.; Minna, J.D.; Mitchell, J.B. Evaluation of a Tetrazolium-based Semiautomated Colorimetric Assay: Assessment of Chemosensitivity Testing. *Cancer Res.* **1987**, *47*, 936–942. [[PubMed](#)]
28. Rigaku Oxford Diffraction. *CrysAlis, PRO*; Version 1.171.40.84a; Rigaku Oxford Diffraction: Yarnton, UK, 2020.
29. Sheldrick, G.M. SHELXT-Integrated space-group and crystal-structure determination. *Acta Cryst. A* **2015**, *71*, 3–8. [[CrossRef](#)] [[PubMed](#)]
30. Sheldrick, G.M. Crystal structure refinement with SHELXL. *Acta Cryst. C* **2015**, *71*, 3–8. [[CrossRef](#)]
31. Farrugia, L.J. WinGX and ORTEP for windows: An update. *J. Appl. Cryst.* **2012**, *45*, 849–854. [[CrossRef](#)]
32. Dolomanov, O.V.; Bourhis, L.J.; Gildea, R.J.; Howard, J.A.K.; Puschmann, H. OLEX2: A complete structure solution, refinement and analysis program. *J. Appl. Cryst.* **2009**, *42*, 339–341. [[CrossRef](#)]
33. Spek, A.L. Structure validation in chemical crystallography. *Acta Cryst.* **2009**, *65*, 148–155. [[CrossRef](#)]

Supplementary information

## Synthesis and Anticancer Activity Evaluation of 5-[-2-Chloro-3-(4-nitrophenyl)-2-propenylidene]-4-thiazolidinones

Kamila Buzun <sup>1</sup>, Anna Kryshchshyn-Dylevych <sup>2</sup>, Julia Senkiv <sup>3</sup>, Olexandra Roman <sup>2</sup>, Krzysztof Bielawski <sup>4</sup>, Anna Bielawska <sup>1</sup> and Roman Lesyk <sup>2,5\*</sup>

<sup>1</sup> Department of Biotechnology, Medical University of Białystok, Jana Kilińskiego 1, Białystok, 15-089, Poland; kamila.buzun@umb.edu.pl (K.B.), anna.bielawska@umb.edu.pl (A.B.)

<sup>2</sup> Department of Pharmaceutical, Organic and Bioorganic Chemistry, Danylo Halatsky Lviv National Medical University, Pekarska 69, Lviv, 79010, Ukraine; kryshchshyn.a@gmail.com (A.K.-D.), lesia\_roman@ukr.net (O.R.), dr\_r\_lesyk@org.lviv.net (R.L.)

<sup>3</sup> Institute of Cell Biology of National Academy of Sciences of Ukraine, 14/16 Drahomanov Str., Lviv 79005, Ukraine; yu.senkiv@gmail.com

<sup>4</sup> Department of Synthesis and Technology of Drugs, Medical University of Białystok, 15-089 Białystok, Poland; kbiel@umb.edu.pl

<sup>5</sup> Department of Public Health, Dietetics and Lifestyle Disorders, Faculty of Medicine, University of Information Technology and Management in Rzeszów, 35-225 Rzeszów, Poland

\* Correspondence: dr\_r\_lesyk@org.lviv.net; Tel.: +380322755966

**Supplementary data:** The NMR spectra of compounds 2a-1

**Citation:** Buzun, K.; Kryshchshyn-Dylevych, A.; Senkiv, J.; Roman, O.; Bielawski, K.; Bielawska, A.; Lesyk, R. Synthesis and Anticancer Activity Evaluation of 5-[-2-Chloro-3-(4-nitrophenyl)-2-propenylidene]-4-thiazolidinones. *Molecules* **2021**, *26*, x. <https://doi.org/10.3390/xxxxx>

Received: date

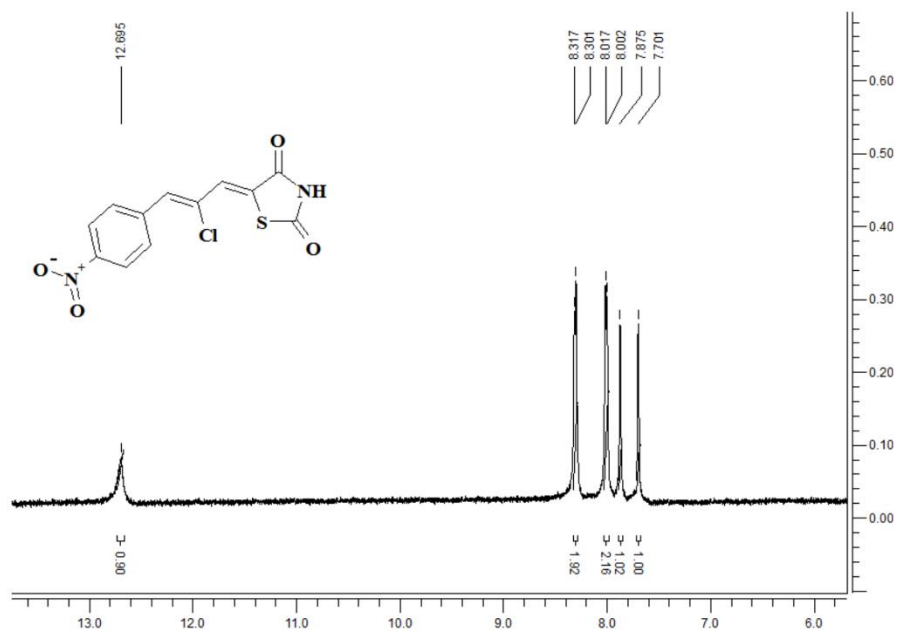
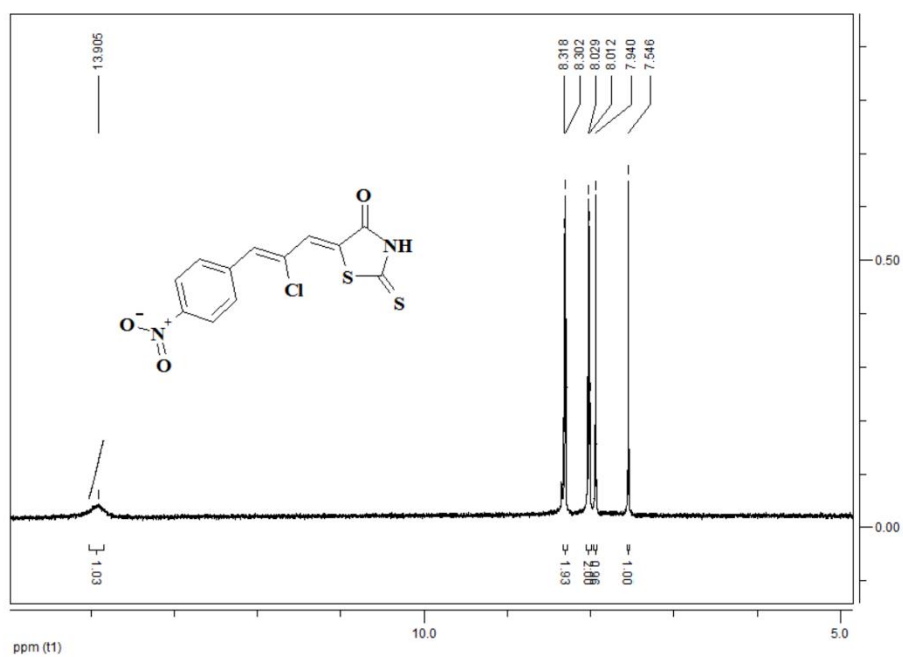
Accepted: date

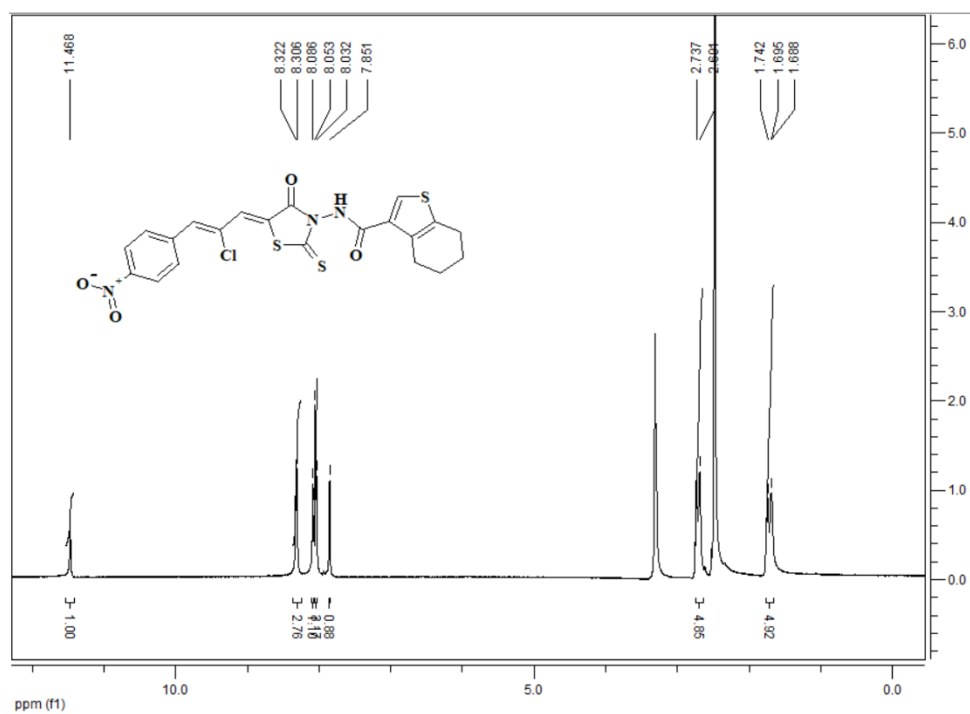
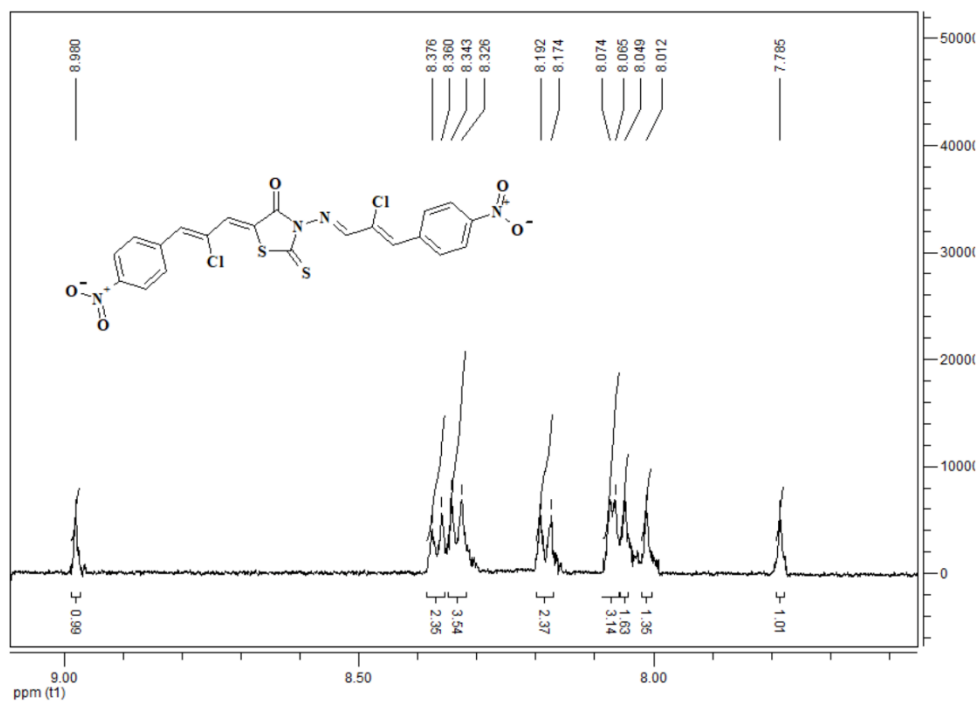
Published: date

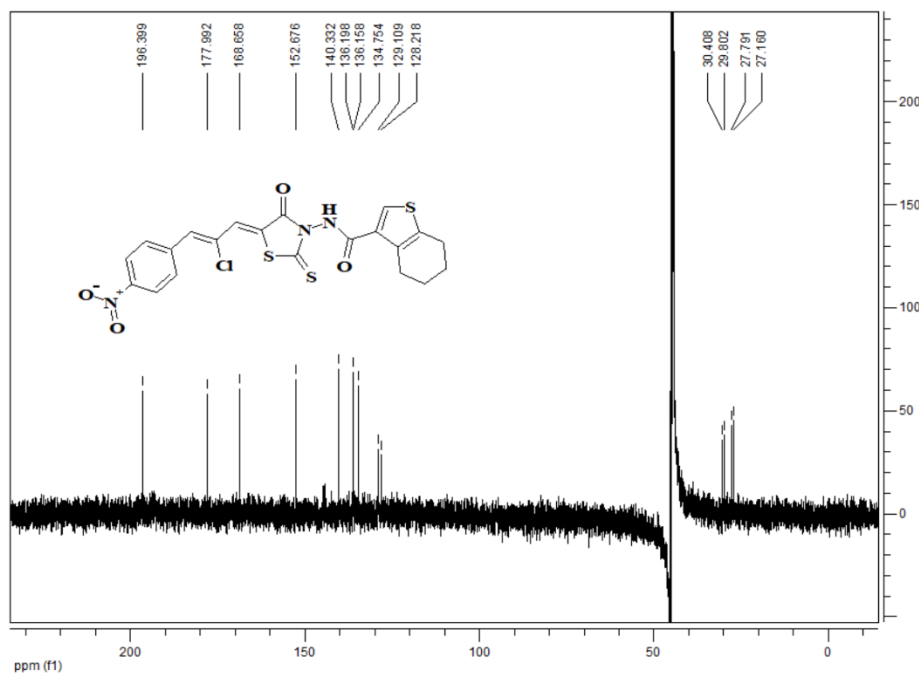
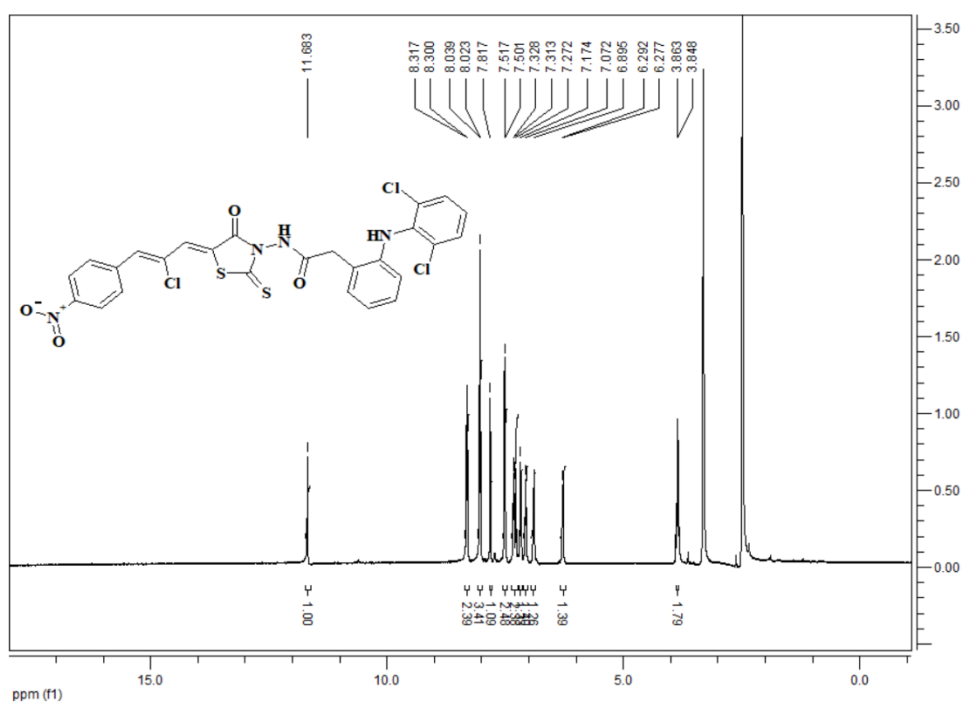
**Publisher's Note:** MDPI stays neutral with regard to jurisdictional claims in published maps and institutional affiliations.

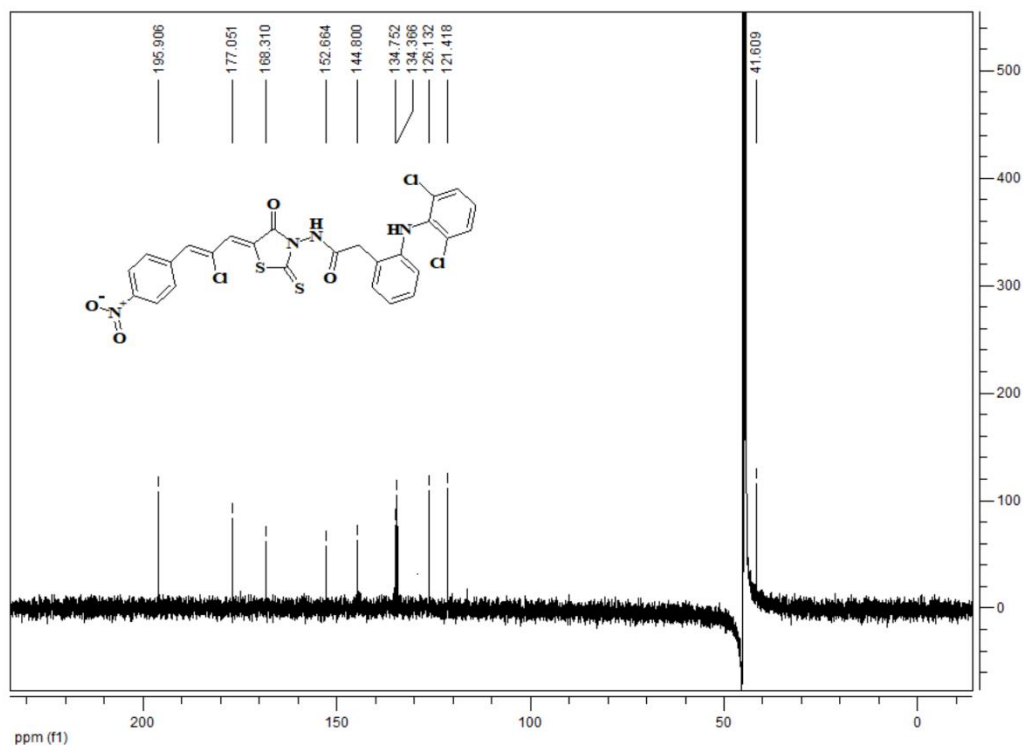
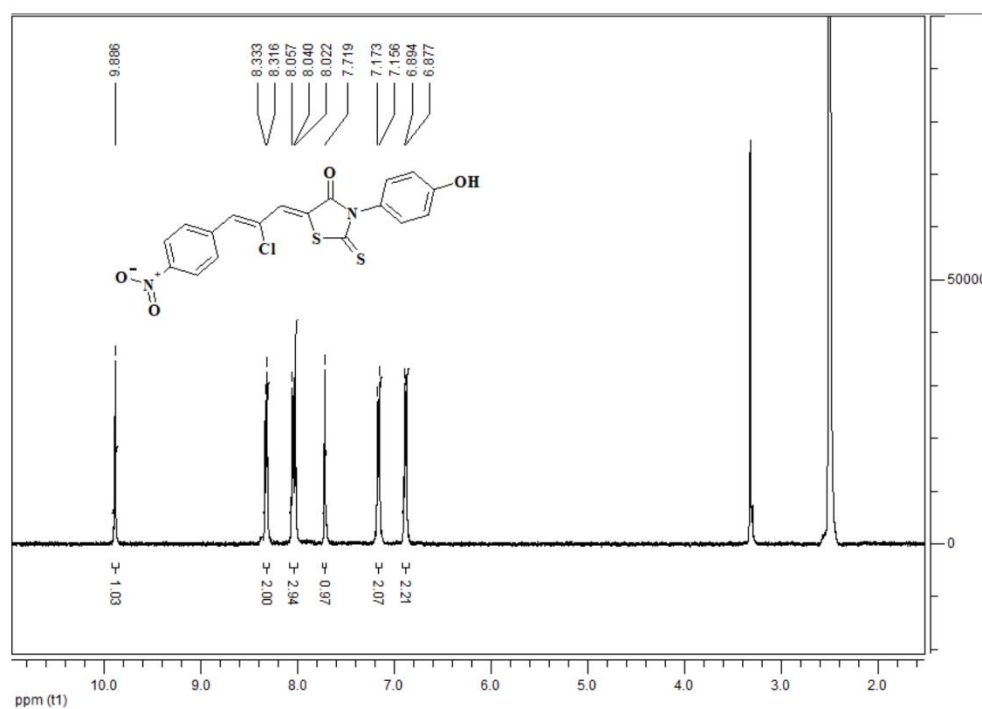


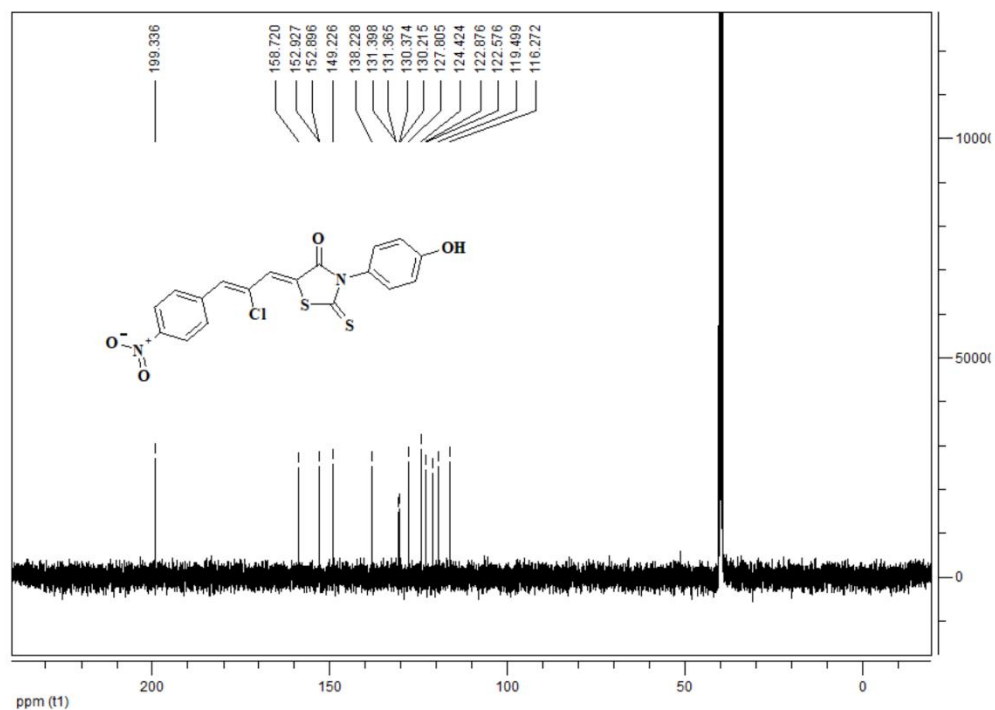
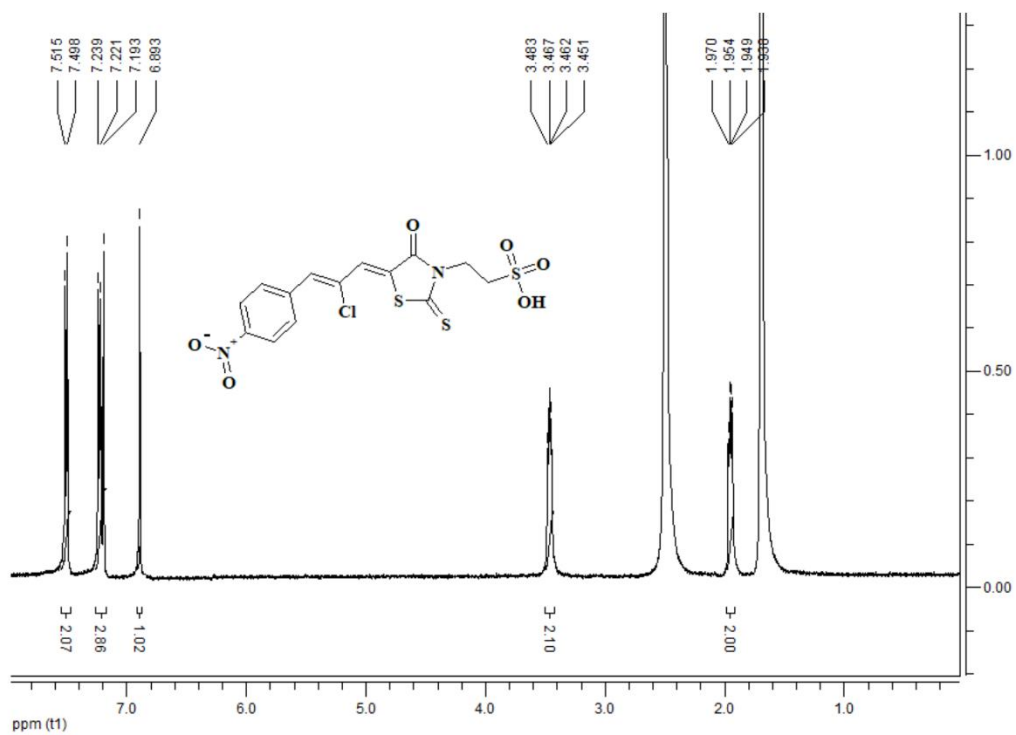
**Copyright:** © 2021 by the authors. Submitted for possible open access publication under the terms and conditions of the Creative Commons Attribution (CC BY) license (<http://creativecommons.org/licenses/by/4.0/>).

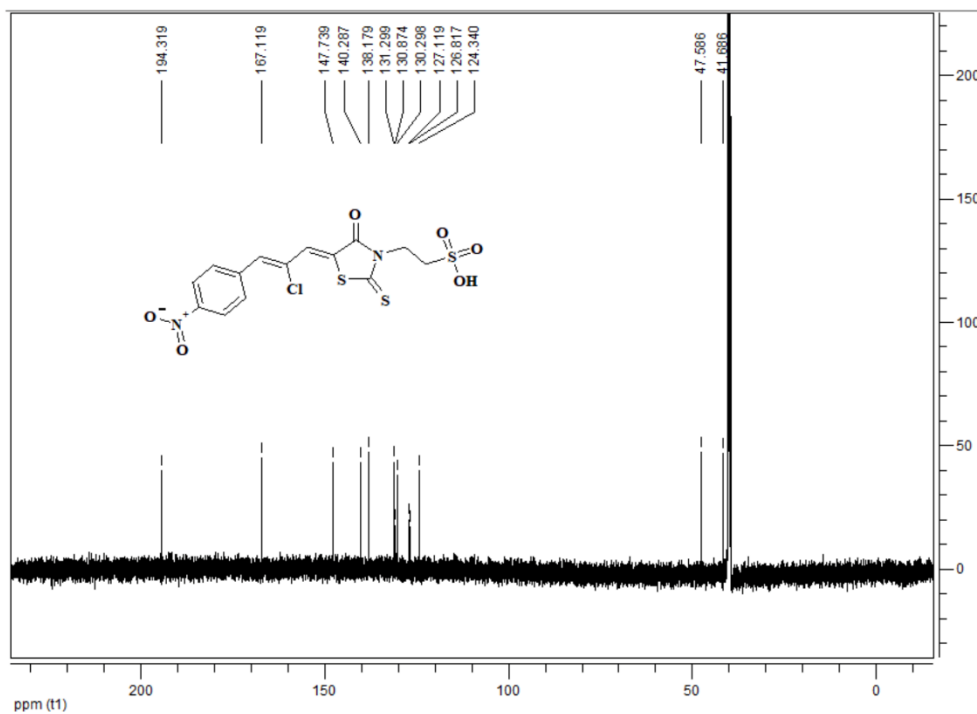
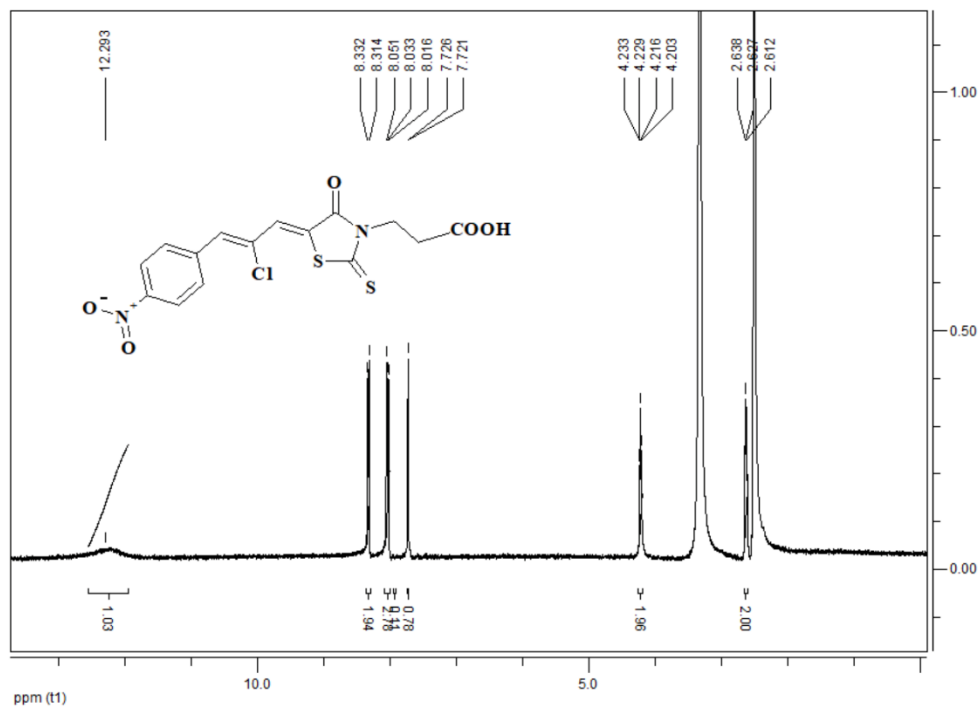
Figure S1. <sup>1</sup>H NMR spectrum 2a.Figure S2. <sup>1</sup>H NMR spectrum 2b.



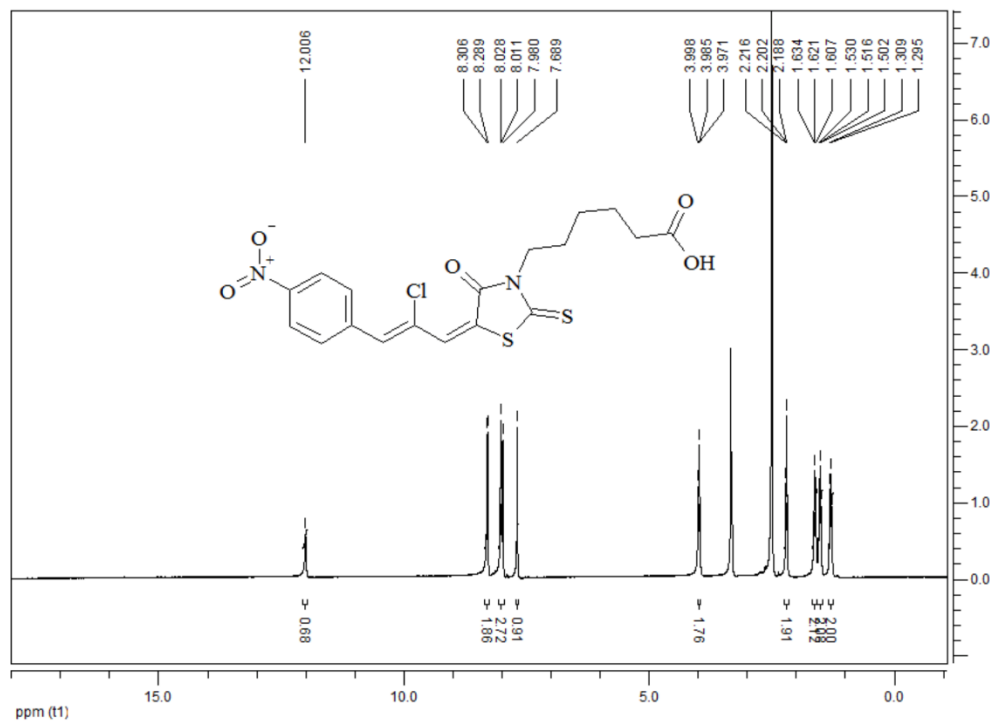
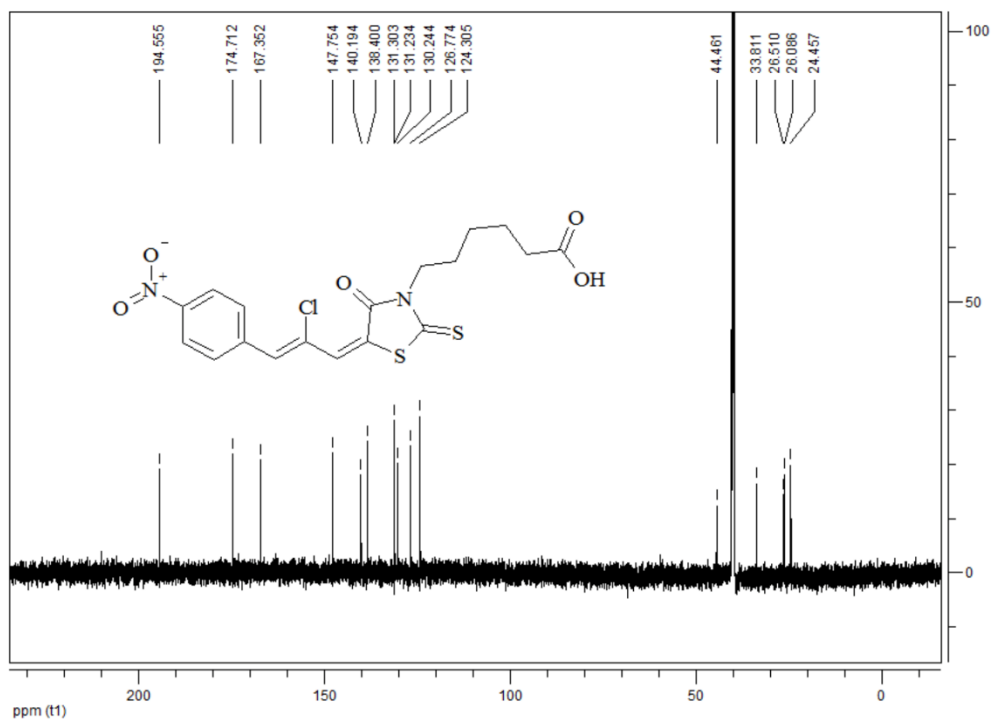
Figure S5. <sup>13</sup>C NMR spectrum 2d.Figure 6. <sup>1</sup>H NMR spectrum 2e.

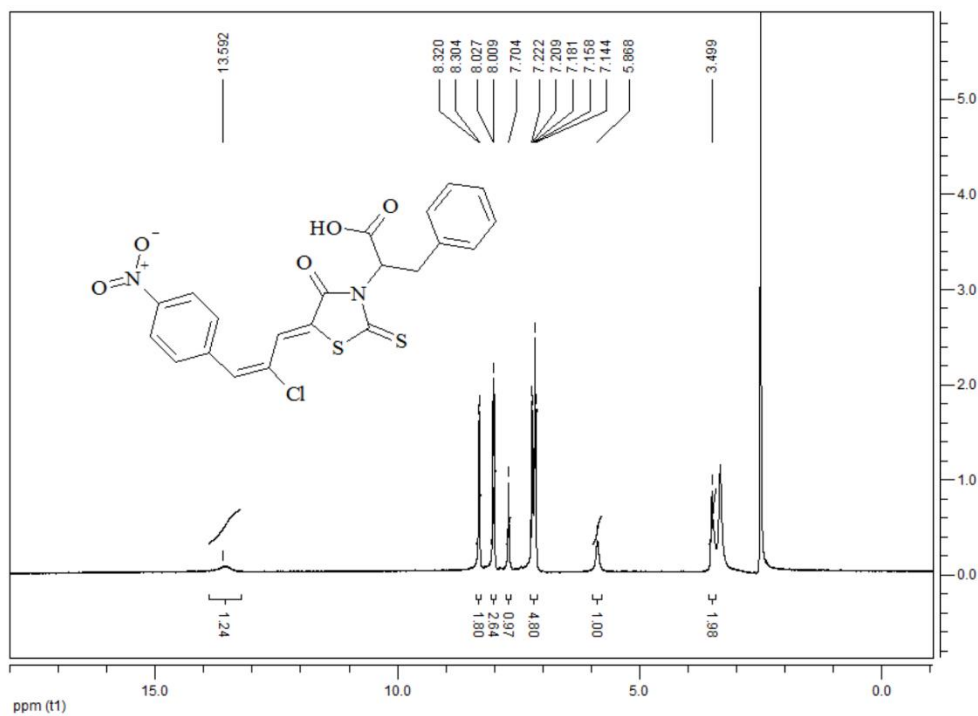
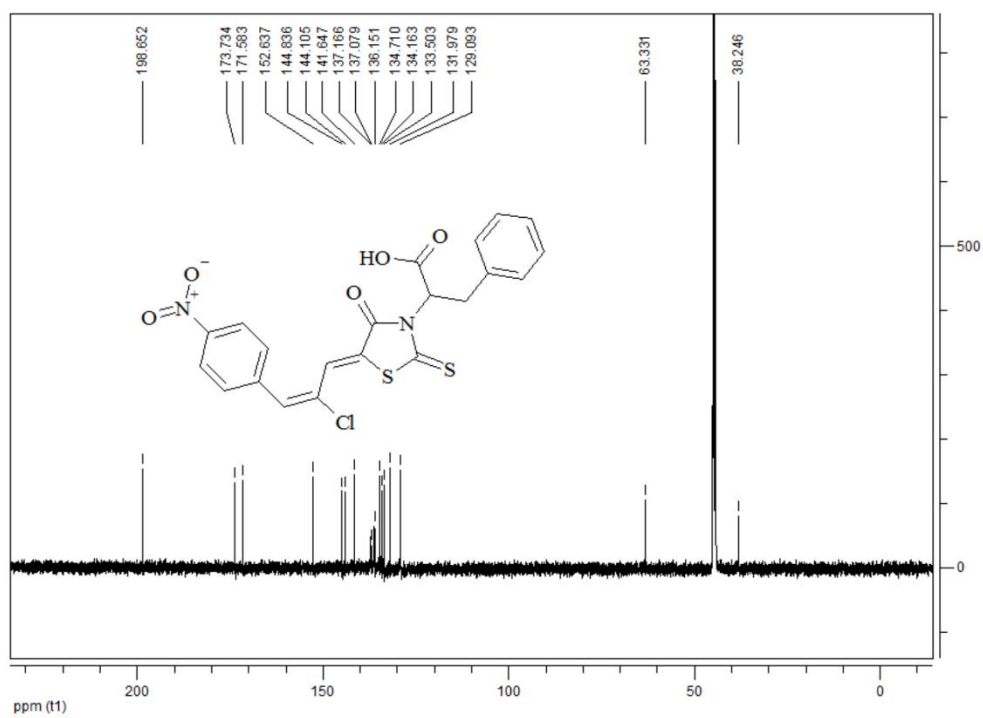
Figure S7. <sup>13</sup>C NMR spectrum 2e.Figure S8. <sup>1</sup>H NMR spectrum 2f.

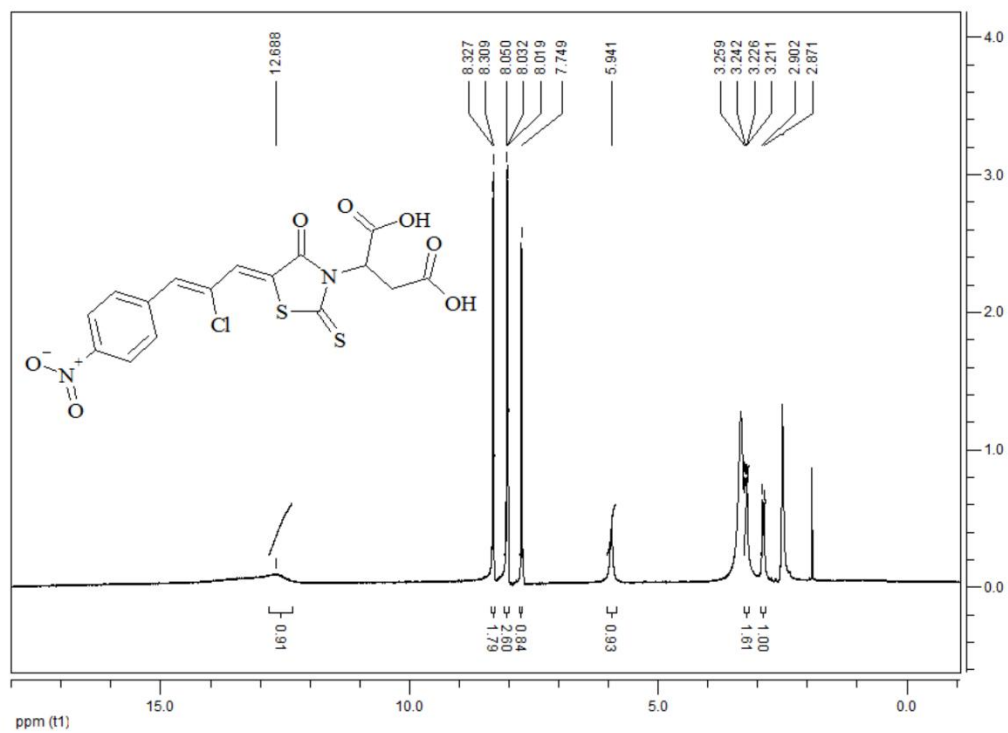
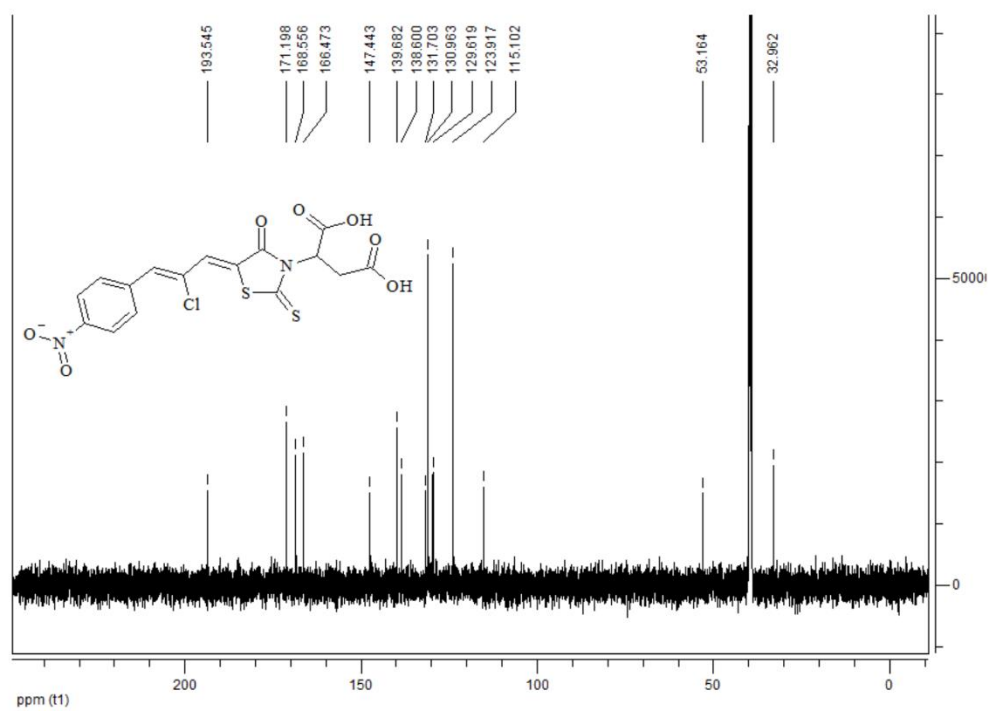
Figure S9.  $^{13}\text{C}$  NMR spectrum 2f.Figure S10.  $^1\text{H}$  NMR spectrum 2g.

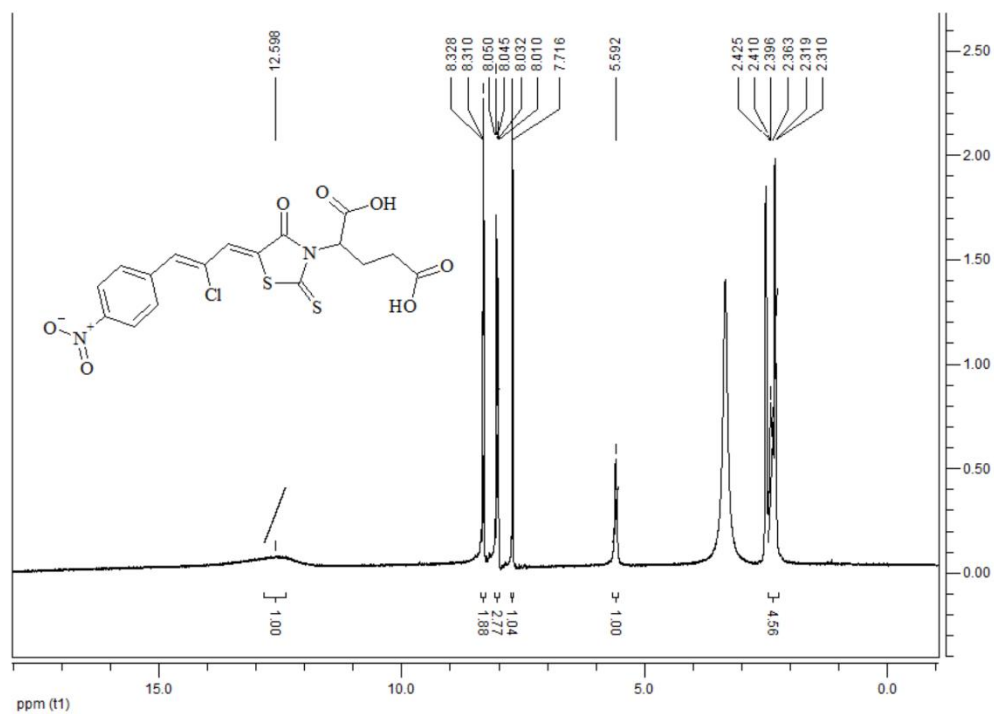
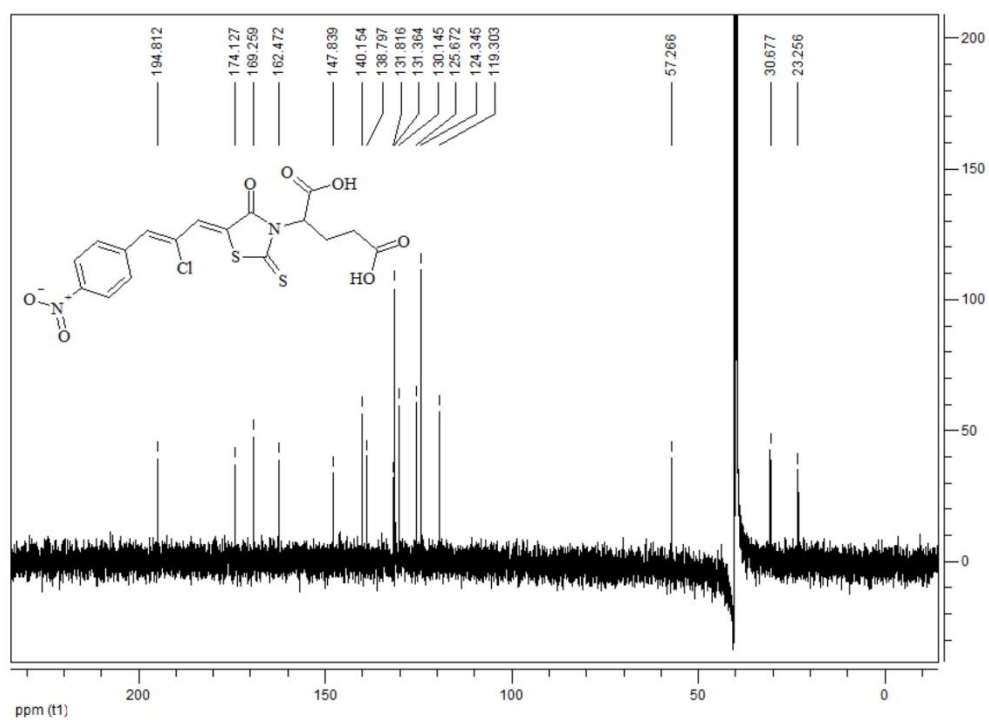
Figure S11.  $^{13}\text{C}$  NMR spectrum 2g.Figure S12.  $^1\text{H}$  NMR spectrum 2h.



Figure S13. <sup>1</sup>H NMR spectrum 2i.Figure S14. <sup>13</sup>C NMR spectrum 2i.

Figure S15. <sup>1</sup>H NMR spectrum 2j.Figure S14. <sup>13</sup>C NMR spectrum 2j.

Figure S15. <sup>1</sup>H NMR spectrum 2k.Figure S14. <sup>13</sup>C NMR spectrum 2k.

Figure S15. <sup>1</sup>H NMR spectrum 21.Figure S16. <sup>13</sup>C NMR spectrum 21.



Article

# 2-{5-[(Z,2Z)-2-Chloro-3-(4-nitrophenyl)-2-propenylidene]-4-oxo-2-thioxothiazolidin-3-yl}-3-methylbutanoic Acid as a Potential Anti-Breast Cancer Molecule

Kamila Buzun <sup>1</sup>, Agnieszka Gornowicz <sup>1,\*</sup>, Roman Lesyk <sup>2,3</sup>, Anna Kryshchysyn-Dylevych <sup>3</sup>,  
Andrzej Gzella <sup>4</sup>, Robert Czarnomysy <sup>5</sup>, Gniewomir Latacz <sup>6</sup>, Agnieszka Olejarz-Maciej <sup>6</sup>,  
Jadwiga Handzlik <sup>6</sup>, Krzysztof Bielawski <sup>5</sup> and Anna Bielawska <sup>1</sup>

- <sup>1</sup> Department of Biotechnology, Faculty of Pharmacy, Medical University of Białystok, 15-089 Białystok, Poland; kamila.buzun@umb.edu.pl (K.B.); anna.bielawska@umb.edu.pl (A.B.)  
<sup>2</sup> Department of Biotechnology and Cell Biology, Medical College, University of Information Technology and Management in Rzeszów, Sucharskiego 2, 35-225 Rzeszów, Poland; dr\_r\_lesyk@org.lviv.net  
<sup>3</sup> Department of Pharmaceutical, Organic and Bioorganic Chemistry, Danylo Halatsky Lviv National Medical University, Pekarska 69, 79010 Lviv, Ukraine; kryshchysyn.a@gmail.com  
<sup>4</sup> Department of Organic Chemistry, Poznan University of Medical Sciences, Grunwaldzka 6, 60-780 Poznan, Poland; akgzella@ump.edu.pl  
<sup>5</sup> Department of Synthesis and Technology of Drugs, Faculty of Pharmacy, Medical University of Białystok, 15-089 Białystok, Poland; robert.czarnomysy@umb.edu.pl (R.C.); kbiel@umb.edu.pl (K.B.)  
<sup>6</sup> Department of Technology and Biotechnology of Drugs, Faculty of Pharmacy, Jagiellonian University Medical College, Medyczna 9, 30-688 Cracow, Poland; glatacz@cm-uj.krakow.pl (G.L.); agnieszka.olejarz@uj.edu.pl (A.O.-M.); j.handzlik@uj.edu.pl (J.H.)  
\* Correspondence: agnieszka.gornowicz@umb.edu.pl



**Citation:** Buzun, K.; Gornowicz, A.; Lesyk, R.; Kryshchysyn-Dylevych, A.; Gzella, A.; Czarnomysy, R.; Latacz, G.; Olejarz-Maciej, A.; Handzlik, J.; Bielawski, K.; et al. 2-{5-[(Z,2Z)-2-Chloro-3-(4-nitrophenyl)-2-propenylidene]-4-oxo-2-thioxothiazolidin-3-yl}-3-methylbutanoic Acid as a Potential Anti-Breast Cancer Molecule. *Int. J. Mol. Sci.* **2022**, *23*, 4091. <https://doi.org/10.3390/ijms23084091>

Academic Editor: Aamir Ahmad

Received: 18 March 2022

Accepted: 5 April 2022

Published: 7 April 2022

**Publisher's Note:** MDPI stays neutral with regard to jurisdictional claims in published maps and institutional affiliations.



**Copyright:** © 2022 by the authors. Licensee MDPI, Basel, Switzerland. This article is an open access article distributed under the terms and conditions of the Creative Commons Attribution (CC BY) license (<https://creativecommons.org/licenses/by/4.0/>).

**Abstract:** It was established that the synthesis of hybrid molecules containing a thiazolidinone and a (Z,Z)-2-chloro-3-(4-nitrophenyl)prop-2-ene structural fragments is an effective approach for the design of potential anticancer agents. Given the results of the previous SAR-analysis, the aim of the study was to synthesize a novel 4-thiazolidinone derivative Les-3331 and investigate its molecular mechanism of action in MCF-7 and MDA-MB-231 breast cancer cells. The cytotoxic properties and antiproliferative potential of Les-3331 were determined. The effect of the tested compound on apoptosis induction and mitochondrial membrane potential was checked by flow cytometry. ELISA was used to determine caspase-8 and caspase-9, LC3A, LC3B, Beclin-1, and topoisomerase II concentration. Additionally, PAMPA, in silico or in vitro prediction of metabolism, CYP3A4/2D6 inhibition, and an Ames test were performed. Les-3331 possesses high cytotoxic and antiproliferative activity in MCF-7 and MDA-MB-231 breast cancer cells. Its molecular mechanism of action is associated with apoptosis induction, decreased mitochondrial membrane potential, and increased caspase-9 and caspase-8 concentrations. Les-3331 decreased LC3A, LC3B, and Beclin-1 concentration in tested cell lines. Topoisomerase II concentration was also lowered. The most probable metabolic pathways and no DDIs risk of Les-3331 were confirmed in in vitro assays. Our studies confirmed that a novel 4-thiazolidinone derivative represents promising anti-breast cancer activity.

**Keywords:** 4-thiazolidinones; breast cancer; apoptosis; autophagy; anticancer agents; chemotherapy; topoisomerase inhibitor; etoposide; 3-MA; ADME-Tox parameters

## 1. Introduction

Cancer is the leading cause of death worldwide. According to the World Health Organization's (WHO) 2019 estimates, cancer is the first or second leading cause of death among people aged 70 in 112 of the 183 studied countries [1]. Based on the latest WHO data, 2.3 million new cases of breast cancer (BC) occurred among women worldwide in 2020 alone and 685,000 deaths were caused by this disease. By the end of 2020, nearly

8 million women diagnosed with BC in the previous five years were alive worldwide. As statistics show, breast cancer is the most common cancer for women in the world [2].

Molecularly, BC is a heterogeneous disease characterized by hormone receptors (progesterone (PR) and estrogen (ER) receptors) activation, human epidermal growth factor receptor 2 (HER2) activation, and/or *BRCA* mutations. We can distinguish three basic subtypes of BC based on its HER2 and hormone receptor status: luminal (ER-positive and PR-positive), HER2-positive (HER2+), and triple-negative breast cancer (TNBC) [3]. Modern, multidisciplinary therapeutic strategies involve both systematic therapies and locoregional approaches (radiotherapy and surgery). Systematic therapies include chemotherapy, anti-HER2 treatment for HER2+ BC, bone-stabilizing agents, endocrine therapy for hormone receptor-positive breast cancer, poly(ADP-ribose) polymerase inhibitors for patients with *BRCA* mutation, and immunotherapy [4]. Systematic chemotherapy used to date involves the use of cytostatic drugs. Their mechanism of action is based on the apoptosis induction and inhibition of mitosis by disrupting the cell cycle. Chemotherapy options in breast cancer treatment strongly depend on the cancer subtype. Currently, for patients with ER+, PR+, and HER− (after or together with endocrine therapy), intravenous treatment with adriamycin–cyclophosphamide, adriamycin–cyclophosphamide–paclitaxel, or docetaxel–cyclophosphamide can be applied. Chemotherapeutic strategies for patients with HER2+ BC are based on intravenous therapy with paclitaxel–trastuzumab, adriamycin–cyclophosphamide–paclitaxel–trastuzumab ± pertuzumab, or docetaxel–carboplatin–trastuzumab ± pertuzumab. Furthermore, therapy of patients with HER2+, ER+, and PR+ breast cancer includes endocrine treatment as well. TNBC patients are treated with intravenous therapy of adriamycin–cyclophosphamide, adriamycin–cyclophosphamide–paclitaxel, or docetaxel–cyclophosphamide [5]. However, available cytostatic drugs have poor selectivity and a low therapeutic index, leading to a number of side effects. Optimal therapy is different for each patient, based on the diagnosed subtype of cancer, stage of disease and individual preferences of the patient.

Advances in knowledge of molecular biology and cancer genetics are contributing to the search for more effective pharmacotherapeutic approaches based on discoveries related to signal transduction in the cell. Therefore, the search for new anticancer drugs with high therapeutic efficacy and low toxicity is particularly important. Since the 1960s, a significant increase in medicinal chemistry and pharmacology of 4-thiazolidinones has been seen [6–8]. Numerous scientific papers, reviews and patents covering novel 4-thiazolidinone analogs have appeared over the last 60 years [9–13]. Compounds belonging to the group of 4-thiazolidinones have demonstrated diversified activity, from anticancer, antimicrobial, antibacterial, and anti-inflammatory to antidiabetic properties [14–16]. Among patented analogs and drugs based on 4-thiazolidinones, we can distinguish e.g., antidiabetic Pioglitazone [17], diuretic Etozoline [12], anti-inflammatory Darbufelon [18], or aldose reductase inhibitor Epalrestat [19]. Derivatives of 4-thiazolidinone are a well-known class of patented, leading compounds and drugs, among which antitumor “small molecules” are of special interest [20]. Thus, indisputable evidence of the affinity of 4-thiazolidinone-based derivatives for validated anticancer biotargets, such as TNF- $\alpha$ -TNFRc-1, JSP-1, and anti-apoptotic complex Bcl-X<sub>L</sub>-BH3, can be found in the literature [14,21,22]. It is important to note that, in this group of heterocyclic compounds, the most interesting for the design of new biologically attractive molecules are 5-ene-4-thiazolidinones [14]. On the other hand, 5-ene-4-thiazolidinones, as possible Michael acceptors, can react with glutathione and other free thiols within a cell; they are treated as frequent hitters or pan-assay interference compounds (PAINS) with low or insufficient selectivity. This may offer a high probability of polar interactions or hydrogen bonds formation, therefore causing a promiscuous behavior in high throughput screening campaigns that is often not confirmed in experimental studies. Moreover, Michael acceptor functionality, as well as the thesis about low selectivity towards biotargets of rhodanines, must be confirmed experimentally and it cannot be based on just the presence of conjugated  $\alpha,\beta$ -unsaturated carbonyl. Additionally, the positive aspects of Michael acceptors must be considered as well as their multitarget properties [13,23].

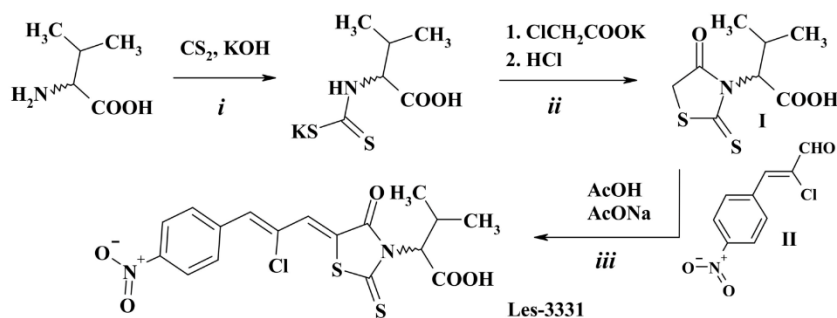
As a continuation of our systematic research of 4-thiazolidinone derivatives, we have established that the synthesis of hybrid molecules containing a thiazolidinone and a (Z,Z)-2-chloro-3-(4-nitrophenyl)prop-2-ene structural fragments (*Ciminalum*-thiazolidinone hybrid molecules) is an effective approach for the design of potential anticancer agents. Our systematic SAR-analysis allowed us to establish that the presence of the *Ciminalum* moiety in position 5 of core heterocycle is crucial to the antitumor activity of various 4-thiazolidinone derivatives, including 2,4-thiazolidinediones [24], isomeric 2- [25], and 4-aminothiazolones [26], 2-thioxo-4-thiazolidinones [24], etc. The role of the substituents in position 3 (especially carboxylic groups) of the 4-thiazolidinone core on the level of anticancer cytotoxicity level is also important for further in-depth research. Thus, high cytotoxicity of 5-[(Z,Z)-2-chloro-3-(4-nitrophenyl)-2-propenylidene]-2-thioxo-4-thiazolidinone-3-carboxylic acids against gastric cancer (AGS), human colon cancer (DLD-1), and breast cancers (MCF-7 and MDA-MB-231) cell lines, and a fairly wide therapeutic range, were established [24].

Given the results of the previous SAR-analysis, as well as the significant effect of the *Ciminalum*-thiazolidinone hybrids on the breast cancer cells, our current research was aimed at the in-depth study of anti-breast activity of novel derivative Les-3331 (2-[5-[(Z,Z)-2-chloro-3-(4-nitrophenyl)-2-propenylidene]-4-oxo-2-thioxothiazolidin-3-yl]-3-methylbutanoic acid).

## 2. Results

### 2.1. Chemistry

Target compound Les-3331 was synthesized via the Knoevenagel condensation of 3-methyl-2-(4-oxo-2-thioxothiazolidin-3-yl)-butanoic acid **I** and (Z,Z)-2-chloro-3-(4-nitrophenyl)prop-2-enal **II** in the presence of sodium acetate under reflux in acetic acid (Scheme 1). The starting 3-methyl-2-(4-oxo-2-thioxothiazolidin-3-yl)-butanoic acid **I** was obtained according to the dithiocarbamate method of 2-thioxo-4-thiazolidinones (rhodanines) synthesis using *D,L*-valine as a starting compound [27].



**Scheme 1.** Synthesis of 2-[5-[(Z,Z)-2-chloro-3-(4-nitrophenyl)-2-propenylidene]-4-oxo-2-thioxothiazolidin-3-yl]-3-methylbutanoic acid (**Les-3331**). Reagents and conditions: (i) *D,L*-Valine (0.03 mol),  $\text{KOH}$  (0.06 mol),  $\text{CS}_2$  (0.03 mol),  $\text{H}_2\text{O}$  (30 mL), stirring, RT, 3 h; (ii) 1.  $\text{CICH}_2\text{COOK}$  (0.03 mol), stirring, RT, 30 min, 2. 2N  $\text{HCl}$  to  $\text{pH} = 2.0$ , heating to  $90^\circ\text{C}$ , 30 min, 70%; (iii) comp. **I** (0.01 mol), (Z,Z)-2-chloro-3-(4-nitrophenyl)prop-2-enal **II** (0.010 mol),  $\text{AcONa}$  (0.01),  $\text{AcOH}$  (20 mL), reflux, 3 h, 64%.

The data characterizing synthesized Les-3331 were presented in the experimental part. Analytical and spectral data (Figures S1–S3, Supplementary Materials) confirmed the structure of the synthesized compound. The  $^1\text{H}$  NMR spectrum of the synthesized Les-3331 is characterized by the signals of the *Ciminalum* residue [24] in the form of two singlets at 7.77 and 8.02 ppm for  $\text{CH}=\text{CCl}-\text{CH}=\text{}$  group, as well as two doublets of the *p*-nitrophenyl substituent at 8.04 and 8.32 ppm. The substituent at position 3 of the rhodanine core is characterized by a subspectrum in the form of two doublets for methyl groups at 0.75 and 1.19 ppm, a multiplet and a doublet for  $\text{CH}$  groups at 2.71 (NCH) and 5.28 ppm ( $\text{CHCOOH}$ ). The carboxylic group forms a broad singlet at 13.28 ppm. In the

$^{13}\text{C}$  NMR spectra of Les-3331 signals of C=O and C=S groups of the core heterocycle were characteristic and appeared at 166.6 and 194.2 ppm, respectively.

The structure of Les-3331 was also confirmed by X-ray crystallography (Table S1, Supplementary Materials). The investigated compound has the structure of 2-[5-[(*Z,Z*)-2-chloro-3-(4-nitrophenyl)-2-propenylidene]-4-oxo-2-thioxothiazolidin-3-yl]-3-methylbutanoic acid and crystallizes as dimethylformamide solvate in a molar ratio of 1:1 (Figure 1), which agrees with the previous data for the specified class of compounds [24]. In the salt crystal lattice of Les-3331, solute and solvent molecules related by translation along the *a* axis are linked by hydrogen bonds O10—H10 $\cdots$ O28, C15—H15 $\cdots$ O9<sup>i</sup>, C29—H29 $\cdots$ O9, and C32—H32A $\cdots$ O9<sup>iii</sup> into tapes (Figure S5A, Table S2, Supplementary Materials). The anti-parallel tapes, related by the center of symmetry, then connect by hydrogen bonds C21—H21 $\cdots$ O26<sup>ii</sup> into columns (Figure S5B, Table S2, Supplementary Materials).

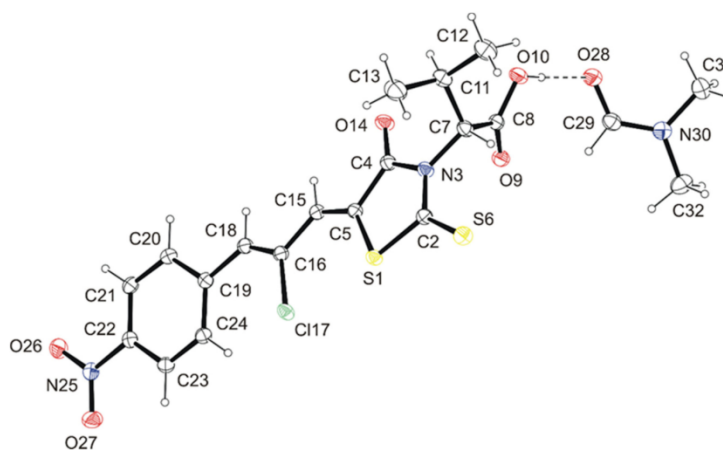


**Figure 1.** ORTEP view of Les-3331\*DMF, showing the atomic labelling scheme. Non-H atoms are drawn as 30% probability displacement ellipsoids and H atoms are drawn as spheres of arbitrary size.

## 2.2. Biological Studies

The influence of Les-3331 on the cell viability of two human breast cancer cell lines and human skin fibroblasts was evaluated using an MTT assay (Figure 2). Cells were incubated with varying concentrations of the tested compound and reference drug (etoposide [28–30]) for 24 h.

Based on the results obtained after 24 h incubation with the tested compound and reference drug, we showed that Les-3331 causes a significant reduction in cell viability of human breast cancer cell lines and  $\text{IC}_{50}$  value for MCF-7 (Figure 2A), and MDA-MB-231 (Figure 2B) cells were 5.02  $\mu\text{M}$  and 15.24  $\mu\text{M}$ , respectively. Etoposide was not as effective in decreasing the viability of human breast cancer cell lines and its  $\text{IC}_{50}$  values were higher than 50  $\mu\text{M}$  in both cases. Furthermore, as presented in Figure 2C, Les-3331 exhibited lower cytotoxicity against human skin fibroblasts compared to the MCF-7 and MDA-MB-231 cancer cell lines. Its  $\text{IC}_{50}$  value was 28.52  $\mu\text{M}$ .

To investigate the effect of novel 2-thioxo-4-thiazolidinone derivative and etoposide on cell proliferation, the level of [ $^3\text{H}$ ]-thymidine incorporation into DNA of human breast cancer cells was measured. The obtained results are shown in Figure 3.

We demonstrated that exposure of cancer cells to Les-3331 inhibited cell proliferation in a concentration-dependent manner. For MCF-7 cancer cells (Figure 3A),  $\text{IC}_{50}$  value of the tested compound was 5.54  $\mu\text{M}$  and for MDA-MB-231 cells (Figure 3B), it was 8.01  $\mu\text{M}$ . Etoposide did not exhibit as strong antiproliferative activity as the newly synthesized compound, and its  $\text{IC}_{50}$  values were higher than 20  $\mu\text{M}$  in both cases.



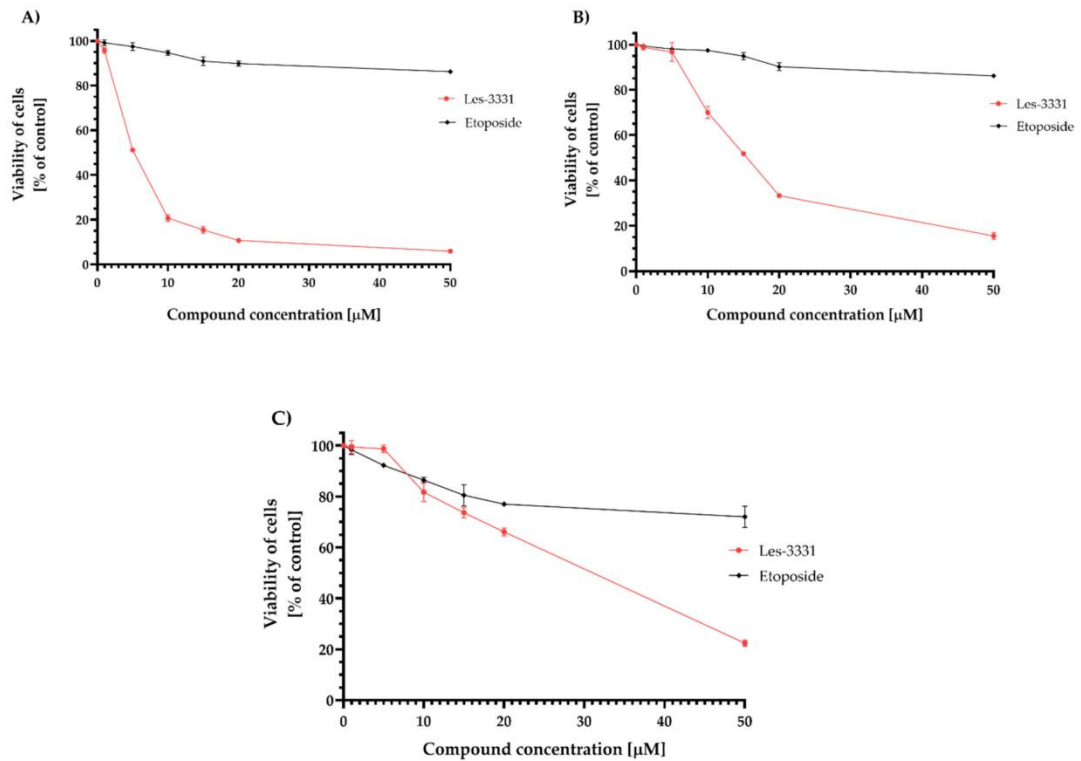


**Figure 2.** Viability of MCF-7 (A), MDA-MB-231 (B), and human skin fibroblasts (C) incubated for 24 h with Les-3331 and a reference drug (etoposide). Mean  $\pm$  SD from three independent experiments performed in duplicate is presented.

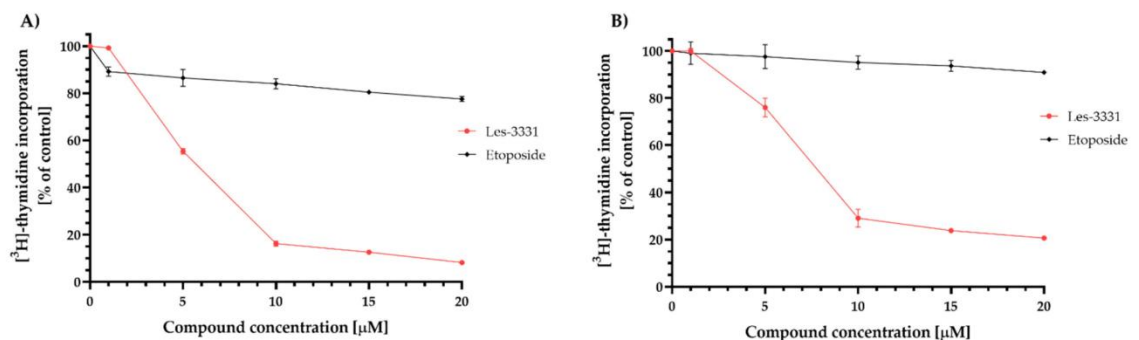


**Figure 3.** The influence of Les-3331 and reference drug on cell proliferation in MCF-7 (A) and MDA-MB-231 (B) cancer cell lines. Antiproliferative activity was measured after 24 h incubation of cancer cells with Les-3331 and a reference drug (etoposide) using  $^3\text{H}$ -thymidine incorporation assay. Mean  $\pm$  SD from three independent experiments performed in duplicate is presented.

In order to evaluate the influence of Les-3331 on the apoptosis process in human breast cancer cells, Annexin V binding assay was performed.

Analysis of results obtained in Annexin V binding assay revealed that Les-3331 induces apoptosis in a concentration-dependent manner. As shown in Figure 4A, we detected 6.5% of late and early apoptotic MCF-7 cells after a 24 h incubation with 1  $\mu\text{M}$  concentration of

Les-3331, whereas after a 24 h incubation of the tested compound with a concentration of five times higher, 40.4% of late and early apoptotic cancer cells were detected. In the case of the MDA-MB-231 cell line (Figure 4B), 5.1% and 18.1% of late- and early-apoptotic cells were detected after 24 h incubation with 1  $\mu$ M and 5  $\mu$ M concentration of novel compound, respectively. The reference compound was not as efficient in apoptosis activation as Les-3331. As demonstrated, 10.7% and 4.7% of late and early apoptotic cells were detected after 24 h exposure of MCF-7 (Figure 4A) and MDA-MB-231 (Figure 4B) cells to 1  $\mu$ M concentration of reference drug, while incubation with 5  $\mu$ M etoposide revealed 10.7% and 7.2% of apoptotic cells, respectively.

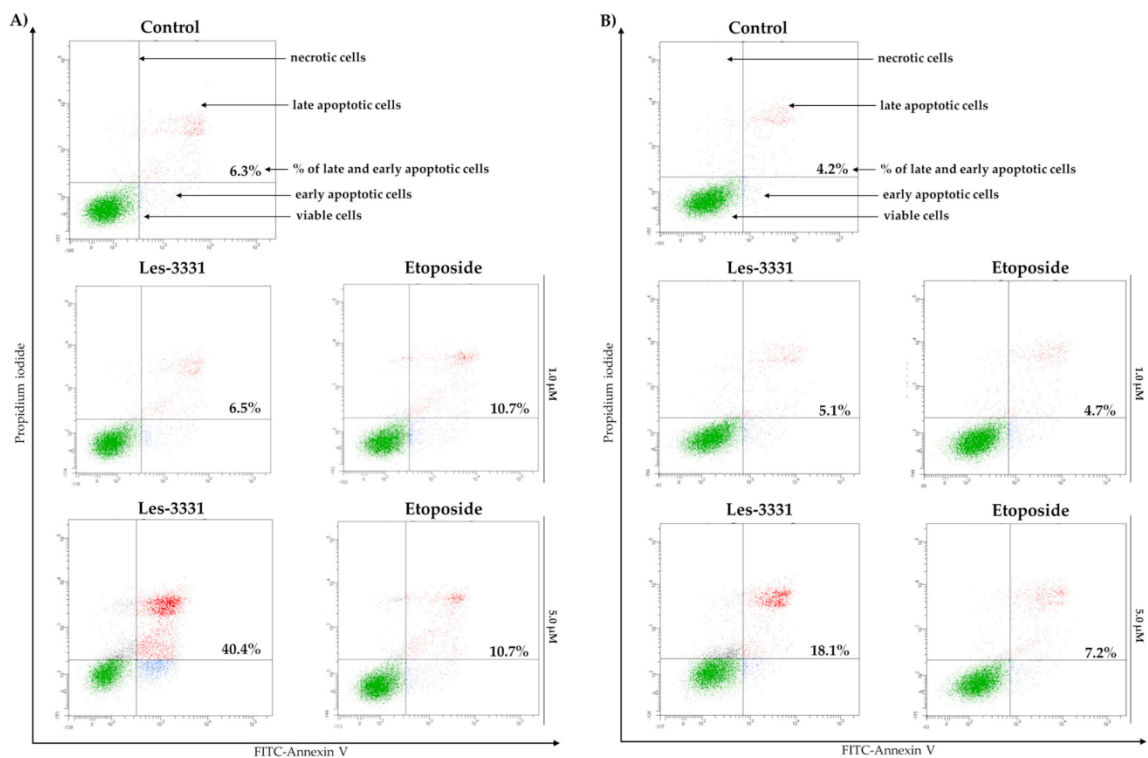


**Figure 4.** Induction of apoptosis in MCF-7 (A) and MDA-MB-231 (B) cells incubated with Les-3331 and a reference drug (etoposide) at 1  $\mu$ M and 5  $\mu$ M concentration for 24 h. The total number of late and early apoptotic human breast cancer cells is presented as the mean percentage from three independent experiments performed in duplicate.

The early stages of apoptosis are correlated with a decrease in mitochondrial membrane potential ( $\Delta\Psi_m$ ) [31]. To investigate the effect of Les-3331 on the intrinsic apoptotic pathway, JC-1 fluorescent dye staining was performed.

It was observed that Les-3331 in tested concentrations decreased  $\Delta\Psi_m$  in MCF-7 (Figure 5A) and MDA-MB-231 (Figure 5B) human breast cancer cells. After 24 h incubation with 1  $\mu$ M Les-3331, 9.8% of MCF-7 and 21.8% of MDA-MB-231 cells had decreased  $\Delta\Psi_m$ , whereas 24 h treatment of cancer cells with a 5  $\mu$ M concentration of Les-3331 resulted in a decrease in  $\Delta\Psi_m$  in 25.5% (MCF-7) and 36.3% (MDA-MB-231) of cells. The weaker effect was observed after incubation with the reference drug (etoposide) in 1  $\mu$ M and 5  $\mu$ M concentrations. As demonstrated, 10.2% of MCF-7 (Figure 5A) and 11.4% of MDA-MB-231 (Figure 5B) cells had decreased  $\Delta\Psi_m$  after incubation with 1  $\mu$ M etoposide, while

treatment of cancer cells with a reference drug concentration of five times higher resulted in a reduction in  $\Delta\Psi_m$  in 18.5% and 15.6% of cells, respectively.

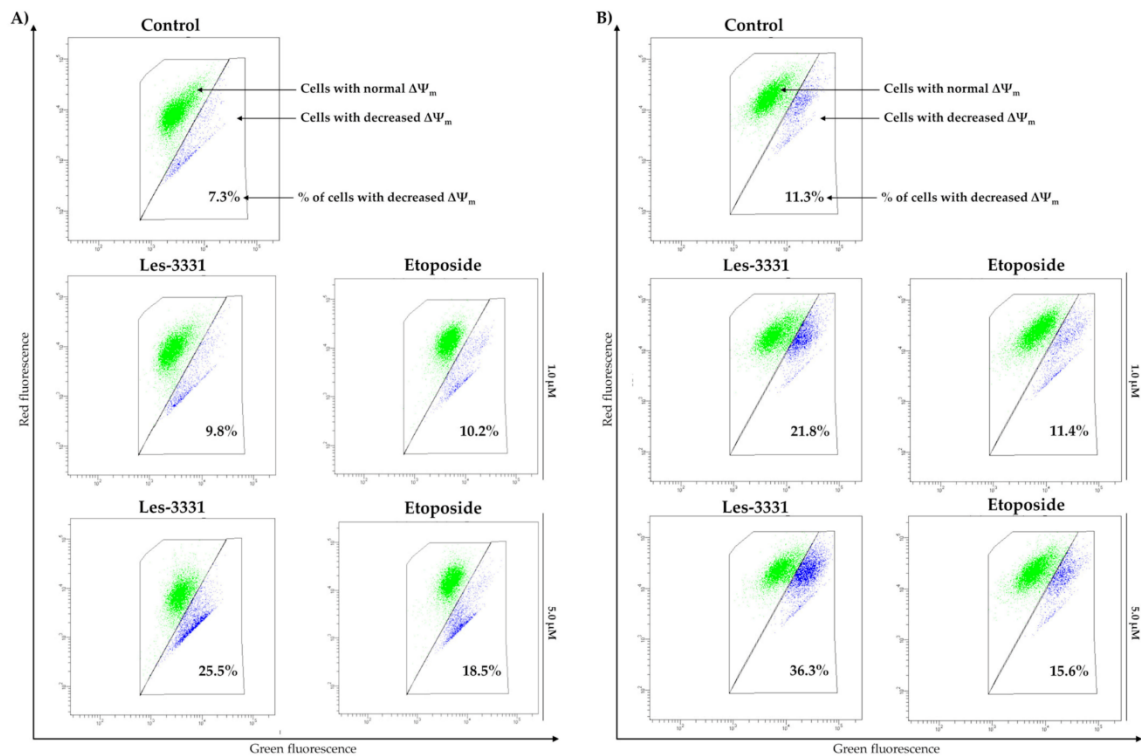


**Figure 5.** Mitochondrial membrane potential analysis in MCF-7 (A) and MDA-MB-231 (B) human breast cancer cells incubated with Les-3331 and reference drug (etoposide) at 1  $\mu\text{M}$  and 5  $\mu\text{M}$  concentration for 24 h. The total number of human breast cancer cells with decreased mitochondrial membrane potential is presented as the mean percentage from three independent experiments performed in duplicate.

Activation of the intrinsic apoptotic pathway by the newly synthesized compound can be confirmed by examining its influence on caspase-9 (Casp-9) concentration. We investigated whether apoptosis in tested human breast cancer cell lines in the presence of 1  $\mu\text{M}$  and 5  $\mu\text{M}$  of Les-3331 occurs through the intrinsic pathway.

Based on the obtained results, we showed that Les-3331 causes an increase in Casp-9 concentration. The most significant effect was observed after the exposure of MCF-7 cancer cells to Les-3331 (Figure 6A). After 24 h incubation with 1  $\mu\text{M}$  and 5  $\mu\text{M}$  Les-3331, we detected 150.187 ng/mL and 168.243 ng/mL of Casp-9, respectively, in MCF-7 cell lysates, compared to the control (120.913 ng/mL). The weaker effect was observed after incubation with a reference drug. Compared to the control, the Casp-9 concentration was 154.960 ng/mL (1  $\mu\text{M}$  etoposide) and 158.900 ng/mL (5  $\mu\text{M}$  etoposide). In MDA-MB-231 cells (Figure 6B), the concentration of Casp-9 after treatment with 1  $\mu\text{M}$  and 5  $\mu\text{M}$  Les-3331 was 84.300 ng/mL and 92.523 ng/mL, respectively, compared to the control (65.073 ng/mL). A similar effect was observed after exposure to 1  $\mu\text{M}$  and 5  $\mu\text{M}$  reference drug, where the concentration of Casp-9 was 86.953 ng/mL and 93.620 ng/mL, respectively.

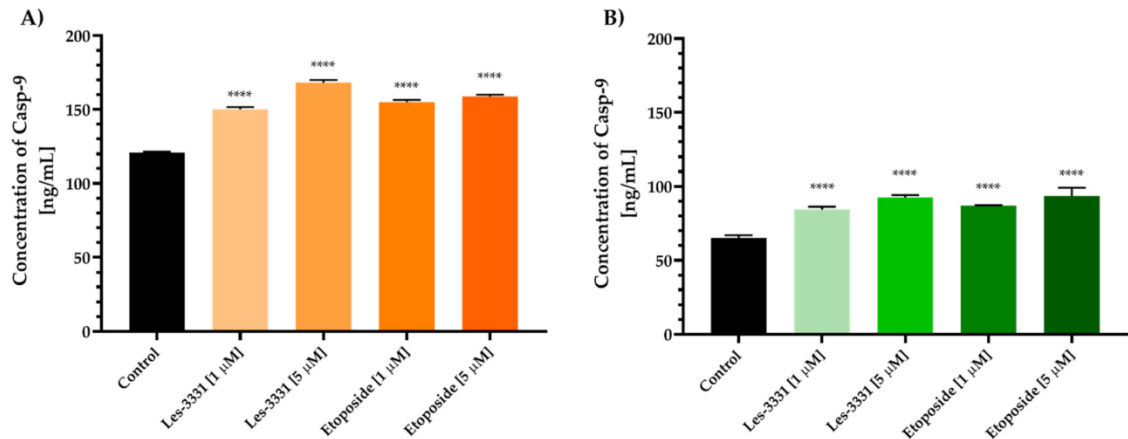


**Figure 6.** The concentration of caspase-9 in MCF-7 (A) and MDA-MB-231 (B) human breast cancer cells after 24 h incubation Les-3331 and reference drug (etoposide) at 1  $\mu$ M and 5  $\mu$ M concentration. Mean  $\pm$  SD from three independent experiments performed in duplicate is presented. Statistical significance was calculated using one-way ANOVA with Bonferroni multiple comparison test. Differences were considered statistically significant at \*\*\*\* ( $p \leq 0.0001$ ).

The involvement of Les-3331 in the extrinsic apoptotic pathway can be confirmed through the determination of its influence on caspase-8 (Casp-8) concentration.

Studies have shown that Les-3331 caused an increase in Casp-8 concentration. The most significant effect on Casp-8 level was observed after 24 h incubation of MCF-7 cells with Les-3331 (Figure 7A). Compared to the control (0.901 ng/mL), we detected 1.050 ng/mL and 1.253 ng/mL of Casp-8 in cell lysates after exposure of MCF-7 cells to 1  $\mu$ M and 5  $\mu$ M Les-3331, respectively. A similar effect of Les-3331 on Casp-8 was shown in MDA-MB-231 cancer cells (Figure 7B). After 24 h incubation of human breast cancer cells with the tested compound, the concentration of Casp-8 was 1.012 ng/mL (1  $\mu$ M Les-3331) and 1.067 ng/mL (5  $\mu$ M Les-3331), compared to the untreated control (0.828 ng/mL). The reference compound (etoposide) did not show as strong an effect on Casp-8 concentration as Les-3331. After 24 h exposure to 1  $\mu$ M etoposide, Casp-8 concentration in cell lysates was 0.812 ng/mL (MCF-7 cells) and 0.836 ng/mL (MDA-MB-231 cells), whereas after treatment with 5  $\mu$ M etoposide, we detected 0.951 ng/mL and 0.857 ng/mL of Casp-8 in MCF-7 and MDA-MB-231 cells, respectively.

The microtubule-associated protein 1A/1B light chain 3A (LC3A) and microtubule-associated protein 1A/1B light chain 3B play (LC3B) an important role in the autophagy process due to their interactions with the autophagosomal membrane [32]. To investigate the influence of Les-3331 on the autophagy process, LC3A concentration was checked.

MCF-7 and MDA-MB-231 human breast cancer cell lines were exposed to Les-3331 in two concentrations, 1 and 5  $\mu$ M, for 24 h. As demonstrated in Figure 8, a decrease in LC3A concentration was observed after the incubation of cancer cells with a newly synthesized compound and reference drugs. The concentration of LC3A in untreated control MCF-7 cells was 6.726 ng/mL. The exposure of MCF-7 to 1 and 5  $\mu$ M Les-3331 (Figure 8A) resulted in a decrease in LC3A concentration to 4.917 ng/mL and 1.127 ng/mL, respectively. Furthermore, 24 h incubation with etoposide decreased the LC3A to 4.505 ng/mL (1  $\mu$ M etoposide) and 4.582 ng/mL (5  $\mu$ M etoposide). Similarly to MCF-7 cells, incubation of MDA-MB-231 cancer cells with Les-3331 caused a reduction in LC3A concentration (Figure 8B) to 2.982 ng/mL (1  $\mu$ M Les-3331) and 1.258 ng/mL (5  $\mu$ M Les-3331), compared to the control (2.965 ng/mL). Etoposide caused a similar effect to Les-3331, decreasing the LC3A concentration to 2.800 ng/mL (1  $\mu$ M concentration) and 1.313 ng/mL (5  $\mu$ M concentration). A 24 h incubation of human breast cancer cells with 5 mM 3-Methyladenine

(3-MA), a known autophagy inhibitor, resulted in a reduction in LC3A concentration to 4.423 ng/mL (MCF-7 cells) and 0.994 ng/mL (MDA-MB-231 cells). The results obtained after incubation with Les-3331 indicated that in MCF-7 cells, 5  $\mu$ M Les-3331 showed an almost fourfold stronger inhibitory effect on LC3A concentration (1.127 ng/mL) compared to 5 mM 3-MA (4.423 ng/mL). In MDA-MB-231 cells, 5  $\mu$ M Les-3331 showed a similar effect on LC3A concentration compared to 5 mM 3-MA: 1.258 ng/mL and 0.994 ng/mL, respectively.

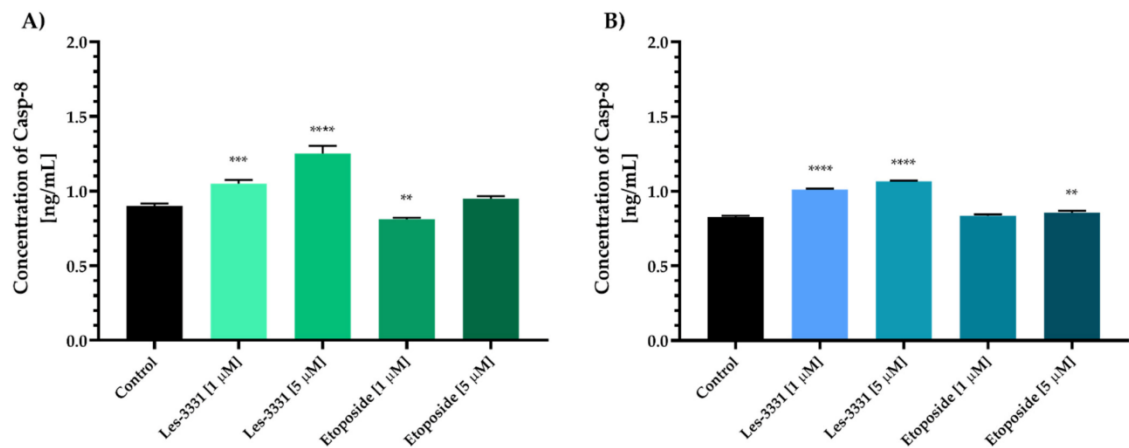


**Figure 7.** The concentration of Caspase-8 in MCF-7 (A) and MDA-MB-231 (B) human breast cancer cells after 24 h incubation with Les-3331 and reference drug (etoposide) at 1  $\mu$ M and 5  $\mu$ M concentration. Mean  $\pm$  SD from three independent experiments performed in duplicate is presented. Statistical significance was calculated using one-way ANOVA with Bonferroni multiple comparison test. Differences were considered statistically significant at: \*\* ( $p \leq 0.01$ ), \*\*\* ( $p \leq 0.001$ ), \*\*\*\* ( $p \leq 0.0001$ ).

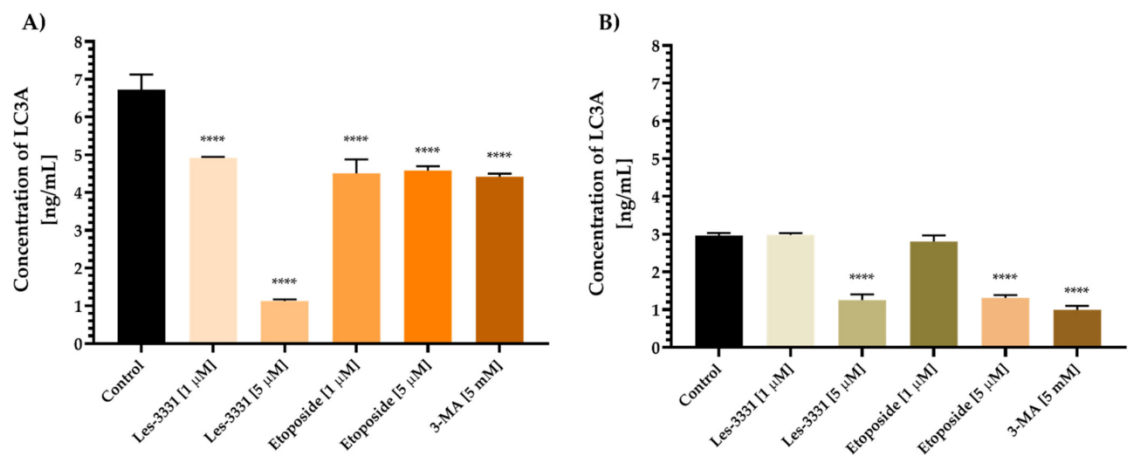


**Figure 8.** The concentration of LC3A in MCF-7 (A) and MDA-MB-231 (B) human breast cancer cells after 24 h incubation with Les-3331 and reference drug (etoposide) at 1  $\mu$ M and 5  $\mu$ M concentration. As a positive control, 3-Methyladenine (3-MA), a known autophagy inhibitor, in 5 mM concentration was used. Mean  $\pm$  SD from three independent experiments performed in duplicate is presented. Statistical significance was calculated using one-way ANOVA with Bonferroni multiple comparison test. Differences were considered statistically significant at: \*\*\*\* ( $p \leq 0.0001$ ).

In order to confirm the above results, the influence of Les-3331 on LC3B concentration was checked.

The basal concentration of LC3B in the untreated control group was 1.194 ng/mL in MCF-7 cells (Figure 9A). After 24 h incubation of the tested cells with 5  $\mu$ M Les-3331, a decrease in LC3B concentration was observed (1.002 ng/mL), while exposure of MCF-7 to 1  $\mu$ M and 5  $\mu$ M etoposide reduced LC3B levels to 1.157 ng/mL and 0.779 ng/mL. The strongest effect on LC3B was observed after incubation with 5 mM 3-MA, which reduced the LC3B levels to 0.664 ng/mL, compared to the control and newly synthesized compound. In MDA-MB-231 cells (Figure 9B), Les-3331 decreased the concentration of LC3B to 1.178 ng/mL (1  $\mu$ M concentration) and 0.996 ng/mL (5  $\mu$ M concentration), compared to the untreated control cells (1.504 ng/mL). In addition, LC3B levels were also reduced after incubation with 1  $\mu$ M and 5  $\mu$ M etoposide, to 0.784 ng/mL and 0.615 ng/mL, respectively. Exposure of MDA-MB-231 cells to 5 mM 3-MA resulted in a decreased LC3B concentration of 0.628 ng/mL.

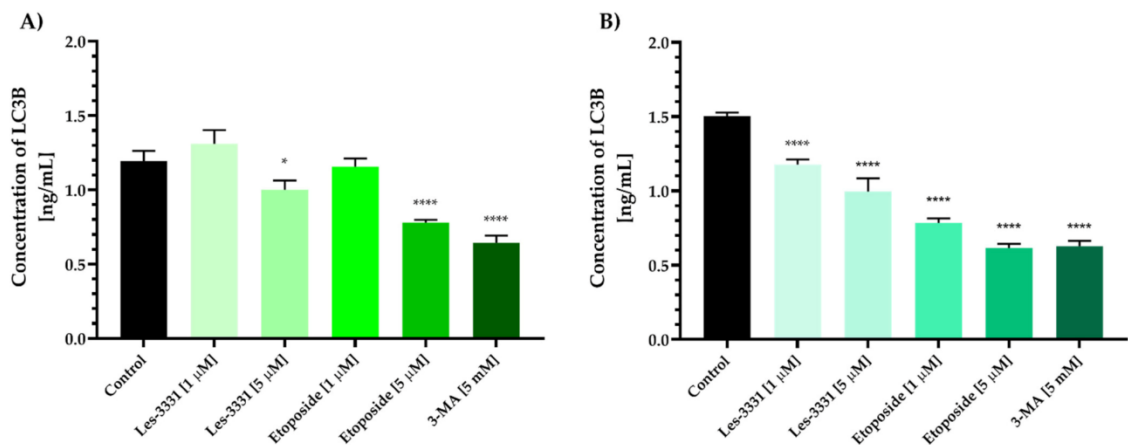


**Figure 9.** The concentration of LC3B in MCF-7 (A) and MDA-MB-231 (B) human breast cancer cells after 24 h incubation with Les-3331 and reference drug (etoposide) at 1  $\mu$ M and 5  $\mu$ M concentration. As a positive control, 3-Methyladenine (3-MA), a known autophagy inhibitor, in 5 mM concentration was used. Mean  $\pm$  SD from three independent experiments performed in duplicate is presented. Statistical significance was calculated using one-way ANOVA with Bonferroni multiple comparison test. Differences were considered statistically significant at: \* ( $p \leq 0.05$ ), \*\*\*\* ( $p \leq 0.0001$ ).

Additionally, to confirm that Les-3331 did not induce the autophagy process, its influence on Beclin-1 concentration was analyzed.

Based on the obtained results (Figure 10), we showed that 24 h exposure of human breast cancer cell lines to Les-3331 causes a decrease in Beclin-1 concentration in comparison with the control, where 7.965 ng/mL (MCF-7 cells) and 3.605 ng/mL (MDA-MB-231 cells) of Beclin-1 was detected. In MCF-7 cell lysates, a newly synthesized compound reduced the levels of analyzed protein more effectively than etoposide or 3-MA (Figure 10A). We detected 7.435 ng/mL and 3.948 ng/mL of Beclin-1 after incubation with 1  $\mu$ M and 5  $\mu$ M Les-3331, while incubation with autophagy inhibitor 3-MA resulted in a reduction in Beclin-1 concentration to 6.344 ng/mL. After exposure to etoposide, Beclin-1 concentration was 7.848 ng/mL (1  $\mu$ M concentration) and 6.686 ng/mL (5  $\mu$ M concentration). The weaker effect on Beclin-1 concentration was observed in MDA-MB-231 cells (Figure 10B). Les-3331 slightly reduced Beclin-1 levels and showed similar activity to 3-MA. Amounts of 3.007 ng/mL and 2568 ng/mL of analyzed protein were detected after exposure to 1  $\mu$ M and 5  $\mu$ M Les-3331, respectively, compared to 5 mM 3-MA (2.399 ng/mL). The level of Beclin-1 after incubation with 1  $\mu$ M etoposide is similar to the control group, which was

3.442 ng/mL, whereas the exposure to 5  $\mu$ M etoposide resulted in a decrease in Beclin-1 to 3.004 ng/mL.

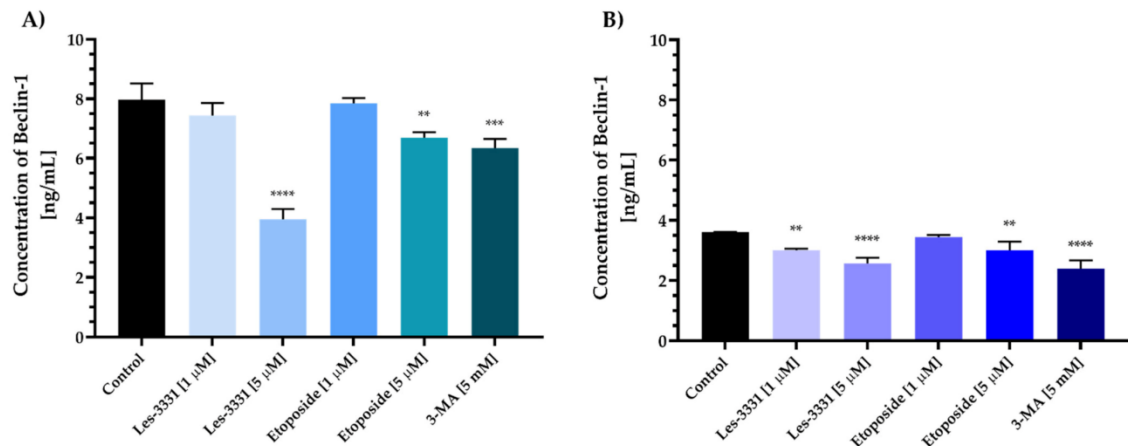


**Figure 10.** The concentration of Beclin-1 in MCF-7 (A) and MDA-MB-231 (B) human breast cancer cells after 24 h incubation with Les-3331 and reference drug (etoposide) at 1  $\mu$ M and 5  $\mu$ M concentration. As a positive control, 3-Methyladenine (3-MA), a known autophagy inhibitor, in 5 mM concentration was used. Mean  $\pm$  SD from three independent experiments performed in duplicate is presented. Statistical significance was calculated using one-way ANOVA with Bonferroni multiple comparison test. Differences were considered statistically significant at: \*\* ( $p \leq 0.01$ ), \*\*\* ( $p \leq 0.001$ ), \*\*\*\* ( $p \leq 0.0001$ ).

Topoisomerases are responsible for controlling the topology of DNA. The presence and proper functioning of these enzymes are significant for most processes, which occur in the cell. In many cancers, an increase in topoisomerase II activity is observed. The use of chemotherapeutics that inhibit enzyme activity results in DNA strand interruption and consequently leads to cell death [33]. To evaluate the effect of Les-3331 on topoisomerase II (Top II) concentration, an ELISA test was performed.

Analysis of the obtained results revealed that Les-3331 causes a reduction in topoisomerase II concentration in both tested human breast cancer cell lines (Figure 11). As shown in Figure 11A, the concentration of Top II was 0.900 ng/mL and 0.625 ng/mL after incubation of MCF-7 cells with 1  $\mu$ M and 5  $\mu$ M Les-3331, respectively, compared to the control (2.260 ng/mL of Top II). The weaker effect was demonstrated after exposure to etoposide, where the concentration of Top II was 1.587 ng/mL (1  $\mu$ M etoposide) and 1.443 ng/mL (5  $\mu$ M etoposide). In MDA-MB-231 cells (Figure 11B), the concentration of analyzed protein was 2.508 ng/mL after incubation with 1  $\mu$ M Les-3331. An almost twofold decrease in Top II concentration was observed after treatment with 5  $\mu$ M Les-3331 (1.436 ng/mL) compared to the control (2.700 ng/mL). Similarly to MCF-7 cells, the weaker effect on Top II concentration was observed after incubation with the reference drug (etoposide) in 1  $\mu$ M and 5  $\mu$ M concentrations, where 2.175 ng/mL and 2.003 ng/mL of Top II was detected, respectively.

To confirm the above results, flow cytometric analysis of topoisomerase II $\alpha$  activity using anti-topoisomerase II $\alpha$  antibody conjugated with PE was performed.

The flow cytometric analysis confirmed the inhibitory effect of Les-3331 on Top II compared to the control and reference drug (Figure 12). It was shown that after a 24 h incubation with Les-3331 in 1  $\mu$ M concentration, 34.1% of MCF-7 (Figure 12A) and 5.4% of MDA-MB-231 cells (Figure 12B) did not exhibit the presence of anti-topoisomerase II $\alpha$  antibody. In the 5  $\mu$ M concentration of the tested compound, that value went up to 49.2% (MCF-7 cells—Figure 12A) and 30.9% (MDA-MB-231 cells—Figure 12B). A weaker effect was observed in 1  $\mu$ M etoposide, where 8.6% (MCF-7) and 7.5% (MDA-MB-231) cells

without anti-topoisomerase II $\alpha$  antibody were detected. For 5  $\mu$ M etoposide, 11.8% of MCF-7 and 9.1% MDA-MB-231 without anti-topoisomerase II $\alpha$  antibody were observed (Figure 12A,B).

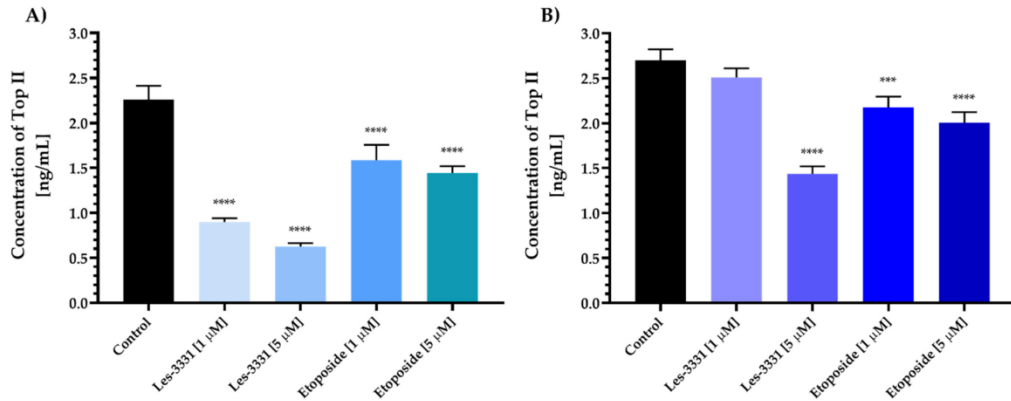


**Figure 11.** The concentration of topoisomerase II in MCF-7 (A) and MDA-MB-231 (B) human breast cancer cells after 24 h incubation with Les-3331 and reference drug (etoposide) at 1  $\mu$ M and 5  $\mu$ M concentration. Mean  $\pm$  SD from three independent experiments performed in duplicate is presented. Statistical significance was calculated using one-way ANOVA with Bonferroni multiple comparison test. Differences were considered statistically significant at \*\*\* ( $p \leq 0.001$ ), \*\*\*\* ( $p \leq 0.0001$ ).

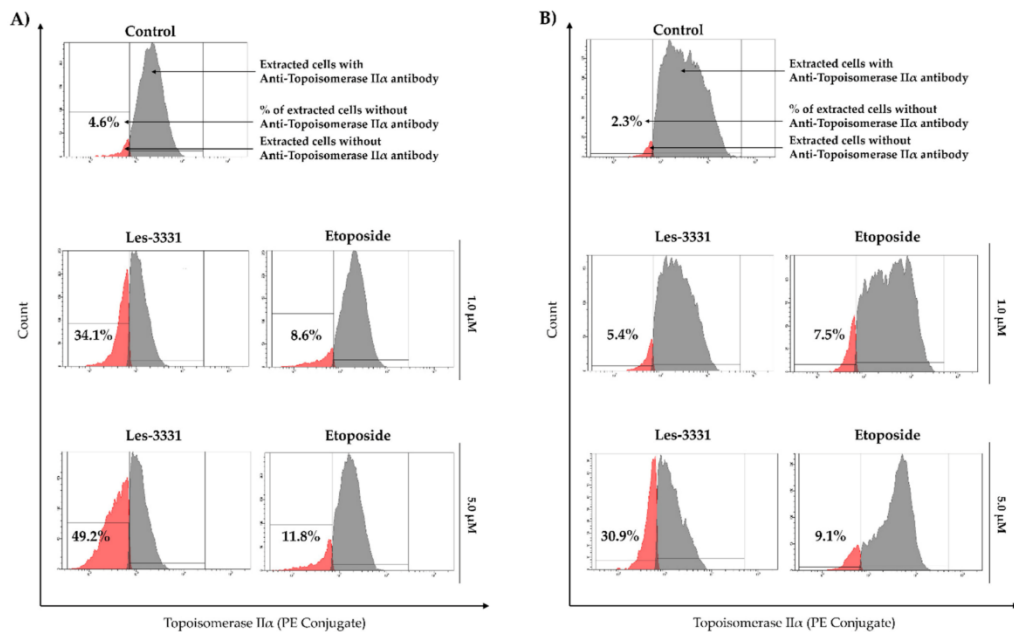


**Figure 12.** Anti-topoisomerase II $\alpha$  antibody analysis of MCF-7 (A) and MDA-MB-231 (B) human breast cancer cells after 24 h incubation with Les-3331 and reference drug (etoposide) at 1  $\mu$ M and 5  $\mu$ M concentration. The total number of human breast cancer cells without anti-topoisomerase II $\alpha$  antibody is presented as the mean percentage from three independent experiments performed in duplicate.



### 2.3. Molecular Docking Simulations

Docking simulations allow for the suggestion that Les-3331 possesses good affinity to Topoisomerase II (Table 1, Figure 13), with the nevertheless summary-binding energy being smaller compared to reference ligand etoposide. The “head” of the molecule incorporates between nucleosides DT9 and DG13 by forming a Pi–Pi-stacked lipophilic interaction. Moreover, the rhodanine core stabilized its position by the hydrogen bond with the Arg503 (2.35 Å). Valine residue of the Les-3331 also connects to DT9 and DG13 by the hydrogen bond (2.22 Å) and Pi–sigma bond (3.73 Å), respectively. Van der Waal forces and Pi–sigma interactions increase the summary energy of the Les-3331–topoisomerase II complex. The nitro group at the tail of the molecule makes two hydrogen bonds with the Ser480 (3.04 Å) and Ala481 (2.66 Å).

**Table 1.** Binding energies and inhibition constants of the Les-3331 and Topoisomerase II.

Compounds	Topoisomerase II	
	Binding Energy, kcal/mol	Inhibition Constant, Ki, nM
Les-3331	−8.79	360.70
Etoposide	−11.97	1.69

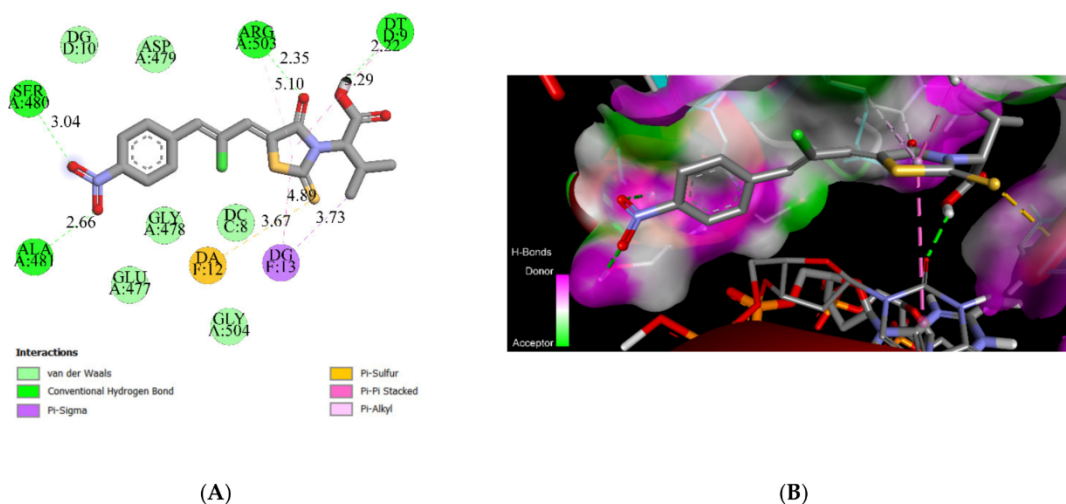


**Figure 13.** 2D (A) and 3D (B) schemes of the Les-3331–Topoisomerase II complex.

Interaction with topoisomerase II possibly contributes to the summary potency of Les-3331 anti-breast cancer activity.

### 2.4. ADME-Tox In Vitro

Les-3331 was tested in the parallel artificial membrane permeability assay (PAMPA) in order to predict its ability to passively penetrate biological membranes. The obtained data confirmed the low passive permeability of Les-3331. The calculated permeability coefficient ( $Pe = 0.96 \times 10^{-6}$  cm/s) was around sixfold lower than estimated for the one used here as highly permeable reference caffeine ( $Pe = 6.58 \times 10^{-6}$  cm/s).

The metabolic stability of Les-3331 was examined with the use of rat liver microsomes (RLMs). The obtained in vitro data were supported by the prediction of the most probable sites of metabolites performed by MetaSite 8.0.1 software (Figure S6, supporting materials). The in silico analysis showed the sulfur atom of the 2-thioxo-4-thiazolidinone moiety as the most susceptible to the metabolism site of Les-3331. The UPLC analysis after 120 min of

incubation with RLMs confirmed that around half of Les-3331 was metabolized into five metabolites M1-M5 (Figure 14). The 52% of compound remained in the reaction mixture and it was a better result than that for the used reference, the unstable drug Verapamil (37.3% remaining). The metabolic stability results were summarized in Table 2.

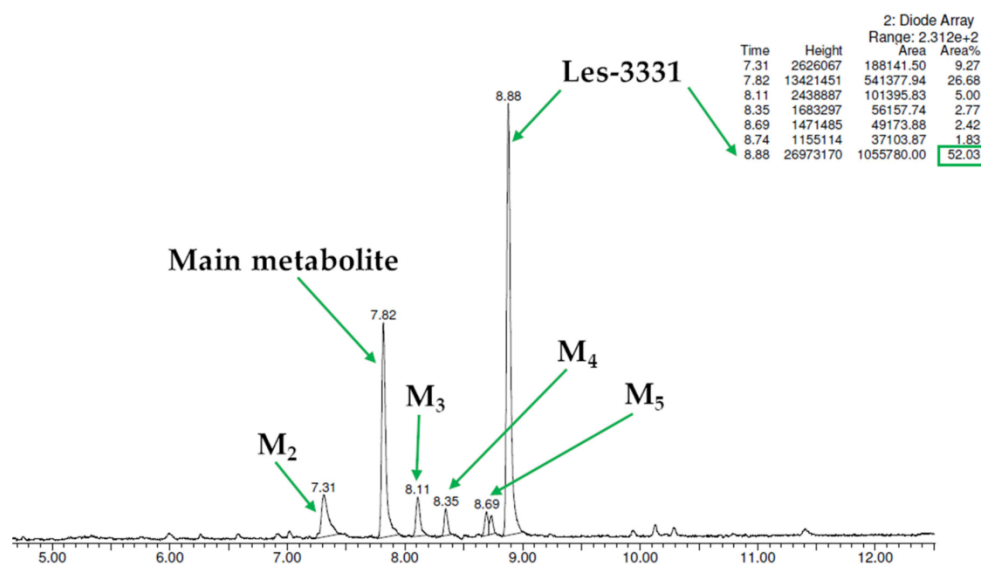


Figure 14. UPLC spectrum of the reaction mixture after 120 min incubation of Les-3331 with RLMs.

Table 2. The molecular masses of metabolites and proposed metabolic pathways of Les-3331.

Substrate	Molecular Mass ( $m/z$ )	% of the Remaining Substrate	The Retention Time of Metabolite (min.)	The Molecular Mass of the Metabolite ( $m/z$ )	Proposed Metabolic Pathway
Les-3331	427.13	52.03	Main metabolite M1 7.82	397.16.	decomposition
			M2 7.31	413.17	decomposition and hydroxylation
			M3 8.11	393.17	decomposition and dehydrogenation
			M4 8.35	397.16	decomposition
			M5 8.69	not estimated	not estimated
Verapamil *	454.60	37.28	M1 4.94	441.42	demethylation (norverapamil)
			M2 3.99	291.35	defragmentation
			M3 4.67	441.42	demethylation

\* Results revealed in previous studies using the procedure similar to Les-3331 [34].

The most probable main metabolic pathway (M1) was estimated next with the use of MS, MS/MS spectra, and in silico data (see Supplementary Materials, Figures S6–S8). The degradation of the 2-thioxo-4-thiazolidinone moiety was found as the reason for compound decomposition into metabolite M1 and the mass decreasing from  $m/z = 427.13$  to 397.16. Moreover, the molecular masses of M2-M3 suggest that the M1 metabolite was further metabolized in the reactions of hydroxylation and dehydrogenation (Table 2, Supplementary Materials: Figures S9–S13).

To predict or exclude potential drug-drug interactions (DDIs) of Les-3331, we examined its influence on cytochromes CYP3A4 and CYP2D6 activities (Figure 15). These two isoforms were chosen because together they are responsible for the metabolism of more than half of all marketed drugs. The ketoconazole and quinidine (both at 1  $\mu\text{M}$ ) were used as the reference inhibitors for CYP3A4 and CYP2D6, respectively. Interestingly, the opposite effects of Les-3331 were shown on the tested CYPs: CYP3A4 was activated at 10 and 25  $\mu\text{M}$  whereas a slight inhibition of CYP2D6 was observed at the highest Les-3331 dose 25  $\mu\text{M}$ . However, when comparing the obtained results to the strong effect of the used references, Les-3331 showed a very low risk of DDIs.

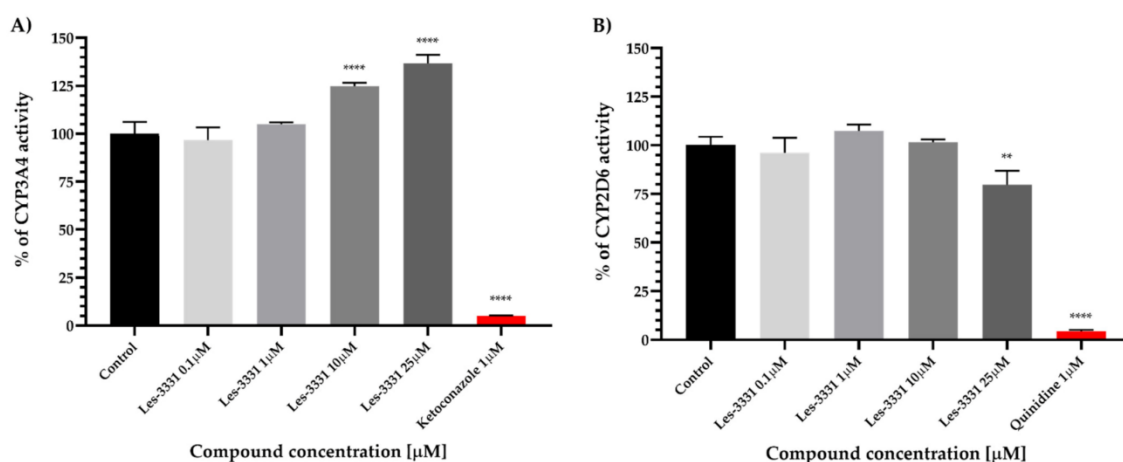


**Figure 15.** The effect of ketoconazole and Les-3331 on CYP3A4 activity (A). The effect of quinidine and Les-3331 on CYP2D6 activity (B). Statistical significance was calculated using one-way ANOVA with Bonferroni multiple comparison test. Differences were considered statistically significant at \*\* ( $p < 0.01$ ), \*\*\*\* ( $p \leq 0.0001$ ).

The mutagenicity of Les-3331 was evaluated using Ames MPF protocol with the use of *Salmonella Typhimurium* TA100. This strain is dedicated to the detection of base-pair substitution. The results were compared to the reference mutagen (4-NQO, 26.3  $\mu\text{M}$ ). According to the assay protocol, a compound can be considered non-mutagenic if the following criteria are filled: (1) the calculated binomial B-value  $\geq 0.99$  and (2) the increase in MCB  $\geq$  twofold. Results indicated that Les-3331 was not mutagenic at the concentration of 1  $\mu\text{M}$  based on both criteria. In the case of a higher concentration of 5  $\mu\text{M}$  of Les-3331, the binomial B-value was equal to the breaking point (0.99), but the probable mutagenic effect was not confirmed by the second criterion, i.e., the twofold increase in MCB was not reached by 5  $\mu\text{M}$  of Les-3331 (Figure S14, Supplementary Materials).

### 3. Discussion

Despite the progress in breast cancer therapy, researchers are still looking for novel strategies and compounds, which will be selective and effective against cancer. Chemotherapy represents one of the therapeutic approaches for the treatment of breast cancer. Other approaches include hormone therapy and targeted therapy.

Apoptosis is a cellular process that plays a pivotal role in carcinogenesis and cancer treatment [35]. Initiator caspases (e.g., caspase-2, -8, -6, -7, -8, -9, and -10) and effector caspases (e.g., caspase-3, -6, and -7) are important players in the initiation and execution of apoptosis. Downregulation, as well as abnormalities in caspase function, may be responsible for decreased programmed cell death. Shen et al. proved that downregulation of caspase-9 in patients with colorectal cancer correlates with poor prognosis [36]. Devarajan et al. demonstrated that downregulation of caspase-3 in breast cancer represents

a possible mechanism of chemoresistance [37]. Additionally, cancer cells avoid apoptosis by changing the functions of anti- or pro-apoptotic proteins [38]. Drugs, which are able to induce apoptotic pathways, are worth attention. In this study, we proved that novel Les-3331 induced apoptosis through the extrinsic pathway as well as the intrinsic pathway. It was confirmed by the analysis in Annexin V binding assay, as well as our observation of the increased caspase-8 and caspase-9 concentrations and decreased mitochondrial membrane potential in comparison with the untreated control in both MCF-7 and MDA-MB-231 breast cancer cells.

Autophagy is a multistep lysosomal degradation process, which is classified into macroautophagy, microautophagy, and chaperone-mediated autophagy [32,39]. It possesses dichotomous roles in cancer and acts as a tumor suppressor as well as a mechanism of cell survival. An important role of autophagy in cancer progression was confirmed in breast cancer. Zhao et al. proved that microtubule-associated protein 1A/1B light chain 3B (LC3B) is reconsidered as a marker of autophagy and related to shorter survival in patients with triple-negative breast carcinoma [40]. Autophagy inhibition could be an important strategy for breast cancer treatment. The inhibition of this process may be a useful tool to overcome the drug resistance and increase cancer cell death by apoptosis induction. Many compounds that are able to inhibit autophagy are being tested at different stages of preclinical and clinical trials. Chloroquine, 3-Methyladenine, SAR405, Lys05, ROC-325, Spautin-1, MM124, and MM137 are under investigation in preclinical studies [32,41]. Hydroxychloroquine, verteporfin, and clarithromycin are tested in clinical trials. The novel compound (Les-3331) tested in that study inhibited LC3A, LC3B, and Beclin-1 concentrations in both analyzed breast cancer cells. The inhibitory effect was enhanced after increasing the dose of Les-3331.

DNA topoisomerases represent important molecular targets in anticancer therapy. In this research, we proved that the novel compound had the ability to decrease topoisomerase II concentration and the inhibitory effect was stronger than the reference drug, etoposide, which was approved by the FDA for cancer treatment in 1983. Its mechanism of action is based on topoisomerase II poisoning by binding to the Top II-DNA covalent complexes [33].

The performed PAMPA showed low passive permeability of Les 3331. However, regarding the high biological activity of Les-3331 against the tested cell lines, it may be presumed that either the concentration inside the cell reached by passive mechanism is sufficient to induce the changes leading to cell death or an additional active transport mechanism may be involved in its permeability. Les-3331 also showed moderate metabolic stability with the degradation of the 2-thioxo-4-thiazolidinone moiety as the most probable metabolic pathway and no risk of DDIs. Although Les-3331 was safe at a lower concentration (1  $\mu$ M) in the AMES test, a risk of mutagenic effects at the higher one (5  $\mu$ M) was shown. These data may suggest possible interactions of Les-3331 with the DNA of the tested breast cancer cells.

## 4. Materials and Methods

### 4.1. General Information

All reagents and solvents were purchased from commercial suppliers and were used directly without further purification. *Ciminalum* was purchased from State Plant for Chemical Reagents STC of Institute for Single Crystals of the NAS of Ukraine. The elemental analyses (C, H, N) were performed using the Perkin-Elmer 2400 CHN analyzer (Perkin-Elmer, Norwalk, CT, USA). NMR spectra were determined with Varian Unity Plus 400 (400 MHz) and Bruker 170 Avance 500 (500 MHz) spectrometers, in DMSO- $d_6$  using tetramethylsilane (TMS) as an internal standard. Melting points were measured on a Kofler hot stage and are uncorrected. LC-MS was performed using a system with an Agilent 1100 Series HPLC equipped with the diode-array detector and Agilent LC\MSD SL mass-selective detector using chemical ionization at atmospheric pressure (APCI).

#### 4.2. Synthesis of 2-[5-[(Z,Z)-2-Chloro-3-(4-nitrophenyl)-2-propenylidene]-4-oxo-2-thioxothiazolidin-3-yl]-3-methylbutanoic Acid (Les-3331)

A mixture of (Z,Z)-2-chloro-3-(4-nitrophenyl)prop-2-enal (0.01 mol) and 3-methyl-2-(4-oxo-2-thioxothiazolidin-3-yl)-butanoic acid (0.01 mol) in the medium of acetic acid (20 mL) and the presence of sodium acetate (0.01 mol) was refluxed for 3 h. Obtained solid product was collected after cooling by filtration and recrystallized from the mixture DMF-ethanol (1:2). Yield: 64%, mp 240–242 °C. <sup>1</sup>H NMR (400 MHz, DMSO-*d*<sub>6</sub>): δ (ppm) 0.75 (d, 3H, *J* = 6.8 Hz, CH<sub>3</sub>), 1.19 (d, 3H, *J* = 6.4 Hz, CH<sub>3</sub>), 2.71 (m, 1H, CH), 5.17 (d, 1H, *J* = 7.6 Hz, CH), 7.77 (s, 1H, CH=), 8.02 (s, 1H, CH=), 8.04 (d, 2H, *J* = 8.8 Hz, arom.), 8.32 (d, 2H, *J* = 8.7 Hz, arom.), 13.28 (br.s, 1H, COOH). <sup>13</sup>C NMR (100 MHz, DMSO-*d*<sub>6</sub>): δ (ppm) 18.9 (CH<sub>3</sub>), 21.6 (CH<sub>3</sub>), 27.2 (CH), 62.1 (CH), 117.0 (C-Cl), 123.9, 129.6 (=CH), 131.0, 132.2 (=CH), 138.9, 139.7, 147.4, 166.6 (C=O), 168.5 (COOH), 194.2 (C=S). LCMS (ESI): *m/z* 426.9/428.9 (100%, [M + H]<sup>+</sup>). Anal. Calc. for C<sub>17</sub>H<sub>15</sub>ClN<sub>2</sub>O<sub>5</sub>S<sub>2</sub>: C 47.83%; H 3.54%; N 6.56%. Found: C 47.90%; H 3.45%; N 6.65%.

#### 4.3. Crystal Structure Determination of Les-3331\*DMF

Single-crystal X-ray data were collected on Rigaku SuperNova, Single source at off-set/far, Atlas [42], using graphite-monochromated CuKα radiation (1.54184 Å). Intensity data were corrected for the Lorentz, polarization, and absorption effects [42]. The structure was solved by the dual-space algorithm (SHELXT) [43,44] and refined against F2 for all data (SHELXL) [44,45]. The position of the H atom bonded to the O atom was obtained from the difference Fourier map and was refined freely. The remaining H atoms were positioned geometrically and were refined using a riding model, with C–H: 0.96 Å (CH<sub>3</sub>), 0.98 Å (Csp<sup>3</sup>H), 0.95 Å (Csp<sup>2</sup>H), and *U*<sub>iso</sub>(H) = 1.2*U*<sub>eq</sub>(C) or 1.5*U*<sub>eq</sub>(C) for methyl H atoms. The methyl groups were refined as rigid groups, which were allowed to rotate. Software used to prepare materials for publication was WINGX [46] and PLATON [47] programs. The molecular illustrations were drawn using ORTEP for Windows [46].

The deposition number CCDC-2129659 for Les-3331 contains supplementary crystallographic data for this paper. These data can be obtained free of charge via [www.ccdc.cam.ac.uk/conts/retrieving.html](http://www.ccdc.cam.ac.uk/conts/retrieving.html), (accessed on 16 March 2022) or from the Cambridge Crystallographic Data Centre, 12, Union Road, Cambridge CB2 1EZ, UK; Fax: +44 1223 336033).

#### 4.4. Cell Culture

Cell culture MCF-7, MDA-MB-231 human breast cancer cells, and fibroblasts skin cells were purchased from the ATCC—American Type Culture Collection. All cell lines were maintained in DMEM (Corning, Kennebunk, ME, USA). The medium was supplemented with 10% fetal bovine serum—FBS (Eurx, Gdansk, Poland) and 1% antimicrobial substances: penicillin–streptomycin (Corning, Kennebunk, ME, USA). The incubator asserted appropriate growth conditions required for these cell lines: 5% of CO<sub>2</sub>, at 37 °C, with the humidity between 90–95%. Cells were seeded in 100 mm round dishes. An amount of 0.05% trypsin containing 0.02% EDTA (Corning, Kennebunk, ME, USA) and phosphate-buffered saline (PBS) without calcium and magnesium (Corning, Kennebunk, ME, USA) was used to detach cells from a plate once 80–90% cell confluence was achieved. In the next step, cells were reseeded in six-well plates (density—5 × 10<sup>5</sup> of cells per well) in 1 mL of DMEM after a 24 h incubation used in the presented tests.

#### 4.5. Cell Viability Assay

To examine the effect of Les-3331 on cell viability, the MTT assay was performed. Etoposide (Sigma-Aldrich, St Louis, MO, USA) was used as a reference drug. Cells, seeded in six-well plates, were incubated for 24 h with serial dilutions of the tested compound and reference drug in duplicates. In the next step, the liquid was aspirated above the cells and cells were washed three times with PBS. Thereafter, 50 µL of 5 mg/mL of MTT (Sigma-Aldrich, St Louis, MO, USA) was added to 1 mL of PBS. After the required time, the MTT solution was removed and resulting formazan crystals were dissolved in DMSO (Sigma-

Aldrich, St Louis, MO, USA). The absorbance was measured using Spectrophotometer UV-VIS Helios Gamma (Unicam/ThermoFisher Scientific Inc., Waltham, MA, USA) at a wavelength of 570 nm. The obtained absorbance in untreated control cells was taken as 100%, while the survival of the cells incubated with tested compounds presented as a percentage of the control value [48].

#### 4.6. [<sup>3</sup>H]-Thymidine Incorporation Assay

The antiproliferative properties of the newly synthesized compound were investigated through the [<sup>3</sup>H]-thymidine incorporation assay, as described in the literature [49]. Cells culture was exposed to various concentrations of Les-3331 acid and reference drug for 24 h. Thereafter, cells were washed with PBS and 1 mL of fresh medium was added to each well. Then, 0.5 µCi of radioactive [<sup>3</sup>H]-thymidine was appended, and the incubation continued for four hours. After the following incubation, the liquid was aspirated and the plate was placed on ice. Cells were washed twice with 1 mL of 0.05 M Tris-HCl buffer comprising 0.11 M NaCl, then twice after that with 1 mL of 5% TCA acid (Stanlab, Lublin, Poland). Finally, the cells were dissolved with 1 mL of 0.1 M NaOH with 1% SDS (Sigma-Aldrich, St. Louis, MO, USA) at room temperature (RT). The resulting cell lysates were transferred into scintillation vials containing 2 mL of scintillation fluid. The radioactivity was determined using Scintillation Counter 1900 TR, TRI-CARB (Packard, Perkin Elmer, Inc., San Jose, CA, USA). The intensity of DNA biosynthesis in cells was expressed in dpm of radioactive thymidine incorporated in the DNA. The radioactivity observed in untreated control cells was taken as 100%. Values from the tested compounds were expressed as a percentage of the control value [41].

#### 4.7. Flow Cytometry Assessment of Annexin V Binding

The effect of Les-3331 and reference drug on the induction of apoptosis process in human breast cancer cell lines was evaluated using a flow cytometer (BD FACSCanto II, Becton Dickinson Biosciences Systems, San Jose, CA, USA) and Annexin V binding Apoptosis Detection Kit II (BD Biosciences, San Diego, CA, USA). The Les-3331 and reference drug were used in 1 µM and 5 µM concentrations. The test was carried out after 24 h incubation with the tested compounds according to the manufacturer's protocol and was previously described by our research group [50]. Analysis of the obtained results was performed using FACSDiva software (version 6.1.3, BD Biosciences Systems, San Jose, CA, USA). The equipment was calibrated with BD Cytometer Setup and Tracking Beads (BD Biosciences, San Diego, CA, USA).

#### 4.8. Mitochondrial Membrane Potential ( $\Delta\Psi_m$ ) Analysis

The JC-1 MitoScreen kit (BD Biosciences, San Diego, CA, USA) was used for the mitochondrial membrane potential ( $\Delta\Psi_m$ ) analysis. The assay was performed using a flow cytometer (BD FACSCanto II, Becton Dickinson Biosciences Systems, San Jose, CA, USA). The Les-3331 and reference drug were used in 1 µM and 5 µM concentrations. After 24 h incubation with tested compounds, the assay was performed as described in the literature [51]. Analysis of the obtained results was performed using FACSDiva software (version 6.1.3, BD Biosciences Systems, San Jose, CA, USA). The equipment was calibrated with BD Cytometer Setup and Tracking Beads (BD Biosciences, San Diego, CA, USA).

#### 4.9. Determination of Caspase-8 and Caspase-9, LC3A, LC3B, Beclin-1, and Topoisomerase II Concentration

High sensitivity assay kits (EIAab Science Co., Ltd., Wuhan, China; Abcam plc., Cambridge, United Kingdom; Cloud-Clone Corp., Katy, TX, USA) were used to determine the concentrations of selected proteins in cell lysates after 24 h incubation with novel compound and reference drug in 1 µM and 5 µM concentrations. In brief, after trypsinization, cells were washed thrice with cold PBS and centrifuged at 1000 × g for 5 min at 4 °C. Then, cells ( $1.5 \times 10^6$ ) were suspended in lysis buffer for whole-cell lysates. After the second

centrifugation, cellular supernatants were frozen immediately at  $-70^{\circ}\text{C}$ . Untreated cancer cells were taken as a control.

The microtiter plates provided in the kits were pre-coated with an antibody specific to the analyzed antigen. The tests were carried out according to the manufacturer's protocols.

#### 4.10. Molecular Docking Studies

Topoisomerase II (PDB code 3QX3) was chosen as target protein for in silico simulations. During the preparing procedures all ligands, cofactors, and water molecules were removed, polar hydrogen atoms were added and nonpolar hydrogen atoms were merged. Moreover, Kollman charges were added and spread over the residues in the prepared pdbqt files of the target protein. For in silico simulations, we used the obtained 3D structure of the Les-3331 obtained from X-ray structure crystallography. Auto Dock Tool was used for calculation of the binding free energy, which includes all types of interaction (hydrogen bonds, lipophilic interaction, Van Der Waals force, etc.) and estimated Inhibition Constant, Ki. Lamarckian Genetic Algorithm (LGA) parameters were used as a default, which includes 50 runs, 300 populations, 2,500,000 energy evaluations, rate of Gene Mutation 0.02, and rate of Crossover 0.8. [52]. Validations of the selected docking were performed using the ability to render the position of reference ligands from X-ray spectrums (RMSD had to be less than 2). Visualization and interpretation of obtained data were performed by the Discovery Studio Visualizer v.21.1.0.20298®.

#### 4.11. Flow Cytometric Analysis of Anti-Topoisomerase II $\alpha$ antibody

To confirm the ELISA results, flow cytometric analysis of Top II activity using an anti-topoisomerase II $\alpha$  antibody conjugated with phycoerythrin (PE) was performed. The Les-3331 and etoposide were used at 1  $\mu\text{M}$  and 5  $\mu\text{M}$  concentrations. Cancer cells were incubated for 24 h with tested compounds and the assay was carried out in accordance with the manufacturer's protocol. Briefly, cells were centrifuged and resuspended in 4% formaldehyde. Then, cells were incubated at RT for 15 min and subsequently washed with excess PBS and centrifuged. Thereafter, ice-cold 90% methanol was added to the cells and they were incubated for 1 h in an ice bath. Next, cells were washed with excess PBS and centrifuged again. In the meantime, the primary antibody was diluted (1:100) in PBS. Then, cells were resuspended in the prepared primary antibody (100  $\mu\text{L}$ ) and incubated at RT, protected from light, for 1 h. Finally, cells were washed and resuspended in PBS (300  $\mu\text{L}$ ). The prepared samples were measured immediately. Analysis of the obtained results was performed using a flow cytometer (BD FACSCanto II, Becton Dickinson Biosciences Systems, San Jose, CA, USA) and FACSDiva software (v6.1.3, BD Biosciences Systems, San Jose, CA, USA). The equipment was calibrated with BD Cytometer Setup and Tracking Beads (BD Biosciences, San Diego, CA, USA).

#### 4.12. ADME-Tox In Vitro

All in vitro assays used for the evaluation of Les-3331 ADME-Tox parameters were described previously [34,53]. In brief, for the determination of permeability, Pre-coated PAMPA Plate System Gentest™ was purchased from Corning (Tewksbury, MA, USA). The solutions of Les-3331 and the reference caffeine (200  $\mu\text{M}$ ) were prepared in PBS buffer (pH = 7.4). PAMPA plates with compounds added to the donor wells were incubated for 5 h at RT. UPLC-MS Waters ACQUITY—TQD system with the TQ Detector (Waters, Milford, MI, USA) was used next for determination of compounds concentrations in donor and acceptor wells, which were required for calculation of permeability coefficient  $Pe$  according to formulas provided by the manufacturer.

The metabolic stability was estimated using rat liver microsomes (RLMs) obtained from Sigma-Aldrich (St. Louis, MO, USA). Les-3331 was incubated in the presence of RLMs and NADPH Regeneration System (Promega, Madison, WI, USA) in Tris-HCl buffer (pH 7.4) for 120 min. Cold ethanol was added next to stop the reaction. The reaction mixture was centrifuged. The aforementioned UPLC-MS device was used to analyze the

supernatant. MS/MS ion fragment analyses were performed for Les-3331 and the main metabolite. The in silico prediction of possible Les-3331 metabolic pathways was performed by MetaSite 8.0.1. Software (Molecular Discovery Ltd., Hertfordshire, UK).

For investigation of potential drug-drug interactions, the luminescent CYP3A4 and CYP2D6 P450-Glo assays obtained from Promega® (Madison, WI, USA) were used. Les-3331 was tested in triplicate at the final concentrations from 0.01 to 25 µM according to the protocols provided by Promega®. The reference inhibitors were tested at 1 µM. The luminescent signal was measured using a microplate reader, EnSpire PerkinElmer (Waltham, MA, USA).

The mutagenicity was evaluated using Ames microplate fluctuation protocol (MPF) from Xenometrix (Allschwil, Switzerland). The applied *Salmonella Typhimurium* TA100 strain was enabled to detect base-pair substitution (hisG46 mutation, for which target is GGG). Les-3331 was tested independently in two final concentrations, 1 and 5 µM, in triplicate. The reference mutagen 4-NQO was tested at 26.3 µM. The occurrence of revertants was visualized using pH indicator dye, which was present in the bacterial medium. The color changes from violet to yellow were confirmed using measurements of absorbance with a microplate reader, EnSpire, at 420 nm. According to the protocols and data sheets provided by Xenometrix, the medium control baseline (MCB) was calculated first, which refers to the number of revertants observed in the control (growth medium + 1% DMSO) plus standard deviation. Next, the Binomial B-value was calculated for tested compounds which indicates the probability that spontaneous mutations occurred. The fold increase  $\geq 2$  over the MCB and/or Binomial B-value  $\geq 0.99$  are considered as the mutagen alert.

#### 4.13. Statistical Analysis

The obtained results are presented as mean  $\pm$  standard deviation (SD) from three independent experiments performed in duplicate. The statistical analysis was performed using GraphPad Prism version 6.0 (San Diego, CA, USA). The one-way ANOVA with Bonferroni multiple comparison tests was used to show differences between the control and the cancer cells exposed to varying concentrations of novel compound and reference drug. Statistically significant differences were defined at: \* ( $p \leq 0.05$ ), \*\* ( $p \leq 0.01$ ), \*\*\* ( $p \leq 0.001$ ), \*\*\*\* ( $p \leq 0.0001$ ).

## 5. Conclusions

We have shown that novel Les-3331 is cytotoxic towards both tested breast cancer cell lines and induce the extrinsic and intrinsic apoptotic pathways. Furthermore, Les-3331 caused a decrease in LC3A, LC3B, and Beclin-1 concentration. Les-3331 caused a reduction in Top II concentration in both tested human breast cancer cell lines. Furthermore, the most probable metabolic pathways for Les-3331 were found in the model in vitro. In general, this agent displayed a moderate ADMET profile in vitro, including no DDIs risk, and some probability of mutagenic effects observed at the higher concentration, but not at the lower one (1 µM). All data proved that Les-3331 is a promising compound, representing multitargeted potential in breast cancer therapy. The obtained results constitute the basis for further in vivo investigation.

**Supplementary Materials:** The following supporting information can be downloaded at: <https://www.mdpi.com/article/10.3390/ijms23084091/s1>.

**Author Contributions:** Conceptualization, A.B., R.L., K.B. (Krzysztof Bielawski) and A.G. (Agnieszka Gornowicz); methodology, K.B. (Kamila Buzun), A.K.-D., A.G. (Agnieszka Gornowicz), R.C., G.L. and R.L.; investigation, K.B. (Kamila Buzun), R.L., A.K.-D., A.G. (Andrzej Gzella), A.G. (Agnieszka Gornowicz), R.C., G.L. and A.O.-M.; writing—original draft preparation, K.B. (Kamila Buzun), A.G. (Agnieszka Gornowicz), G.L. and R.L.; writing—review and editing, A.B., R.L., K.B. (Krzysztof Bielawski) and J.H.; supervision, A.B., R.L. and J.H. All authors have read and agreed to the published version of the manuscript.

**Funding:** This work was supported by European Union funds (project No. POWR.03.02.00-00-I051/16-00), grant No. 02/IMSD/G/2019, Medical University of Białystok, grant No. SUB/2/DN/22/002/2229, grant



0121U100690 of Ministry of Healthcare of Ukraine, and grant 2020.02/0035 of National Research Foundation of Ukraine.

**Institutional Review Board Statement:** Not applicable.

**Informed Consent Statement:** Not applicable.

**Data Availability Statement:** The datasets used and/or analyzed during the current study are available from the corresponding author on reasonable request.

**Acknowledgments:** The authors would like to thank all the brave defenders of Ukraine who made the finalization of this article possible.

**Conflicts of Interest:** The authors declare no conflict of interest.

**Sample Availability:** A sample of the compound is available from the authors.

### Abbreviations

3-MA	3-Methyladenine
ANOVA	analysis of variance
BC	breast cancer
Casp-8	caspase-8
Casp-9	caspase-9
DDIs	drug-drug interactions
ELISA	enzyme-linked immunosorbent assay
ER	estrogen receptor
FBS	fetal bovine serum
LC3A	microtubule-associated protein 1A/1B light chain 3A
LC3B	microtubule-associated protein 1A/1B light chain 3B
MCB	medium control baseline
MPF	microplate fluctuation protocol
MTT	3-(4,5-dimethylthiazol-2-yl)-2,5-diphenyl-2H-tetrazolium bromide
PAMPA	parallel artificial membrane permeability assay
PBS	phosphate-buffered saline
PE	phycoerythrin
PR	progesterone receptor
RLMs	rat liver microsomes
RT	room temperature
TCA	trichloroacetic acid
TMS	tetramethylsilane
TNBC	triple-negative breast cancer
Top II	topoisomerase II
UPLC	ultra-performance liquid chromatography
WHO	World Health Organization
$\Delta\Psi_m$	mitochondrial membrane potential

### References

1. Bray, F.; Laversanne, M.; Weiderpass, E.; Soerjomataram, I. The ever-increasing importance of cancer as a leading cause of premature death worldwide. *Cancer* **2021**, *127*, 3029–3030. [CrossRef] [PubMed]
2. World Health Organization—Breast Cancer. Available online: <https://www.who.int/news-room/fact-sheets/detail/breast-cancer> (accessed on 19 January 2022).
3. Loibl, S.; Poortmans, P.; Morrow, M.; Denkert, C.; Curigliano, G. Breast cancer. *Lancet* **2021**, *397*, 1750–1769. [CrossRef]
4. Harbeck, N.; Penault-Llorca, F.; Cortes, J.; Gnant, M.; Houssami, N.; Poortmans, P.; Ruddy, K.; Tsang, J.; Cardoso, F. Breast cancer. *Nat. Rev. Dis. Primers* **2019**, *5*, 66. [CrossRef] [PubMed]
5. Waks, A.G.; Winer, E.P. Breast Cancer Treatment: A Review. *JAMA* **2019**, *321*, 288–300. [CrossRef]
6. Brown, F.C. 4-Thiazolidinones. *Chem. Rev.* **1961**, *61*, 463–521. [CrossRef]
7. Newkome, G.R.; Nayak, A. 4-Thiazolidinones. In *Advances in Heterocyclic Chemistry*; Katritzky, A.R., Boulton, A.J., Eds.; Academic Press: Cambridge, MA, USA, 1980; Volume 25, pp. 83–112.
8. Singh, S.P.; Parmar, S.S.; Raman, K.; Stenberg, V.I. Chemistry and biological activity of thiazolidinones. *Chem. Rev.* **1981**, *81*, 175–203. [CrossRef]

9. Tomašić, T.; Peterlin Mašič, L. Rhodanine as a scaffold in drug discovery: A critical review of its biological activities and mechanisms of target modulation. *Expert Opin. Drug Discov.* **2012**, *7*, 549–560. [[CrossRef](#)]
10. Tripathi, A.C.; Gupta, S.J.; Fatima, G.N.; Sonar, P.K.; Verma, A.; Saraf, S.K. 4-Thiazolidinones: The advances continue. *Eur. J. Med. Chem.* **2014**, *72*, 52–77. [[CrossRef](#)]
11. Lesyk, R.B.; Zimenkovsky, B.S. 4-Thiazolidinones: Centenarian history, current status and perspectives for modern organic and medicinal chemistry. *Curr. Org. Chem.* **2004**, *8*, 1547–1577. [[CrossRef](#)]
12. Lesyk, R.B.; Zimenkovsky, B.S.; Kaminsky, D.V.; Kryshchshyn, A.P.; Havryluk, D.Y.; Atamanyuk, D.V.; Subtel'na, I.Y.; Khylyuk, D.V. Thiazolidinone motif in anticancer drug discovery. Experience of DH LNMU medicinal chemistry scientific group. *Biopolym. Cell* **2011**, *27*, 107–117. [[CrossRef](#)]
13. Tomasic, T.; Masic, P.L. Rhodanine as a privileged scaffold in drug discovery. *Curr. Med. Chem.* **2009**, *16*, 1596–1629. [[CrossRef](#)] [[PubMed](#)]
14. Kaminsky, D.; Kryshchshyn, A.; Lesyk, R. 5-Ene-4-thiazolidinones—An efficient tool in medicinal chemistry. *Eur. J. Med. Chem.* **2017**, *140*, 542–594. [[CrossRef](#)] [[PubMed](#)]
15. Tahmasvand, R.; Bayat, P.; Vahdaniparast, S.M.; Dehghani, S.; Kooshafar, Z.; Khaleghi, S.; Almasirad, A.; Salimi, M. Design and synthesis of novel 4-thiazolidinone derivatives with promising anti-breast cancer activity: Synthesis, characterization, in vitro and in vivo results. *Bioorg. Chem.* **2020**, *104*, 104276. [[CrossRef](#)] [[PubMed](#)]
16. Jain, A.K.; Vaidya, A.; Ravichandran, V.; Kashaw, S.K.; Agrawal, R.K. Recent developments and biological activities of thiazolidinone derivatives: A review. *Bioorg. Med. Chem.* **2012**, *20*, 3378–3395. [[CrossRef](#)]
17. Sohda, T.; Momose, Y.; Meguro, K.; Kawamatsu, Y.; Sugiyama, Y.; Ikeda, H. Studies on antidiabetic agents. Synthesis and hypoglycemic activity of 5-[4-(pyridylalkoxy)benzyl]-2,4-thiazolidinediones. *Arzneimittelforschung* **1990**, *40*, 37–42. [[CrossRef](#)]
18. Charlier, C.; Michaux, C. Dual inhibition of cyclooxygenase-2 (COX-2) and 5-lipoxygenase (5-LOX) as a new strategy to provide safer non-steroidal anti-inflammatory drugs. *Eur. J. Med. Chem.* **2003**, *38*, 645–659. [[CrossRef](#)]
19. Ramirez, M.A.; Borja, N.L. Epalrestat: An aldose reductase inhibitor for the treatment of diabetic neuropathy. *Pharmacotherapy* **2008**, *28*, 646–655. [[CrossRef](#)]
20. Elkaeed, E.B.; Salam, H.A.A.E.; Sabt, A.; Al-Ansary, G.H.; Eldehna, W.M. Recent advancements in the development of anti-breast cancer synthetic small molecules. *Molecules* **2021**, *26*, 7611. [[CrossRef](#)]
21. Lesyk, R. Drug design: 4-thiazolidinones applications. Part 1. Synthetic routes to the drug-like molecules. *J. Med. Sci.* **2020**, *89*, 33–49. [[CrossRef](#)]
22. Lesyk, R. Drug design: 4-thiazolidinones applications. Part 2. Pharmacological profiles. *J. Med. Sci.* **2020**, *89*, 132–141. [[CrossRef](#)]
23. Kaminsky, D.; Kryshchshyn, A.; Lesyk, R. Recent developments with rhodanine as a scaffold for drug discovery. *Expert Opin. Drug Discov.* **2017**, *12*, 1233–1252. [[CrossRef](#)] [[PubMed](#)]
24. Buzun, K.; Kryshchshyn-Dylevych, A.; Senkiv, J.; Roman, O.; Gzella, A.; Bielawski, K.; Bielawska, A.; Lesyk, R. Synthesis and anticancer activity evaluation of 5-[2-chloro-3-(4-nitrophenyl)-2-propenylidene]-4-thiazolidinones. *Molecules* **2021**, *26*, 3057. [[CrossRef](#)] [[PubMed](#)]
25. Subtel'na, I.; Atamanyuk, D.; Szymańska, E.; Kieć-Kononowicz, K.; Zimenkovsky, B.; Vasylenko, O.; Gzella, A.; Lesyk, R. Synthesis of 5-arylidene-2-amino-4-azolones and evaluation of their anticancer activity. *Bioorg. Med. Chem.* **2010**, *18*, 5090–5102. [[CrossRef](#)] [[PubMed](#)]
26. Panchuk, R.; Chumak, V.; Fil, M.R.; Havrylyuk, D.; Zimenkovsky, B.S.; Lesyk, R.; Stoika, R.S. Study of molecular mechanisms of proapoptotic action of novel heterocyclic 4-thiazolidone derivatives. *Biopolym. Cell* **2012**, *28*, 121–128. [[CrossRef](#)]
27. Slepikas, L.; Chiriano, G.; Perozzo, R.; Tardy, S.; Kranjc, A.; Patthey-Vuadens, O.; Ouertatani-Sakouhi, H.; Kicka, S.; Harrison, C.F.; Scrignari, T.; et al. In silico driven design and synthesis of Rhodanine derivatives as novel antibacterials targeting the enoyl reductase InhA. *J. Med. Chem.* **2016**, *59*, 10917–10928. [[CrossRef](#)] [[PubMed](#)]
28. Jagiello-Gruszfeld, A.I.; Meluch, M.; Kunkiel, M.; Gorniak, A.; Majstrak-Hulewska, A.; Gorska, K.; Konieczna, A.; Nowecki, Z. Oral etoposide in heavily pre-treated metastatic breast cancer: A retrospective study. *J. Clin. Oncol.* **2021**, *39*, e13070. [[CrossRef](#)]
29. Hu, N.; Zhu, A.; Si, Y.; Yue, J.; Wang, X.; Wang, J.; Ma, F.; Xu, B.; Yuan, P. A Phase II, Single-Arm Study of Apatinib and Oral Etoposide in Heavily Pre-Treated Metastatic Breast Cancer. *Front. Oncol.* **2021**, *10*, 3246. [[CrossRef](#)]
30. Giannone, G.; Milani, A.; Ghisoni, E.; Genta, S.; Mittica, G.; Montemurro, F.; Valabrega, G. Oral etoposide in heavily pre-treated metastatic breast cancer: A retrospective series. *Breast* **2018**, *38*, 160–164. [[CrossRef](#)]
31. Gornowicz, A.; Kałuża, Z.; Bielawska, A.; Gabryel-Porowska, H.; Czarnomysy, R.; Bielawski, K. Cytotoxic efficacy of a novel dinuclear platinum(II) complex used with anti-MUC1 in human breast cancer cells. *Mol. Cell. Biochem.* **2014**, *392*, 161–174. [[CrossRef](#)]
32. Buzun, K.; Gornowicz, A.; Lesyk, R.; Bielawski, K.; Bielawska, A. Autophagy modulators in cancer therapy. *Int. J. Mol. Sci.* **2021**, *22*, 5804. [[CrossRef](#)]
33. Buzun, K.; Bielawska, A.; Bielawski, K.; Gornowicz, A. DNA topoisomerases as molecular targets for anticancer drugs. *J. Enzym. Inhib. Med.* **2020**, *35*, 1781–1799. [[CrossRef](#)] [[PubMed](#)]
34. Sniecikowska, J.; Gluch-Lutwin, M.; Bucki, A.; Więckowska, A.; Siwek, A.; Jastrzebska-Wiesek, M.; Partyka, A.; Wilczyńska, D.; Pytka, K.; Latacz, G.; et al. Discovery of novel pERK1/2- or  $\beta$ -arrestin-preferring 5-HT<sub>1A</sub> receptor-biased agonists: Diversified therapeutic-like versus side effect profile. *J. Med. Chem.* **2020**, *63*, 10946–10971. [[CrossRef](#)] [[PubMed](#)]
35. Wong, R.S.Y. Apoptosis in cancer: From pathogenesis to treatment. *J. Exp. Clin. Cancer Res.* **2011**, *30*, 87. [[CrossRef](#)] [[PubMed](#)]

36. Shen, X.-G.; Wang, C.; Li, Y.; Wang, L.; Zhou, B.; Xu, B.; Jiang, X.; Zhou, Z.-G.; Sun, X.-F. Downregulation of caspase-9 is a frequent event in patients with stage II colorectal cancer and correlates with poor clinical outcome. *Colorectal Dis.* **2010**, *12*, 1213–1218. [[CrossRef](#)] [[PubMed](#)]
37. Devarajan, E.; Sahin, A.A.; Chen, J.S.; Krishnamurthy, R.R.; Aggarwal, N.; Brun, A.-M.; Sapino, A.; Zhang, F.; Sharma, D.; Yang, X.-H.; et al. Down-regulation of caspase 3 in breast cancer: A possible mechanism for chemoresistance. *Oncogene* **2002**, *21*, 8843–8851. [[CrossRef](#)]
38. Fernald, K.; Kurokawa, M. Evading apoptosis in cancer. *Trends Cell Biol.* **2013**, *23*, 620–633. [[CrossRef](#)]
39. Amaravadi, R.K.; Kimmelman, A.C.; Debnath, J. Targeting autophagy in cancer: Recent advances and future directions. *Cancer Discov.* **2019**, *9*, 1167–1181. [[CrossRef](#)]
40. Zhao, H.; Yang, M.; Zhao, J.; Wang, J.; Zhang, Y.; Zhang, Q. High expression of LC3B is associated with progression and poor outcome in triple-negative breast cancer. *Med. Oncol.* **2013**, *30*, 475. [[CrossRef](#)]
41. Gornowicz, A.; Szymanowska, A.; Mojzych, M.; Bielawski, K.; Bielawska, A. The effect of novel 7-methyl-5-phenyl-pyrazolo[4,3-*e*]tetrazolo[4,5-*b*][1,2,4]triazine sulfonamide derivatives on apoptosis and autophagy in DLD-1 and HT-29 colon cancer cells. *Int. J. Mol. Sci.* **2020**, *21*, 5221. [[CrossRef](#)]
42. CrysAlis. *PRO, Version 1.171.41.110a*; Rigaku Oxford Diffraction: Yarnton, UK, 2021.
43. Sheldrick, G. SHELXT-Integrated space-group and crystal-structure determination. *Acta Crystallogr. A* **2015**, *71*, 3–8. [[CrossRef](#)]
44. Dolomanov, O.V.; Bourhis, L.J.; Gildea, R.J.; Howard, J.A.K.; Puschmann, H. OLEX2: A complete structure solution, refinement and analysis program. *J. Appl. Crystallogr.* **2009**, *42*, 339–341. [[CrossRef](#)]
45. Sheldrick, G. Crystal structure refinement with SHELXL. *Acta Crystallogr. C* **2015**, *71*, 3–8. [[CrossRef](#)] [[PubMed](#)]
46. Farrugia, L.J. WinGX and ORTEP for Windows: An update. *J. Appl. Crystallogr.* **2012**, *45*, 849–854. [[CrossRef](#)]
47. Spek, A. Structure validation in chemical crystallography. *Acta Crystallogr. D* **2009**, *65*, 148–155. [[CrossRef](#)] [[PubMed](#)]
48. Pawłowska, N.; Gornowicz, A.; Bielawska, A.; Surażyński, A.; Szymanowska, A.; Czarnomysy, R.; Bielawski, K. The molecular mechanism of anticancer action of novel octahydropyrazino[2,1-*a*:5,4-*a'*]diisoquinoline derivatives in human gastric cancer cells. *Investig. New Drugs* **2018**, *36*, 970–984. [[CrossRef](#)] [[PubMed](#)]
49. Mullick, P.; Khan, S.A.; Begum, T.; Verma, S.; Kaushik, D.; Alam, O. Synthesis of 1,2,4-triazine derivatives as potential anti-anxiety and anti-inflammatory agents. *Acta Pol. Pharm.* **2009**, *66*, 379–385. [[PubMed](#)]
50. Gornowicz, A.; Bielawska, A.; Czarnomysy, R.; Gabryel-Porowska, H.; Muszyńska, A.; Bielawski, K. The combined treatment with novel platinum(II) complex and anti-MUC1 increases apoptotic response in MDA-MB-231 breast cancer cells. *Mol. Cell. Biochem.* **2015**, *408*, 103–113. [[CrossRef](#)]
51. Czarnomysy, R.; Surażyński, A.; Muszyńska, A.; Gornowicz, A.; Bielawska, A.; Bielawski, K. A novel series of pyrazole-platinum(II) complexes as potential anti-cancer agents that induce cell cycle arrest and apoptosis in breast cancer cells. *J. Enzyme Inhib. Med.* **2018**, *33*, 1006–1023. [[CrossRef](#)]
52. Morris, G.M.; Goodsell, D.S.; Halliday, R.S.; Huey, R.; Hart, W.E.; Belew, R.K.; Olson, A.J. Automated docking using a Lamarckian genetic algorithm and an empirical binding free energy function. *J. Comput. Chem.* **1998**, *19*, 1639–1662. [[CrossRef](#)]
53. Latacz, G.; Lubelska, A.; Jastrzębska-Więsek, M.; Partyka, A.; Marć, M.A.; Satała, G.; Wilczyńska, D.; Kotańska, M.; Więcek, M.; Kamińska, K.; et al. The 1,3,5-triazine derivatives as innovative chemical family of 5-HT<sub>6</sub> serotonin receptor agents with therapeutic perspectives for cognitive impairment. *Int. J. Mol. Sci.* **2019**, *20*, 3420. [[CrossRef](#)]

## Supplementary Material

# 2-{5-[(Z,2Z)-2-Chloro-3-(4-nitrophenyl)-2-propenylidene]-4-oxo-2-thioxothiazolidin-3-yl}-3-methylbutanoic Acid as a Potential Anti-Breast Cancer Molecule

Kamila Buzun <sup>1</sup>, Agnieszka Gornowicz <sup>1,\*</sup>, Roman Lesyk <sup>2,3</sup>, Anna Kryshchshyn-Dylevych <sup>3</sup>, Andrzej Gzella <sup>4</sup>, Robert Czarnomysy <sup>5</sup>, Gniewomir Latacz <sup>6</sup>, Agnieszka Olejarz-Maciej <sup>6</sup>, Jadwiga Handzlik <sup>6</sup>, Krzysztof Bielawski <sup>5</sup> and Anna Bielawska <sup>1</sup>

- <sup>1</sup> Department of Biotechnology, Faculty of Pharmacy, Medical University of Bialystok, 15-089 Bialystok, Poland; kamila.buzun@umb.edu.pl (K.B.); anna.bielawska@umb.edu.pl (A.B.)
  - <sup>2</sup> Department of Biotechnology and Cell Biology, Medical College, University of Information Technology and Management in Rzeszow, Sucharskiego 2, 35-225 Rzeszow, Poland; dr\_r\_lesyk@org.lviv.net
  - <sup>3</sup> Department of Pharmaceutical, Organic and Bioorganic Chemistry, Danylo Halytsky Lviv National Medical University, Pekarska 69, 79010 Lviv, Ukraine; kryshchshyn.a@gmail.com
  - <sup>4</sup> Department of Organic Chemistry, Poznan University of Medical Sciences, Grunwaldzka 6, 60-780 Poznan, Poland; akgzella@ump.edu.pl
  - <sup>5</sup> Department of Synthesis and Technology of Drugs, Faculty of Pharmacy, Medical University of Bialystok, 15-089 Bialystok, Poland; robert.czarnomysy@umb.edu.pl (R.C.); kbiel@umb.edu.pl (K.B.)
  - <sup>6</sup> Department of Technology and Biotechnology of Drugs, Faculty of Pharmacy, Jagiellonian University, Medical College, Medyczna 9, PL 30-688 Cracow, Poland; glatacz@cm-uj.krakow.pl (G.L.); agnieszka.olejarz@uj.edu.pl (A.O.-M.); jhandzlik@uj.edu.pl (J.H.)
- \* Correspondence: agnieszka.gornowicz@umb.edu.pl

### Table of contents:

1.	Copies of <sup>1</sup> H, <sup>13</sup> C NMR and LC-MS spectra of Les-3331.....	2-3
2.	Crystal structure determination (X-ray) of Les-3311.....	4-7
3.	<i>In silico</i> prediction of the most probable sites of metabolism.....	7
4.	MS spectrum and MS ion fragment analyses of Les-3331.....	8
5.	MS spectrum and MS ion fragment analyses of Les-3331 main metabolite M1.....	9
6.	MS spectra of Les-3331 metabolites M2-M5.....	9-10
7.	<i>In silico</i> prediction of the most probable sites of the main metabolite M1 hydroxylation.....	10
8.	The AMES test results.....	11

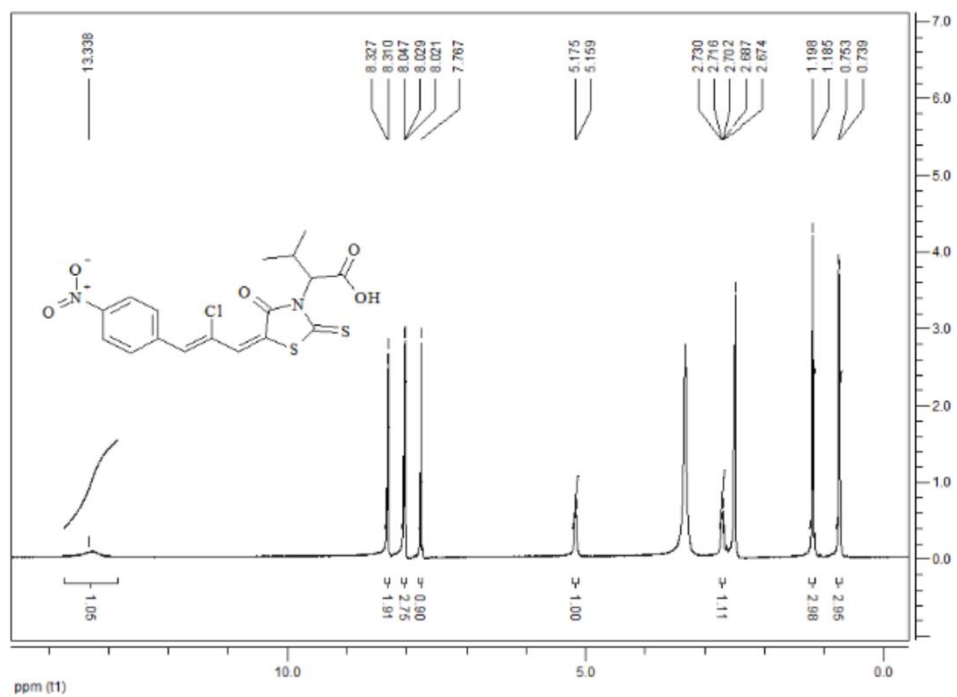


Figure S1. <sup>1</sup>H NMR spectrum of Les-3331

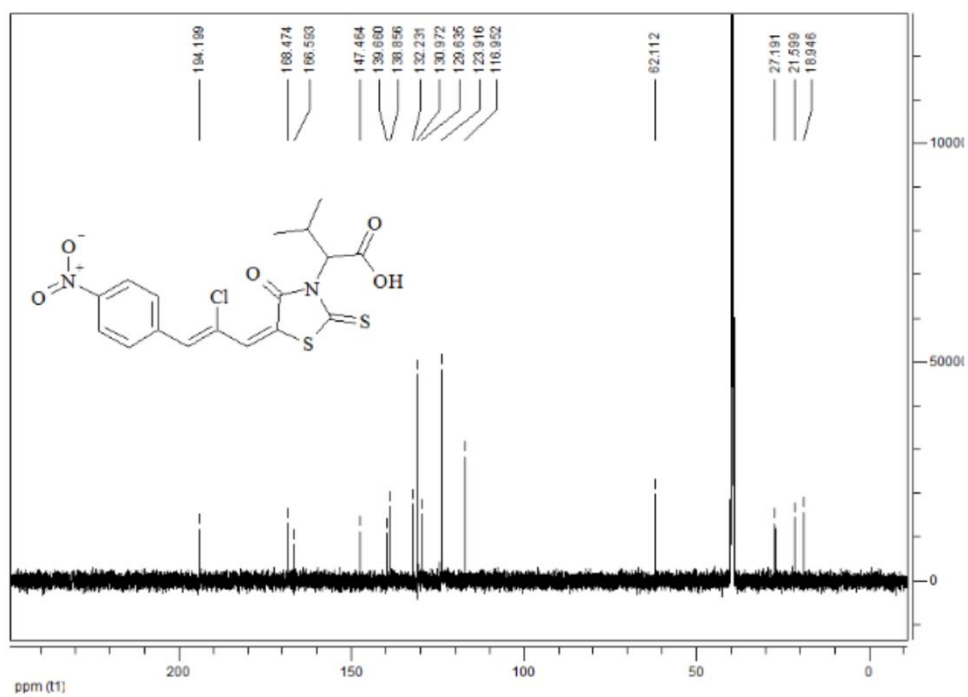


Figure S2. <sup>13</sup>C NMR spectrum of Les-3331

MaxPeak: 100.00%  
Ret\_Time: 1.650 min

CLQ227651



**Mol Wt**  
**Exact Mass**

#	Time	Area%
1	1.650	100.00

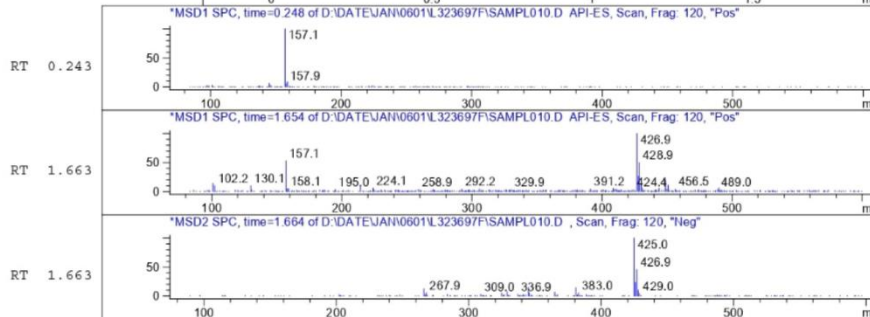
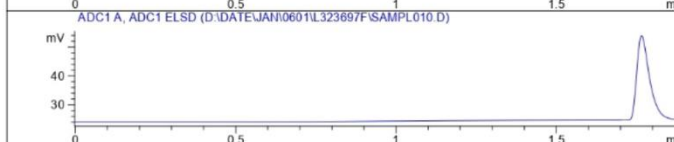
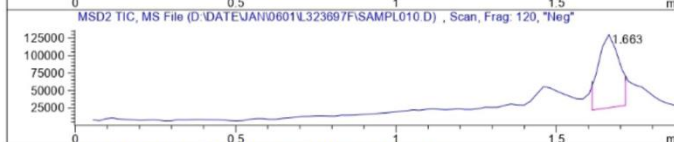
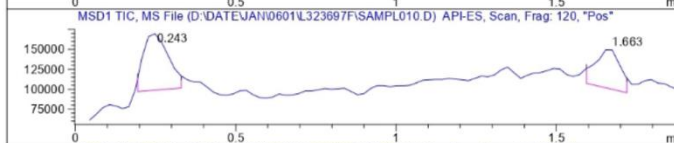
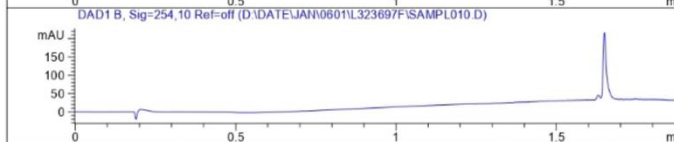
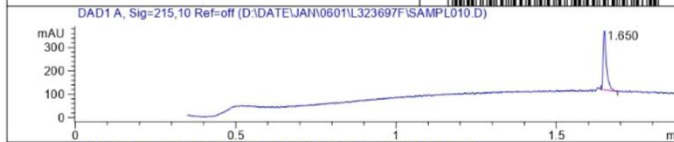


Figure S3. LC-MS spectrum of Les-3331

### Crystal structure determination (X-ray) of Les-3331

In the salt crystal lattice of Les-3331 (Table S1) solute and solvent molecules related by translation along the *a*-axis are linked by hydrogen bonds O10—H10<sup>⋯</sup>O28, C15—H15<sup>⋯</sup>O9<sup>i</sup>, C29—H29<sup>⋯</sup>O9 and C32—H32A<sup>⋯</sup>O9<sup>iii</sup> into tapes (Figure S5, Table S2). The anti-parallel tapes, related by the center of symmetry, are then connected by hydrogen bonds C21—H21<sup>⋯</sup>O26<sup>ii</sup> into columns (Figure S5, Table S2).

The carboxyl group present in the molecule, which is a fragment of the isobutylcarboxylic residue, forms a dihedral angle of 69.92(4)° with the mean plane of the 2-thioxo-1,3-thiazolidin-4-one system. The spatial orientation of this functional group is also determined by torsion angles C2—N3—C7—C8 and N3—C7—C8—O9 of 117.20(14) and -27.28(17)°, respectively. According to the values of the latter, bonds C2—N3 and C7—C8 take an anticlinal (*+ac*) conformation to each other, whereas bonds N3—C7 and C8—O9 an intermediate conformation between synperiplanar and synclinal (*sp/-sc*) ones. Spatial orientation of the remaining isobutyl fragment of the isobutylcarboxylic moiety is determined by torsion angles C2—N3—C7—C11, N3—C7—C11—C12 and N3—C7—C11—C13 of -112.25(15), 31.69(19) and 153.72(13)°, respectively. The values found to indicate that the C2—N3 and C7—C11 bonds adopt the anticlinal conformation (*-ac*), the N3—C7 and C11—C12 bonds an intermediate conformation between the synperiplanar and syncline (*sp/+sc*), and the N3—C7 and C11—C13 bonds an intermediate conformation between anticlinal and antipleriplanar (*+ac/ap*). The C5—C15 and C16—C18 bond lengths of 1.345(2) and 1.352(2) Å found in the 3-(4-nitrophenyl)-2-chloroprop-2-en-1-ylidene residue confirmed the presence of double bonds between these carbons. The mean planes of the 1,3-thiazolidine and phenyl rings present in the molecule form a dihedral angle of 16.91(4)°. The arrangement of atoms C15, C16, C17 and C18 belonging to the 3-(4-nitrophenyl)-2-chloroprop-2-en-1-ylidene moiety is flat (r.m.s.d. = 0.0008 Å) and lies almost in the plane of the 2-thioxo-1,3-thiazolidin-4-one system. The dihedral angle is only 1.76(6)°. Moreover, the mentioned arrangement of atoms C15, C16, C17 and C18 is positioned with respect to the phenyl ring at an angle of 15.44(6)°. The spatial arrangement of the 3-(4-nitrophenyl)-2-chloroprop-2-en-1-ylidene residue in the molecule is additionally determined by the torsion angles S1—C5—C15—C16, C5—C15—C16—C18 and C17—C16—C18—C19 of -1.8 (2), 179.34 (13) and -3.2(2)°, respectively, indicating the *Z* configuration of the bond pairs S1—C5/C15—C16 and C17—C16/C18—C19 and the *s-trans* conformation of the double bonds pair C5—C15/C16—C18. In the crystal, the conformation of the molecule is stabilized by the intra- and intermolecular hydrogen bonding (Figure S4 and Figure S5A, Table S2). The bond lengths O10—H10<sup>⋯</sup>O28, C29—H29<sup>⋯</sup>O9 and C32—H32A<sup>⋯</sup>O9<sup>iii</sup> stabilize the spatial arrangement of the isobutylcarboxylic moiety whereas the hydrogen bonds C15—H15<sup>⋯</sup>O9<sup>i</sup>, C21—H21<sup>⋯</sup>O26<sup>ii</sup> and C24—H24<sup>⋯</sup>C17 stabilize the spatial arrangement of the 3-(4-nitrophenyl)-2-chloroprop-2-en-1-ylidene residue.

In the crystal lattice, solute molecules related by translation along the *a*-axis are linked by hydrogen bonds C15—H15<sup>⋯</sup>O9<sup>i</sup> into tapes (Figure S4 and Figure S5A, Table S2). Solvent molecules do not participate in the formation of the tape but only attach to it through hydrogen bonds O10—H10<sup>⋯</sup>O28, C29—H29<sup>⋯</sup>O9 and C32—H32A<sup>⋯</sup>O9<sup>iii</sup>. The anti-parallel tapes, related by the center of symmetry, are connected by hydrogen bonds C21—H21<sup>⋯</sup>O26<sup>ii</sup> into columns (Figure S5B, Table S2).

**Table S1.** Crystal data, data collection and structure refinement for Les-3331

<b>Formula</b>	C <sub>17</sub> H <sub>15</sub> N <sub>2</sub> O <sub>5</sub> S <sub>2</sub> , C <sub>3</sub> H <sub>7</sub> NO
<b>Formula weight</b>	499.97
<b>Temperature/K</b>	130.0(1)
<b>Wavelength/Å</b>	1.54184
<b>Crystal system</b>	triclinic
<b>Space group</b>	<i>P</i> $\bar{1}$
<b>Unit cell parameters (Å, °)</b>	<i>a</i> = 6.3403(2)
	<i>b</i> = 10.3925(4)
	<i>c</i> = 18.2404(7)
	$\alpha$ = 81.365(3)
	$\beta$ = 84.987(3)
	$\gamma$ = 76.138(3)
<b>Volume (Å<sup>3</sup>)</b>	1152.00(7)
<b>Z (Z')</b>	2 (1)
<b><i>D</i><sub>c</sub>/g cm<sup>-3</sup></b>	1.441
<b><math>\mu</math>/mm<sup>-1</sup></b>	3.530
<b><i>F</i>(000)</b>	520
<b>Crystal dimensions [mm]</b>	0.42*0.13*0.04
<b>Color/Shape</b>	Yellow/lath
<b>Measurement method</b>	$\omega$ scans
<b><math>\theta</math> range for data collection (°)</b>	2.45–76.28
<b>Max/min. indices <i>h, k, l</i></b>	<i>h</i> : –7 → 7
	<i>k</i> : –12 → 12
	<i>l</i> : –22 → 21
<b>Collected reflections</b>	8975
<b>Independent reflections</b>	4666
<b><i>R</i><sub>int</sub></b>	0.0204
<b>Observed reflections [<i>I</i> ≥ 2σ(<i>I</i>)]</b>	4352
<b>Completeness to <math>\theta_{\max}</math> = 76.28° /%</b>	97.2
<b>Completeness to <math>\theta_{\text{full}}</math> = 67.68° /%</b>	99.9
<b>Restraints/Parameters</b>	0/297
<b>Abs. correction method</b>	Multi-scan
<b><i>T</i><sub>min</sub>, <i>T</i><sub>max</sub></b>	0.68721, 1.00000
<b>Goodness-of-fit on <i>F</i><sup>2</sup></b>	1.060
<b>Final <i>R</i> indices [<i>I</i> ≥ 2σ(<i>I</i>)]</b>	<i>R</i> 1 = 0.0309, <i>wR</i> 2 = 0.0823
<b><i>R</i> indices (all data)</b>	<i>R</i> 1 = 0.0331, <i>wR</i> 2 = 0.0847
<b>Largest diff. peak and hole /eÅ<sup>3</sup></b>	0.336 and -0.284



Table S2. Hydrogen bonds in the crystal structure of Les-3331

$D-H\cdots A$	$D-H$ (Å)	$H\cdots A$ (Å)	$D\cdots A$ (Å)	$D-H\cdots A$ (°)
<b>O10—H10<sup>i</sup>—O28</b>	0.90(3)	1.67(3)	2.5620(17)	169(3)
<b>C13—H13C<sup>i</sup>—O10</b>	0.98	2.44	3.062(2)	121
<b>C15—H15<sup>i</sup>—O9<sup>i</sup></b>	0.95	2.37	3.2218(17)	149
<b>C21—H21<sup>ii</sup>—O26<sup>ii</sup></b>	0.95	2.47	3.2175(18)	135
<b>C24—H24<sup>ii</sup>—C117</b>	0.95	2.53	3.2045(14)	128
<b>C29—H29<sup>iii</sup>—O9</b>	0.95	2.56	3.2280(18)	127
<b>C32—H32A<sup>iii</sup>—O9<sup>iii</sup></b>	0.98	2.58	3.527(2)	16159

Symmetry codes: (i)  $-1+x, y, z$ ; (ii)  $-1-x, 2-y, 1-z$ ; (iii)  $1+x, y, z$

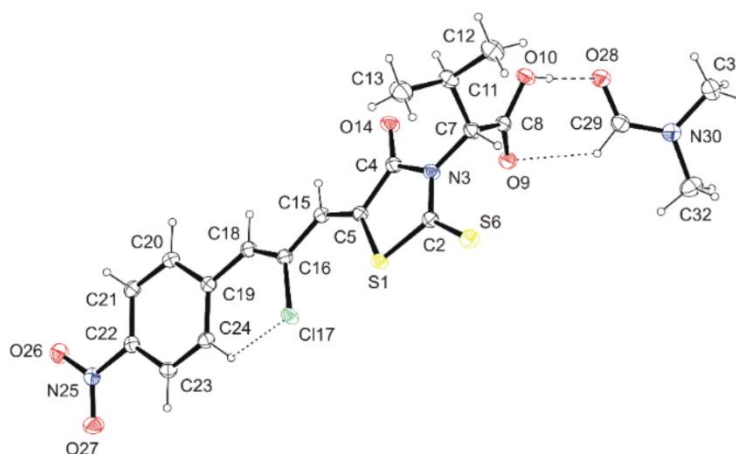


Figure S4. ORTEP view of Les-3331-DMF, showing the atomic labelling scheme. Non-H atoms are drawn as 30% probability displacement ellipsoids and H atoms are drawn as spheres of arbitrary size.

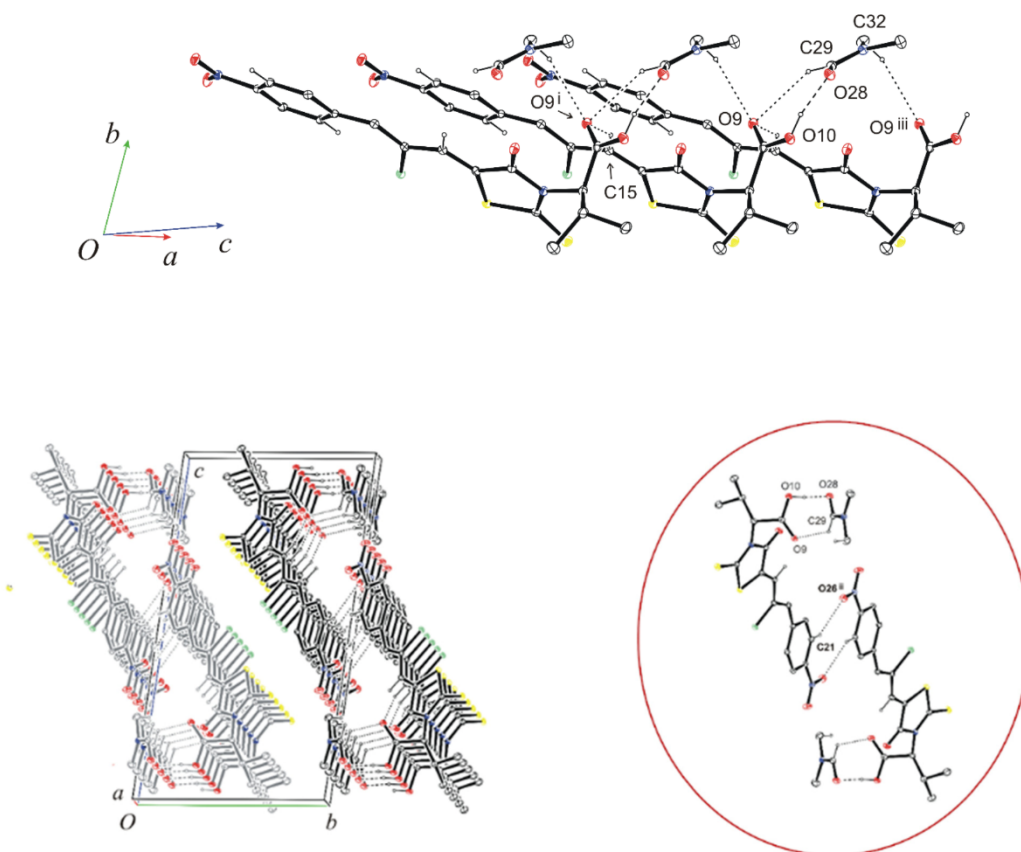


Figure S5. Hydrogen bonds linking molecules (A) into tapes growing along the a-axis, (B) linking inversion tapes into columns.

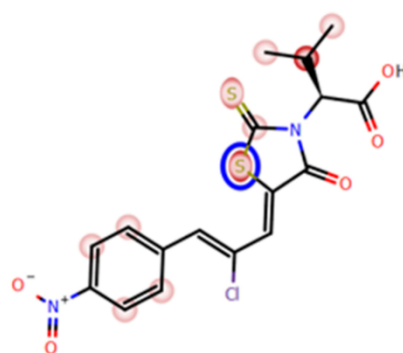
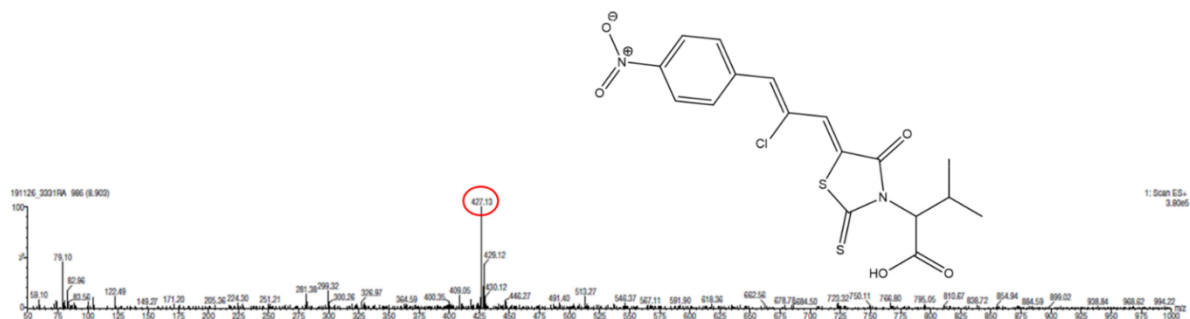


Figure S6. The MetaSite 8.0.1. *in silico* prediction of the most probable sites of Les-3331 metabolism

A)



B)

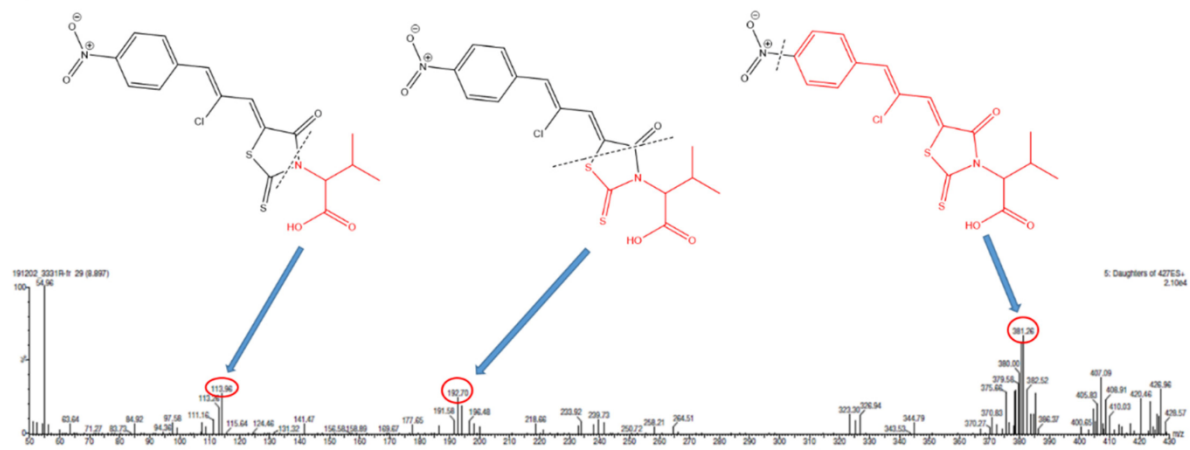
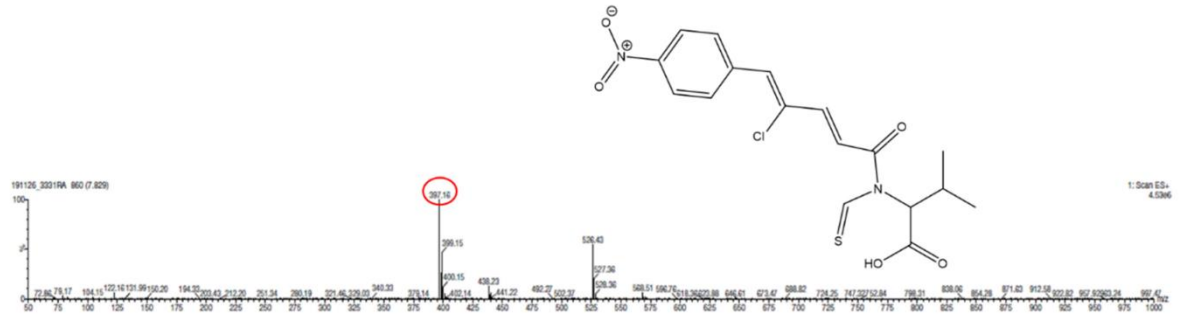


Figure S7. The MS spectrum (A) and MS ion fragment analyses (B) of compound Les-3331. The produced fragments of Les-3331 were marked in red.

A)



B)

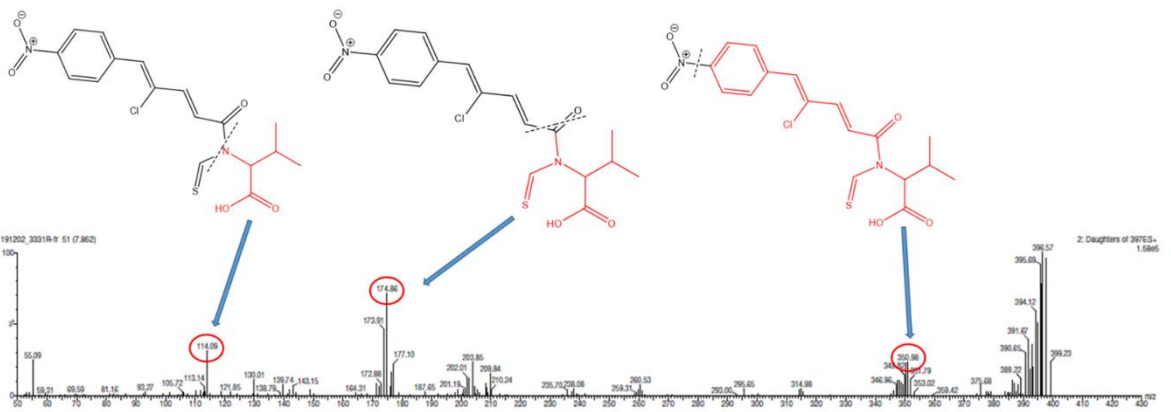


Figure S8. The MS spectrum and the most probable structure of Les-3331 main metabolite M1 (A). MS ion fragment analyses of compound Les-3331 main metabolite M1 (B). The produced fragments were marked in red.

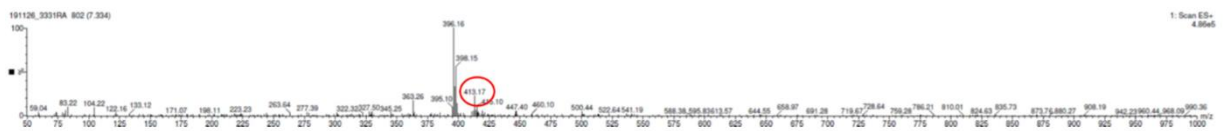


Figure S9. The MS spectrum of Les-3331 metabolite M2.

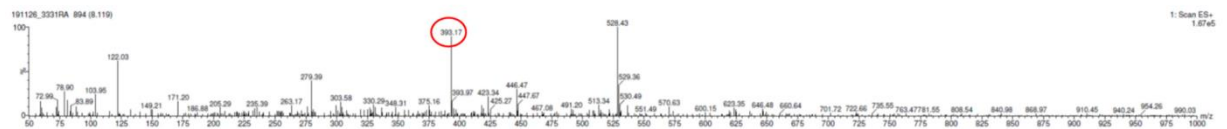


Figure S10. The MS spectrum of Les-3331 metabolite M3.

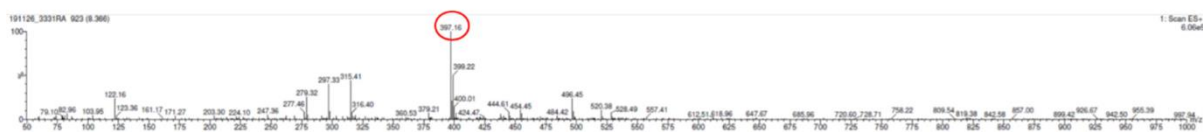


Figure S11. The MS spectrum of Les-3331 metabolite M4.

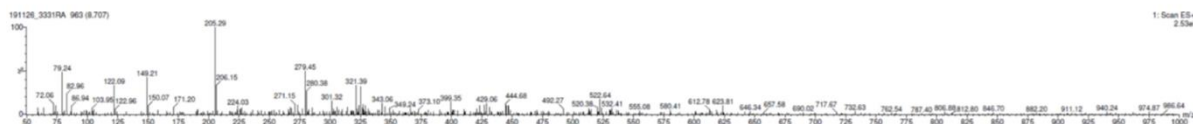


Figure S12. The MS spectrum of Les-3331 metabolite M5. Due to illegible data, the molecular weight of M5 was not estimated.

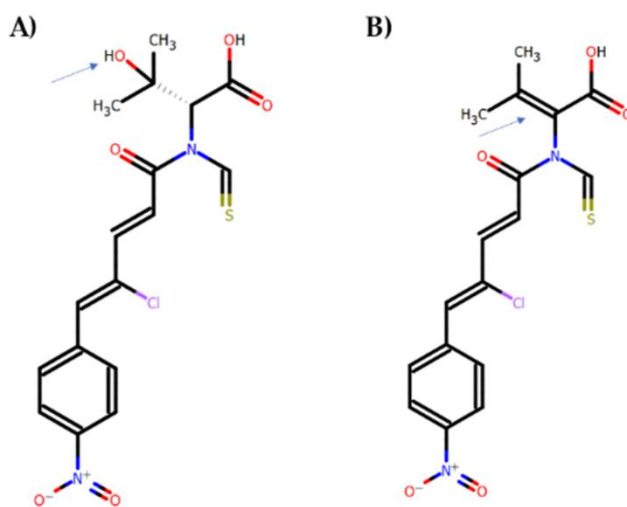
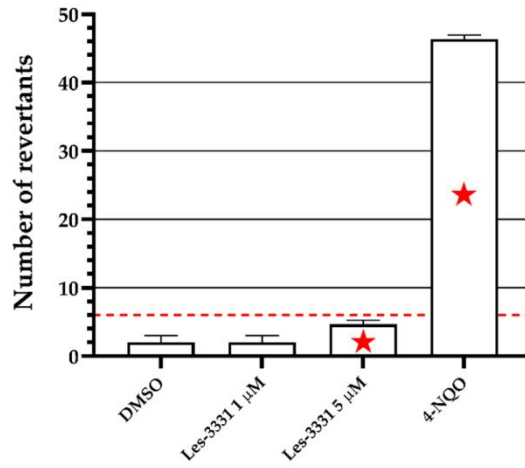


Figure S13. The MetaSite 8.0.1. *in silico* prediction of the most probable sites of the main metabolite M1 hydroxylation (A, metabolite M2) and dehydrogenation (B, metabolite M3).



\* Binomial B  $\geq$  0.99

**Figure S14.** The number of histidine prototrophic revertants of *Salmonella Typhimurium* strain TA100 exposed to the reference mutagen nonyl-4-hydroxyquinoline-N-oxide (4-NQO, 26.3  $\mu$ M) and Les-3331 at 1  $\mu$ M and 5  $\mu$ M concentrations.

\* the Binomial B-value  $\geq$  0.99 and  $2 \geq$  fold increase of medium control baseline (dashed line) indicates the mutagenic effect

**MSc Kamila Buzun**

Department of Biotechnology,  
Medical University of Białystok,  
Jana Kilinskiego 1  
15-089 Białystok, Poland

**Author Statement**

I hereby declare that my contribution to the preparation of publication:

1. Kamila Buzun, Anna Bielawska, Krzysztof Bielawski, Agnieszka Gornowicz, *DNA topoisomerases as molecular targets for anticancer drugs*, Journal of Enzyme Inhibition and Medicinal Chemistry, 2020, 35, 1781–1799, DOI: 10.1080/14756366.2020.1821676.

contained in my doctoral dissertation was collection and review of the literature, analysis and interpretation of the data and preparation of the manuscript, figures and tables, which I define as 70% participation in the preparation of the mentioned publication.

2. Kamila Buzun, Agnieszka Gornowicz, Roman Lesyk, Krzysztof Bielawski, Anna Bielawska, *Autophagy Modulators in Cancer Therapy*, International Journal of Molecular Sciences, 2021, 22, 5804, DOI: 10.3390/ijms22115804.

contained in my doctoral dissertation was collection and review of the literature, analysis and interpretation of the data, and preparation of the manuscript, figures and tables, which I define as 70% participation in the preparation of the mentioned publication.

3. Kamila Buzun, Anna Kryshchychyn-Dylevych, Julia Senkiv, Olexandra Roman, Andrzej Gzella, Krzysztof Bielawski, Anna Bielawska, Roman Lesyk, *Synthesis and Anticancer Activity Evaluation of 5-[2-Chloro-3-(4-nitrophenyl)-2-propenylidene]-4-thiazolidinones*, Molecules, 2021, 26, 3057, DOI: 10.3390/molecules26103057.

contained in my doctoral dissertation was conducting part of the experimental research, interpretation of the obtained results, participation in original draft preparation, which I define as 51% participation in the preparation of the mentioned publication.

4. Kamila Buzun, Agnieszka Gornowicz, Roman Lesyk, Anna Kryshchychyn-Dylevych, Andrzej Gzella, Robert Czarnomysy, Gniewomir Latacz, Agnieszka Olejarz-Maciej, Jadwiga Handzlik, Krzysztof Bielawski, Anna Bielawska, *2-{5-[(Z,Z)-2-Chloro-3-(4-nitrophenyl)-2-propenylidene]-4-oxo-2-thioxothiazolidin-3-yl}-3-methylbutanoic Acid as a Potential Anti-Breast Cancer Molecule*, International Journal of Molecular Sciences, 2022, 23, 4091, DOI: 10.3390/ijms23084091.

contained in my doctoral dissertation was conducting part of the experimental research, statistical analysis of the results, participation in original draft preparation, preparation of figures and tables, which I define as 51% participation in the preparation of the above mentioned publication.

*Kamila Buzun*  
.....  
Signature of the Author

*Anna Bielawska*  
.....  
Signature of the Supervisor

*Roman Lesyk*  
.....  
Signature of the Supervisor

Białystok, 11.04.2022

**Prof. Anna Bielawska**

Department of Biotechnology,  
Medical University of Białystok,  
Jana Kilinskiego 1  
15-089 Białystok, Poland

**Co-author Statement**

I hereby declare that my contribution to the preparation of publication:

1. Kamila Buzun, Anna Bielawska, Krzysztof Bielawski, Agnieszka Gornowicz, *DNA topoisomerases as molecular targets for anticancer drugs*, Journal of Enzyme Inhibition and Medicinal Chemistry, 2020, 35, 1781–1799, DOI: 10.1080/14756366.2020.1821676.

contained in the doctoral dissertation of Kamila Buzun, MSc was review and editing of the manuscript, supervision.

2. Kamila Buzun, Agnieszka Gornowicz, Roman Lesyk, Krzysztof Bielawski, Anna Bielawska, *Autophagy Modulators in Cancer Therapy*, International Journal of Molecular Sciences, 2021, 22, 5804, DOI: 10.3390/ijms22115804.

contained in the doctoral dissertation of Kamila Buzun, MSc was review and editing of the manuscript and supervision.

3. Kamila Buzun, Anna Kryshchshyn-Dylevych, Julia Senkiv, Olexandra Roman, Andrzej Gzella, Krzysztof Bielawski, Anna Bielawska, Roman Lesyk, *Synthesis and Anticancer Activity Evaluation of 5-[2-Chloro-3-(4-nitrophenyl)-2-propenylidene]-4-thiazolidinones*, Molecules, 2021, 26, 3057, DOI: 10.3390/molecules26103057.

contained in the doctoral dissertation of Kamila Buzun, MSc was review and editing of the manuscript and supervision.

4. Kamila Buzun, Agnieszka Gornowicz, Roman Lesyk, Anna Kryshchshyn-Dylevych, Andrzej Gzella, Robert Czarnomysy, Gniewomir Latacz, Agnieszka Olejarz-Maciej, Jadwiga Handzlik, Krzysztof Bielawski, Anna Bielawska, *2-{5-[(Z,Z)-2-Chloro-3-(4-nitrophenyl)-2-propenylidene]-4-oxo-2-thioxothiazolidin-3-yl}-3-methylbutanoic Acid as a Potential Anti-Breast Cancer Molecule*, International Journal of Molecular Sciences, 2022, 23, 4091, DOI: 10.3390/ijms23084091.

contained in the doctoral dissertation of Kamila Buzun, MSc review and editing of the manuscript and supervision.

I agree to submit the above-mentioned papers by Kamila Buzun, MSc as part of her doctoral dissertation in the form of a thematically coherent series of papers published in scientific journals.

  
Signature



Lviv, 11.04.2022

**Prof. Roman Lesyk**

Department of Pharmaceutical, Organic  
and Bioorganic Chemistry,  
Danylo Halytsky Lviv National Medical University,  
Pekarska 69, 79010 Lviv, Ukraine

Department of Biotechnology and Cell Biology,  
University of Information Technology  
and Management in Rzeszow, Medical College,  
Sucharskiego 2, 35-225 Rzeszow, Poland

**Co-author Statement**

I hereby declare that my contribution to the preparation of publication:

1. Kamila Buzun, Agnieszka Gornowicz, Roman Lesyk, Krzysztof Bielawski, Anna Bielawska, *Autophagy Modulators in Cancer Therapy*, International Journal of Molecular Sciences, 2021, 22, 5804, DOI: 10.3390/ijms22115804.

contained in the doctoral dissertation of Kamila Buzun, MSc was conceptualization of the paper, review and editing of the publication, supervision.

2. Kamila Buzun, Anna Kryshchyshyn-Dylevych, Julia Senkiv, Olexandra Roman, Andrzej Gzella, Krzysztof Bielawski, Anna Bielawska, Roman Lesyk, *Synthesis and Anticancer Activity Evaluation of 5-[2-Chloro-3-(4-nitrophenyl)-2-propenylidene]-4-thiazolidinones*, Molecules, 2021, 26, 3057, DOI: 10.3390/molecules26103057

contained in the doctoral dissertation of Kamila Buzun, MSc was conceptualization of the paper, supervision and project administration.

3. Kamila Buzun, Agnieszka Gornowicz, Roman Lesyk, Anna Kryshchyshyn-Dylevych, Andrzej Gzella, Robert Czarnomysy, Gniewomir Latacz, Agnieszka Olejarz-Maciej, Jadwiga Handzlik, Krzysztof Bielawski, Anna Bielawska, *2-{5-[(Z,Z)-2-Chloro-3-(4-nitrophenyl)-2-propenylidene]-4-oxo-2-thioxothiazolidin-3-yl}-3-methylbutanoic Acid as a Potential Anti-Breast Cancer Molecule*, International Journal of Molecular Sciences, 2022, 23, 4091, DOI: 10.3390/ijms23084091

contained in the doctoral dissertation of Kamila Buzun, MSc was conceptualization of the paper, review and editing of the publication and supervision.

I agree to submit the above mentioned papers by Kamila Buzun, MSc as part of her doctoral dissertation in the form of a thematically coherent series of papers published in scientific journals.

  
.....  
Signature

Białystok, 20.04.2022

**Prof. Krzysztof Bielawski**

Department of Synthesis and Technology of Drugs,  
Medical University of Białystok,  
Jana Kilinskiego 1  
15-089 Białystok, Poland

**Co-author Statement**

I hereby declare that my contribution to the preparation of publication:

1. Kamila Buzun, Anna Bielawska, Krzysztof Bielawski, Agnieszka Gornowicz, *DNA topoisomerases as molecular targets for anticancer drugs*, Journal of Enzyme Inhibition and Medicinal Chemistry, 2020, 35, 1781–1799, DOI: 10.1080/14756366.2020.1821676.

contained in the doctoral dissertation of Kamila Buzun, MSc was review and editing of the publication, supervision.

2. Kamila Buzun, Agnieszka Gornowicz, Roman Lesyk, Krzysztof Bielawski, Anna Bielawska, *Autophagy Modulators in Cancer Therapy*, International Journal of Molecular Sciences, 2021, 22, 5804, DOI: 10.3390/ijms22115804.

contained in the doctoral dissertation of Kamila Buzun, MSc was review and editing of the publication, supervision.

3. Kamila Buzun, Anna Kryshchyshyn-Dylevych, Julia Senkiv, Olexandra Roman, Andrzej Gzella, Krzysztof Bielawski, Anna Bielawska, Roman Lesyk, *Synthesis and Anticancer Activity Evaluation of 5-[2-Chloro-3-(4-nitrophenyl)-2-propenylidene]-4-thiazolidinones*, Molecules, 2021, 26, 3057, DOI: 10.3390/molecules26103057.

contained in the doctoral dissertation of Kamila Buzun, MSc was review and editing of the publication, supervision.

4. Kamila Buzun, Agnieszka Gornowicz, Roman Lesyk, Anna Kryshchyshyn-Dylevych, Andrzej Gzella, Robert Czarnomysy, Gniewomir Latacz, Agnieszka Olejarz-Maciej, Jadwiga Handzlik, Krzysztof Bielawski, Anna Bielawska, *2-{5-[(Z,Z)-2-Chloro-3-(4-nitrophenyl)-2-propenylidene]-4-oxo-2-thioxothiazolidin-3-yl}-3-methylbutanoic Acid as a Potential Anti-Breast Cancer Molecule*, International Journal of Molecular Sciences, 2022, 23, 4091, DOI: 10.3390/ijms23084091.

contained in the doctoral dissertation of Kamila Buzun, MSc was review and editing of the publication, supervision.

I agree to submit the above-mentioned papers by Kamila Buzun, MSc as part of her doctoral dissertation in the form of a thematically coherent series of papers published in scientific journals.

  
.....  
Signature

Cracow, 12.04.2022

**Prof. Jadwiga Handzlik**

Department of Technology and Biotechnology of Drugs,  
Jagiellonian University Medical College,  
Medyczna 9,  
30-688 Cracow, Poland

**Co-author Statement**

I hereby declare that my contribution to the preparation of publication:

1. Kamila Buzun, Agnieszka Gornowicz, Roman Lesyk, Anna Kryshchyshyn-Dylevych, Andrzej Gzella, Robert Czarnomysy, Gniewomir Latacz, Agnieszka Olejarz-Maciej, Jadwiga Handzlik, Krzysztof Bielawski, Anna Bielawska, 2-{5-[(Z,Z)-2-Chloro-3-(4-nitrophenyl)-2-propenylidene]-4-oxo-2-thioxothiazolidin-3-yl}-3-methylbutanoic Acid as a Potential Anti-Breast Cancer Molecule, International Journal of Molecular Sciences, 2022, 23, 4091, DOI: 10.3390/ijms23084091.

contained in the doctoral dissertation of Kamila Buzun, MSc was review and editing of the manuscript and supervision over determination of ADMETox parameters of novel 4-thiazolidinone derivative.

I agree to submit the above mentioned papers by Kamila Buzun, MSc as part of her doctoral dissertation in the form of a thematically coherent series of papers published in scientific journals.

Katedra i Zakład Technologii  
i Biotechnologii Środków Leczniczych UJ CM

  
prof. dr hab. n. t. Jadwiga Handzlik  
Signature

Poznan, 11.04.2022

**Prof. dr hab. Andrzej Gzella**

Department of Organic Chemistry,  
Poznan University of Medical Sciences,  
Grunwaldzka 6,  
60-780 Poznan, Poland

#### Co-author Statement

I hereby declare that my contribution to the preparation of publication:

1. Kamila Buzun, Anna Kryshchysyn-Dylevych, Julia Senkiv, Olexandra Roman, Andrzej Gzella, Krzysztof Bielawski, Anna Bielawska, Roman Lesyk, *Synthesis and Anticancer Activity Evaluation of 5-[2-Chloro-3-(4-nitrophenyl)-2-propenylidene]-4-thiazolidinones*, *Molecules*, 2021, 26, 3057, DOI: 10.3390/molecules26103057

contained in the doctoral dissertation of Kamila Buzun, MSc was performing X-ray analysis and interpretation of its data for selected synthesized compound.

2. Kamila Buzun, Agnieszka Gornowicz, Roman Lesyk, Anna Kryshchysyn-Dylevych, Andrzej Gzella, Robert Czarnomysy, Gniewomir Latacz, Agnieszka Olejarz-Maciej, Jadwiga Handzlik, Krzysztof Bielawski, Anna Bielawska, *2-{5-[(Z,Z)-2-Chloro-3-(4-nitrophenyl)-2-propenylidene]-4-oxo-2-thioxothiazolidin-3-yl}-3-methylbutanoic Acid as a Potential Anti-Breast Cancer Molecule*, *International Journal of Molecular Sciences*, 2022, 23, 4091, DOI: 10.3390/ijms23084091

contained in the doctoral dissertation of Kamila Buzun, MSc was X-ray structure analysis of the studied compound.

I agree to submit the above mentioned papers by Kamila Buzun, MSc as part of her doctoral dissertation in the form of a thematically coherent series of papers published in scientific journals.



.....  
Signature

Lviv, 11.04.2022

**Anna Kryshchyshyn-Dylevych**

Department of Pharmaceutical, Organic  
and Bioorganic Chemistry,  
Danylo Halytsky Lviv National Medical University,  
Pekarska 69,  
79010 Lviv, Ukraine

**Co-author Statement**

I hereby declare that my contribution to the preparation of publication:

1. Kamila Buzun, Anna Kryshchyshyn-Dylevych, Julia Senkiv, Olexandra Roman, Andrzej Gzella, Krzysztof Bielawski, Anna Bielawska, Roman Lesyk, *Synthesis and Anticancer Activity Evaluation of 5-[2-Chloro-3-(4-nitrophenyl)-2-propenylidene]-4-thiazolidinones*, *Molecules*, 2021, 26, 3057, DOI: 10.3390/molecules26103057

contained in the doctoral dissertation of Kamila Buzun, MSc was synthesis of new rhodanine derivatives and formal analysis of spectral data.

2. Kamila Buzun, Agnieszka Gornowicz, Roman Lesyk, Anna Kryshchyshyn-Dylevych, Andrzej Gzella, Robert Czarnomysy, Gniewomir Latacz, Agnieszka Olejarz-Maciej, Jadwiga Handzlik, Krzysztof Bielawski, Anna Bielawska, *2-{5-[(Z,Z)-2-Chloro-3-(4-nitrophenyl)-2-propenylidene]-4-oxo-2-thioxothiazolidin-3-yl}-3-methylbutanoic Acid as a Potential Anti-Breast Cancer Molecule*, *International Journal of Molecular Sciences*, 2022, 23, 4091, DOI: 10.3390/ijms23084091

contained in the doctoral dissertation of Kamila Buzun, MSc was selection of research methodology and synthesis of studied compound.

I agree to submit the above mentioned papers by Kamila Buzun, MSc as part of her doctoral dissertation in the form of a thematically coherent series of papers published in scientific journals.

*Anna Kryshchyshyn-Dylevych*  
Signature

Cracow, 12.04.2022

**Assoc. Prof. Gniewomir Latacz**

Department of Technology and Biotechnology of Drugs,  
Jagiellonian University Medical College,  
Medyczna 9,  
30-688 Cracow, Poland

**Co-author Statement**

I hereby declare that my contribution to the preparation of publication:

1. Kamila Buzun, Agnieszka Gornowicz, Roman Lesyk, Anna Kryshchysyn-Dylevych, Andrzej Gzella, Robert Czarnomysy, Gniewomir Latacz, Agnieszka Olejarz-Maciej, Jadwiga Handzlik, Krzysztof Bielawski, Anna Bielawska, *2-{5-[(Z,Z)-2-Chloro-3-(4-nitrophenyl)-2-propenylidene]-4-oxo-2-thioxothiazolidin-3-yl}-3-methylbutanoic Acid as a Potential Anti-Breast Cancer Molecule*, International Journal of Molecular Sciences, 2022, 23, 4091, DOI: 10.3390/ijms23084091.

contained in the doctoral dissertation of Kamila Buzun, MSc was selection of the research methods in ADMETox parameters studies and participation in original draft preparation.

I agree to submit the above mentioned papers by Kamila Buzun, MSc as part of her doctoral dissertation in the form of a thematically coherent series of papers published in scientific journals.

Katedra i Zakład Technologii  
i Biotechnologii Środków Leczniczych UJ CM  
Signature  
dr hab. Gniewomir Latacz  
adiunkt

Białystok, 20.04.2022

**PhD Agnieszka Gornowicz**

Department of Biotechnology,  
Medical University of Białystok,  
Jana Kilinskiego 1  
15-089 Białystok, Poland

**Co-author Statement**

I hereby declare that my contribution to the preparation of publication:

1. Kamila Buzun, Anna Bielawska, Krzysztof Bielawski, Agnieszka Gornowicz, *DNA topoisomerases as molecular targets for anticancer drugs*, Journal of Enzyme Inhibition and Medicinal Chemistry, 2020, 35, 1781–1799, DOI: 10.1080/14756366.2020.1821676.

contained in the doctoral dissertation of Kamila Buzun, MSc was conceptualization of the paper, review and editing of the publication.

2. Kamila Buzun, Agnieszka Gornowicz, Roman Lesyk, Krzysztof Bielawski, Anna Bielawska, *Autophagy Modulators in Cancer Therapy*, International Journal of Molecular Sciences, 2021, 22, 5804, DOI: 10.3390/ijms22115804.

contained in the doctoral dissertation of Kamila Buzun, MSc was conceptualization of the paper, review and editing of the publication.

3. Kamila Buzun, Agnieszka Gornowicz, Roman Lesyk, Anna Kryshchychyn-Dylevych, Andrzej Gzella, Robert Czarnomysy, Gniewomir Latacz, Agnieszka Olejarz-Maciej, Jadwiga Handzlik, Krzysztof Bielawski, Anna Bielawska, *2-{5-[(Z,2Z)-2-Chloro-3-(4-nitrophenyl)-2-propenylidene]-4-oxo-2-thioxothiazolidin-3-yl}-3-methylbutanoic Acid as a Potential Anti-Breast Cancer Molecule*, International Journal of Molecular Sciences, 2022, 23, 4091, DOI: 10.3390/ijms23084091.

contained in the doctoral dissertation of Kamila Buzun, MSc conceptualization of the paper, selection of the research methods of evaluation of molecular mechanism of compound's activity, review and editing of the publication.

I agree to submit the above mentioned papers by Kamila Buzun, MSc as part of her doctoral dissertation in the form of a thematically coherent series of papers published in scientific journals.

  
Signature

Białystok, 20.04.2022

**PhD Robert Czarnomysy**

Department of Synthesis and Technology of Drugs,  
Medical University of Białystok,  
Jana Kilinskiego 1  
15-089 Białystok, Poland

**Co-author Statement**

I hereby declare that my contribution to the preparation of publication:

1. Kamila Buzun, Agnieszka Gornowicz, Roman Lesyk, Anna Kryshchyn-Dylevych, Andrzej Gzella, Robert Czarnomysy, Gniewomir Latacz, Agnieszka Olejarz-Maciej, Jadwiga Handzlik, Krzysztof Bielawski, Anna Bielawska, *2-{5-[(Z,Z)-2-Chloro-3-(4-nitrophenyl)-2-propenylidene]-4-oxo-2-thioxothiazolidin-3-yl}-3-methylbutanoic Acid as a Potential Anti-Breast Cancer Molecule*, International Journal of Molecular Sciences, 2022, 23, 4091, DOI: 10.3390/ijms23084091.

contained in the doctoral dissertation of Kamila Buzun, MSc was flow cytometric analysis of the compound (Annexin V Binding Assay, Mitochondrial Membrane Potential Analysis and Analysis of Anti-Topoisomerase II $\alpha$  antibody).

I agree to submit the above mentioned papers by Kamila Buzun, MSc as part of her doctoral dissertation in the form of a thematically coherent series of papers published in scientific journals.

  
Signature



Lviv, 11.04.2022

**Olexandra Roman**

Department of Pharmaceutical, Organic  
and Bioorganic Chemistry,  
Danylo Halytsky Lviv National Medical University,  
Pekarska 69, 79010 Lviv, Ukraine

**Co-author Statement**

I hereby declare that my contribution to the preparation of publication:

1. Kamila Buzun, Anna Kryshchyshyn-Dylevych, Julia Senkiv, Olexandra Roman, Andrzej Gzella, Krzysztof Bielawski, Anna Bielawska, Roman Lesyk, *Synthesis and Anticancer Activity Evaluation of 5-[2-Chloro-3-(4-nitrophenyl)-2-propenylidene]-4-thiazolidinones*, *Molecules*, 2021, 26, 3057, DOI: 10.3390/molecules26103057

contained in the doctoral dissertation of Kamila Buzun, MSc was the development and validation of the synthesis method of 5-[2-chloro-3-(4-nitrophenyl)-2-propenylidene]-4-thiazolidinones.

I agree to submit the above mentioned papers by Kamila Buzun, MSc as part of her doctoral dissertation in the form of a thematically coherent series of papers published in scientific journals.

*Olexandra Roman*

.....  
Signature

Lviv, 11.04.2022

**Julia Senkiv**

Institute of Cell Biology  
National Academy of Sciences of Ukraine,  
Drahomanov Str. 14/16,  
79005 Lviv, Ukraine

**Co-author Statement**

I hereby declare that my contribution to the preparation of publication:

1. Kamila Buzun, Anna Kryshchyshyn-Dylevych, Julia Senkiv, Olexandra Roman, Andrzej Gzella, Krzysztof Bielawski, Anna Bielawska, Roman Lesyk, *Synthesis and Anticancer Activity Evaluation of 5-[2-Chloro-3-(4-nitrophenyl)-2-propenylidene]-4-thiazolidinones*, *Molecules*, 2021, 26, 3057, DOI: 10.3390/molecules26103057

contained in the doctoral dissertation of Kamila Buzun, MSc was determination of the influence of studied compounds on normal human blood lymphocytes, calculation of therapeutic index (TI) and visualization of these data.

I agree to submit the above mentioned papers by Kamila Buzun, MSc as part of her doctoral dissertation in the form of a thematically coherent series of papers published in scientific journals.

  
.....  
Signature

Cracow, 12.04.2022

**MSc Agnieszka Olejarz-Maciej**

Department of Technology and Biotechnology of Drugs,  
Jagiellonian University Medical College,  
Medyczna 9,  
30-688 Cracow, Poland

#### Co-author Statement

I hereby declare that my contribution to the preparation of publication:

1. Kamila Buzun, Agnieszka Gornowicz, Roman Lesyk, Anna Kryshchyshyn-Dylevych, Andrzej Gzella, Robert Czarnomysy, Gniewomir Latacz, Agnieszka Olejarz-Maciej, Jadwiga Handzlik, Krzysztof Bielawski, Anna Bielawska, *2-{5-[(Z,Z)-2-Chloro-3-(4-nitrophenyl)-2-propenylidene]-4-oxo-2-thioxothiazolidin-3-yl}-3-methylbutanoic Acid as a Potential Anti-Breast Cancer Molecule*, International Journal of Molecular Sciences, 2022, 23, 4091, DOI: 10.3390/ijms23084091.

contained in the doctoral dissertation of Kamila Buzun, MSc was the assessment of mutagenicity of new compound using the Ames microplate fluctuation (MPF) protocol.

I agree to submit the above mentioned papers by Kamila Buzun, MSc as part of her doctoral dissertation in the form of a thematically coherent series of papers published in scientific journals.

Agnieszka Olejarz-Maciej  
.....  
Signature

#### **XIV. Scientific achievements**

Total Impact Factor: **33.688**

*h*-index: **4.00**

#### **List of publications constituting the doctoral dissertation:**

Total Impact Factor for the publication series: **21.311**

Total points according to the list of scientific journals by the MES: **520 points**

1. Kamila Buzun, Agnieszka Gornowicz, Roman Lesyk, Anna Kryshchyshyn-Dylevych, Andrzej Gzella, Robert Czarnomysy, Gniewomir Latacz, Agnieszka Olejarz-Maciej, Jadwiga Handzlik, Krzysztof Bielawski, Anna Bielawska, *2-{5-[(Z,2Z)-2-Chloro-3-(4-nitrophenyl)-2-propenylidene]-4-oxo-2-thioxothiazolidin-3-yl}-3-methylbutanoic Acid as a Potential Anti-Breast Cancer Molecule*, International Journal of Molecular Sciences, 2022, Vol. 23, No. 8, 34 pp., Article ID: 4091, DOI: 10.3390/ijms23084091, IF = 5.924, MES scores: 140.00 points
2. Kamila Buzun, Anna Kryshchyshyn-Dylevych, Julia Senkiv, Olexandra Roman, Andrzej Gzella, Krzysztof Bielawski, Anna Bielawska, Roman Lesyk, *Synthesis and Anticancer Activity Evaluation of 5-[2-Chloro-3-(4-nitrophenyl)-2-propenylidene]-4-thiazolidinones*, Molecules, 2021, Vol. 26, No. 10, 15 pp., Article ID: 3057, DOI: 10.3390/molecules26103057, IF = 4.412, MES scores: 100.00 points
3. Kamila Buzun, Agnieszka Gornowicz, Roman Lesyk, Krzysztof Bielawski, Anna Bielawska, *Autophagy Modulators in Cancer Therapy*, International Journal of Molecular Sciences, 2021, Vol. 22, No. 11, 35 pp., Article ID: 5804, DOI: 10.3390/ijms22115804, IF = 5.924, MES scores: 140.00 points
4. Kamila Buzun, Anna Bielawska, Krzysztof Bielawski, Agnieszka Gornowicz, *DNA topoisomerases as molecular targets for anticancer drugs*, Journal of Enzyme Inhibition and Medicinal Chemistry, 2020, Vol. 35, No. 1, 1781-1799, DOI: 10.1080/14756366.2020.1821676, IF = 5.051, MES scores: 140.00 points

### **List of additional scientific publications:**

Total Impact Factor for the publications: **12.377**

Total points according to the list of scientific journals by the MES: **240 points**

1. Iwona Radziejewska, Katarzyna Supruniuk, Robert Czarnomysy, Kamila Buzun, Anna Bielawska, *Anti-Cancer Potential of Afzelin towards AGS Gastric Cancer Cells*, Pharmaceuticals, 2021, Vol. 14, No. 10, 16 pp., Article ID: 973, DOI: 10.3390/ph14100973, IF = 5.863, MES scores: 100 points
2. Sylwia Sudół, Katarzyna Kucwaj-Brysz, Rafał Kurczab, Natalia Wilczyńska, Magdalena Jastrzębska-Więsek, Grzegorz Satała, Gniewomir Latacz, Monika Głuch-Lutwin, Barbara Mordyl, Ewa Żesławska, Wojciech Nitek, Anna Partyka, Kamila Buzun, Agata Doroz-Płonka, Anna Wesołowska, Anna Bielawska, Jadwiga Handzlik, *Chlorine substituents and linker topology as factors of 5-HT<sub>6</sub>R activity for novel highly active 1,3,5-triazine derivatives with procognitive properties in vivo*, European Journal of Medicinal Chemistry, 2020, Vol. 203, 16 pp., Article ID: 112529, DOI: 10.1016/j.ejmech.2020.112529, IF = 6.514, MES scores: 140 points
3. Kamila Buzun, Anna Bielawska, Krzysztof Bielawski, *Nanotechnology in cosmetology*, Polish Journal of Cosmetology, 2019, Vol. 22, No. 1, 14-19

### List of conference reports:

1. Kamila Buzun, Agnieszka Gornowicz, Robert Czarnomysy, Roman Lesyk, Krzysztof Bielawski, Anna Bielawska, *The pro-apoptotic effect of new 2-thioxo-4-thiazolidinone derivative Les-3331 on MCF-7 and MDA-MB-231 cell lines*, Ninth International Conference on Radiation in Various Fields of Research, Herceg Novi, Montenegro, 14-18.06.2021
2. Anna Szymanowska, Kamila Buzun, Wojciech Szymanowski, Robert Czarnomysy, Agnieszka Gornowicz, Mariusz Mojzych, Anna Bielawska, Krzysztof Bielawski, *The pro-apoptotic effect of novel pyrazolo[4,3-e]tetrazolo[4,5-b][1,2,4]triazine derivatives in HT-29 colon cancer cells*, Ninth International Conference on Radiation in Various Fields of Research, Herceg Novi, Montenegro, 14-18.06.2021
3. Wojciech Szymanowski, Kamila Buzun, Anna Szymanowska, Agnieszka Gornowicz, Roman Lesyk, Krzysztof Bielawski, Anna Bielawska, *The cytotoxic potential of a novel 2-thioxo-4-thiazolidinone derivative used with anti-HER2 antibodies in AGS gastric cancer cells*, Ninth International Conference on Radiation in Various Fields of Research, Herceg Novi, Montenegro, 14-18.06.2021
4. Kamila Buzun, Agnieszka Gornowicz, Robert Czarnomysy, Roman Lesyk, Anna Bielawska, Krzysztof Bielawski, *Anticancer activity of a new 2-thioxo-4-thiazolidinone derivative Les-3331 against MDA-MB-231 cancer cell line*, X Konserwatorium Chemii Medycznej, Lublin, Poland, 03-05.09.2021
5. Krzysztof Bielawski, Agnieszka Gornowicz, Wojciech Szymanowski, Robert Czarnomysy, Kamila Buzun, Anna Bielawska, *The influence of anti-HER2 monoclonal antibodies with etoposide on autophagy in gastric cancer cells*, X Konserwatorium Chemii Medycznej, Lublin, Poland, 03-05.09.2021
6. Kamila Buzun, Gniewomir Latacz, Roman Lesyk, Jadwiga Handzlik, Olga Szewczyk, Krzysztof Bielawski, Anna Bielawska, *In silico and in vitro prediction of metabolic stability of new 2-thioxo-4-thiazolidinone derivatives*, 18th Hellenic Symposium on Medicinal Chemistry, on-line, 25-27.02.2021
7. Kamila Buzun, Bożena Popławska, Anna Szymanowska, Wojciech Szymanowski, Agnieszka Gornowicz, Roman Lesyk, Anna Bielawska, Krzysztof Bielawski, *Molekularny mechanizm działania przeciwnowotworowego nowych pochodnych 2-tioksytiazolidyno-4-onu w komórkach raka piersi MCF-7*, IV Sympozjum Szkoła Chemii Medycznej, Wrocław, Poland, 25-27.09.2019

8. Anna Szymanowska, Wojciech Szymanowski, Kamila Buzun, Robert Czarnomysy, Agnieszka Gornowicz, Mariusz Mojzych, Anna Bielawska, Krzysztof Bielawski, *Wpływ sulfonamidowych pochodnych 1,2,4-triazyny na proces apoptozy w komórkach raka jelita grubego HT-29*, IV Sympozjum Szkoła Chemii Medycznej, Wrocław, Poland, 25-27.09.2019
9. Wojciech Szymanowski, Anna Szymanowska, Kamila Buzun, Agnieszka Gornowicz, Roman Lesyk, Krzysztof Bielawski, Anna Bielawska, *Ocena skojarzonego działania trastuzumabu oraz pertuzumabu ze związkami 4367 na komórki raka piersi HCC1954*, IV Sympozjum Szkoła Chemii Medycznej, Wrocław, Poland, 25-27.09.2019
10. Kamila Buzun, Anna Szymanowska, Wojciech Szymanowski, Bożena Popławska, Agnieszka Gornowicz, Mariusz Mojzych, Anna Bielawska, Krzysztof Bielawski, *The cytotoxic potential of novel tricyclic 1,2,4-triazine derivatives in MDA-MB-231 breast cancer cells*, XV International Scientific Conference for Students and PhD Students "Youth and Progress of Biology", Lviv, Ukraine, 09-11.04.2019
11. Anna Szymanowska, Wojciech Szymanowski, Kamila Buzun, Agnieszka Gornowicz, Robert Czarnomysy, Mariusz Mojzych, Anna Bielawska, Krzysztof Bielawski, *The influence of novel 1,2,4-triazine derivatives on the activity of caspase-8 and caspase-10 in human colon cancer cells*, XV International Scientific Conference for Students and PhD Students "Youth and Progress of Biology", Lviv, Ukraine, 09-11.04.2019
12. Wojciech Szymanowski, Anna Szymanowska, Kamila Buzun, Agnieszka Gornowicz, Robert Czarnomysy, Bożena Popławska, Mariusz Mojzych, Krzysztof Bielawski, Bielawska Anna, *The expression of caspase -3 and -9 after treatment with novel series of 1,2,4-triazine derivatives in DLD-1 colon cancer cells*, XV International Scientific Conference for Students and PhD Students "Youth and Progress of Biology", Lviv, Ukraine, 09-11.04.2019

**List of other scientific activities:**

A scientific internship in the field of ADME-Tox techniques at the Department of Technology and Biotechnology of Drugs, Jagiellonian University Medical College, 20.10.2019-28.02.2020, Cracow, Poland